Habilitation à Diriger les Recherches _ Habilitation à Diriger les Recherches

David Chiron

UNIVERSITÉ DE NANTES

DOCTORAT BIOLOGIE BRETAGNE SANTE LOIRE

CRCINA

Inserm

cnrs

UNIVERSITE DE NANTES

ECOLE DOCTORAL BIOLOGIE-SANTE (BS)

Habilitation à Diriger les Recherches

par

Dr. David CHIRON

Centre de Recherche en Cancérologie et Immunologie Nantes-Angers

Equipe_10 Regulation of Bcl-2 and p53 networks
in Multiple Myeloma and Mantle Cell Lymphoma

Jury de soutenance du 24/03/2022

Rapporteurs : Dr. Véronique Baud, Université de Paris
Dr. Gaétan Jego, Université de Bourgogne
Dr. Nicolas Bidère, Nantes Université

Examinateurs : Dr. Brigitte Sola, Université de Caen Normandie
Dr. Gaël Roué, IJC Barcelone
Dr. Catherine Pellat, Nantes Université

1. Curriculum vitae

Nom: David Chiron
Date et lieu de Naissance: 16/06/84, Nantes. **Nationalité:** F
E-mail: david.chiron@univ-nantes.fr

1.1_ Parcours universitaire

- Doctorat en Aspects moléculaires et cellulaires de la biologie - 2007-2010
  Spécialités: Oncologie, Hématologie, Immunologie
  Encadrement : Dr. Pellat-Deceunynck C. et Dr. Jego G.
  Ecole doctorale Biologie-Santé, Université de Nantes, France
  Financement : Allocation du Ministère de la Recherche
  Soutenu le : 18 Octobre 2010

- Master en Sciences Biologiques et Médicales – 2005-2007
  Spécialités : Biologie, Biotechnologie et Recherche Thérapeutique
  Faculté des Sciences, Université de Nantes, France

- Licence de Biologie-Biochimie - 2005
  Université de Grenade, Espagne (Programme Echange Erasmus)

1.2 _ Carrière professionnelle

- Chargé de Recherche CNRS __ 2016 -
  Centre Régional de Recherche en Cancérologie et Immunologie Nantes-Angers, France (UMR1232)
  Equipe : Dr. Pellat-Deceunynck C. et Dr. Amiot M.
  Intitulé du projet : Etude du microenvironnement dans le Lymphome à Cellules du Manteau

- Chercheur Post-doctorant __ 2014 - 2016
  Centre Régional de Recherche en Cancérologie Nantes-Angers, France
  Equipe : Dr. Amiot M. et Dr. Pellat-Deceunynck C.
  Intitulé du projet : Régulation de la Famille Bcl2 par le microenvironnement des Lymphomes B
  Financement : Allocation Ligue Contre Le Cancer "Aide au retour de l'étranger"

- Chercheur Post-doctorant __ 2011 - 2014
  Weill-Cornell Medical College, Cornell University, New York, USA
  Directeur : Pr. Chen-Kiang S.
  Intitulé du projet : - Mechanism-based targeting of the cell cycle in Lymphomas

Publications : Auteur de 33 publications dans des journaux internationaux à comité de lecture (dont 16 en tant que premier ou dernier auteur).

Réseaux **:** Institut Carnot Calym, CNRS GDR 3697 Micronit, European MCL network

Animation de la Recherche
- Co-direction de l'équipe "Molecular Vulnerabilities in B-cell malignancies" **reMOVE-B**
  (*à partir de 2022*)
- Membre du conseil de gestion de la faculté de médecine de Nantes
- Membre du comité d'animation scientifique du CRCINA.
- Responsable scientifique du comité junior du Cluster l'HéMA-NexT (*i-site NexT, ANR*).

1.3 _ Enseignement, formation et diffusion de la culture scientifique

Thèses co-encadrées

- Antonin Papin _ 2016-2019
Rôle du microenvironnement tumoral dans l'expansion des lymphomes B
Sous la direction de Steven Le Gouill (50) et de **David Chiron** (50).
Thèse soutenue le 08-10-2019 et ayant donné lieu à 5 Publications.
Dr. Antonin Papin est actuellement en Post-doctorat dans le laboratoire du Dr. Ary Melnyk au Weill Cornell Medical College de New York.

- Salomé Decombis _ 2019
Rôle du microenvironnement immunitaire dans l'expansion des lymphomes B matures
Sous la direction de Catherine Pellat-Deceunynck (50) et de **David Chiron** (50).
En préparation depuis le 02-09-2019

Encadrement d'étudiants Master 2 recherche

- Antonin Papin _ 2015-2016 _ Master Biologie-Santé de Nantes
Étude de l'impact des monocytes macrophages sur la survie et la prolifération des cellules du lymphome du manteau in vitro.

- Thiphanie Riveron _ 2018-2019 _ Master Biologie-Santé de Nantes
Rôle de l'IL-32 dans le dialogue entre le lymphome à cellules du Manteau et son microenvironnement myéloïde.

- Mathieu Rouel _ 2018-2019 _ Master Informatique de Nantes _ Co-encadrement du Stage avec Dr. Benoit Tessoulin (50%)
Analyse du transcriptome des hémopathies B mature.

- Clara Sortais _ 2019-2020 _ Master 2 «Biochimie, cellules et cibles thérapeutiques» (B2CT) de Paris Diderot
Caractérisation moléculaire et fonctionnelle des macrophages associés aux lymphomes à cellules du manteau.

Enseignement

2017 : Licence 3 Advanced Biology Training _ Nantes Université _ 4h
2018 : Licence 3 Advanced Biology Training _ Nantes Université _ 4h
Licence 2 Advanced Biology Training _ Nantes Université _ 1h30
M2 BBRT - Master Biologie-Santé _ Nantes Université _ 4h
2019 : M2 BBRT - Master Biologie-Santé _ Nantes Université _ 4h
2020 : M2 BBRT - Master Biologie-Santé _ Nantes Université _ 4h

Tous les cours mentionnés ci-dessus avaient pour thématique l'étude du microenvironnement dans les hémopathies B mature.

Jurys de soutenance de Master-2

- 2019 : M2 GGBS - Master Biologie-Santé _ Nantes Université
- 2020 : M2 GGBS - Master Biologie-Santé _ Nantes Université

Jury de thèse:

- 2019 : Rôle de la β-caténine dans le dialogue entre les cellules B tumorales et leur microenvironnement par Souhail Ouriemmi. Université Paris 13, le 20-11-2019 (examinateur)

Vulgarisation

1. **Chiron D**. Physiopathologie du lymphome à cellules du manteau. Horizons Hémato // Avril / Mai / Juin 2016 // Volume 06 // Numéro 02

2. Après-midi de visite et réunion au laboratoire avec les bénévoles de Action Cancer 44 (Comité local de l'association France Cancer), 2017

3. Participation à L'HéMA Day, Place du commerce, Nantes, 2019, https://www.chu-nantes.fr/entrez-dans-la-melee-contre-les-cancers-du-sang-91184.kjsp, organisé par Lok A & Le Gouill S

Travaux d'expertise

- Reviewer de publications depuis 2016 dans des journaux internationaux Q1. Ce travail d'expertise s'est notamment concrétisé par la publication de 2 commentaires issus de ces «reviewing» :

1. **Chiron D**. Three targets in 1 shot against ibrutinib resistance.
   Blood. 2019;133(9):888-889
   Editorial de l'article : Dobrovolsky et al., Bruton tyrosine kinase degradation as a therapeutic strategy for cancer. Blood. 2019 Feb 28;133(9):952-961.

2. **Chiron D**. Towards ecosystem integration for a better understanding of aggressiveness of B-cell lymphomas.
   Br J Haematol. 2021 Feb 22. doi: 10.1111/bjh.17367
   Editorial de l'article : Rodrigues et al., Infiltration of CD163-, PD-L1- and FoxP3-positive cells adversely affects outcome in patients with mantle cell lymphoma independent of established risk factors. Br J Haematol. 2021 Mar 8.

- Evaluation de projets scientifiques pour la Région Nouvelle-Aquitaine (AAP 2018)

- Evaluation de projets scientifique pour Ligue National contre le cancer (comité Normandie 2018).

- Jury de recrutement d'un maître de conférences sur l'emploi n° 64/65 MCF 1309 - 4369. Université Sorbonne Paris Nord (2019-2020)

Activités collectives au sein de l'unité

2017-__ Commission 'Animalerie' et 'Informatique' du CRCINA

2020-__ Comité d'Animation Scientifique (CAS) du CRCI²NA. Ce CAS composé d'une dizaine de personnes a eu pour mission de préparer la coordination de l'animation scientifique du futur centre de Recherche (2022) à travers l'organisation des séminaires hebdomadaires, de symposia, de clubs d'animation, …

1.4 _ Contrat de Recherche

Contrats locaux

1- Young Investigator call, l'Hema, 2019-2020, investigateur principal, 40 k€
2- Lauréat du concours "Jeunes Chercheurs", CHU de Nantes, 2015-2016, 50 k€
3- SIRIC ILIAD Internal Research Call 2019, investigateur principal, 25 k€

Fondations

1- Ligue Régionale Contre le Cancer 2019, investigateur principal, 27 k€
2016, co-investigateur principal, 20 k€

Contrats Nationaux

1- ANR _ Abondement Calym 2019-2020, budget attribué aux projets « Lymphomes », 78 k€

2- ANR *CHICHE (Carnot/Findmed*_ANR) 2020-2021, co-investigateur principal, 65 k€

3- Allocation Ligue Contre Le Cancer "Aide au retour de l'étranger", 2014-2015, investigateur principal, 110 k€

Contrats partenaires industriels

1- Jansen 2015-2016, investigateur principal, 80 k€

2- Institut Roche 2016-2017, investigateur principal, 60 k€

Tous les contrats mentionnés ci-dessus avaient pour thématique l'étude du microenvironnement dans les hémopathies B mature.

Prix

1- Travel Scholarship Award, International Myeloma Society (IMS), 2011

2- The Philippe Foundation Inc Grant Award, 2012

3- American Society of Hematology (ASH) Abstract Achievement Award, 2012-2013

4- Cancer Research and Treatment (CRT) Fellowship (USA) 2013

2. Publications

2.1 _ Listes détaillée des publications classées par type et par année

- publications originales dans des journaux à comité de lecture

2021

Tessoulin B, **Chiron D**, Thieblemont C, Oberic L, Bouadballah K, Gyan E, Damaj G, Ribrag V, Gressin R, Feugier P, Casasnovas O, Zerazhi H, Lemonnier F, Maisonneuve H, Joubert C, Van Den Neste E, Lamy T, Tilly H, Moreau A, Hermine O, Le Gouill S.
Oxaliplatin before autologous transplantation in combination with high-dose cytarabine and rituximab provides longer disease control than cisplatin or carboplatin in patients with mantle-cell lymphoma: results from the LyMA prospective trial. **Bone Marrow Transplant**. 2021 Mar 3. (IF : 5)

Le Gouill S, Morschhauser F, **Chiron D**, Bouabdallah K, Cartron G, Casasnovas O, Bodet-Milin C, Ragot S, Bossard C, Nadal N, Herbaux C, Tessoulin B, Tchernonog E, Rossi C, McCulloch R, Gastinne T, Callanan MB, Rule S.
Ibrutinib, Obinutuzumab And Venetoclax In Relapsed and Untreated Patients with Mantle-Cell Lymphoma, a phase I/II trial. **Blood**. 2021 Feb 18;137(7):877-887. doi: 10.1182. (IF : 17.5)

2020

Le Bris Y, Magrangeas F, Moreau A, **Chiron D**, Guérin-Charbonnel C, Theisen O, Pichon O, Canioni D, Burroni B, Maisonneuve H, Thieblemont C, Oberic L, Gyan E, Pellat-Deceunynck C, Hermine O, Delfau-Larue MH, Tessoulin B, Béné MC, Minvielle S, Le Gouill S.
Whole genome copy number analysis in search of new prognostic biomarkers in first line treatment of mantle cell lymphoma. A study by the LYSA group. **Hematological Oncology**. 2020;38(4):446-455. (IF : 3)

Lazarian G, Friedrich C, Quinquenel A, Tran J, Ouriemmi S, Dondi E, Martin A, Mihoub I, **Chiron D**, Bellanger C, Fleury C, Gélébart P, McCormack E, Ledoux D, Thieblemont C, Marzec J, Gribben JG, Cymbalista F, Varin-Blank N, Gardano L, Baran-Marszak F.
Stabilization of β-catenin upon B-cell receptor signaling promotes NF-kB target genes transcription in mantle cell lymphoma. **Oncogene**. 2020;39(14):2934-2947. (IF : 8)

2019

Papin A, Tessoulin B, Bellanger C, Moreau A, Le Bris Y, Maisonneuve H, Moreau P, Touzeau C, Amiot M, Pellat-Deceunynck C, Le Gouill S, **Chiron D**.
CSF1R and BTK inhibitions as novel strategies to disrupt the dialog between mantle cell lymphoma and macrophages. **Leukemia**. 2019;33(10):2442-2453. (IF : 9)

Tessoulin B, Papin A, Gomez-Bougie P, Bellanger C, Amiot M, Pellat-Deceunynck C, **Chiron D.**
BCL2-family dysregulation in B-cell malignancies: from gene expression regulation to a targeted therapy biomarker. **Frontiers in oncology**. 2019;8:645. (IF : 4)

Douanne T, André-Grégoire G, Trillet K, Thys A, Papin A, Feyeux M, Hulin P, **Chiron D**, Gavard J, Bidère N. Pannexin-1 limits the production of proinflammatory cytokines during necroptosis. **EMBO reports**. 2019;20(10):e47840. (IF : 7.5)

2018

Tessoulin B, Moreau-Aubry A, Descamps G, Gomez-Bougie P, Maïga S, Gaignard A, **Chiron D**, Ménoret E, Le Gouill S, Moreau P, Amiot M, Pellat-Deceunynck C.
Whole-exon sequencing of human myeloma cell lines shows mutations related to myeloma patients at relapse with major hits in the DNA regulation and repair pathways. **Journal of hematology & oncology**. 2018;11(1):1-13. (IF : 9)

Gillardin PS, Descamps G, Maiga S, Tessoulin B, Djamai H, Lucani B, **Chiron D**, Moreau P, Le Gouill S, Amiot M, Pellat-Deceunynck C, Moreau-Aubry A.
Decitabine and melphalan fail to reactivate p73 in p53 deficient myeloma cells. **International journal of molecular sciences**. 2018;19(1):40. (IF : 4)

Lok A, Descamps G, Tessoulin B, **Chiron D**, Eveillard M, Godon C, Le Bris Y, Vabret A, Bellanger C, Maillet L, Barillé-Nion S, Gregoire M, Fonteneau JF, Le Gouill S, Moreau P, Tangy F, Amiot M, Moreau-Aubry A, Pellat-Deceunynck C.
p53 regulates CD46 expression and measles virus infection in myeloma cells. **Blood advances**. 2018;2(23):3492-3505. (IF : 4.5)

2017

Tessoulin B, Eveillard M, Lok A, **Chiron D**, Moreau P, Amiot M, Moreau-Aubry A, Le Gouill S, Pellat-Deceunynck C.
p53 dysregulation in B-cell malignancies: More than a single gene in the pathway to hell. **Blood reviews**. 2017;31(4):251-259. (IF : 7)

Karvonen H, **Chiron D**, Niininen W, Ek S, Jerkeman M, Moradi E, Nykter M, Heckman CA, Kallioniemi O, Murumägi A, Ungureanu D.
Crosstalk between ROR1 and BCR pathways defines novel treatment strategies in mantle cell lymphoma. **Blood advances**. 2017;1(24):2257-2268. (IF : 4.5)

Dousset C, Maïga S, Gomez-Bougie P, Le Coq J, Touzeau C, Moreau P, Le Gouill S, **Chiron D**, Pellat-Deceunynck C, Moreau-Aubry A, Amiot M.
BH3 profiling as a tool to identify acquired resistance to venetoclax in multiple myeloma. **British journal of haematology**. 2017;179(4):684-688. (IF : 5)

2016

Chiron D, Bellanger C, Papin A, Tessoulin B, Dousset C, Maiga S, Moreau A, Esbelin J, Trichet V, Chen-Kiang S, Moreau P, Touzeau C, Le Gouill S, Amiot M, Pellat-Deceunynck C.
Rational targeted therapies to overcome microenvironment-dependent expansion of mantle cell lymphoma. **Blood**, The Journal of the American Society of Hematology. 2016;128(24):2808-2818. (IF : 13)

Hanf M, **Chiron D**, de Visme S, Touzeau C, Maisonneuve H, Jardel H, Pellat-Deceunynck C, Amiot M, le Gouill S.
The REFRACT-LYMA cohort study: a French observational prospective cohort study of patients with mantle cell lymphoma. **BMC Cancer**. 2016;16(1):802. (IF : 3)

2015

Chiron D, Dousset C, Brosseau C, Touzeau C, Maïga S, Moreau P, Pellat-Deceunynck C, Le Gouill S, Amiot M.
Biological rational for sequential targeting of Bruton tyrosine kinase and Bcl-2 to overcome CD40-induced ABT-199 resistance in mantle cell lymphoma. **Oncotarget**. 2015;6(11):8750-8759. (IF : 5)

Maïga S, Brosseau C, Descamps G, Dousset C, Gomez-Bougie P, **Chiron D**, Ménoret E, Kervoelen C, Vié H, Cesbron A, Moreau-Aubry A, Amiot M, Pellat-Deceunynck C.
A simple flow cytometry-based barcode for routine authentication of multiple myeloma and mantle cell lymphoma cell lines. **Cytometry Part A.** 2015;87(4):285-288. (IF : 3)

2014

Chiron D, Di Liberto M, Martin P, Huang X, Sharman J, Blecua P, Mathew S, Vijay P, Eng K, Ali S, Johnson A, Chang B, Ely S, Elemento O, Mason CE, Leonard JP, Chen-Kiang S.
Cell-cycle reprogramming for PI3K inhibition overrides a relapse-specific C481S BTK mutation revealed by longitudinal functional genomics in mantle cell lymphoma. **Cancer discovery**. 2014;4(9):1022-1035. (IF : 19.5)

2013

Chiron D, Maïga S, Surget S, Descamps G, Gomez-Bougie P, Traore S, Robillard N, Moreau P, Le Gouill S, Bataille R, Amiot M, Pellat-Deceunynck C.
Autocrine insulin-like growth factor 1 and stem cell factor but not interleukin 6 support self-renewal of human myeloma cells. **Blood cancer journal**. 2013;3(6):e120-e120. (IF : 3)

Chiron D, Martin P, Di Liberto M, Huang X, Ely S, Lannutti BJ, Leonard JP, Mason CE, Chen-Kiang S.
Induction of prolonged early G1 arrest by CDK4/CDK6 inhibition reprograms lymphoma cells for durable PI3Kδ inhibition through PIK3IP1. **Cell cycle.** 2013;12(12):1892-1900. (IF : 5)

2012

Chiron D, Maïga S, Descamps G, Moreau P, Le Gouill S, Marionneau S, Ouiller T, Moreaux J, Klein B, Bataille R, Amiot M, Pellat-Deceunynck C.
Critical role of the NOTCH ligand JAG2 in self-renewal of myeloma cells. **Blood Cells, Molecules, and Diseases**. 2012;48(4):247-253. (IF : 2)

Surget S, **Chiron D**, Gomez-Bougie P, Descamps G, Ménoret E, Bataille R, Moreau P, Le Gouill S, Amiot M, Pellat-Deceunynck C.
Cell death via DR5, but not DR4, is regulated by p53 in myeloma cells. **Cancer research**. 2012;72(17):4562-4573. (IF : 9)

2011

Chiron D, Surget S, Maïga S, Bataille R, Moreau P, Le Gouill S, Amiot M, Pellat-Deceunynck C.
The peripheral CD138+ population but not the CD138-population contains myeloma clonogenic cells in plasma cell leukaemia patients**. British journal of haematology.** 2011;156(5):679-683. (IF : 5)

Geffroy-Luseau A, **Chiron D**, Descamps G, Jégo G, Amiot M, Pellat-Deceunynck C.
TLR9 ligand induces the generation of CD20+ plasmablasts and plasma cells from CD27+ memory B-cells. **Frontiers in immunology**. 2011;2:83. (IF : 6)

2010

Chiron D, Pellat-Deceunynck C, Amiot M, Bataille R, Jego G.
TLR3 ligand induces NF-κB activation and various fates of multiple myeloma cells depending on IFN-α production. **The Journal of Immunology**. 2009;182(7):4471-4478. (IF : 6)

Chiron D, Pellat-Deceunynck C, Maillasson M, Bataille R, Jego G.
Phosphorothioate-modified TLR9 ligands protect cancer cells against TRAIL-induced apoptosis. **The Journal of Immunology.** 2009;183(7):4371-4377. (IF : 6)

- publications de revues dans des journaux à comité de lecture

2020

Jullien M, Gomez-Bougie P, **Chiron D**, Touzeau C.
Restoring apoptosis with BH3 mimetics in mature B-cell malignancies. **Cells**. 2020;9(3):717. (IF : 4)

2018

Papin A, Le Gouill S, **Chiron D**.
Rationale for targeting tumor cells in their microenvironment for mantle cell lymphoma treatment. **Leukemia & lymphoma**. 2018;59(5):1064-1072 (IF : 3)

2012

Jego G, **Chiron D**, Berthenet K, Pellat-Deceunynck C.
Modulation of normal and malignant plasma cells function by toll-like receptors. **Front Biosci**. 2012;4:2289-2301. (IF : NC)

2010

Chiron D, Jego G, Pellat-Deuceunynck C.
Toll-like receptors: expression and involvement in multiple myeloma. **Leukemia research**. 2010;34(12):1545-1550. (IF : 3)

2008

Chiron D, Bekeredjian-Ding I, Pellat-Deceunynck C, Bataille R, Jego G.
Toll-like receptors: lessons to learn from normal and malignant human B cells. **Blood**, The Journal of the American Society of Hematology. 2008;112(6):2205-2213. (IF : 10)

- Editoriaux

2021

Chiron D.
Towards ecosystem integration for a better understanding of B-cell lymphomas aggressiveness. **British Journal of Haematology**. 2021. (IF : 5.5)

2019

Chiron D.
Three targets in 1 shot against ibrutinib resistance. **Blood**, The Journal of the American Society of Hematology. 2019;133(9):888-889. (IF : 17.5)

2.2 _ Cinq publications représentatives de l'activité actuelle

Papin A, Tessoulin B, Bellanger C, Moreau A, Le Bris Y, Maisonneuve H, Moreau P, Touzeau C, Amiot M, Pellat-Deceunynck C, Le Gouill S, **Chiron D**.
CSF1R and BTK inhibitions as novel strategies to disrupt the dialog between mantle cell lymphoma and macrophages. **Leukemia**. 2019;33(10):2442-2453. (IF : 9)

Tessoulin B, Papin A, Gomez-Bougie P, Bellanger C, Amiot M, Pellat-Deceunynck C, **Chiron D.**
BCL2-family dysregulation in B-cell malignancies: from gene expression regulation to a targeted therapy biomarker. **Frontiers in oncology**. 2019;8:645. (IF : 4)

Chiron D, Bellanger C, Papin A, Tessoulin B, Dousset C, Maiga S, Moreau A, Esbelin J, Trichet V, Chen-Kiang S, Moreau P, Touzeau C, Le Gouill S, Amiot M, Pellat-Deceunynck C.
Rational targeted therapies to overcome microenvironment-dependent expansion of mantle cell lymphoma. **Blood**, The Journal of the American Society of Hematology. 2016;128(24):2808-2818. (IF : 13)

Chiron D, Dousset C, Brosseau C, Touzeau C, Maïga S, Moreau P, Pellat-Deceunynck C, Le Gouill S, Amiot M.
Biological rational for sequential targeting of Bruton tyrosine kinase and Bcl-2 to overcome CD40-induced ABT-199 resistance in mantle cell lymphoma. **Oncotarget**. 2015;6(11):8750-8759. (IF : 5)

Chiron D, Di Liberto M, Martin P, Huang X, Sharman J, Blecua P, Mathew S, Vijay P, Eng K, Ali S, Johnson A, Chang B, Ely S, Elemento O, Mason CE, Leonard JP, Chen-Kiang S.
Cell-cycle reprogramming for PI3K inhibition overrides a relapse-specific C481S BTK mutation revealed by longitudinal functional genomics in mantle cell lymphoma. **Cancer discovery**. 2014;4(9):1022-1035. (IF : 19.5)

Ces cinq publications sont placées en annexe.

2.3 _ **Communications** *(Orateur souligné)*

- conférences invitées dans des congrès

1. **Chiron D**. Mantle cell lymphoma microenvironment. L'Héma-Day, Nantes November 20, 2018

2. Papin A, **Chiron D.** Rational for targeting tumor cells in their microenvironment for mantle cell lymphoma treatment. Annual meeting of Czech Hematology Society, Olomouc, May 28th 2018.

3. **Chiron D**. Mantle cell lymphoma microenvironment: Proliferation, Bcl-2 family imbalance and drug resistance. Annual meeting of Czech Hematology Society, Olomouc, May 28th, 2017.

4. **Chiron D**, Cell cycle, PI3K inhibition and C481S BTK mutations. European MCL Network Rotterdam 2014

5. **Chiron D**, Pellat-Deceunynck C, Le Gouill S and Amiot M. Le microenvironnement du lymphome du manteau : Inducteur de prolifération et de résistance aux thérapies. Symposium Tours 2014

- communications à des congrès, symposium

1. Papin A, Bellanger C, Tessoulin B, Amiot M, Le Gouill S, Pellat-Deceunynck C and **Chiron D.** The dialog between mantle cell lymphoma and monocytes/macrophages can be disrupted by BTK inhibition and monitored through CD163 modulation in vivo. Annual meeting of the European Hematology Association. Stockholm June 14-17, 2018. Abstract selected for **oral** presentation

2. **Chiron D**. Characterization and integration of mantle cell lymphoma microenvironments are determinant for the development of rational targeted therapies. ESH 2nd Scientific Workshop on the Tumour Environment in Haematological Malignancies and its Therapeutic Targeting. Berlin 7-9 April 2017. Abstract selected for **oral** presentation

3. **Chiron D**, Bellanger C, Papin A, Tessoulin B, Dousset C, Maiga S, Moreau A, Esbelin J, Trichet V, Chen-Kiang S, Moreau P, Touzeau C, Le Gouill S, Amiot M, Pellat-Deceunynck C. Microenvironment-dependent proliferation and mitochondrial priming loss in mantle cell lymphoma is overcome by anti-CD20. The American Society of Hematology, San Diego, 9-12 December 2016. Abstract selected for **oral** presentation

4. **Chiron D**, B-cell lymphoma microenvironment : Bcl-2 family unbalance and drug resistance. 10èmes Journées du Cancéropôle Grand Ouest. 16 et 17 juin 2016. Les Sables d'Olonnes, Abstract selected for **oral** presentation

5. **Chiron D**, Microenvironnement Tumoral : Mécanismes Moléculaires de la Régulation du Cycle Cellulaire et de la Famille Bcl-2 dans le Lymphome du Manteau. 9 èmes Journées du Cancéropôle Grand Ouest. 18 et 19 juin 2015. Nantes, Abstract selected for **oral** presentation

6. **Chiron D**, Martin P, Maurizio Di Liberto M, Huang X, Vijay P, Blueca P, Ely S, Elemento O, Mason C, Leonard JP, and Chen-Kiang S. Integrative Whole Transcriptome and Exome Sequencing Reveals Reprogramming of Mantle Cell Lymphoma in Prolonged Early G1 Arrest for Clinical Response to Selective Inhibition of CDK4 in Combination Therapy. Blood. ASH Annual Meeting, New Orleans 2013. Abstract selected for **oral** presentation

7. **Chiron D,** Martin P, Di Liberto M, Huang X, Ely SA, Lannutti BJ, Leonard JP, Mason CE and Chen-Kiang S. Induction of early G1-arrest by CDK4/CDK6 inhibition sensitizes mantle cell lymphoma cells to selective PI3Kd inhibition by GS-1101 through enhancing the duration of p-AKT inhibition. Blood. ASH Annual Meeting, Atlanta 2012. Abstract selected for **oral** presentation

8. **Chiron D**, Amiot M, Moreaux J, Klein B, Bataille R, Pellat-Deceunynck C. Myeloma cells self-renew depends on JAG2 expression and is mediated by IGF1 or SCF loop. Blood. ASH Annual Meeting, Orlando 2010. Abstract selected for **oral** presentation

9. Papin A, Bellanger C, Tessoulin B, Amiot M, Le Gouill S, Pellat-Deceunynck C, **Chiron D.** CSF1R and BTK Inhibitions as Novel Strategies to Disrupt the Dialogue between Mantle Cell Lymphoma and Macrophages. ESH 3rd Scientific Workshop on the Tumour Environment in Haematological Malignancies and its Therapeutic Targeting. London. February 24 - 26, 2019 Abstract selected for **poster** presentation

10. Papin A, Bellanger C, Tessoulin B, Amiot M, Le Gouill S, Pellat-Deceunynck C, **Chiron D.** CSF1R and BTK Inhibitions as Novel Strategies to Disrupt the Dialogue between Mantle Cell Lymphoma and Macrophages. 60th Annual Meeting of the American-Society-of-Hematology, San Diego 1-4 December 2018 Abstract selected for **poster** presentation

11. **Chiron D**, Papin A, Bellanger C, Amiot M, Le Gouill S and Pellat-Deceunynck C. Characterization and integration of mantle cell lymphoma microenvironments are determinant for the development of rational targeted therapies. International Conference on Malignant Lymphoma, June 17-20, 2017, Lugano. Abstract selected for **poster** presentation

12. **Chiron D**, Maïga S, Descamps G, Moreau P, Harousseau JL, Bataille R, Le Gouill S, Amiot M, Pellat-Deceunynck C. Myeloma self-renewal is mainly mediated by IGF1 and only supported by CD138+ cells. Blood. 13th International Myeloma Workshop, Paris 2011 Abstract selected for **poster** presentation

13. **Chiron D**, Amiot M, Moreaux J, Klein B, Bataille R, Pellat-Deceunynck C. Involvement of the notch pathway in the clonogenicity of human multiple myeloma cell lines. Cancer Research. AACR 101st Annual Meeting,Washington D.C 2010 Abstract selected for **poster** presentation

- séminaires, workshops

1. Cheminant M and **Chiron D**. Driving toward precision medicine for Mantle Cell Lymphoma. RedTalks #4, e-meeting Calym. Janvier 2021

2. Decombis S, Papin A, Bellanger C, Sortais C, Dousset C, Le Bris Y, Amiot M, Moreau-Aubry A, Le Gouill S, Pellat-Deceunynck C and **Chiron D** The pro-tumoral IL32/BAFF axis in MCL ecosystem is disrupted by Nik inhibition. GDR MicroNit. e-meeting. 23,24,25 Novembre 2020

3. Papin A, Tessoulin B, Bellanger C, Moreau A, Le Bris Y, Amiot M, Pellat-Deceunynck C, Le Gouill S and **Chiron D**. CSF1R and BTK Inhibitions as Novel Strategies to Disrupt the Dialogue between Mantle Cell Lymphoma and Macrophages. GDR MicroNit. Le Croisic. 3-5 Décembre 2019. Oral

4. Papin A, Le Gouill S, Pellat-Deceunynck C, **Chiron D**. The dialog between mantle cell lymphoma and monocytes/macrophages can be disrupted by BTK inhibition. GDR MicroNit. 31 Janv - 2 Fev _Marseille 2018 Oral

5. Papin A, Bellanger C, Tessoulin B, Amiot M, Le Gouill S, Pellat-Deceunynck C and **Chiron D**. Caractérisation de la niche tumorale du lymphome à cellules du manteau: interactions bidirectionnelles avec les monocytes/macrophages. GDR MicroNit. La Rochelle. 18-20 Janvier 2017 Oral

6. **Chiron D**, Bellanger C, Papin A, Tessoulin B, Dousset C, Le Gouill S, Amiot M, Pellat-Deceunynck C. Microenvironment-dependent regulation of Bcl2 family in B-cell lymphoma. GDR MicroNit. La Rochelle, 20 au 22 janvier 2016 Oral

7. Papin A, Bellanger C, Tessoulin B, Amiot M, Le Gouill S, Pellat-Deceunynck C and **Chiron D**. The dialog between mantle cell lymphoma and monocytes/macrophages can be disrupted by BTK inhibition and monitored through CD163 modulation in vivo. Calym Workshop, Lyon, 6-7 Novembre 2018 Poster

- logiciels

Rouel M, Chiron D. 2019 dge−seq_secondary−analysis_software. Logiciel d'analyse de données RNA−seq sur la plateforme R−shiny.

- Brevets

Inventor(s): Chen-kiang S, Di Liberto M, Chiron D.
Combination or composition useful for treating a B cell proliferative disorder e.g. non-Hodgkins lymphoma or mantle cell lymphoma in an individual, comprises an ibrutinib, a cyclin-dependent kinase-4 inhibitor, and an excipient. Patent Number: WO2015084892-A1. Patent Assignee: UNIV CORNELL; CHIRON D

3. Synthèse des Travaux de Recherche *(2011-2021)*

3.1 _ Interconnexion des voies du cycle cellulaire et du BCR dans le Lymphome à Cellules du Manteau _ *Weill Cornell Medical College, NYC _ Chen-Kiang Lab _ 2011-2013*

A la fin de ma thèse portant sur l'étude du rôle des Toll-like Receptors dans la survie et la croissance du Myélome Multiple ainsi que le rôle de la signalisation Notch / IGF-1 dans l'autorenouvellement des cellules CD138+, j'ai souhaité rejoindre le laboratoire du Pr. Chen-Kiang à l'Université Cornell de New York.

Ce laboratoire est spécialisé dans l'étude du rôle de la dérégulation du cycle cellulaire dans la résistance tumorale. Au cours de ce post-doctorat je me suis intéressé aux cyclines D, et particulièrement à la cycline D1, dans le modèle du lymphome à cellules du manteau (LCM). Le LCM est une tumeur de Lymphocytes B matures naïfs IgM+ CD5+ localisée initialement dans les organes lymphoïdes secondaires (ganglions, rate) où elle présente généralement un fort index de prolifération. L'une des caractéristiques primaires du LCM est la translocation t(11 ;14) qui juxtapose une copie de l'enhancer des chaines lourdes des immunoglobulines (IGH) et le locus CCND1, menant à l'expression aberrante de la Cycline-D1 et résultant en une activité constitutive de l'holoenzyme Cycline-D1/CDK4. Cette kinase qui phosphoryle et inactive la protéine Rb, gardien du point de contrôle en phase G1, soutient l'entrée des cellules en phase S. Elle n'est cependant pas suffisante pour induire une lymphomagenèse *in vivo* (*Bodrug et al., Embo j. 1994*), suggérant des interconnexions avec d'autres voies oncogéniques et/ou un rôle complémentaire du microenvironnement.

Dans le LCM, le récepteur B à l'antigène (BCR) transcrit à partir de l'allèle IgH non transloqué est fonctionnel. Une activation constante du BCR sans activation antigénique, dite ''activation tonique'', est impliquée dans l'expansion des lymphomes IgM+ (*Young and Staudt, Nat Rev Drug Discov, 2013*). Cependant, bien qu'exprimant fortement les kinases PI3K∂ et BTK, en aval du BCR, la majorité des lignées de LCM sont réfractaires à leur inhibiteur respectif et malgré une réponse initiale à ces mêmes inhibiteurs *in vivo*, les patients rechutent, souvent de façon agressive (*Cheah et al., Ann Oncol. 2015*).

J'ai démontré que l'inhibition sélective du complexe Cycline-D1/CDK4 prévient non seulement la prolifération des cellules tumorales (arrêt du cycle en phase G1) mais les sensibilise aussi à la mort induite par l'inhibition des kinases en aval du BCR (PI3K∂ ou BTK). Cette sensibilisation est médiée par PIK3IP1 qui induit une inhibition forte et durable d'AKT. PIK3IP1 est un régulateur négatif de l'activité PI3K et mes données suggéraient qu'il s'exprime préférentiellement en phase G1. Cette induction de *PIK3IP1* a été confirmée *in vivo* chez des patients traités en monothérapie par un inhibiteur du CDK4/6.

Mes travaux ont démontré que, en plus de déréguler le cycle cellulaire, la surexpression de la Cyclin-D1 neutralise *PIK3IP1* et soutient une activation continue du BCR qui induit les voies BTK/NFKB et PI3K∂/AKT. L'efficacité de l'inhibition des kinases PI3K∂ ou BTK pour neutraliser AKT n'étant que transitoire, notre stratégie d'inhibition durable par un blocage préalable du cycle cellulaire avait pour objectif de stabiliser la réponse moléculaire et de retarder *in fine* la rechute *in vivo*. Nos travaux ont participé au rationnel d'une combinaison thérapeutique reposant sur l'inhibiteur des CDK4/6 (palbociclib) et l'inhibiteur du BTK (ibrutinib). Cette stratégie a été évaluée en clinique dans le LCM à la rechute (Phase 1,

NCT#02159755, NYC) et les premiers résultats ont montré que la combinaison est sans toxicité particulière pour ces patients et que la nature et la durée des réponses cliniques sont supérieures à celles de l'Ibrutinib seul (*Martin et al., Blood 2019*).

Pour étudier la régulation du BCR *in vivo*, j'ai saisi l'opportunité d'un essai clinique de phase-1 évaluant un inhibiteur sélectif de BTK (Ibrutinib). Par RNA-seq et Exon-seq, j'ai ainsi mis en évidence, pour 2 patients, l'apparition d'une mutation spécifiquement associée à la résistance acquise à l'Ibrutinib, faisant suite à une réponse partielle durable (14 à 30 mois). En effet, bien qu'indétectable dans les biopsies avant traitement, la mutation BTK^{C481S}, qui abroge la liaison irréversible de l'Ibrutinib sur le BTK, représente 50 à 90% des allèles à la rechute. Cette mutation n'est pas présente chez des patients caractérisés par une courte réponse partielle (<3 mois) ou réfractaires à l'Ibrutinib (n=8), confirmant l'existence d'une résistance primaire comme cela a été observée dans les lignées. De façon remarquable, malgré la présence de la mutation BTK^{C481S}, l'inhibition du complexe Cyclin-D1/CDK4 reste efficace pour bloquer les voies BCR/AKT et induire la mort cellulaire en synergie avec l'inhibition de PI3K*∂*.

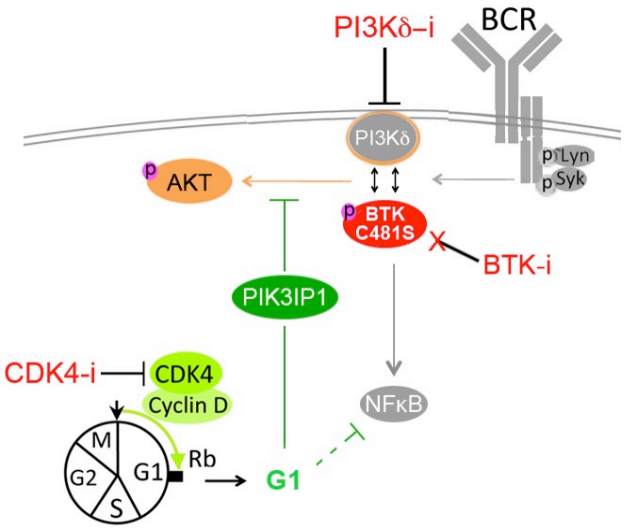

Représentation schématique de la régulation négative par PIK3IP1 de la signalisation du BCR. Les mécanismes moléculaires d'interconnexion des voies du cycle cellulaire et PI3K représente une stratégie alternative pour les patients présentant la mutation BTK^{C481S}.

Notre étude mettait pour la première fois en évidence les mécanismes moléculaires responsables de la résistance acquise à l'Ibrutinib dans le LCM et posait les bases pour le développement de combinaisons thérapeutiques contrecarrant cette résistance. Depuis ce projet, de nombreux travaux ont étudié les mécanismes de résistance aux inhibiteurs de la signalisation BCR et cette thématique reste un champ d'étude très actif dans les hémopathies B (*Ondrisova and Mraz, Front Onco 2020*).

D'autre part, la dérégulation du cycle cellulaire a été mise en évidence dans de nombreux cancers. Par l'inhibition sélective des CDK4/6, cette stratégie de sensibilisation aux voies d'addictions oncogéniques est donc applicable à de nombreuses pathologies. Ainsi, l'association d'un inhibiteur des CDK4/6 à un anti-estrogène permet le doublement de la survie sans progression de patientes atteintes de cancer du sein métastatique ER+ (Finn et al., Lancet Oncol, 2014, Garber et al., Science 2014). Sur ces bases les inhibiteurs sélectifs des CDK4/6 ont été approuvés dans le cancer du sein en 2016 et de nombreuses études

évaluent leurs rôles dans le contrôle du cycle cellulaire (*Rubin et al., Mol Cell, 2020*) mais aussi dans l'immunomodulation (*Petroni et al., Nat. Rev, 2020*)

Mes travaux effectués au cours de ce post-doctorat au Weill Cornell Medical College ont été publiés dans Cell Cycle *(Chiron et al., 2013)* et *Cancer Discovery (Chiron et al., 2014)* et ont fait l'objet d'un brevet (WO2015084892-A1) et de plusieurs présentations lors de congrès internationaux.

3.2 Etude du microenvironnement dans le Lymphome à Cellules du Manteau

_ CRCINA, Nantes _ Laboratoire C. Pellat/ M. Amiot _ 2014-2021

A mon retour de post-doctorat, j'ai continué mon activité de Recherche au CRCINA au sein de l'équipe « Regulation of Bcl2 and p53 networks in Multiple Myeloma and Mantle Cell Lymphoma » co-dirigée par Dr. Catherine Pellat-Deceunynck (DR1, CNRS) et Dr. Martine Amiot (DR1, CNRS). J'ai été recruté au CNRS en tant que CRCN en 2016 et je développe depuis mon projet qui a pour objectif de comprendre le rôle du microenvironnement tumoral dans l'expansion et la résistance aux traitements des lymphomes B agressifs.

A- Contexte scientifique du projet

Au cours des 30 dernières années, la Recherche en cancérologie s'est focalisée sur l'identification des anomalies intrinsèques à la cellule tumorale (marqueurs de (sous-groupe) de tumeurs, expression/régulation des voies oncogéniques, anomalies (épi)-génétiques, …) en omettant largement l'étude de la tumeur dans son microenvironnement. A présent, cette bonne connaissance des anomalies intrinsèques permet de replacer la tumeur dans son environnement et de repenser le cancer comme un écosystème tumoral. Les études démontrant que l'écosystème tumoral joue un rôle central dans l'expansion des tumeurs et la résistance au traitement n'ont cessé de s'accumuler depuis l'émergence du concept de microenvironnement tumoral (TME) il y a plus d'un siècle (*Maman et al., Nat. Rev. Cancer 2018*). En effet, l'écosystème tumoral a depuis montré de multiples facettes allant de son rôle essentiel dans le métabolisme du cancer à l'influence des contraintes mécaniques, sans oublier la diversité des infiltrats immunitaires.

Tout d'abord observé dans les tumeurs solides, le rôle central du TME a également été mis en évidence dans les hémopathies et notamment les lymphomes B (*Scott et al., Nat. Rev. Cancer 2014*). Plusieurs études fonctionnelles ont démontré que les lymphocytes B tumoraux influencent la formation d'un TME protecteur, qui en retour fournit des signaux protumoraux optimaux grâce à des interactions complexes de type cellulaire, soluble ou encore vésiculaire. Une meilleure compréhension du TME favorise désormais le développement de nouvelles stratégies thérapeutiques telles que des combinaisons rationnelles et ciblées pour contourner la résistance microenvironnement-induite, des inhibiteurs des points de contrôle immunitaires ou encore les anticorps bispécifiques.

Le lymphome à cellules du manteau (LCM) est une hémopathie B mature rare mais ayant pour caractéristique d'être à la fois agressive et incurable dans la majorité des cas. Ainsi de nouvelles stratégies s'avèrent nécessaires pour contrecarrer cette résistance résultant de rechutes itératives. Ces 2 dernières décennies, la plupart des études se sont concentrées sur les anomalies génomiques structurelles et fonctionnelles de cette pathologie, ce qui a conduit à caractériser l'origine moléculaire du LCM (t(11;14)), les facteurs impliqués dans son évolution clinique hétérogène (*SOX11*, *TP53*, *CDKN2A*) ainsi que des marqueurs de la résistance à différents traitements (*Nadeu et al. Blood 2020*).

Contrairement aux anomalies intrinsèques aux cellules tumorales, le dialogue entre le LCM et son TME était, jusqu'à récemment, largement ignoré. Néanmoins, ces dernières années plusieurs études, incluant celles résultant de mes travaux, ont mis en évidence un dialogue

dynamique au sein de la zone d'expansion primaire du LCM, les ganglions lymphatiques (LN pour « Lymph node »). Ainsi, nous avons démontré que les cellules de LCM sont capables de façonner leur microenvironnement, ce dernier étant nécessaire pour enclencher l'activation du cycle cellulaire ou encore des voies oncogéniques NFKB ou BCR (« B-cell Receptor »). Les conséquences fonctionnelles de ce dialogue incluent l'inhibition de l'apoptose et la résistance aux traitements. Ces résultats ont confirmé la nécessité d'intégrer le TME dans la biologie du LCM et encouragent à poursuivre les études dans la compréhension de la complexité des dialogues cellulaires et moléculaires au sein de l'écosystème tumoral.

B - Etude transcriptomique des modulations dépendantes du microenvironnement

Contrairement aux autres lymphomes B, le LCM se caractérise par une dissémination précoce, dès le diagnostic chez pratiquement tous les patients, résultant en une quantité importante de cellules tumorales circulantes (principalement dans la moelle osseuse et le sang périphérique (PB pour « Peripheral Blood »)). Cette caractéristique permet de comparer les cellules tumorales dans plusieurs tissus et d'identifier les régulations spécifiques des niches lymphoïdes.

B_1- Comparaison des profils tumoraux issus du sang et des ganglions

Afin de déchiffrer les régulations moléculaires qui se produisent dans le LCM au sein de ses écosystèmes, nous avons analysé l'expression différentielle des gènes dans des sections de ganglions tumoraux (LN, n=107) et des échantillons de sang périphérique (PB, n=77). Notre première observation concernant la prolifération différentielle (index de prolifération Ki67) des cellules tumorales dans les compartiments PB et LN a rapidement confirmé notre hypothèse d'un rôle majeur de l'écosystème ganglionnaire dans cette pathologie (Figure 1A). Nous avons observé que 38% des gènes analysés (n=5887/15396) étaient modulés dans les LN, ce qui suggère le rôle central de l'environnement dans la régulation transcriptionnelle du LCM (Figure 1B).

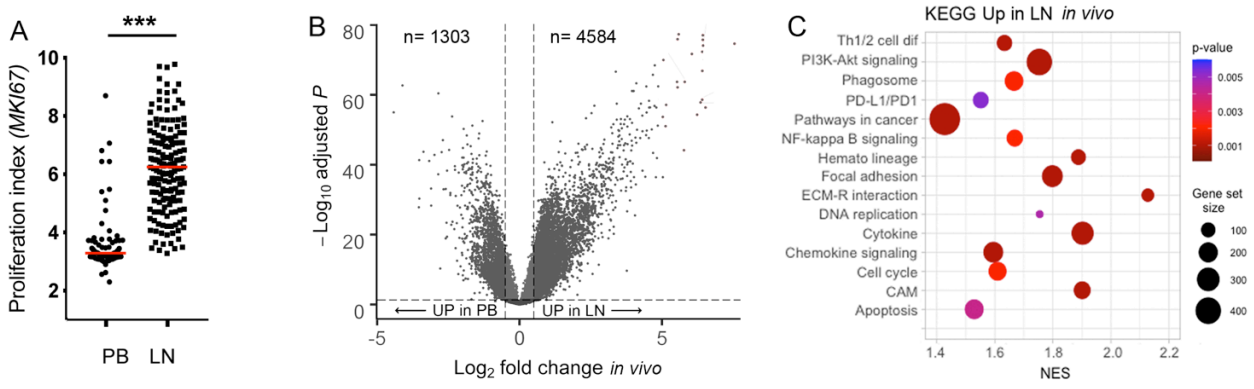

Figure 1. Profil transcriptomique des cellules de LCM issues du sang et des ganglions. ***A****) Proliferation différentielle des cellules tumorales en fonction de leur écosystème et mesurée à travers l'expression du gène MKI67 (codant pour l'antigène Ki-67).* ***B****) Représentation par Volcano-plot de l'analyse du transcriptome (Affimetrix U133, données publiques) à partir d'échantillons de ganglions tumoraux (LN, n=107) comparés à des échantillons de sang périphérique de LCM (PB, n=77), (padj<0,05, log2Fc>0,5).* ***C****) Analyse de l'enrichissement fonctionnel (KEGG) de l'ensemble des gènes régulés à la hausse dans les ganglions tumoraux in vivo tel que représenté dans la figure 1B (n=4584 gènes). L'axe des abscisses représente le score d'enrichissement normalisé (NES).*

Nos analyses d'annotations fonctionnelles (KEGG) reflètent une communication active au sein de l'écosystème entre les cellules tumorales et leur environnement. Nous observons ainsi des signatures d'infiltrats immunitaires (Th1/2, PD1/PDL1, Phagosome), de dialogues cellulaires et solubles (molécules d'adhésion cellulaire (CAM), matrice extracellulaire-récepteur (ECM-R), Cytokines, Chemokines), d'activation de voies de signalisation (NFkB, PI3K/AKT), de la prolifération (Réplication ADN, Cycle cellulaire) ou encore de régulation de l'apoptose (Figure 1C).

Nous avons au sein de notre équipe une forte expertise concernant l'étude la famille Bcl-2, que cela soit au niveau fondamental (Dr Martine Amiot) ou translationnel (Prof. Steven Le Gouill et Cyrille Touzeau). Ce contexte favorable m'a encouragé à étudier dans un premier temps les mécanismes impliqués dans la régulation de l'apoptose par le microenvironnement tumoral.

B_2- L'écosystème tumoral modifie profondément l'équilibre de la famille Bcl-2

L'apoptose est un processus physiologique et essentiel pour le développement et l'homéostasie des organismes multicellulaires mais sa dérégulation est une caractéristique fréquente dans le Cancer, augmentant la survie des cellules tumorales et leur résistance au traitement. Les protéines de la famille Bcl-2 (B-cell lymphoma 2) sont des régulateurs clés de l'apoptose mitochondriale et sont structurellement caractérisées par la présence d'un ou plusieurs domaines d'Homologie Bcl-2 (BH) (BH1-BH4). En termes de fonction, la famille Bcl-2 comprend des membres pro- et anti-apoptotiques. Les «BH3-only» dits activateurs (BID, PUMA et BIM) se lient directement et activent les protéines BAX/BAK, dont l'oligomérisation forment des macropores dans la membrane externe mitochondriale entraînant l'engagement de l'apoptose. Les protéines anti-apoptotiques à multi-domaines (BCL2, BCLXL, MCL1, BCLW, BFL1) inhibent l'apoptose en se liant et en séquestrant les protéines pro-apoptotiques par l'interaction avec leur domaine BH3. Enfin, les protéines pro-apoptotiques «BH3-only» dites sensibilisatrices (BAD, BIK, NOXA, HRK, BMF) ne peuvent pas activer directement BAX/BAK, mais contrecarrent l'action des protéines anti-apoptotiques en libérant les «BH3-only» activateurs et/ou les oligomères BAX/BAK par liaison compétitive (Figure 2A).

Afin de déterminer les régulations de la famille Bcl-2 dépendantes du TME, nous nous sommes tout d'abord basés sur des données transcriptomiques de LCM. Nous avons étudié leur régulation dans les échantillons de LCM issus de ganglions lymphatiques (LN, n=175) et de sangs périphériques (PB, n=81). Nous avons mis en évidence que tous les gènes étudiés, à l'exception de BFL1, étaient significativement différentiellement exprimés dans les ganglions et le sang (Figure 2B). Bien que ces échantillons ne soient pas appariés, ces données suggéraient que les cellules de LCM ont des profils Bcl-2 divergents en fonction de leur TME. Il est intéressant de noter qu'un déséquilibre global pro- et anti-apoptotique est observé dans les ganglions de LCM avec une augmentation générale de tous les membres anti-apoptotiques et une diminution de plusieurs membres pro-apoptotique (NOXA, BIM et BMF) (Figure 2B).

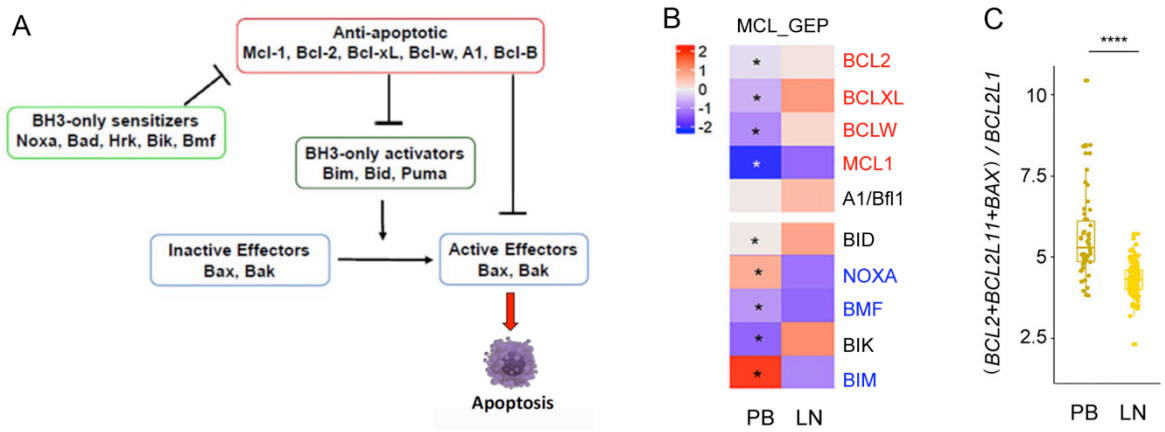

Figure 2. Régulation TME-dépendante de la famille Bcl-2. ***A****) Représentation graphique du réseau interconnecté des membres de la famille Bcl-2.* ***B****) "Heat-map" des profils d'expression des gènes Bcl-2 en fonction de leur localisation dans les tissus. Tests de Wilcoxon-Mann-Whitney. *p < 0.05.* ***C****) Évaluation du rapport (BCL2 + BIM + BAX)/BCLXL en fonction de la localisation tissulaire des cellules de LCM (sang périphérique, PB, ganglions lymphatiques, LN). ****p < 0,0001.*

Afin d'étendre nos résultats à d'autres histologies, nous avons intégré l'expression des gènes de la famille Bcl-2 de 10 sous-types d'hémopathies B matures par normalisation informatique de 21 ensembles de données (de type puce Affimetrix U133 et accessibles au public), rassemblant 1219 échantillons de patients. Pour mieux comprendre les modulations observées, nous avons comparé les profils d'expression des lymphocytes B tumoraux à leur équivalent normal (du lymphocyte B naïf au plasmocyte, n = 37). Les membres anti-apoptotiques de la famille Bcl-2 ont tendance à être surexprimés dans la plupart des tumeurs par rapport à leur équivalent normal, à l'exception notable de BCLXL. La protéine BCL2 est surexprimée comme décrit précédemment dans le LCM, le Lymphome diffus à grandes cellules (DLBCL), le Lymphome Folliculaire (FL) ou la Leucémie Lymphoïde Chronique (LLC). BFL1 est le gène le plus fréquemment surexprimé dans notre étude (dans 8 hémopathies sur 10). Concernant les gènes pro-apoptotiques «BH3-only», ils ont tendance à être sous-exprimés dans toutes les hémopathies B matures par rapport à leur équivalent normal, BIM étant le plus fréquemment significativement sous-exprimé (7 hémopathies sur 10).

Nous avons ensuite réévalué l'expression de la famille Bcl-2 en fonction de la localisation tissulaire (sang, moelle, ganglions), des sous-groupes moléculaires connus de chaque histologie ou du statut de la maladie. Il ressort de cette analyse que BIM et NOXA sont tous deux régulés à la baisse par le microenvironnement tumoral dans toutes hémopathies B étudiées (MCL, FL, LLC et SMZL), suggérant un rôle fondamental du contrôle de ces protéines « BH3-only» dans la survie dépendante du TME. Des stratégies rationnelles visant à contrecarrer leur régulation pourraient alors s'avérer essentielles pour cibler les cellules de lymphome dans leur écosystème protecteur.

Les membres de la famille Bcl-2 sont impliqués dans la résistance au cancer principalement en raison du déséquilibre entre les protéines pro- et anti-apoptotiques favorisant la survie. Cependant, les protéines anti-apoptotiques sont aussi devenues des cibles thérapeutiques avec le développement de petites molécules appelées « BH3-mimetics ». Ces dernières miment les protéines pro-apoptotiques «BH3-only» dites

sensibilisatrices et induisent ainsi l'apoptose à travers une perturbation sélective des interactions pro- et anti-apoptotiques. L'addiction à une ou plusieurs protéines anti-apoptotiques est variable selon la nature de la tumeur et nous avions montré que le BH3-mimetics Venetoclax, qui cible spécifiquement la protéine BCL2, était particulièrement efficace *ex vivo* dans les cellules de LCM circulantes (*Chiron et al. Oncotarget 2015*). Cependant même si les études cliniques ont mis en évidence une réponse globale encourageante chez les patients atteints de LCM traités par le Venetoclax en monothérapie, la durée de survie sans progression observée est apparue beaucoup plus courte que dans d'autres pathologies BCL2-dependante telle que la LLC (« modèle » de dépendance à BCL2).

En intégrant des données récentes sur l'activité clinique du Venetoclax en monothérapie avec l'expression transcriptomique des membres de la famille Bcl-2, nous avons déterminé qu'une signature basée sur le ratio (BCL2+BIM+BAX)/BCLXL était le plus fort prédicteur de la réponse au Venetoclax pour les hémopathies B matures *in vivo*. Cette signature est hétérogène entre les hémopathies mais aussi en fonction des tissus analysés. Ainsi notre étude suggère que les cellules de LCM issues des ganglions pourraient être plus résistantes au Venetoclax que les cellules du sang périphérique, et par conséquent pourraient être impliquées dans les rechutes systématiques (Figure 2C).

Notre étude montre donc un déséquilibre global de la famille Bcl-2 dépendent du TME et tendant vers la survie, dans les niches du LCM mais aussi d'autres hémopathies B. Ces résultats nous ont amenés à faire l'hypothèse d'un rôle majeur de ce déséquilibre dans la résistance aux traitements et au constat de la nécessité de développer *ex vivo* des modèles fonctionnels intégrant ces modulations TME-dépendantes.

Ces travaux sur la régulation transcriptomique de la famille Bcl-2 dans les hémopathies B ont été possible grâce à une collaboration entre Benoit Tessoulin (médecin hémato en thèse de Sciences sous la supervision de C. Pellat) et Antonin Papin (thèse de Sciences sous ma supervision). Ces travaux ont donné lieu à une publication, pour laquelle je suis dernier auteur, dans Frontiers in Oncology en 2018 (Tessoulin et al.) et à la participation dans une revue publiée dans Cells en 2020 (Jullien et al.).

C - Développement de modèles *ex vivo* pour l'étude fonctionnelle de l'impact du microenvironnement immunitaire

Afin de déterminer les mécanismes de régulations TME-dépendants de la famille Bcl-2 ainsi que leurs conséquences sur l'expansion tumorale et la résistance aux traitements, j'ai fait le pari de développer des systèmes de coculture *ex vivo* permettant de mimer les régulations présentes dans les ganglions de LCM. Ces systèmes originaux avaient aussi pour objectif de palier la difficulté d'accès aux cellules vivantes issues des tissus ganglionnaires et indispensables pour des études fonctionnelles.

C_1- Etablir une cohorte de cellules de LCM et déterminer quelles sont les interactions tumeur/TME pertinentes à évaluer.

A partir de 2016, nous avons participé à la mise en place d'une cohorte clinico-biologique de LCM portée par le Prof. Steven Le Gouill (chef de service d'hématologie, CHU de Nantes). Malgré la faible incidence de notre modèle cellulaire (2-3/100,000 par an), cette cohorte assure la collecte d'un grand nombre d'échantillons sanguins et médullaires de LCM stockés en DMSO dans notre laboratoire (Refract-Lyma; 2016-2020*, n> 300*) (*Hanf et al., BMC 2016*). Les échantillons sont annotés au niveau clinique (diagnostic, rechute, sous-type morphologique, indolent, ...) et biologique (envahissement, phénotype, statut p53, ...) et les données sont renseignées dans une base de donnée accessible à tous les acteurs de ce circuit (échantillons anonymisés côté EPST). Nous avons aussi accès à de nombreux échantillons de ganglions de LCM référencés et stockés sous forme FFPE par le service d'anatomopathologie du CHU de Nantes (Pr. Céline Bossard PU-PH ; n>100). De façon complémentaire, l'utilisation de lignées cellulaires, indépendantes du microenvironnement pour leur survie, supporte la découverte des mécanismes moléculaires (voie de signalisation, régulations,…) impliqués dans la biologie du LCM. Cette collection (EBV- n=12, EBV+ n=3) est caractérisée aux niveaux phénotypique, mutationnel, transcriptionel et fonctionnel (réponse aux drogues).

Les cellules circulantes de LCM entrent rapidement en apoptose spontanée *ex vivo* (>50% mortalité en 24h), ne prolifèrent pas contrairement aux cellules dans les ganglions, et ceci quelle que soit la nature des anomalies génomiques (translocation, mutations, CNV, …), suggérant un rôle essentiel du TME (Figure 1A). La nature de ce dernier étant inconnu dans le LCM, nous avons dans un premier temps utilisé un algorithme de déconvolution pour les données transcriptomiques des tumeurs (*Chen et al., Cancer systems biology 2018*). Cette caractérisation "basse résolution" du TME des ganglions de LCM met en évidence de fréquentes infiltrations lymphoïdes et myéloïdes, plaidant en faveur d'un dialogue potentiel entre le LCM et son TME immunitaire *in vivo* (Figure 3).

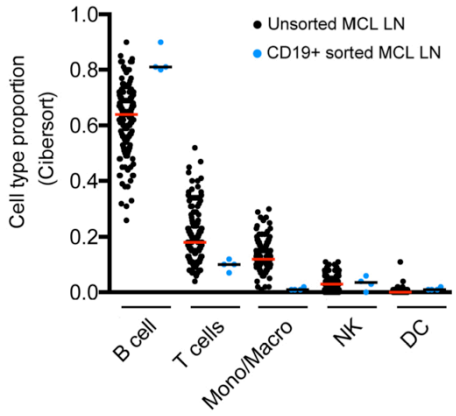

Figure 3. *Analyse de déconvolution de données de transcriptomic issus des ganglions (LN) de LCM à travers l'utilisation de l'algorithme Cibersort.*
Quatre échantillons de cellules de LCM triés par le CD19+ à partir de ganglions tumoraux servent de contrôles internes à l'analyse de déconvolution (points bleus).

C_2 - Etudes des interactions de type lymphoïde-T à travers l'axe CD40/CD40L

J'ai dans un premier temps modélisé les potentielles interactions lymphoïdes de type T_{FH} à travers l'axe CD40/CD40L, en les comparant avec des cocultures de cellules souches mésenchymateuses (MSC) pour lesquelles un rôle protumoral avait été suggéré (*Medina et al, Haematologica 2012*). Alors que les cellules primaires de LCM ne survivent pas isolées *ex vivo*, ces 2 cocultures maintiennent leur viabilité sur le long terme, mais seul le CD40L entraine une entrée en phase S (BrdU+, Figure 4A). La signalisation CD40 induit aussi la progression dans le cycle cellulaire des lymphocytes B normaux mais des facteurs de croissance sont essentiels pour maintenir cette prolifération. En me basant sur l'expression des récepteurs par la tumeur *in situ,* déterminée par RNA-seq de biopsies de ganglions de LCM (collaboration Dr. Chen-Kiang, Cornell University), j'ai développé un cocktail de cytokines propre au LCM (Ck : IL6/IGF1/BAFF/IL10) qui s'est avéré efficace pour maintenir et potentialiser la prolifération (Figure 4B).

J'ai ainsi mis au point un modèle de coculture baptisé ''CD40L+Ck'' permettant l'étude de la pathologie *ex vivo* par la réactivation durable (> 21 jours) du cycle cellulaire de cellules primaires circulantes, de façon similaire aux cellules tumorales présentes *in situ* dans les ganglions (Figure 4C).

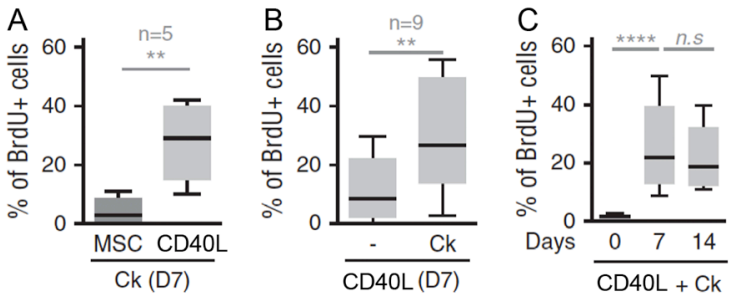

Figure 4. L'axe CD40/CD40L, mais pas les MSC, soutiennent la prolifération des cellules primaires de LCM ex vivo. A) *Marquage BrdU/IP de cellules de LCM (n = 5) en présence de MSC humaines ou en coculture avec des cellules CD40L+ associées à des cytokines (Ck) pendant 7 jours comme indiqué. (B) Marquage BrdU/IP de cellules LCM (n = 9) en coculture avec des cellules CD40L+ avec ou sans cytokines pendant 7 jours comme indiqué. (C) Analyse du cycle cellulaire (% de cellules BrdU+) des cellules de LCM pendant la durée et dans les conditions indiquées (n = 9). **P , .01,****P , .0001.*

En plus d'induire la prolifération, la coculture « CD40L+Ck » entraîne également une modulation de l'expression de membres anti et pro-apoptotique de la famille Bcl-2. Ainsi notre étude met notamment en évidence une forte induction de MCL1 et BCLXL et une baisse de BIM. Cette dernière, à l'inverse des régulations de MCL1 et BCLXL, est par ailleurs régie par des mécanismes spécifiques à la tumeur car elle n'est pas retrouvée dans les lymphocytes B normaux (NBC, Figure 5A).

J'ai pu démontré par la suite que la forte induction de BCLXL est la conséquence directe de l'activation des voies NFkB (classique et alterne) par la coculture «CD40L+Ck». Nous avons donc démontré que cette dernière reproduit plusieurs modulations précédemment observées *in situ* au cours nos études transcriptomiques (Figure 1C, cycle cellulaire, voie NFkB, modulation de la famille Bcl-2). Ainsi, notre modèle de coculture «CD40L+Ck» reproduit bien dans les cellules primaires circulantes un programme moléculaire similaire à celui observé dans les ganglions.

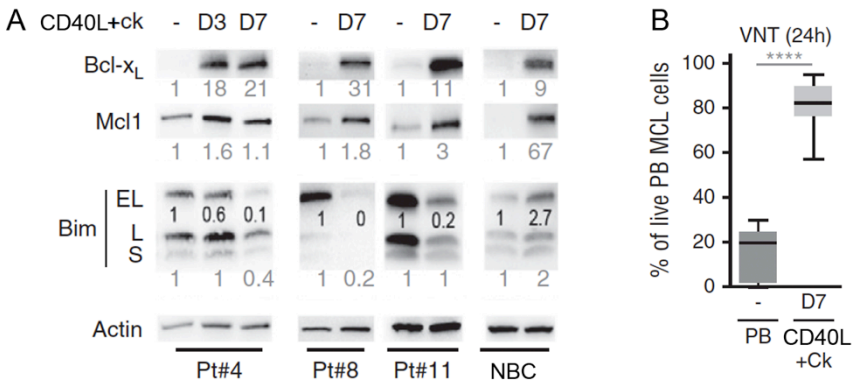

Figure 5. Les stimulations extrinsèques entraînent une modulation déséquilibrée de la famille Bcl-2 dans le LCM. *A) Immunoblot de la famille Bcl-2 dans les cellules de LCM en coculture 'CD40L+Ck' pour le temps indiqué. NBC : Normal B cells. B) Des cellules de LCM fraîchement isolées du sang périphérique (PB) ou après 7 jours en coculture 'CD40L+Ck' ont été traitées avec du Venetoclax (VNT, 25 nM) pendant 24 heures. La viabilité a ensuite été analysée par marquage Annexin-V,. **** p< .0001*

Pour évaluer les conséquences fonctionnelles de cette modulation de la famille Bcl-2 au niveau cellulaire, j'ai évalué la sensibilité des cellules primaires de LCM fraîchement isolées du sang (PB) et après 7 jours de coculture sur «CD40L+Ck ». J'ai observé que, contrairement au cellules circulantes, les cellules en coculture deviennent fortement résistantes à plusieurs agents chimiothérapeutiques (agents alkylants, intercalants) mais aussi au «BH3 mimetics» spécifique de BCL2, le Venetoclax (Figure 5B). Ces résultats fonctionnels confortent notre hypothèse que les cellules de LCM nichées dans les ganglions pourraient être plus résistantes aux traitements et seraient alors impliquées dans les rechutes systématiques caractéristiques de cette pathologie.

Afin de déterminer les mécanismes moléculaires responsables de cette résistance TME-dépendante, nous avons étudié la dynamique des complexes de la famille Bcl-2 directement au niveau mitochondrial par la technique du «BH3-profiling». A l'échelle mitochondriale, les protéines anti-apoptotique, BCL2, BCLXL et MCL1, assurent la viabilité cellulaire en séquestrant les protéines pro-apoptotiques dites «BH3-only» (Certo et al., Cancer Cell 2006, Touzeau et al., Leukemia 2015). En effet, la libération des BH3-only provoque le relargage de cytochrome C, la dépolarisation mitochondriale et *in fine* l'apoptose (Figure 2A). Le BH3-profiling est un test fonctionnel qui mesure la dépolarisation mitochondriale après addition de peptides ou de BH3-mimetics sélectifs de BCL2, BCLXL ou MCL1, et reflète ainsi le potentiel apoptotique, aussi appelé «priming» mitochondrial.

Dans les cellules circulantes, mes données montrent que la dépolarisation est exclusivement dépendante de la dissociation des «BH3-only» de leurs complexes avec BCL2. Cet état est défini comme «priming BCL2». Cependant, j'observe une perte totale du priming dans les cellules en coculture qui sont caractérisées par l'induction de BCLXL. Cette absence de priming reflète parfaitement la résistance observée au niveau cellulaire et m'a permis de poser les bases du concept de modulation du priming par le microenvironnement du lymphome. Nous avons finalement démontré que la perte du priming mitochondrial était exclusivement du à une séquestration dynamique du «BH3-only» activateur BIM par BCLXL, faisant de ce dernier un acteur central de la résistance TME-dépendent dans le LCM (Figure 6).

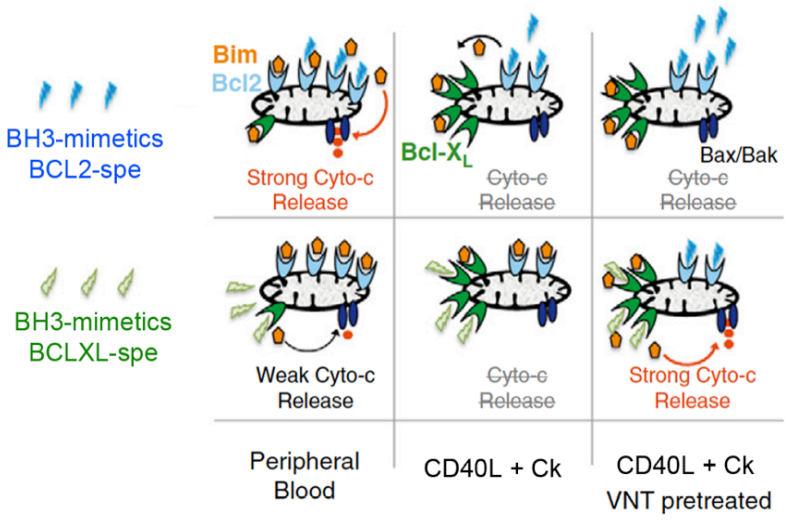

Figure 6. *Représentation schématique des mécanismes impliqués dans la perte de priming mitochondriale dépendante de l'induction de Bcl-xL par le microenvironnement.*

L'ensemble de nos résultats nous a logiquement amené à rechercher des stratégies thérapeutiques ciblant BCLXL dans le LCM afin de lever la résistance TME-dépendante, et plus particulièrement la résistance au Venetoclax. En effet une inhibition de BCL2 et BCLXL semblait nécessaire pour cibler à la fois les cellules circulantes de LCM et celles localisées dans les niches ganglionnaires (Figure 6). Les molécules ciblant BCLXL et BCL2 telles que le Navitoclax sont disponibles mais leur utilisation clinique a été grandement limitée par l'induction de toxicité *in vivo* (thrombocytopénie). Des approches novatrices contrecarrant l'induction TME-dépendante de BCLXL directement dans les cellules tumorales étaient alors nécessaires.

Nous avons tout d'abord observé que l'utilisation d'inhibiteurs de la kinase BTK pourrait être une stratégie efficace pour contrecarrer cette résistance TME-dépendante. En effet, l'inhibition sélective du BTK par l'Ibrutinib inhibe les signaux émanant de l'activation du BCR (*Chiron et al., Cancer Discovery 2014*) mais interfère aussi avec le homing des cellules de LCM dans les ganglions et la moelle osseuse (*Chang BY et al., Blood 2013*) . La lymphocytose qui en résulte est due à l'inhibition d'axes chimiokiniques BTK-dépendant, principalement l'axe CXCR4/SDF1 dans le LCM. En conséquence, *in vivo*, l'Ibrutinib provoque une lymphocytose. Nous avons démontré que ces cellules tumorales, en dehors du TME, ont une faible expression de BCLXL et sont particulièrement sensibles au Venetoclax (Figure 7).

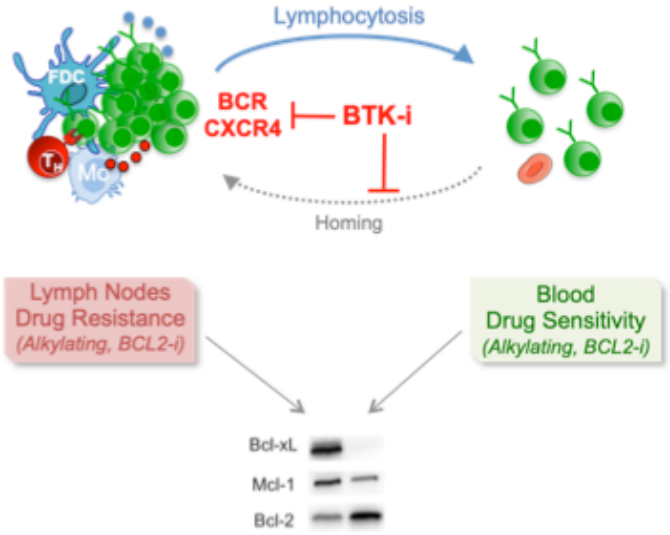

Figure 7. Représentation schématique du rationnel de la combinaison séquentielle entre les inhibiteurs du BTK et les agents cytotoxiques tel que les BH3-mimetics. *L'ibrutinib induit une lymphocytose in vivo, éloignant les cellules malignes de leur microenvironnement protecteur. Nos résultats apportent la preuve que la résistance in situ au venetoclax peut être contrecarrée lorsque les cellules de LCM s'échappent des ganglions lymphatiques.*

Nous avons ensuite démontré que la surexpression TME-dépendante de BCLXL pouvait aussi être contrecarrée par l'Obinutuzumab, un anticorps monoclonal anti-CD20 de nouvelle génération (de type II, décrit pour avoir un effet direct sur la cellule tumorale plus important que les anti-CD20 de type I comme le Rituximab, Illidge T et al, Cancer Treat Rev. 2015). L'Obinutuzumab inhibe efficacement l'expression de BCLXL dans les cellules primaires de LCM *ex vivo*, l'inhibition étant plus profonde dans les cellules exprimant des niveaux élevés de CD20 membranaire. Nous avons également démontré que l'inhibition de BCLXL par l'Obinutuzumab était la conséquence de l'inhibition des voies classique et alterne de NFKB. De façon cohérente, cette baisse du BCLXL sensibilise les cellules primaires de LCM au Venetoclax.

Le transfert à la clinique de notre approche fondamentale intégrant le microenvironnement a participé au rationnel de l'essai clinique international de phase 1 OAsIs (*Prof. S. Le Gouill NCT#02558816*). Ce dernier a été conçu pour évaluer la faisabilité d'un traitement séquentiel avec l'Ibrutinib (inhibiteur du BTK) et l'Obinutuzumab (anti-CD20), suivi du Venetoclax chez des patients atteints de LCM au diagnostic ou à la rechute. Les résultats de cet essai sans « chimiothérapie » ont été récemment publiés et montrent que la combinaison a été bien tolérée et a permis un contrôle de la maladie, y compris des réponses complètes au niveau moléculaire chez des patients au diagnostique ou à la rechute avec des profils génétiques à haut risque (ex : *TP53* muté) (Figure 8).

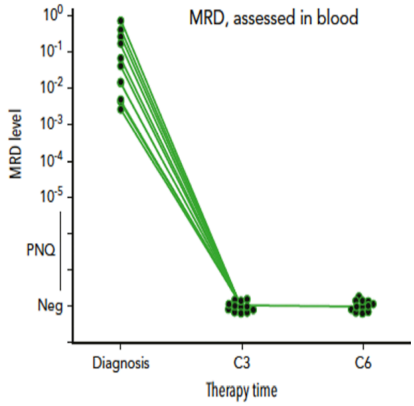

Figure 8. Evolution de la maladie résiduelle chez les patients au diagnostique inclus dans l'essai OAsIs. *Changements absolus du niveau de la maladie résiduelle (MRD) dans le sang périphérique par ASO-qPCR, chez 12 patients en première ligne. Les points de traitement C3 (fin du cycle 3) et C6 (fin du cycle 6) de l'Ibrutinib, de l'Obinutuzumab et du Venetoclax sont indiqués. Les niveaux de MRD détectables, mais non quantifiables, sont indiqués comme positifs non quantifiables (PNQ).*

Ces travaux sur le développement de modèles *ex vivo* pour l'étude fonctionnelle de l'impact du microenvironnement immunitaire ont donné lieu à plusieurs publications dans Oncotarget en 2015 (Chiron et al. Biological rational for sequential targeting of Bruton tyrosine kinase and Bcl-2 to overcome CD40-induced ABT-199 resistance in mantle cell lymphoma), dans Blood en 2016 (Chiron et al. Rational targeted therapies to overcome microenvironment-dependent expansion of mantle cell lymphoma) et en 2021 (Le Gouill et al. Ibrutinib, Obinutuzumab And Venetoclax In Relapsed and Untreated Patients with Mantle-Cell Lymphoma, a phase I/II trial.).

C_3 - Etudes du dialogue entre les cellules tumorales et leur microenvironnement myéloïde

En plus d'un infiltrat lymphoïde-T, nos données préliminaires suggéraient la présence d'un infiltrat myéloïde conséquent dans les ganglions de LCM (Figure 3). Le rôle protumoral des macrophages associés à la tumeur (TAM) est largement démontré que ce soit dans les tumeurs solides ou hématologiques. Des études antérieures ont suggéré la présence de macrophages dans les ganglions de LCM, mais leur phénotype et le dialogue moléculaire qui résulte des interactions entre les cellules du LCM et les TAM étaient inconnus. Nous avons donc décidé d'étudier le rôle des macrophages dans l'écosystème du LCM et ce projet a été le sujet principal de la thèse d'Antonin Papin (2016-2019).

Après avoir confirmé la présence de macrophages dans les ganglions de LCM par IHC (CD68+), nous avons mis en place des modèles de co-culture entre cellules primaires tumorales et monocytes issus de donneurs sains. L'utilisation de ces modèles *ex vivo* nous a permis de montrer dans un premier temps que les monocytes supportent la survie et la prolifération tumorale, au moins en partie à travers un dialogue soluble (Figure 9).

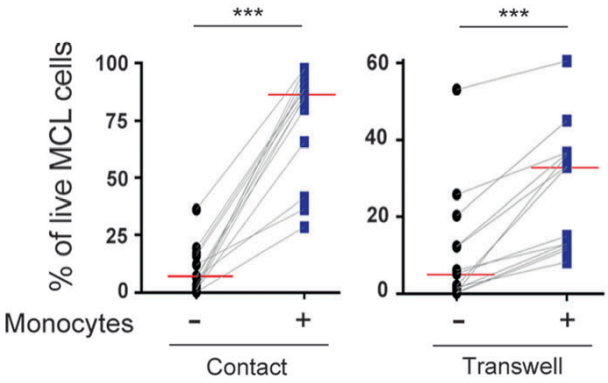

Figure 9. Les monocytes soutiennent la survie des cellules de LCM. *Le pourcentage de cellules tumorales vivantes a été évalué par marquage Annexin-V après 7 jours de culture seule(-) ou avec des monocytes, soit en contact (n = 17, panel de gauche), soit séparés par des inserts transwell (n = 13, panel de droite).*
****p < .001.*
Les lignes rouges représentent les médianes.

Alors que les macrophages favorisent la survie tumorale, nous avons observé que la tumeur elle-même peut corrompre le microenvironnement myéloïde. En effet, au cours des cocultures, les monocytes se différentient en «macrophages associés au LCM» (MϕLCM). Afin de définir la nature de ces MϕLCM, nous avons comparé leur transcriptome à celui de macrophages de type M1 (pro-inflammatoire, différentié par CSF2/IFNγ) et M2 (anti-inflammatoire, différentié par CSF1/IL10), tous deux représentant les extrémités du spectre de différentiation des macrophages *ex vivo*. Ces analyses démontrent que, même si ils se rapprochent des macrophages de type M2, les MϕLCM forment un groupe spécifique, notamment caractérisé par une expression intermédiaire du marqueur de TAM CD163, par la sécrétion de facteurs immuno-régulateurs tels que l'IL10 mais également de facteurs pro-inflammatoires tels que l'IL6 (Figure 10A).

Afin de déterminer les mécanismes impliqués dans la différenciation des monocytes en MϕLCM CD163+ protumoraux, nous avons analysé l'expression par les cellules tumorales de facteurs solubles décrits pour être impliqués dans la polarisation macrophagique. Nous avons ainsi observé une surexpression des gènes *CSF1* et *IL10*, 2 facteurs connus pour leur propriété M2 polarisatrices, en comparaison aux lymphocytes B normaux (NBC) (Figure 10B). De façon importante, la neutralisation de l'axe CSF1/CSF1R (par un inhibiteur spécifique du CSF1R, le GW2580), mais pas de l'IL-10, est suffisante pour bloquer la polarisation des MϕLCM et contrecarrer leur propriété protumorale *ex vivo* (Figure 10C).

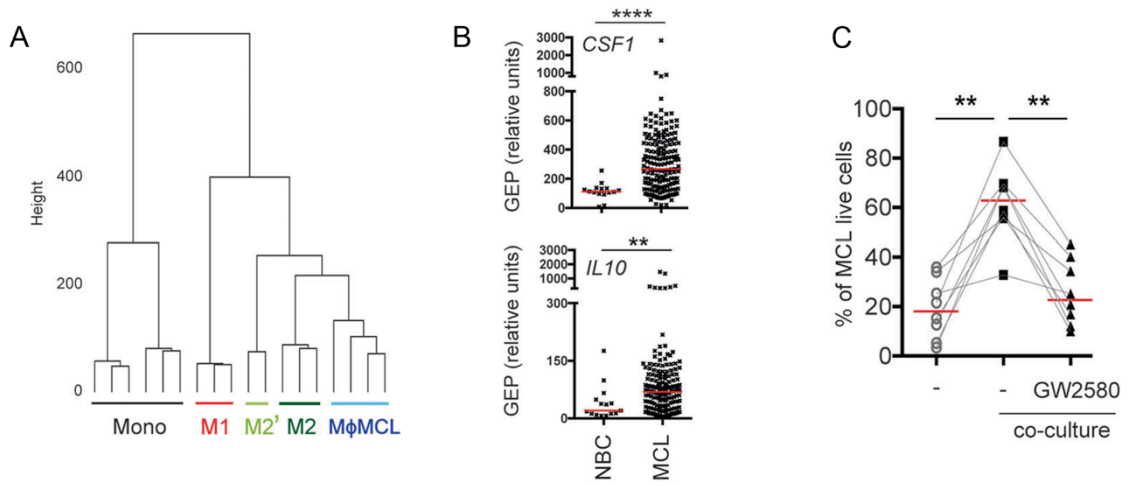

Figure 10. La tumeur rééduque les monocytes en macrophages protumoraux spécifiques à travers la sécrétion de CSF1/IL10. A) *Les cellules tumorales polarisent les monocytes en MϕMCL spécifiques avec des caractéristiques semblables à celles de M2. Un regroupement hiérarchique ascendant a été construit avec la méthode 'Ward.D2' de la distance euclidienne. Les macrophages M2 ont été générés à partir de monocytes humains cultivés avec CSF1/IL-10, M2' avec du CSF1 seul (GSE20484), et M1 avec LPS/IFNg (GSE95405).* ***B)*** *Les cellules de LCM expriment les facteurs de polarisation M2 CSF1 et IL-10. L'expression de CSF1 et IL-10 dans les cellules tumorales (n = 183) a été comparée aux lymphocytes B normaux (NBC, n = 15) selon les bases de données publiques de GEP. ****p < 0,0001 ; **p < 0,01.* ***C)*** *Pourcentage de cellules vivantes de LCM en coculture avec des monocytes en présence d'inhibiteur du CSF1R (GW2580, 1 μM ; n = 8). La mort cellulaire a été évaluée par marquage Annexin-V. **p < .01. Les lignes rouges représentent les médianes.*

Nous avons ensuite étudié l'origine de la surexpression du CSF1 et de l'IL10 dans le contexte tumoral et nous avons démontré que ces deux facteurs solubles sont sous le contrôle du BCR constitutivement activé dans le LCM. Ainsi, l'inhibition du BCR par la neutralisation de la kinase BTK par l'Ibrutinib, abroge la sécrétion du CSF1 et de l'IL10 dans les cellules sensibles à l'Ibrutinib (Mino) mais pas dans les cellules résistantes (Granta) (Figure 11A). Comme attendu, l'inhibitions du CSF1 et de l'IL10 (polarisateurs M2) résultent en une réduction conséquente de la polarisation des monocytes en MϕLCM, observée à travers la baisse du CD163 membranaire (Figure 11B). Comme observé précédemment avec l'inhibiteur du CSF1R (Figure 10C), l'inhibition de la sécrétion du CSF1 tumoral par l'Ibrutinib est suffisante pour bloquer la polarisation des MϕLCM mais aussi pour contrecarrer leur propriété protumorale *ex vivo* (Figure 11C).

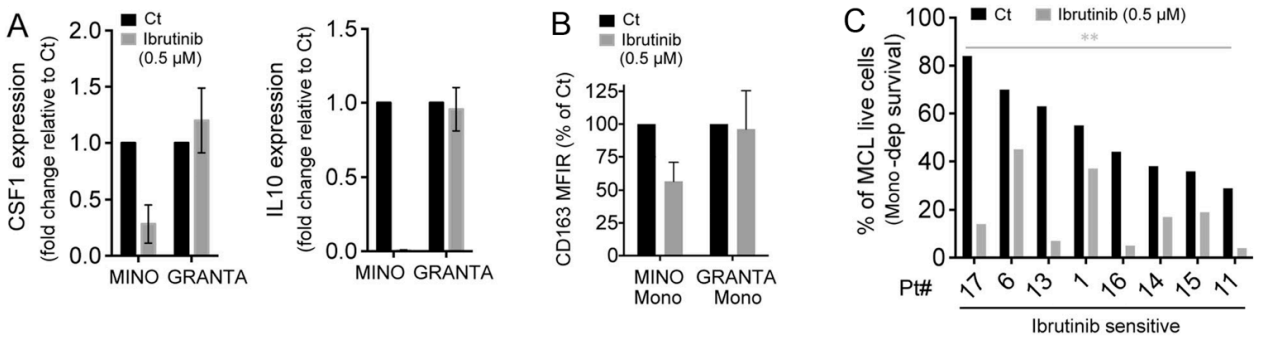

Figure 11. L'Ibrutinib contrecarre le dialogue LCM/MϕLCM par l'inhibition du CSF1. ***A****) Analyse par RT-qPCR des cellules Mino sensibles à l'Ibrutinib et des cellules Granta résistantes à l'ibrutinib avec ou sans traitement à l'Ibrutinib (72 h ; 0,5 µM). L'expression des gènes a été normalisée par rapport à la condition de contrôle non traitée de chaque lignée cellulaire.* ***B)*** *Modulation du CD163 (ratio de MFI) sur des cellules CD14+ en coculture avec MINO et GRANTA +/- Ibrutinib.* ***C)*** *Pourcentage de cellules primaires de LCM vivantes en coculture avec des monocytes +/- Ibrutinib (72 h ; 0,5 µM ; n = 8) (marquage Annexin-V). **p <0,01*

De façon importante, nous avons pu confirmer ces régulations *in vivo* chez des patients de LCM. Nous retrouvons des concentrations élevées de CSF1 et d'IL-10 dans le plasma de patients, au diagnostic comme à la rechute, en comparaison avec des donneurs sains. Nous montrons également que le marqueur de TAM CD163 est surexprimé à la surface des monocytes circulants des patients, ce qui est cohérent avec les propriétés d'induction du CD163 par le CSF1 et l'IL-10. Grâce au suivi longitudinal de huit patients traités par l'Ibrutinib, nous avons évalué les modulations d'IL-10 et de CSF1 dans le plasma ainsi que l'expression du CD163 sur les monocytes avant et après traitement. Nous observons une réduction des concentrations plasmatiques d'IL-10 et de CSF1 ainsi qu'une diminution de l'expression du CD163 sur les monocytes circulants pour 6/8 patients après 8 jours de traitement. L'étude rétrospective de ces modulations montre que les modulations de l'IL-10, du CSF1 et du CD163 peuvent être des marqueurs précoces de réponse à l'Ibrutinib. Une plus large cohorte de patients est maintenant nécessaire pour confirmer ces observations préliminaires.

L'Ibrutinib en monothérapie a fait preuve d'une efficacité clinique sans précédent dans le LCM. Néanmoins, plusieurs mécanismes de résistance tels que l'acquisition de mutations (ex : *BTK*, *PLCG2, SMARCA4*), de délétion (ex : *CDKN2A*, *SMARCA2*) ou encore l'activation de voies compensatrices (ex : NFκB alterne) ont été décrits et des études rétrospectives ont révélé une faible survie des patients de LCM réfractaire à l'Ibrutinib. Nous avons montré que le ciblage du CSF1R pourrait être une alternative pour perturber le dialogue protumoral entre les cellules de LCM et les MϕMCL, en particulier pour les patients réfractaires à l'Ibrutinib pour lesquels peu d'alternatives thérapeutiques sont disponibles. En effet, l'inhibition du CSF1R par le GW2580 réduit efficacement la viabilité des cellules de LCM lors de co-culture avec les MϕLCM, indépendamment de la réponse à l'Ibrutinib. De plus, la combinaison de l'Ibrutinib et du GW2580 à des concentrations faibles induit un effet supra-additif pour les cellules de LCM sensibles à l'Ibrutinib lors des co-cultures. Ceci suggère que cette stratégie pourrait également être bénéfique pour les patients sensibles à l'Ibrutinib.

En conclusion, en modélisant le dialogue entre les cellules de LCM et leurs niches immunitaires protectrices, nous avons découvert une nouvelle combinaison rationnelle qui pourrait contrecarrer la résistance. Nos données renforcent le rôle central du microenvironnement dans le LCM et montrent que les monocytes/macrophages sont une cible potentielle pour le développement de nouvelles stratégies thérapeutiques (Figure 12).

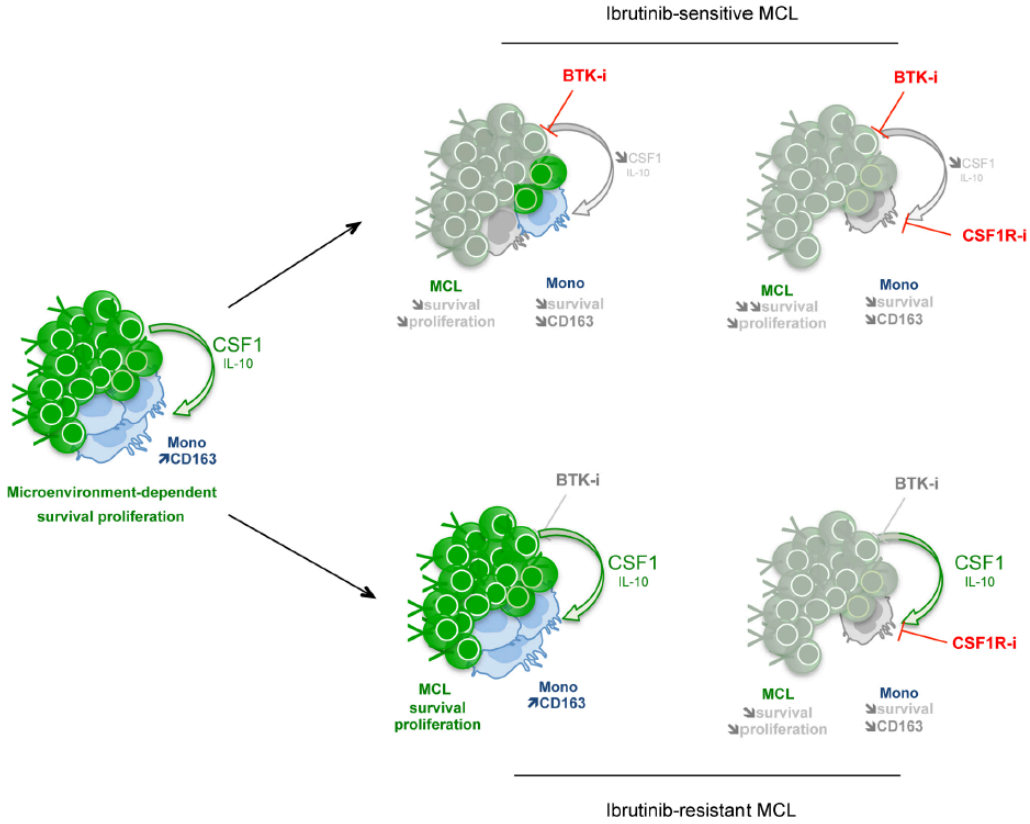

Figure 12. *Les cellules de LCM sécrètent du CSF1 et de l'IL-10 qui polarisent les monocytes en macrophages CD163+. Chez les patients sensibles, l'Ibrutinib inhibe les productions de CSF1 et d'IL-10 et, en conséquence, la polarisation des monocytes et la survie MϕLCM -dépendante des cellules tumorales. Chez les patients résistants, l'Ibrutinib est inefficace mais le traitement avec un inhibiteur du CSF1R (GW2580) altère le dialogue entre les MϕLCM et les cellules tumorales et contrecarre la résistance TME-dépendante.*

Ces travaux sur le dialogue entre les cellules tumorales et leur microenvironnement myéloïde ont donné lieu à une publication dans Leukemia en 2019 (Papin et al.). L'efficacité de l'inhibition de l'axe CSF1/CSF1R vient d'être démontrée dans le Lymphome Folliculaire (*Valero et al., Leukemia 2021*), mettant en évidence que nos travaux dans le modèle du LCM s'appliquent à d'autres hémopathies B mâture.

Notre étude a permis de caractériser le dialogue entre le LCM et les macrophages associés. Cependant plusieurs questions restent en suspens. Même si l'analyse du transcriptome a montré que les macrophages associés aux LCM (MϕLCM) présentent plus de similitudes avec les macrophages M2, ces derniers sont caractérisés par un profil sécrétoire spécifique et intermédiaire aux M1/M2. Ceci reflète la plasticité phénotypique et fonctionnelle de la polarisation des TAM et suggère que des facteurs complémentaires à IL10 et au CSF1 sont impliqués dans la polarisation tumorale des MϕLCM. D'autre part, ces MϕLCM supportent la survie et la prolifération des cellules tumorales par l'intermédiaire d'un dialogue soluble dont la nature n'avait pas été adressée dans cette étude.

D - Etude des dialogues solubles dans l'écosystème tumoral du LCM

D_1 - Identification d'une expression de l'IL32 dépendante du TME et spécifique à la tumeur par analyse transcriptomique non supervisée.

Afin de poursuivre la caractérisation du dialogue moléculaire présent dans les niches tumorales du LCM, j'ai repris l'étude des modulations transcriptomiques mis à jour précédemment (Figure 13A). Les sections de ganglions tumoraux utilisées dans ces analyses transcriptomiques présentent des infiltrations hétérogènes de cellules tumorales et immunitaires, ce qui suggère que les gènes identifiés pourraient provenir à la fois de cellules tumorales et non tumorales. Afin de nous concentrer sur les modulations spécifiques aux cellules tumorales *in situ*, nous avons comparé ces données transcriptomiques issues de ganglions tumoraux avec les modulations observées dans les cellules purifiées (triées par l'antigène CD19+) et cocultivées dans notre modèle *ex vivo* «CD40L+Ck» précédemment décrit (Partie C_2).

Les résultats de cette analyse transcriptomique ont tout d'abord confirmé la pertinence du modèle «CD40L+Ck», plus de 70 % des gènes régulés à la hausse *ex vivo* dans la co-culture étant également induits dans les ganglions *in vivo* (n=3217/4524) (Figure 13B, panel de gauche). Ensuite, la comparaison des gènes TME-dépendant (à la fois *ex* et *in vivo*, n=3217) avec des lymphocytes B normaux (NBC) en co-culture, a révélé que 39% des modulations observées étaient spécifiques à la tumeur (Figure 13, panel de droite). Les annotations fonctionnelles montrent que le dialogue soluble est spécifiquement enrichi dans l'écosystème tumoral, contrairement, par exemple, à l'activation du cycle cellulaire héritée des NBC. Le classement des gènes induits par le TME et spécifique de la tumeur a mis en évidence l'interleukine-32 (IL32) (Figure 13C). Les mécanismes de régulation et les rôles biologiques potentiels de la cytokine IL32 étant inconnus, nous avons décidé d'évaluer son rôle dans le LCM. Ce sujet a été confié à Salomé Decombis qui a commencé sa thèse de Sciences fin 2019 sous ma supervision et celle de Catherine Pellat.

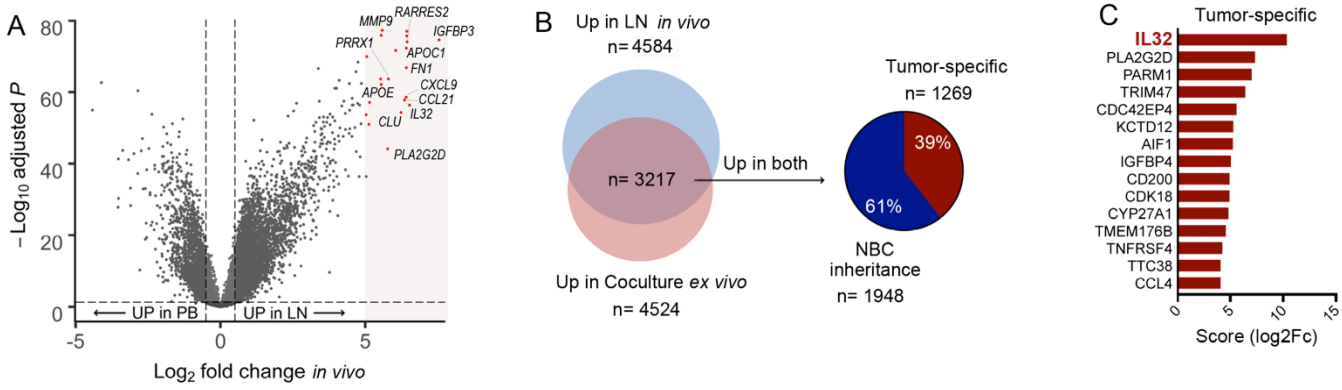

Figure 13. Expression de l'IL32 spécifique de la tumeur et dépendante du microenvironnement A) *Représentation par Volcano-plot de l'analyse du transcriptome (Affimetrix U133, données publiques) comme présenté Figure 1B. Les gènes les plus fortement modulés sont annotés sur le graphique (log2Fc>5).*
B) *Panel gauche : Comparaison de l'ensemble des gènes induits dans les cellules de LCM CD19+ co-cultivées ex vivo (RNA-seq) avec l'ensemble des gènes induits dans les ganglions tumoraux in vivo, en comparaison au cellules de LCM circulantes. Panel de droite : Les gènes communs in vivo et ex vivo uprégulés (n=3217 gènes) ont été comparés aux gènes induits dans des lymphocytes B CD5+ normaux (NBC) co-cultivées de manière similaire afin de déterminer les ensembles de gènes "d'héritage NBC" et "spécifiques à la tumeur".* ***C)*** *Les 15 principaux gènes ''spécifiques à la tumeur" ont été définis. Le score (log2Fc) intègre à la fois les modulations ex vivo et in vivo.*

D_2 - L' IL32β secrétée par la tumeur conduit à une rééducation spécifique des monocytes en macrophages protumoraux CD163+ (Mϕ-32)

L'IL32 est une cytokine nouvellement caractérisée et dont les isoformes ont des rôles biologiques différentiels. L'IL32β est le plus fréquemment décrit dans le Cancer comme nous avons pu le constater dans le LCM. Il est à noter que le récepteur de l'IL-32 est inconnu et que l'absence d'expression de cette interleukine chez les rongeurs limite considérablement nos connaissances sur ses rôles physiologiques. Néanmoins, l'expression de l'IL-32 a été documentée dans plusieurs cancers solides et semble être impliquée dans de nombreux processus biologiques (ex : migration, métastase, prolifération, apoptose) (*Sloot et al., Seminar in immunology 2018*).

Nous avons tout d'abord mis en évidence que la production d'IL32β par le LCM était sous le contrôle de la voie alterne de NFkB, elle même induite par l'activation du CD40. L'activation du CD40 induit cette voie de façon similaire dans les cellules de LCM et les lymphocytes B normaux. La sécrétion tumeur-spécifique de l'IL32 nous a conduit à rechercher une potentielle régulation épigénétique. Par la technique du «séquençage bisulfite», nous avons démontré que les cellules IL32+ (tumeur) et IL32- (B normaux) présentaient un schéma de méthylation significativement différent dans les régions du promoteur et des îlots CpG, suggérant que l'hypométhylation favorise l'expression de l'IL32 dans le contexte tumoral.

Nous avons ensuite démontré que l'IL32β n'a pas d'impact direct sur la survie tumorale mais que cette cytokine participe à la formation d'un écosystème myéloïde spécifique à la tumeur. Un tel rôle paracrin de l'IL32 a été récemment décrit dans le Myélome Multiple, renforçant l'hypothèse d'un rôle important de ce facteur soluble dans l'écosystème des hémopathies B mature (*Zahoor et al., Blood advances 2017*). L'IL32 a été initialement caractérisée pour ses propriétés pro-inflammatoires. Néanmoins, des études plus récentes ont mis en évidence que l'IL32 est exprimée de préférence par les lymphocytes T régulateur (*Zavidij et al., Nature Cancer 2020*) et qu'elle est impliquée dans certaines réponses immunorégulatrices, notamment par l'induction de l'IL10 ou de l'IDO par les macrophages. Dans notre étude, nous avons confirmé, par une analyse transcriptomique non supervisée des gènes induits dans les monocytes/macrophages par l'IL32β, la capacité de cette dernière à induire à la fois la production de facteurs solubles pro- et anti-inflammatoires (Figure 14).

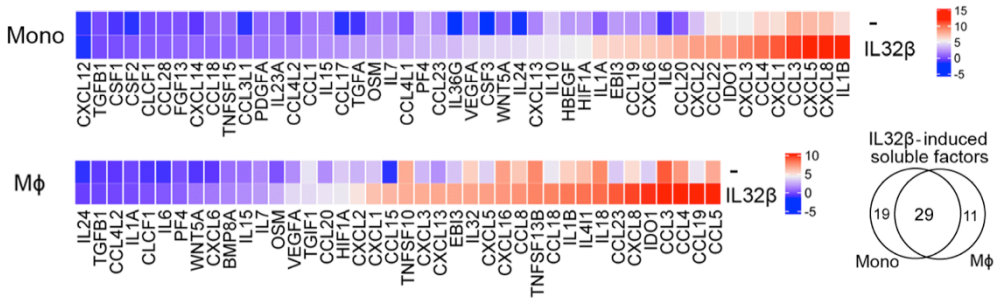

Figure 14. L'IL32β sécrété par les cellules de LCM induit une rééducation spécifique des monocytes en macrophages protumoraux Mϕ-32. *''Heat-map'' des transcrits de facteurs solubles modulés dans les monocytes (Mono, n=3) et les macrophages (Mφ, n=3) stimulés par de l'IL32β recombinant humain. Les couleurs indiquent l'intensité de l'expression génique médiane (échelle logarithmique). Parmi les gènes des facteurs solubles modulés par l'IL32β, 29 sont communs aux Mono et Mφ (RNA-seq, log2Fc>0,1).*

Il convient de noter que ces résultats obtenus par l'utilisation d'IL32β recombinant humain ont été confirmés avec le surnageant tumoral provenant de cellules de LCM isogéniques exprimant ou non l'IL32 (générées par la technologie CRISPR/CAS9).

Nous avions précédemment démontré que les MϕLCM exprimaient des facteurs solubles de type pro- (M1) et anti-inflammatoires (M2), suggérant que des facteurs autres que les facteurs classiques de polarisation M2 (tels que l'IL-10 et le CSF-1 sécrétés par le LCM) pourraient être impliqués dans la corruption de l'écosystème (Partie C_3). Dans la présente étude, nous avons constaté que l'IL32β sécrétée par la tumeur est très probablement impliquée dans ce processus, la plupart des facteurs caractérisant les MϕLCM étant induits par cette cytokine. D'autre part, les macrophages différenciés par l'IL32β (Mϕ32) partagent les caractéristiques phénotypiques et fonctionnelles des MϕMCL telles que l'expression de CD163^{mid} ou le soutien de la survie tumorale par le biais du dialogue soluble (Figure 15).

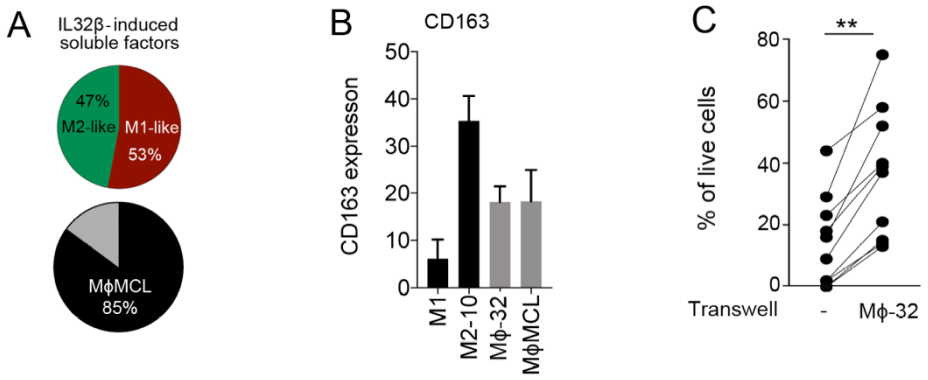

Figure 15. ***L'IL32β sécrétée par les cellules de LCM participe aux caractéristiques phénotypiques et fonctionnelles des MϕMCL.*** **A)** Les facteurs solubles induits par l'IL32β sur Mono/Macro (Figure 14) ont été classés comme M1-like, M2-like (panneau supérieur) ou MϕMCL-like (panneau inférieur). **B)** Le rapport d'intensité moyenne de fluorescence CD163 a été déterminé par cytométrie en flux pour les macrophages de type M1 (M1, n=3), de type M2 (M2, n=4), les macrophages dérivés de monocytes polarisés avec le CSF1 pendant 5 jours puis stimulés avec l'IL32β pendant 48h (Mϕ-32, n=3) et les macrophages associés au LCM (MϕMCL, n=3). **C)** Le pourcentage de cellules vivantes de LCM a été évalué par marquage Annexin-V après 3 jours de coculture seule (-) ou avec Mϕ32 et séparées par des inserts transwell (n=10). **p < .002.

D_3- BAFF est au centre du dialogue protumoral des Mϕ-32 à travers l'activation de la voie alterne de NFkB

Parmi les facteurs solubles induits par IL32β, plusieurs d'entre eux avaient été précédemment décrits comme étant impliqués dans l'expansion du LCM, tels que l'IL6, l'IL10, BAFF ou WNT5A (Figure 14). Néanmoins, nous avons constaté que seul BAFF soutient seul la survie à long terme des cellules primaires de LCM (7 jours), à un niveau similaire à celui observé avec le surnageant Mϕ-32 (Figure 16). Si BAFF est un facteur de survie bien décrit pour les lymphocytes B (normaux et malins), seules quelques publications ont abordé l'impact fonctionnel de BAFF dans le LCM. Nous avons observé que la plupart des échantillons de LCM expriment le récepteur BAFF (BAFF-R), son activation conduisant à l'induction sélective de la voie alterne de NFkB.

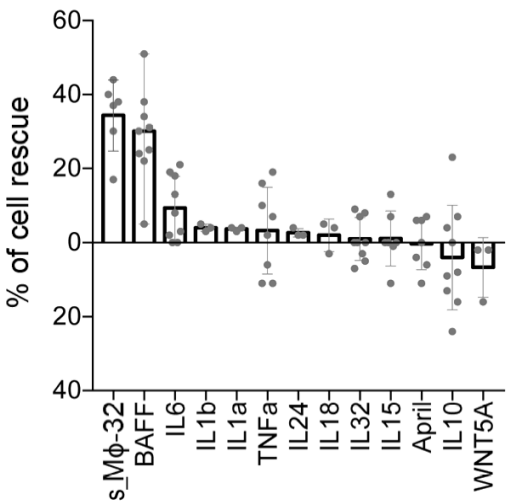

Figure 16. BAFF est au centre du dialogue protumoral des Mϕ-32. *Les cellules de LCM ont été cultivées avec le surnageant Mϕ-32 (s_Mϕ-32, n=6) ou des facteurs de croissance : BAFF, IL6, IL10, IL32b, TNFa, IL15, April, IL1b, IL1a, IL24, IL18 ou Wnt5a (n>3). Le « % of cell rescue » reflète l'augmentation de la survie (marquage Annexin-V) induit par le facteur indiqué après 7 jours de culture ex vivo.*

D_4 - Rôle central de la voie alterne de NFKB dans le LCM ?

En plus de la signalisation pro-survie dépendante de BAFF, la voie alterne de NFkB semble jouer un rôle plus large dans le LCM. En effet, plusieurs acteurs clés de cette voie tels que *MAP3K14* (codant pour NIK) ou *TRAF2* sont parmi les gènes les plus fréquemment mutés à la rechute et des anomalies de *BIRC3* ou *TRAF3* ont également été décrites (*Hill, Blood advances 2020*). Toutes ces mutations conduisent à une activation constitutive de la voie alterne de NFkB. En plus des anomalies intrinsèques, cette voie est également actionnable par le TME. Saba et al (*Blood, 2016*) ont mis en évidence qu'une "signature NIK", reflétant l'activité de cette voie, était enrichie dans les ganglions de LCM par rapport au sang périphérique. Conformément à ces résultats, nous observons de façon similaire une forte activation dans notre modèle de coculture «CD40L+Ck», conçu pour mimer l'écosystème ganglionnaire.

Le rôle central des voies NFkB dans la différenciation B normale ainsi que dans les hémopathies B est bien documenté (*Kennedy et al., Cells 2018*). Le rôle essentiel de la voie classique a été récemment confirmée *in vivo* par l'efficacité considérable de l'inhibition de l'axe BCR/NFkB, grâce à l'émergence des inhibiteurs du BTK (ex : Ibrutinib). Alors que les conséquences fonctionnelles et les cibles sélectives de l'activation de la voie alterne de NFkB sont encore largement inconnues, des études récentes ont suggéré un rôle de cette voie dans la résistance aux traitements. Ainsi, Rahal et al. (*Nat. Med., 2014*) ont montré que des mutations induisant son activité constitutive était impliquée dans la résistance à l'Ibrutinib. Une étude récente a démontré que la voie alternative contrôle aussi l'expression de BCLXL dans la LLC (Haselager et al., CDD 2021). Cette étude est en accord avec nos travaux démontrant que BCLXL est fortement induit dans les cellules primaires stimulées par le CD40L, entraînant une perte du priming mitochondrial et une résistance conséquente au Venetoclax (Partie C_2). D'autre part, nous montrons à présent que, en plus de son impact direct sur la cellule tumorale, l'activation de la voie NFkB alterne influence également l'écosystème du LCM à travers une induction TME-dépendante de l'IL32. Cette induction spécifique de la tumeur résulte en une reprogrammation des macrophages environnants.

L'inhibition spécifique de la voie alterne de NFkB était difficilement réalisable avant le développement très récent d'inhibiteurs sélectifs de NIK (*Brightbill et al, Nat Commun 2018 ; Mondragon et al., Cancer Cell 2019*). NIK est une kinase spécifiquement impliquée dans la voie alterne à travers l'activation d'IKKa, qui à son tour induit le clivage de p100 en p52, ceci sans affecter la voie classique de NFKB.

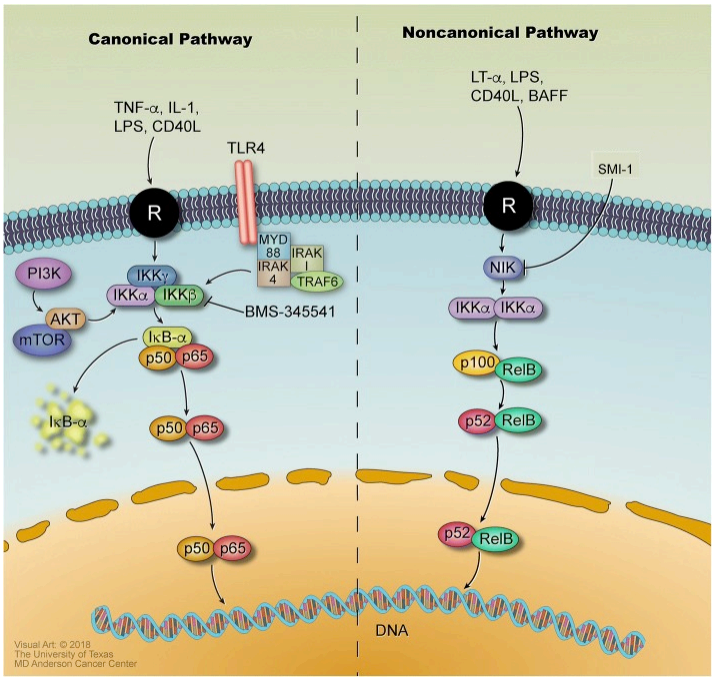

Représentation schématique des voies classiques (canonical) et alterne (noncanonical) NFkB.
R : recepteurs
Adaptée de Balaji et al, JHO 2018

Nous avons confirmé l'efficacité de l'inhibition de NIK pour contrecarrer l'induction de l'IL32 dépendante du TME (Figure 17A) mais aussi la survie dépendante de BAFF dans les cellules primaires de LCM (Figure 17BC). D'autre part nous avons observé que l'inhibition de NIK était efficace dans les cellules de LCM quelle que soit leur sensibilité aux inhibiteurs du BTK, ce qui suggère que l'inhibition de NIK pourrait présenter un intérêt particulier pour les patients résistants à l'Ibrutinib.

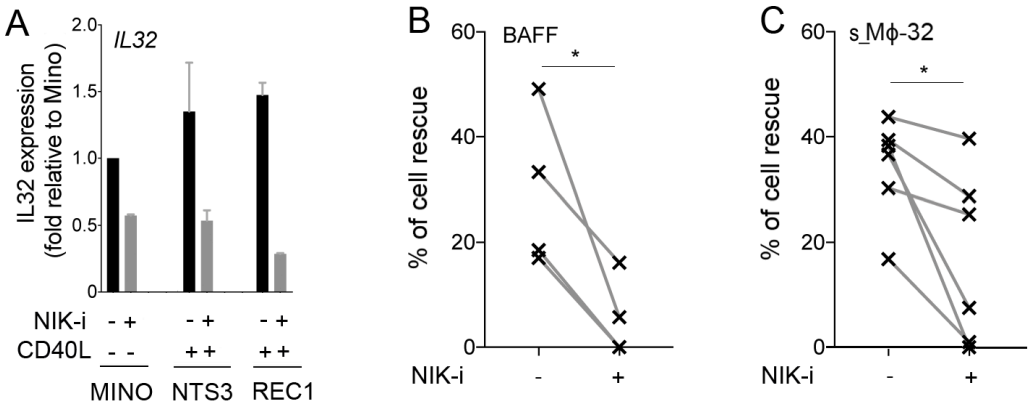

Figure 17. La voie alterne de NFkB control l'axe IL32/BAFF dans l'écosystème tumoral du LCM. A) *RT-qPCR dans des lignées cellulaires de LCM co-cultivées sur des cellules exprimant CD40L pendant 96h en présence ou en absence de l'inhibiteur de NIK (NIK-i, 10 µmol)).* ***B)*** *Pourcentage de survie dépendant du BAFF dans les cellules de LCM (n=4) cultivée avec ou sans inhibiteur NIK (NIK-i, 10 µmol) pendant 7 jours. *p < 0.05.* ***C)*** *Pourcentage de survie dépendant du surnageant Mϕ-32 (s_Mϕ-32) dans les cellules de LCM (n=6) cultivée avec ou sans inhibiteur NIK (NIK-i, 10 µmol) pendant 7 jours. *p < 0.05.*

En conclusion, sur la base d'une analyse transcriptomique globale, nous avons identifié un nouvel axe IL32/BAFF dans le dialogue protumoral du LCM au sein de son écosystème ganglionnaire. Bien que des outils cliniques ciblant l'IL32 doivent encore être développés, nos données mettent en évidence le rôle central de la voie alterne de NFkB dans sa régulation (Figure 18). Des études supplémentaires sont à présent nécessaires pour déterminer l'implication de cette voie dans d'autres régulations TME-dépendante issues des nombreux dialogues ayant lieu au sein de la triade Lymphocyte CD40L^{+}T / LCM / TAM CD163^{+}.

Je suis le principal investigateur de ces travaux sur l'axe IL32/BAFF et le rôle central de la voie alterne de NFkB dans le dialogue LCM/TME. Ce projet, partie intégrante du travail de thèse de Salomé Decombis (2019-2022) que je codirige avec Catherine Pellat-Deceunynck, est en cours de finalisation et sera soumis à publication courant 2021.

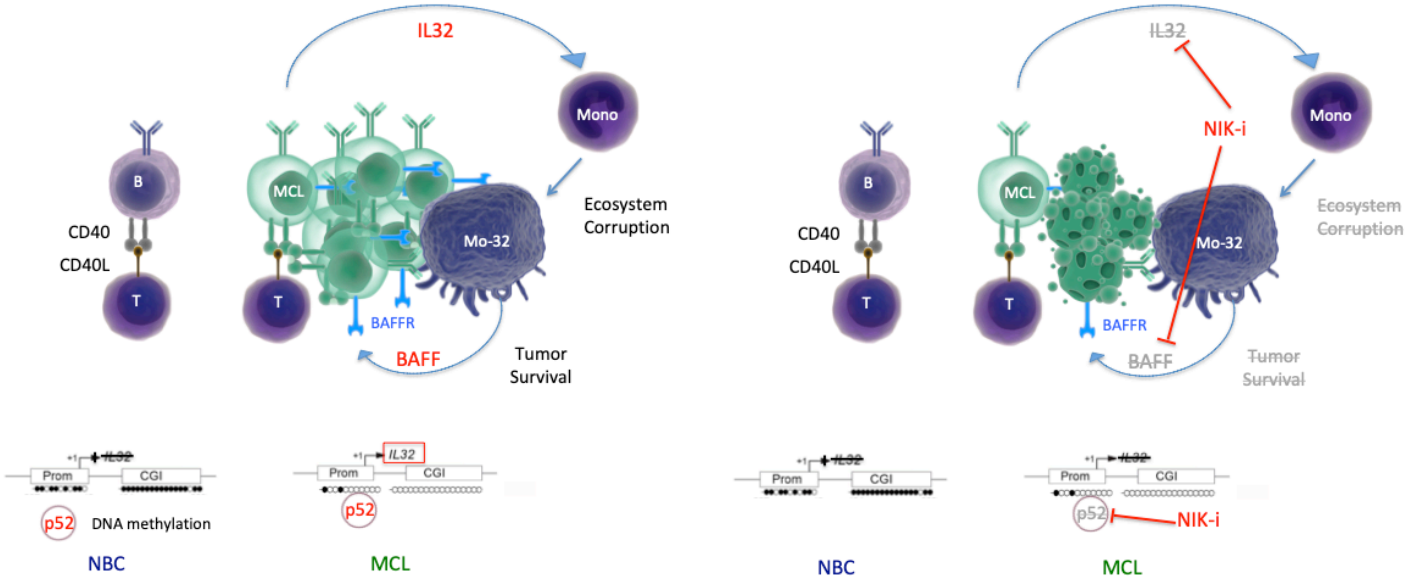

Figure 18. *Panel de gauche : L'activation du CD40 sur les cellules de LCM (MCL) induit notamment l'activation de la voie NFkB alterne (p52). Cette dernière induit la production d'IL32 par les cellules tumorales (promoteurs et CGI hypométhylés) mais pas par les lymphocytes B normaux (B, promoteurs et CGI hyperméthylés). L'IL32 sécrété par les cellules de LCM est impliquée dans la rééducation spécifique des monocytes en macrophages protumoraux Mϕ-32, qui a leur tour produise un sécrétome protumoral notamment composé de BAFF. Ce dernier induit la survie tumorale à travers l'activation de la voie NFkB alterne. Panel de droite : L'inhibition sélective de la voie NFkB alterne via l'inhibition de la kinase NIK, contrecarre ce dialogue au niveau de l'induction d'IL32 mais aussi au niveau de la survie dépendante de BAFF.*

3.3 _ Autres travaux / Collaboration avec des partenaires académiques

En plus de ces projets que je dirige, j'ai apporté mon expertise et ma participation depuis 2016 à des projets de l'équipe ou d'autres laboratoires.

_ Au sein de notre équipe de Recherche sur les thématiques des hémopathies B, p53 et Bcl-2

Dousset C, Maïga S, Gomez-Bougie P, Le Coq J, Touzeau C, Moreau P, Le Gouill S, **Chiron D**, Pellat-Deceunynck C, Moreau-Aubry A, Amiot M. **BH3 profiling** as a tool to identify acquired resistance to venetoclax in multiple myeloma. British journal of haematology. 2017

Tessoulin B, Eveillard M, Lok A, **Chiron D,** Moreau P, Amiot M, Moreau-Aubry A, Le Gouill S, Pellat-Deceunynck C. **p53** dysregulation in B-cell malignancies: More than a single gene in the pathway to hell. Blood reviews. 2017

Gillardin PS, Descamps G, Maiga S, Tessoulin B, Djamai H, Lucani B, **Chiron D**, Moreau P, Le Gouill S, Amiot M, Pellat-Deceunynck C, Moreau-Aubry A. Decitabine and melphalan fail to reactivate p73 in **p53** deficient myeloma cells. International journal of molecular sciences. 2018

Lok A, Descamps G, Tessoulin B, **Chiron D**, Eveillard M, Godon C, Le Bris Y, Vabret A, Bellanger C, Maillet L, Barillé-Nion S, Gregoire M, Fonteneau JF, Le Gouill S, Moreau P, Tangy F, Amiot M, Moreau-Aubry A, Pellat-Deceunynck C. **p53** regulates CD46 expression and measles virus infection in myeloma cells. Blood advances. 2018

Le Bris Y, Magrangeas F, Moreau A, **Chiron D,** Guérin-Charbonnel C, Theisen O, Pichon O, Canioni D, Burroni B, Maisonneuve H, Thieblemont C, Oberic L, Gyan E, Pellat-Deceunynck C, Hermine O, Delfau-Larue MH, Tessoulin B, Béné MC, Minvielle S, Le Gouill S. Whole genome copy number analysis in search of new prognostic biomarkers in first line treatment of **mantle cell lymphoma**. A study by the LYSA group. Hematological Oncology. 2020

_ Au sein de notre centre de Recherche (CRCINA) avec Dr. N Bidere sur l'étude de cytokines pro-inflammatoires

Douanne T, André-Grégoire G, Trillet K, Thys A, Papin A, Feyeux M, Hulin P, **Chiron D**, Gavard J, Bidère N. Pannexin-1 limits the production of proinflammatory cytokines during necroptosis. EMBO reports. 2019

_ Au niveau national avec l'équipe du Dr. N Varin-Blank (INSERM_U978) sur la voie WNT dans le LCM

Lazarian G, Friedrich C, Quinquenel A, Tran J, Ouriemmi S, Dondi E, Martin A, Mihoub I, **Chiron D**, Bellanger C, Fleury C, Gélébart P, McCormack E, Ledoux D, Thieblemont C, Marzec J, Gribben JG, Cymbalista F, Varin-Blank N, Gardano L, Baran-Marszak F. Stabilization of β-catenin upon B-cell receptor signaling promotes NF-kB target genes transcription in **mantle cell lymphoma**. Oncogene. 2020

_ Au niveau international avec l'équipe du Dr. D Ungureanu (Faculty of Medicine and Life Sciences, University of Tampere, Tampere, Finland) sur le BCR dans le LCM

Karvonen H, **Chiron D**, Niininen W, Ek S, Jerkeman M, Moradi E, Nykter M, Heckman CA, Kallioniemi O, Murumägi A, Ungureanu D. Crosstalk between ROR1 and BCR pathways defines novel treatment strategies in **mantle cell lymphoma**. Blood advances. 2017

4. Projets scientifiques *(2021-2026)*

Dans la continuité de mon projet actuel, je poursuis mes activités visant à identifier et à cibler les vulnérabilités (talon d'Achille) résultant de la dépendance des hémopathies B mature à leur écosystème tumoral. Plus précisément, mes efforts se concentreront sur A) les principales voies moléculaires impliquées dans la résistance dépendante du TME à travers la modulation de la famille Bcl-2 ainsi que sur B) l'utilisation de nouvelles technologies pour caractériser la nature du TME du LCM *in situ*.

A - Caractériser et cibler les dérégulations TME-dépendantes des membres de la famille Bcl-2

A_1 Contrecarrer BCLXL, inducteur majeur de résistance dans le LCM

L'expression élevée de BCLXL est associée à la résistance aux traitements (BH3-mimetics ciblant BCL2, MCL1, alkylants, …) dans le LCM. Nos données préliminaires montrent que cette expression (soit dans des sous-clones ou induite par le microenvironnement) semble être associée à une activité élevée de la voie alterne de NFkB, qui est intrinsèquement (anomalies de TRAF2/3, BIRC3, NIK) ou extrinsèquement (CD40, BAFF) activée dans le LCM. Étant donné la difficulté d'utilisation des BH3-mimetics ciblant BCLXL en raison de la toxicité sur les plaquettes *in vivo*, nous étudierons l'efficacité d'outils innovants pour contrecarrer l'induction du BCLXL. Ainsi nous évaluerons si les inhibiteurs de NIK récemment développés (voir D_4 dans Activité de Recherche) inhibent sélectivement l'induction de BCLXL et restaurent ainsi la sensibilité aux BH3-mimetics. La voie alterne de NFkB ayant aussi été impliquée dans la résistance aux inhibiteurs du BTK (Rahal et al., Nat Med. 2014), nous évaluerons l'impact de l'inhibition de NIK sur la réponse à l'Ibrutinib.

En plus des inhibiteurs de NIK, nous expertiserons la technologie PROTAC (Proteolysis Targeting Chimeric), qui a récemment été décrite comme étant capable d'inhiber BCLXL dans les cellules tumorales tout en épargnant les plaquettes (*Khan et al., Nat. Med. 2019*), et qui pourrait être efficace dans les cellules de LCM.

A_2 Déterminer les mécanismes d'inhibition TME-dépendent de BIM et comprendre son implication dans la survie tumorale

La protéine BH3-only activatrice BIM a un rôle majeur dans l'initiation de la dépolarisation mitochondriale et un faisceau d'arguments nous suggère que sa régulation par le TME est centrale pour la survie du LCM :
1) Le développement de LCM dans les souris EμCCND1 CD19^{CRE}BIM$^{fl/fl}$, contrairement aux souris EμCCND1, suggère un rôle physiopathologique majeur (*Katz et al., Blood 2014*).
2) 6 des 12 lignées cellulaires de LCM caractérisées ont une double délétion de BIM (2q13).
3) Aucune délétion homozygote de BIM n'a été retrouvée dans 95 échantillons primaires de LCM (*Le Bris et al., Hematological Oncology 2020*). Cette discordance suggère d'autres mécanismes de régulation, souligne les limites du modèle 'lignée cellulaire' dans le LCM et renforce l'intérêt de notre stratégie de modélisation du microenvironnement tumoral (TME).

Alors que les cellules de LCM expriment BIM dans le sang, une forte inhibition est observée dans les ganglions au niveau transcriptionel (Figure 19A). Mes données confirment la régulation de la protéine BIM *ex vivo* par les TME 'myéloïde' et 'lymphoïde', la corrélant ainsi avec la survie des cellules primaires. De façon remarquable cette régulation n'est pas retrouvée dans les lymphocytes B normaux (NBC) (Figure 19B) et nous avions précédemment observé que l'inhibition TME-dépendante de BIM était similaire dans les autres hémopathies B matures étudiées (voir B_2 dans Activité de Recherche).

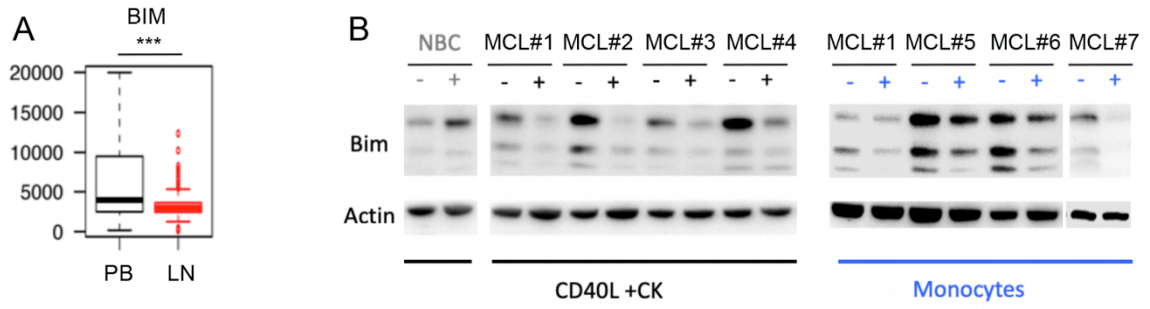

Figure 19. Inhibition du pro-apoptotique BIM de façon TME-dépendante et spécifique de la tumeur dans les cellules primaires de LCM. A*) Au niveau transcriptionnel in vivo dans les ganglions (LN) par rapport aux cellules circulantes (PB).* ***B****) Au niveau protéique ex vivo après coculture dans le système ''CD40L+Ck'' ou au contact de monocytes pendant 7 jours.*

En m'appuyant sur nos différents modèles intégrant le rôle central du TME développés ces dernières années, je propose d'étudier les fonctions de BIM ainsi que les mécanismes moléculaires qui contrôlent sa régulation TME-dépendante dans les cellules primaires de LCM.

Nos données préliminaires suggèrent qu'une diminution/extinction de BIM pourrait permettre aux cellules tumorales d'échapper à leur dépendance au TME pour leur survie. Je propose d'évaluer les conséquences de son extinction dans les cellules primaires de LCM par CRISPR/Cas9 (développé dans l'équipe par les Dr. A. Moreau) et vecteurs lentiviraux. Malgré les difficultés techniques inhérentes à l'infection des Lymphocytes B primaires, des résultats prometteurs ont été récemment publiés par l'équipe du Dr D. Hodson à Cambridge (*Caeser et al., Nat. Com. 2019*). Grâce aux outils moléculaires développés par ces derniers, nous évaluerons l'efficacité d'infection dans les cellules primaires tumorales par des lentivirus à enveloppe GALV_MTR. En plus de nous aider à déchiffrer le rôle de BIM, le développement de cette technologie nous permettrait d'étudier, à moyen terme, d'autres mécanismes TME-dépendants dans les cellules primaires de LCM.

Mes données préliminaires suggèrent que le contrôle de BIM par le microenvironnement dans le LCM est déterminé au niveau de l'ARN (Figure 19A). BIM est finement régulé par de multiples facteurs de transcription ou encore des régulations épigénétiques (méthylation). Afin de déterminer les mécanismes dépendants du microenvironnement, je propose d'évaluer ces différentes régulations. Au niveau transcriptionel nous étudierons le rôle

potentiel de la voie NFkB, ou encore AKT/FoxO3a, deux voies modulées par le TME et décrites comme impliquées dans la régulation de BIM. D'autre part, nous résultats préliminaires montre une régulation TME-dépendante de TSC22D3 (GILZ), similaire à celle de BIM. Notre équipe ayant précédemment suggéré un control de l'expression de BIM par TSC22D3 dans le MM (*Kervoelen et al., Oncotarget 2015*) nous évoluerons son rôle potentiel dans le LCM. Concernant le contrôle épigénétique, comme précédemment documenté par notre équipe (*Brousseau et al., Cell Death Dis 2014*), la méthylation de l'ADN est déterminante dans la régulation de la famille Bcl-2. La présence d'un large ilot CpG (>500) au niveau du promoteur de BIM ainsi que mes données préliminaires qui montrent une augmentation des DNMT1 et 3a dans les cellules primaires en coculture renforcent cette hypothèse. La modulation du profil d'expression de BIM par un inhibiteur de la méthylation (5azadC) sera évaluée. D'autre part, nous déterminerons le niveau de méthylation des régions CpG (conversion bisulfite et pyroséquençage).

A_3 Etudier le rôle de la famille Bcl-2 à la résolution cellule unique dans la résistance à OAsIs

Le paradigme du traitement des patients atteints de LCM va probablement changer dans les années à venir notamment grâce à l'efficacité des thérapies ciblées, inhibiteurs de BTK et BH3-mimetics. Cependant, malgré les résultats très encourageants de ces nouvelles combinaisons « sans chimio », environ un tiers des patients présente une résistance primaire ou une rechute à moyen terme (*Agarwal et al., Nat Med 2018*).

J'ai fait l'hypothèse que l'analyse de l'hétérogénéité fonctionnelle du LCM au niveau de la cellule unique permettrait de découvrir des mécanismes impliqués dans l'expansion des lymphomes et leur résistance à ces nouvelles thérapies. La technologie de séquençage à haut débit de cellules uniques (scRNA-seq, 10X Genomics) est accessible au sein de notre centre (technologie rendue disponible sur site grâce au SIRIC ILLIAD) et ouvre de nouvelles possibilités pour comprendre les mécanismes impliqués dans les rechutes aux thérapies innovantes. Dans l'essai OAsIs (Obinutuzumab, Ibrutinib, Venetoclax) nous avons collecté des échantillons (sang et moelle majoritairement) avant traitement et à la rechute pour certains d'entre eux. Nous concentrerons dans un premier temps notre effort sur ces échantillons longitudinaux appariés (diagnostic et rechute).

La bioinformatique étant essentielle pour l'analyse de technologies innovantes à haut débit (principalement basée sur l'interface R), en plus d'une collaboration l'équipe du Dr. S. Minvielle (équipe 11, CRCINA), des efforts ont été mis dans la formation de plusieurs membres de notre équipe. Sur la base de cette stratégie, une 'pipeline' (comprenant Seurat, SoupX, DEseq2, Cellphonedb, ...) est en cours de développement et permettra une analyse indépendante de nos données à haut débit.

Nos résultats préliminaires nous apportent des informations intéressantes à travers l'identification de cellules très minoritaires avant traitement et très probablement responsable de la rechute (Figure 20). L'analyse en profondeur de ce cluster de cellules résistantes à Oasis montre un profil d'expression de la famille Bcl-2 particulier que nous allons à présent étudier au niveau fonctionnel, et notamment au niveau de la régulation par le microenvironnement. Aussi ces cellules montrent plusieurs caractéristiques de cellules

dites « persistantes » (très rares, non cyclantes,…(*Shen et al., Cell 2020*). Nous évaluerons donc si leurs caractéristiques phénotypiques et fonctionnelles sont spécifiques de la résistance à OAsIs ou si elles sont plus largement impliquées dans les rechutes systématiques dont souffrent les patients atteints de LCM.

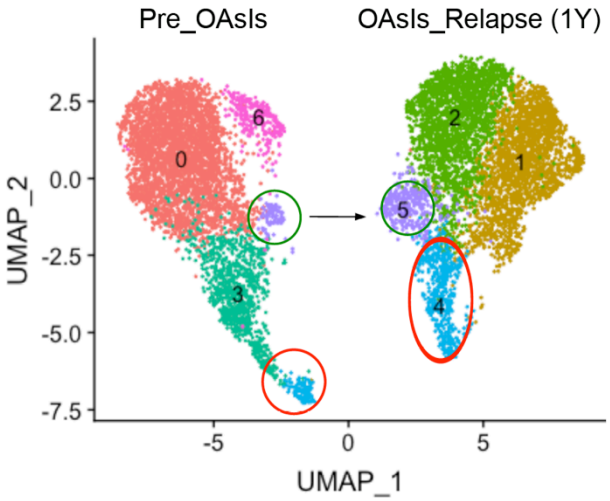

Figure 20. Analyse à l'échelle 'cellule unique' du transcriptome des cellules tumorales de patients inclus dans OAsIs.

Représentation en UMAP de cellules tumorales issues d'échantillons médullaires d'un patient de LCM avant traitement (Pre_OAsIs) et à la rechute après 1 an de réponse (OAsIs_Relapse (1Y)).

Le Cluster#4 entouré en rouge est porté par une signature du cycle cellulaire est représente les cellules en prolifération dans chaque échantillon.

Le Cluster#5 entouré en vert représente des cellules non cyclantes présentes avant traitement et à la rechute

En outre, en collaboration avec Yannick Le Bris (PH, hémato-bio, CHU de Nantes) chaque échantillon sera caractérisé pour un panel prédéfini (approche de capture IDT®) de mutations/CNV dans environ 49 gènes, y compris les voies p53, BCR ou NFkB, et une région spécifique du chromosome 9p récemment décrite comme étant impliquée dans la résistance à l'Ibrutinib/Venetoclax (*Agarwal et al., Nat Med 2018*). Je prévois donc de réaliser une analyse génomique, transcriptomique et fonctionnelle intégrée afin de découvrir les mécanismes de résistance impliqués dans la rechute des thérapies ciblées de type OAsIs.

B - Caractériser la nature des écosystèmes tumoraux du LCM

Nos résultats de ces dernières années montrent clairement un impact des écosystèmes immunitaires dans la biologie du LCM. Cependant nous n'avons aujourd'hui que très peu d'information sur la nature précise et la composition des différents écosystèmes des cellules de LCM.

B_1- Etude du Microenvironnement médullaire par la technologie scRNA-seq

Parallèlement à l'étude des cellules tumorales issues des échantillons médullaires collectés au cours de l'essai clinique OAsIs, je prévois d'analyser les cellules de l'écosystème par scRNA-seq. En effet la résistance peut être la conséquence de modification au niveau moléculaire de la cellule tumorale (déterminants génomiques de la réponse), mais aussi au niveau cellulaire, nos travaux récents démontrant un rôle central du microenvironnement dans l'expansion du LCM et sa résistance aux traitements. L'analyse conjointe et intégrée par sc-RNA-seq des cellules tumorales et de leur microenvironnement nous permettra de mieux comprendre la dynamique des cellules de LCM dans leurs niches de protection.

La LCM se caractérise par une dissémination précoce et la survie de la tumeur est soutenue par divers écosystèmes dans les ganglions lymphatiques, la moelle osseuse ou le sang périphérique. Mon choix d'analyser des échantillons de moelle osseuse dans le cadre du présent projet est basé sur : 1) Même si la moelle osseuse n'est pas le principal site d'expansion du LCM, 60 à 80 % des patients présentent une infiltration médullaire au moment du diagnostic. 2) La nature et la composition de la moelle osseuse dans le LCM sont totalement inconnues et sous-étudiées. 3) Contrairement aux cellules viables issues de ganglions lymphatiques dissociés, les échantillons de moelle osseuse sont accessibles et, comme les biopsies liquides, sont appropriées pour générer des données de qualité en utilisant la technologie 10X. 4) L'acquisition d'échantillons de moelle osseuse de LCM permettra l'intégration et la comparaison de notre ensemble de données à l'analyse d'échantillons de moelle osseuse normale (chirurgie de la hanche) et de myélome multiple effectué par notre équipe dans le contexte du projet SIRIC ILIAD (Projet porté par Catherine Pellat-Deceunynck en collaboration avec Stéphane Minvielle).

Nos premières analyses nous permettent d'ores et déjà d'identifier de profondes modifications des compartiments T et myéloïdes dans les moelles de patients de LCM par rapport aux moelles normales (Figure 21). Ces données doivent à présent être validées et consolidées avant d'étudier leurs conséquences fonctionnelles.

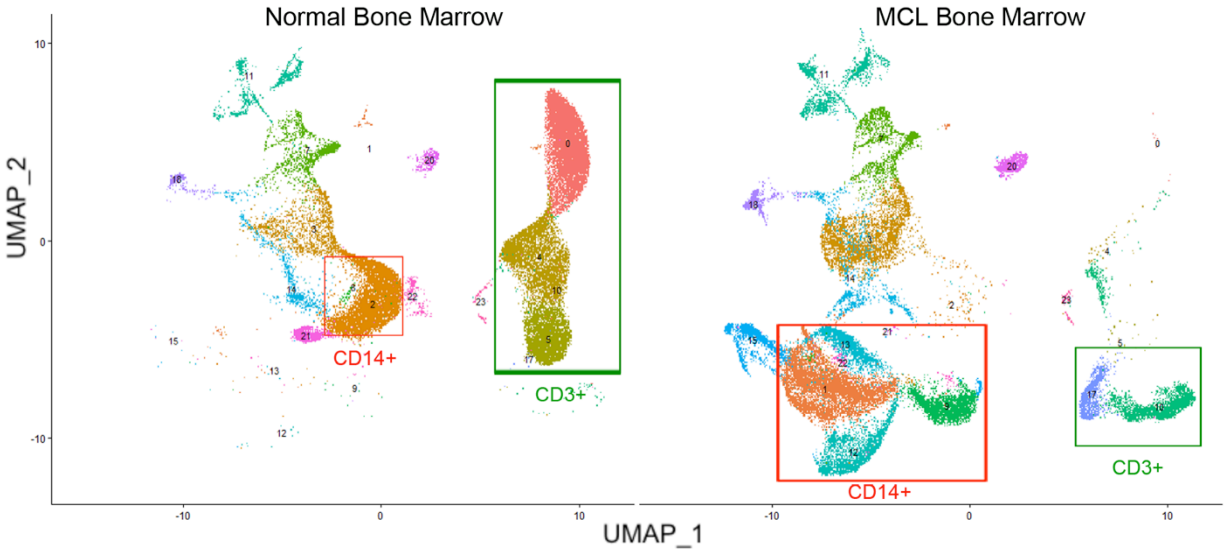

Figure 21. Analyse à l'échelle 'cellule unique' du transcriptome des cellules de l'écosystème médullaire de patients de LCM. *Représentation en UMAP de cellules de l'écosystème médullaire de donneurs sains (à gauche) et de patients de LCM. Le profil des cellules CD14+ ou encore CD3+ semble être particulièrement modifié dans le contexte tumoral (à droite).*

B_2 - Etude du microenvironnement ganglionnaire par immunohistochimie multispectrale

La difficulté d'accès à des échantillons de ganglions dissociés de LCM de qualité suffisante pour une analyse au niveau cellule unique m'a poussé à développer une stratégie alternative d'étude du microenvironnement ganglionnaire.

Ainsi nous développons en collaboration avec la plateforme MicropiCell (SFR Bonamy, Nantes) l'analyse par immunohistochimie multispectrale de ganglions de LCM fixés. Cette technologie nous permettra de mieux caractériser les infiltrats myéloïdes (CD68, 163, SIRPA, CD47) et lymphoïdes (CD40L, 8,4, FOXP3), et de déterminer les interactions potentiellement ciblables *in vivo* au sein de la structure lymphoïde (PD1/PDL1, CD86/CTLA4, TIM3). Ce projet sera facilité par un accès à de nombreux échantillons de ganglions de LCM référencés et stockés sous forme FFPE par le service d'anatomopathologie du CHU de Nantes (Pr. Céline Bossard PU-PH ; n>100).

Cette technologie nécessite de nombreuses mises au point que cela soit pour les marquages ou les analyses d'images mais nos données préliminaires confirment la faisabilité de cette approche sur les sections de tissu de LCM (Figure 22)

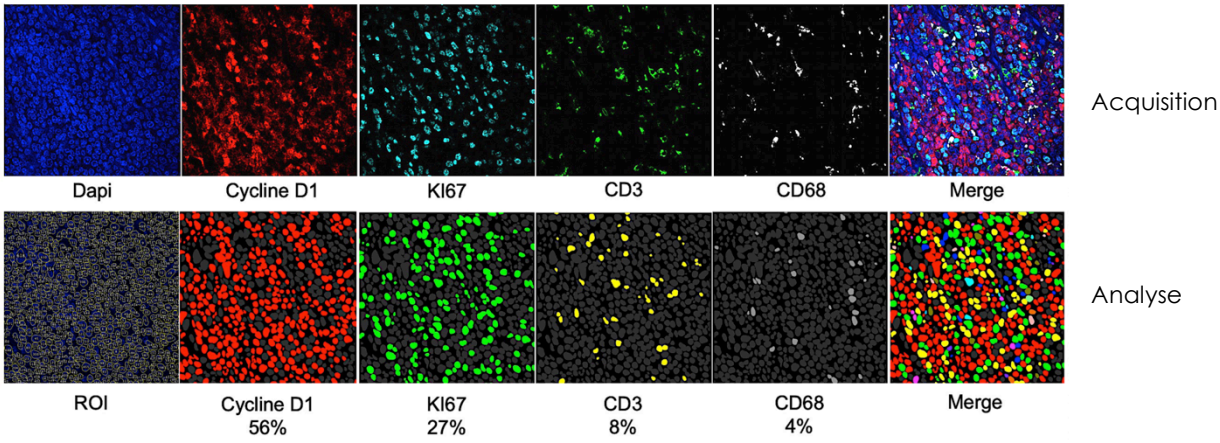

Figure 22. Etude du microenvironnement ganglionnaire du LCM par Immunohistochimie multispectrale. *Panel supérieur: Section de tissu tumoral analysé par microscopie confocale après marquage des noyaux par Dapi et 5 anticorps, associés à des Opal différents, et ciblant les cellules tumorales (Cyclin D1), les cellules proliférantes (Ki67), les lymphocytes T (CD3) et les macrophages (CD68). Le 'Merge' représente la superposition de toutes les images. Panel inférieur : Analyse informatique des images acquises en microscopie à l'aide d'un script développé par MicropiCell.*

C - Développer des modèles de culture ex vivo plus complexes et pertinents

Nos modèles de coculture en 2D nous ont fourni des informations essentielles sur les régulations moléculaires dépendantes du microenvironnement. Cependant nous aspirons à développer, à plus long terme, des modèles plus complexes qui intègrent la complexité de tout un écosystème.

Nous avons récemment développé un modèle murin humanisé (souris NSG greffées par des cellules souches CD34+ humaines) de PDX de LCM avec infiltration de tumeurs dans le sang périphérique, la moelle osseuse et les organes lymphoïdes secondaires, imitant la pathologie humaine (2018, collaboration Plate-forme de souris humanisée, Nantes). Ce protocole d'humanisation permet de reconstituer les différents composants hématopoïétiques humains tels que les lymphocytes T régulateurs et les populations de macrophages. Néanmoins, même si nos données préliminaires ont confirmé un rôle de soutien de l'écosystème humain pour la croissance tumorale *in vivo* (Figure 23), plusieurs limitations telles que les GVH/GVL ainsi que le coût et la durée des expériences limitent fortement l'utilisation de ce modèle.

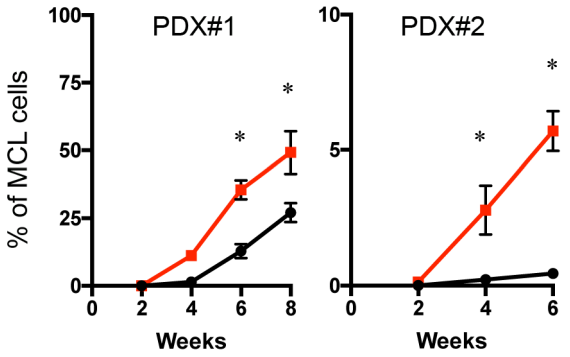

Figures 23. Développement de modèles de PDX de LCM.

Pourcentage de cellules tumorales circulantes détectées dans le sang périphérique de souris NSG (courbe noire) ou NSG préalablement humanisées (courbe rouge), après greffe des cellules primaires de LCM pour le temps indiqué en abscisse.

Deux PDX différents obtenus après greffe de cellules primaires issus de patients de LCM sont représentés (PDX#1 et PDX#2)

Afin de mimer la complexité des niches de protection immunitaire tout en contournant ces limitations, nous souhaitons développer des modèles innovants et autologues *ex vivo* basés sur des cellules primaires et des organoïdes 3D. Etant donné le rôle central de l'écosystème immunitaire dans l'expansion du LCM, nous allons dans un premier temps développer un organoïde (protéine bioadhésive + nanoparticule de silicate) qui se concentrera sur la triade Lymphocytes-T/ LCM /Macrophage. L'implémentation progressive de ce modèle s'appuiera sur nos nouvelles découvertes concernant la nature du TME ainsi que sur de nouvelles technologies de biologie cellulaire, telle que la bio-impression ou des dispositifs de microfluidiques ('tumor on chip'), et des outils de biologie moléculaires adaptés aux cellules primaires (ex : CRISPR/CAS9). Cette partie du projet sera développée à plus long terme et sera soutenue par l'expertise actuelle de plusieurs groupes de notre centre de Recherche en cancérologie.

5. Fiche de Synthèse

Nom: David Chiron
E-mail: david.chiron@univ-nantes.fr

Travaux et Projets

J'ai obtenu mon doctorat en 2010 pour mes travaux sur les récepteurs Toll-like et la clonogénicité dans le myélome multiple à l'INSERM_601 (*Dir. Dr. M. Bonneville*). Au cours de mon post-doctorat à New York à l'Université Cornell (*Lab. Prof. S. Chen-Kiang*), j'ai caractérisé les interactions moléculaires entre la signalisation BCR et le cycle cellulaire dans le lymphome à cellules du manteau. J'ai aussi identifié des mutations spécifiques impliquées dans la résistance aux inhibiteurs du BCR. Depuis 2014, je développe mon projet sur la résistance des hémopathies B matures en intégrant le rôle clé des écosystèmes tumoraux, au sein du CRCINA (*INSERM_1232, CNRS ERL_6001_Dir. Dr. M. Grégoire*). J'ai rejoint le CNRS en 2016 (*CRCN, section 24*) et mes recherches actuelles portent sur l'intégration, dans les mécanismes de résistance, des interactions cellulaires (immunitaires : lymphocytes-T, macrophages) et des régulations moléculaires associées (BCR, CD40, dialogues solubles). Je porte ce projet en m'appuyant sur des technologies à haut débit ((single-cell)*RNA-seq, IHC multispectrale)* et des modèles de coculture de cellules primaires permettant la compréhension fonctionnelle des régulations et le développement de nouvelles stratégies de ciblages thérapeutiques.

Je suis co-auteur de 33 publications dans des journaux internationaux à comité de lecture (dont 16 en tant que premier ou dernier auteur).

Mots-clés : Hémopathies B mature, microenvironnement immunitaire, BCR

Synthèse des encadrements et publications associées

Thèses co-encadrées

- Antonin Papin _ 2016-2019
Rôle du microenvironnement tumoral dans l'expansion des lymphomes B
Sous la direction de Steven Le Gouill (50) et de **David Chiron** (50).
Thèse soutenue le 08-10-2019 et ayant donné lieu à 5 Publications :
Papin et al., Leukemia. 2019;33(10):2442-2453. (IF : 9)
Tessoulin B, Papin A et al., Frontiers in oncology. 2019;8:645. (IF : 4)
Douanne T et al., EMBO reports. 2019;20(10):e47840. (IF : 7.5)
Chiron D, Bellanger C, Papin A, et al. Blood, 2016;128(24):2808-2818. (IF : 13)
Papin A, et al. Leukemia & lymphoma. 2018;59(5):1064-1072 (IF : 3)

- Salomé Decombis _2019
Rôle du microenvironnement immunitaire dans l'expansion des lymphomes B matures
Sous la direction de Catherine Pellat-Deceunynck (50) et de **David Chiron** (50).
En préparation depuis le 02-09-2019 et ayant un manuscrit en cours de reviewing :
Decombis et al, 2021

Encadrement d'étudiants Master 2 recherche

- Antonin Papin _ 2015-2016 _ Master Biologie-Santé de Nantes
- Thiphanie Riveron _ 2018-2019 _ Master Biologie-Santé de Nantes
- Mathieu Rouel _ 2018-2019 _ Master Informatique de Nantes
- Clara Sortais, MD _ 2019-2020 _ Master 2 «B2CT» de Paris Diderot

6. Annexe : Copie des cinq publications les plus représentatives de mon activité actuelle

Vous trouverez en annexe les publications suivantes :

- Chiron D, Di Liberto M, Martin P, et al. Cell-cycle reprogramming for PI3K inhibition overrides a relapse-specific C481S BTK mutation revealed by longitudinal functional genomics in mantle cell lymphoma. **Cancer discovery**. 2014;4(9):1022-1035.

- Chiron D, Dousset C, Brosseau C, et al. Biological rational for sequential targeting of Bruton tyrosine kinase and Bcl-2 to overcome CD40-induced ABT-199 resistance in mantle cell lymphoma. **Oncotarget**. 2015;6(11):8750-8759.

- Chiron D, Bellanger C, Papin A, et al. Rational targeted therapies to overcome microenvironment-dependent expansion of mantle cell lymphoma. **Blood**, The Journal of the American Society of Hematology. 2016;128(24):2808-2818.

- Tessoulin B, Papin A, Gomez-Bougie P, et al. BCL2-family dysregulation in B-cell malignancies: from gene expression regulation to a targeted therapy biomarker. **Frontiers in oncology**. 2019;8:645.

- Papin A, Tessoulin B, Bellanger C, et al. CSF1R and BTK inhibitions as novel strategies to disrupt the dialog between mantle cell lymphoma and macrophages. **Leukemia**. 2019;33(10):2442-2453.

Published OnlineFirst July 31, 2014; DOI: 10.1158/2159-8290.CD-14-0098

RESEARCH ARTICLE

Cell-Cycle Reprogramming for PI3K Inhibition Overrides a Relapse-Specific C481S *BTK* Mutation Revealed by Longitudinal Functional Genomics in Mantle Cell Lymphoma

David Chiron[1], Maurizio Di Liberto[1], Peter Martin[2], Xiangao Huang[1], Jeff Sharman[3], Pedro Blecua[4,5], Susan Mathew[1], Priyanka Vijay[4,6], Ken Eng[4,6], Siraj Ali[7], Amy Johnson[8], Betty Chang[9], Scott Ely[1], Olivier Elemento[4,5], Christopher E. Mason[4,5], John P. Leonard[2], and Selina Chen-Kiang[1,10]

Published OnlineFirst July 31, 2014; DOI: 10.1158/2159-8290.CD-14-0098

ABSTRACT Despite the unprecedented clinical activity of the Bruton tyrosine kinase (BTK) inhibitor ibrutinib in mantle cell lymphoma (MCL), acquired resistance is common. By longitudinal integrative whole-exome and whole-transcriptome sequencing and targeted sequencing, we identified the first relapse-specific C481S mutation at the ibrutinib binding site of BTK in MCL cells at progression following a durable response. This mutation enhanced BTK and AKT activation and tissue-specific proliferation of resistant MCL cells driven by CDK4 activation. It was absent, however, in patients with primary resistance or progression following transient response to ibrutinib, suggesting alternative mechanisms of resistance. Through synergistic induction of PIK3IP1 and inhibition of PI3K–AKT activation, prolonged early G_1 arrest induced by PD 0332991 (palbociclib) inhibition of CDK4 sensitized resistant lymphoma cells to ibrutinib killing when BTK was unmutated, and to PI3K inhibitors independent of C481S mutation. These data identify a genomic basis for acquired ibrutinib resistance in MCL and suggest a strategy to override both primary and acquired ibrutinib resistance.

SIGNIFICANCE: We have discovered the first relapse-specific BTK mutation in patients with MCL with acquired resistance, but not primary resistance, to ibrutinib, and demonstrated a rationale for targeting the proliferative resistant MCL cells by inhibiting CDK4 and the cell cycle in combination with ibrutinib in the presence of BTK^{WT} or a PI3K inhibitor independent of BTK mutation. As drug resistance remains a major challenge and CDK4 and PI3K are dysregulated at a high frequency in human cancers, targeting CDK4 in genome-based combination therapy represents a novel approach to lymphoma and cancer therapy. *Cancer Discov; 4(9); 1022–35. ©2014 AACR.*

INTRODUCTION

Mantle cell lymphoma (MCL), a non-Hodgkin lymphoma of pregerminal center mature B cells, remains incurable due to the development of drug resistance (1). Bruton tyrosine kinase (BTK) is a TEC family cytoplasmic tyrosine kinase required for the development, activation, and differentiation of B cells (2), as shown by the development of X-linked agammaglobulinemia when BTK is genetically inactivated (3). By mediating B-cell receptor (BCR) signaling, BTK is also indispensable for the survival of B cells and lymphoma cells (4). Targeting BTK with the irreversible, orally bioavailable inhibitor ibrutinib (PCI 32765; ref. 5) achieved an unprecedented objective response rate of 68% in a phase II single-agent clinical trial in patients with relapsed/refractory MCL (6), and was similarly efficacious in chronic lymphocytic leukemia (CLL; ref. 7). On this basis, ibrutinib was approved by the FDA in late 2013 for treatment of patients with recurrent MCL and in 2014 for patients with CLL (8).

However, disease progression while on ibrutinib treatment is frequent in MCL. It was reported as the principal reason for discontinuation of ibrutinib in 50 of 65 patients in the phase II trial, and has been associated with a highly proliferative state and poor clinical outcomes (ref. 6; data not shown). Although the mechanism is unknown, the unrestrained proliferation of MCL cells at relapse suggests that targeting the cell cycle in combination therapy may delay the expansion of resistant clones or override some mechanisms of ibrutinib resistance. Because a hallmark of MCL is cell-cycle dysregulation (9) due to aberrant cyclin D1 expression from a t(11;14)(q13;q32) chromosomal translocation and activation of CDK4, targeting cyclin D1 or CDK4 represents a rational approach to controlling the cell cycle in MCL. Supporting this possibility, targeting CDK4/CDK6 with the selective and potent oral inhibitor PD 0332991 (palbociclib; ref. 10) in the first single-agent clinical trial in patients with recurrent MCL effectively arrested MCL cells in early G_1, resulting in a durable clinical response with an excellent toxicity profile (11).

CDK4 is overexpressed or activated at a high frequency in both hematologic malignancies and solid tumors, and PD 0332991 is now a breakthrough therapy for breast cancer owing to its ability to more than double the progression-free survival (PFS) of patients with metastatic breast cancer when combined with letrozole (12). The clinical efficacy of PD 0332991 may stem from induction of prolonged early G_1

[1]Department of Pathology and Laboratory Medicine, Weill Cornell Medical College, New York, New York. [2]Department of Medicine, Weill Cornell Medical College, New York, New York. [3]Willamette Valley Cancer Institute and Research Center/US Oncology Research, Springfield, Oregon. [4]Department of Physiology and Biophysics, Weill Cornell Medical College, New York, New York. [5]Institute for Computational Biomedicine, Weill Cornell Medical College, New York, New York. [6]Tri-Institutional Training Program in Computational Biology and Medicine, Weill Cornell Medical College, New York, New York. [7]Foundation Medicine, Inc., Cambridge, Massachusetts. [8]Ohio State University, Columbus, Ohio. [9]Pharmacyclics, Sunnyvale, California. [10]Graduate Program in Immunology and Microbial Pathogenesis, Weill Cornell Medical College, New York, New York.

Note: Supplementary data for this article are available at Cancer Discovery Online (http://cancerdiscovery.aacrjournals.org/).

D. Chiron, M. Di Liberto, and P. Martin contributed equally to this article.

Corresponding Author: Selina Chen-Kiang, Department of Pathology and Laboratory Medicine, 1300 York Avenue, New York, NY 10065. Phone: 212-746-6440; Fax: 212-746-7996; E-mail: sckiang@med.cornell.edu

doi: 10.1158/2159-8290.CD-14-0098

Published OnlineFirst July 31, 2014; DOI: 10.1158/2159-8290.CD-14-0098

arrest (pG1) beyond the scheduled early G_1 transit time by sustained CDK4/CDK6 inhibition (13), which reprograms cancer cells for killing by diverse clinically relevant agents (14). These include dexamethasone (13) and the proteasome inhibitor bortezomib in primary myeloma cells *ex vivo* and in animal models (14, 15), and PI3K inhibitors in primary MCL cells *ex vivo* (16).

Here, we demonstrate by longitudinal functional genomics and targeted sequencing a relapse-specific C481S missense mutation at the ibrutinib binding site of BTK in both patients who progressed on ibrutinib after a durable response, but not in patients ($n = 6$) with a transient response or primary resistance to ibrutinib. A further analysis of 1 patient revealed that the *BTK*^{C481S} mutation is associated with heightened BTK and AKT activation, exacerbated genomic instability, and preferential CDK4-driven proliferation of resistant MCL cells in the spleen. Induction of pG1 by selective inhibition of CDK4 reprogrammed lymphoma cells for killing by ibrutinib when BTK is unmutated, and by selective PI3K inhibitors regardless of the presence of the *BTK*^{C481S} mutation, suggesting a novel strategy to override ibrutinib resistance by targeting CDK4 in genome-based combination therapy.

RESULTS

Relapse-Specific *BTK*^{C481S} Mutation in MCL

To elucidate the mechanism of acquired resistance to ibrutinib, we investigated the dynamic tumor evolution and discerned mutations that were expressed in MCL tumors by longitudinal integrative analysis of whole-exome sequencing (WES) and whole-transcriptome sequencing (WTS) of five serial biopsies of a representative male patient with MCL (Patient 1). This patient achieved a partial response (PR; equal to or greater than 50% reduction of tumor mass) on single-agent ibrutinib therapy for 14 months before progression with mild lymphadenopathy and massive splenomegaly (see Methods).

Single-nucleotide variant (SNV) analysis of serial WES and Sanger sequencing detected a dinucleotide substitution of G1442C and C1443T in *BTK* in MCL cells at relapse in both the bone marrow (r_IbBM, 74% of the reads) and the spleen (r_IbSP, 83% of the reads). This substitution resulted in a cysteine-to-serine missense mutation at residue 481 (C481S), localized in the tyrosine kinase domain of BTK (Fig. 1A–C). Importantly, the C481S mutation was not detected in any of the three lymph node biopsies taken 8 months (p_Ib1 and p_Ib2) or immediately (p_Ib3) before initiating ibrutinib, or in the cheek swab germline control (Fig. 1A).

Longitudinal WTS analysis of serial biopsies corroborated the very high frequency (~80%) of C481S mutation in *BTK* exclusively at relapse in MCL cells in both the bone marrow (read depth, 129) and the spleen (read depth, 372; Fig. 1D). The abundance of *BTK* mRNA was increased at relapse (2-fold) in bone marrow MCL cells along with the selective elevation of mRNA expression from genes in the BCR signaling pathway (*CD79A*, *LYN*, *PLCG2*, and *PRKCB*; Fig. 1D). However, no SNV was identified in other genes of the BCR signaling pathway (Fig. 1D) or in genes frequently mutated in MCL such as *ATM*, *NOTCH1*, and *UBR5*, except for SNVs in the 5′ untranslated region (5′-UTR) of *CCND1* (Fig. 1E; refs. 17, 18). *BTK*^{C481S} has not been detected in ibrutinib-naïve primary MCL cells by WTS or WES by us and others (refs. 16, 18–21; data not shown). These data demonstrate the specificity of *BTK*^{C481S} mutation at relapse from ibrutinib in MCL.

Further integrative WES and WTS analysis revealed 190 SNVs that were expressed in MCL cells but not present in the germline: 35 in coding sequences (CDS) and 155 in UTRs (Fig. 2A and Supplementary Tables S1 and S2). Sixteen of the CDS SNVs were nonsynonymous and predicted to be damaging at the protein level (Supplementary Table S3), of which 11 were constitutive and five increased in frequency with time in *BRAP*, *RC3H1*, *C14ORF159*, *BTK*, and *TRAPPC10* (Fig. 2B–D). Only C481S in *BTK* and V600F in *TRAPPC10* (22) were detected at a very high frequency exclusively at relapse in MCL cells in both the bone marrow and the spleen (Fig. 2B and Supplementary Table S3). The significance of the concurrent *TRAPPC10*^{V600F} mutation is unknown. However, its unique association with *BTK*^{C481S} in both bone marrow and splenic MCL cells at relapse implicates a clonal origin for ibrutinib-resistant MCL cells.

BTK^{C481S} was identified in a second male patient with MCL (Patient 2), who progressed on ibrutinib after achieving a PR that lasted for 30 months (see Methods). By targeted and Sanger sequencing of cells present in the pleural effusion, which comprised 69% CD19$^+$/CD5$^+$ MCL cells, G1442C was present at relapse in 31% of the sequence reads but not before ibrutinib treatment or in the germline (Supplementary Table S4). The *BTK*^{C481S} mutation has been identified in CLL at the time of relapse following a durable response by WES as well (23). Collectively, these findings highlight the remarkable specificity of the *BTK*^{C481S} mutation at ibrutinib resistance after a durable response in CLL and MCL.

Absence of *BTK*^{C481S} Mutation in Transient Ibrutinib Response and Primary Resistance

BTK^{C481S} was absent in serial peripheral blood or lymph node MCL cells of 6 patients with primary resistance to ibrutinib or acquired resistance following a transient (<5 months) PR, using cheek swab DNA as controls for individual patients (Supplementary Table S5). No gain-of-function R665W mutation in the downstream PLCγ2 observed in ibrutinib relapse in CLL (23) was detected (Supplementary Table S5). Thus, mechanisms other than *BTK*^{C481S} mutation or PLCγ2 activation must have contributed to the rapid resistance to ibrutinib in patients with MCL who retain the wild-type (WT) BTK.

This led us to ask whether *BTK*^{WT} was inhibited by ibrutinib *in vivo* in resistant MCL cells. *BTK*^{WT} was autophosphorylated (pY223) in peripheral blood MCL cells before (p_Ib1) but not at 3 weeks of ibrutinib treatment (Ib1) in Patient 4, who had a PR for more than 10 months, or in Patient 8, who maintained stable disease (SD; <50% reduction of tumor mass) for more than 4 months (Fig. 3A). A prominent loss of AKT activation (pS473) by mTORC2 was concurrent with BTK inhibition, even taking into account the reduction in total AKT, whereas PLCγ2 activation (pY759) was diminished only modestly (Fig. 3A). Of interest, *BTK*^{WT} was also

Published OnlineFirst July 31, 2014; DOI: 10.1158/2159-8290.CD-14-0098

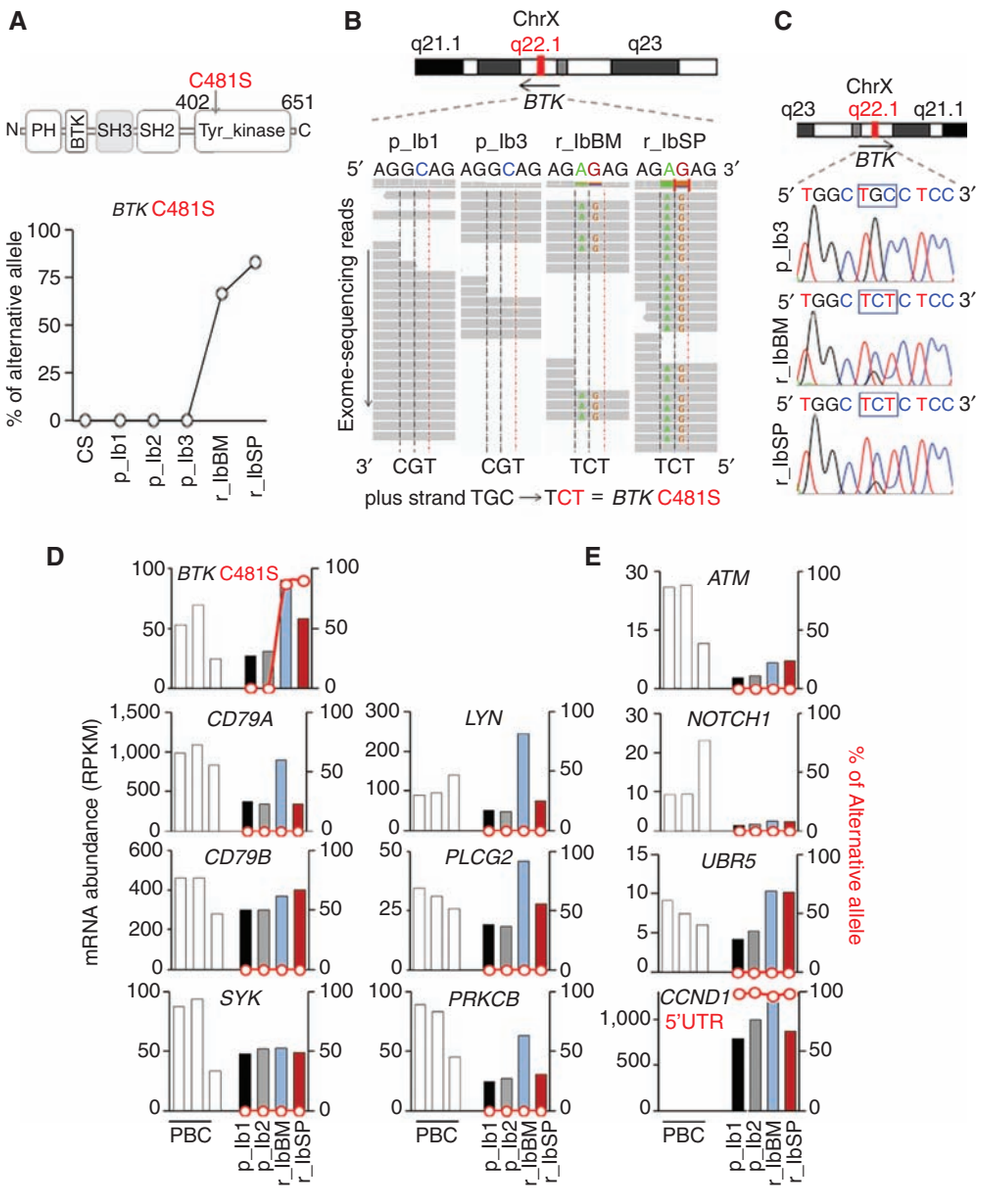

Figure 1. Identification of a relapse-specific *BTK*^{C481S} mutation in MCL by longitudinal integrative WES and WTS. **A,** schema for the C481S mutation in BTK (red) and WES analysis of SNVs (% of alternative allele) in the DNA of cheek swab (CS) and MCL cells from serial biopsies of Patient 1. The accession number for the protein sequence is NP_000052.1. **B,** integrative genomics viewer (IGV) visualization of nucleotide substitutions (red and green) and alignments of *BTK* on chromosome X (ChrX):100611161-100611166. **C,** identification by Sanger sequencing of G1442C and C1443T in *BTK* in bone marrow and spleen biopsies at relapse (r_IbBM, r_IbSP), and the wild-type sequence in the bone marrow biopsy immediately before initiation of ibrutinib treatment (p_Ib3). **D** and **E,** WTS analysis of mRNA abundance (RPKM, reads per kilobase per million reads; bars) and nonsynonymous SNVs (% of alternative allele, red line) in CDS and UTRs of genes commonly mutated in MCL. PBC, CD19^{+} B cells isolated from peripheral blood of healthy donors.

inactivated in lymph node (Patient 6) and peripheral blood (Patient 9) MCL cells of primary ibrutinib-resistant patients while on ibrutinib treatment, in which AKT was expressed at a high level and activated.

Primary MCL cells predominantly express PI3Kδ (*PIK3CD*), the hematologic lineage-restricted PI3K isoform (24), whereas PI3Kα (*PIK3CA*) is expressed at a lower level in some cases of MCL. PI3Kβ (*PIK3CB*) and PI3Kγ (*PIK3CG*) were barely expressed, and the regulatory subunits *PIK3R5* and *PIK3R6* were undetectable (16). However, expression of PI3Kα was not associated with the ibrutinib response, as PI3Kα was expressed in MCL cells of Patient 4 (PR), Patient 1, and Patient 3 (progression following a transient PR) and all 3 primary resistant patients, but not in Patient 8 (SD) or Patient 5 (progression following transient PR; Fig. 3A and B). Primary ibrutinib resistance or transient response, therefore, seems not to stem from defective ibrutinib inhibition of *BTK*^{WT} in MCL cells but rather may involve sustained PI3K–AKT activation.

Published OnlineFirst July 31, 2014; DOI: 10.1158/2159-8290.CD-14-0098

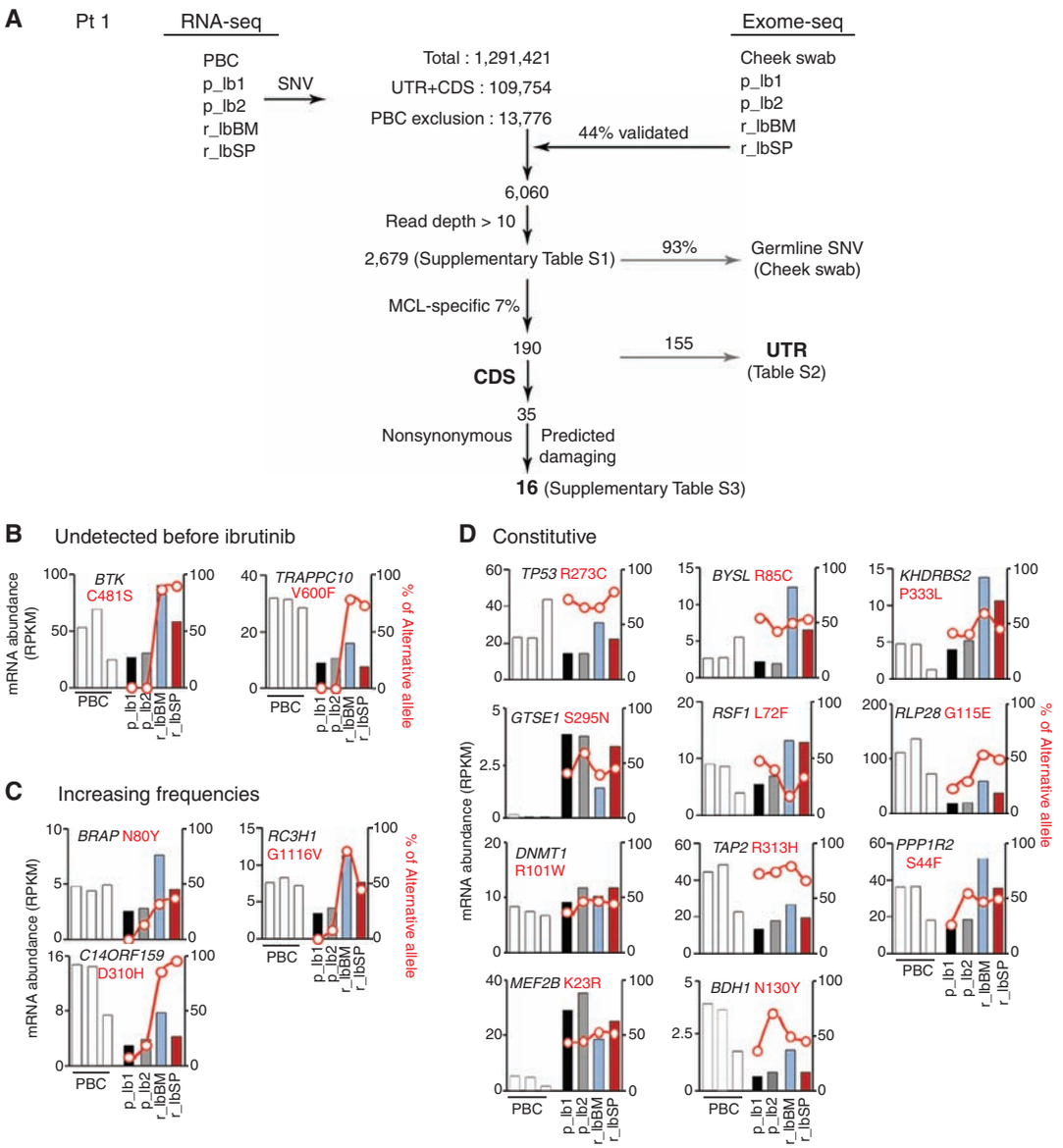

Figure 2. Longitudinal integrative WES and WTS analysis of acquired resistance following a durable response in MCL harboring *BTK*^{C481S}. **A,** SNVs (1,291,421) were identified in MCL cells from serial biopsies of Patient (Pt) 1 before ibrutinib treatment (p_lb1, p_lb2) and after relapse from ibrutinib (r_lbBM, r_lbSP) by WTS using the Illumina platform and Genesifter (Geospiza). After exclusion of SNVs detected in PBC libraries, 44% ($n = 6,060$) of the 13,776 SNVs were also detected by WES analysis. A threshold of 10× coverage was applied, which reduced the number of SNVs to 2,679. After exclusion of the germline SNVs present in the cheek swabs, 190 SNVs were specific to the MCL cells of this patient: 155 detected in UTRs and 35 in CDS, of which 16 were predicted to be damaging at the protein level by SIFT, PROVEAN, or PolyPhen-2. Among them, 5 were detected at increasing frequency in serial biopsies but only *BTK*^{C481S} and *TRAPPC10*^{V600F} mutations were detected at relapse exclusively (**B** and **C**), and 11 were present in all biopsies (**D**). The percentage of alternative allele (red) and mRNA abundance (RPKM) of the indicated genes are shown. Mutations are shown in red text.

Activation of BTK and AKT at Relapse in MCL Cells Harboring *BTK*^{C481S} Mutation

The functional consequence of C481S mutation *in vivo* was then characterized in MCL cells isolated from serial biopsies of Patient 1. Ibrutinib inhibits BTK activity irreversibly by covalently binding to cysteine 481 *in vitro* and in cell lines (5), and the C481S mutation has been shown to markedly reduce (~25-fold) the affinity of BTK for ibrutinib in a model chicken lymphoma DT40 cell line (23). Notably, BTK was constitutively active in lymph node MCL cells before ibrutinib therapy and in peripheral blood B cells (PBC) from healthy donors, presumably for their survival (Fig. 3C). Activation of BTK was increased in bone marrow MCL cells at relapse, concurrent with a modest increase in PI3Kα and PI3Kδ and activation of AKT (pS473; Fig. 3C).

Published OnlineFirst July 31, 2014; DOI: 10.1158/2159-8290.CD-14-0098

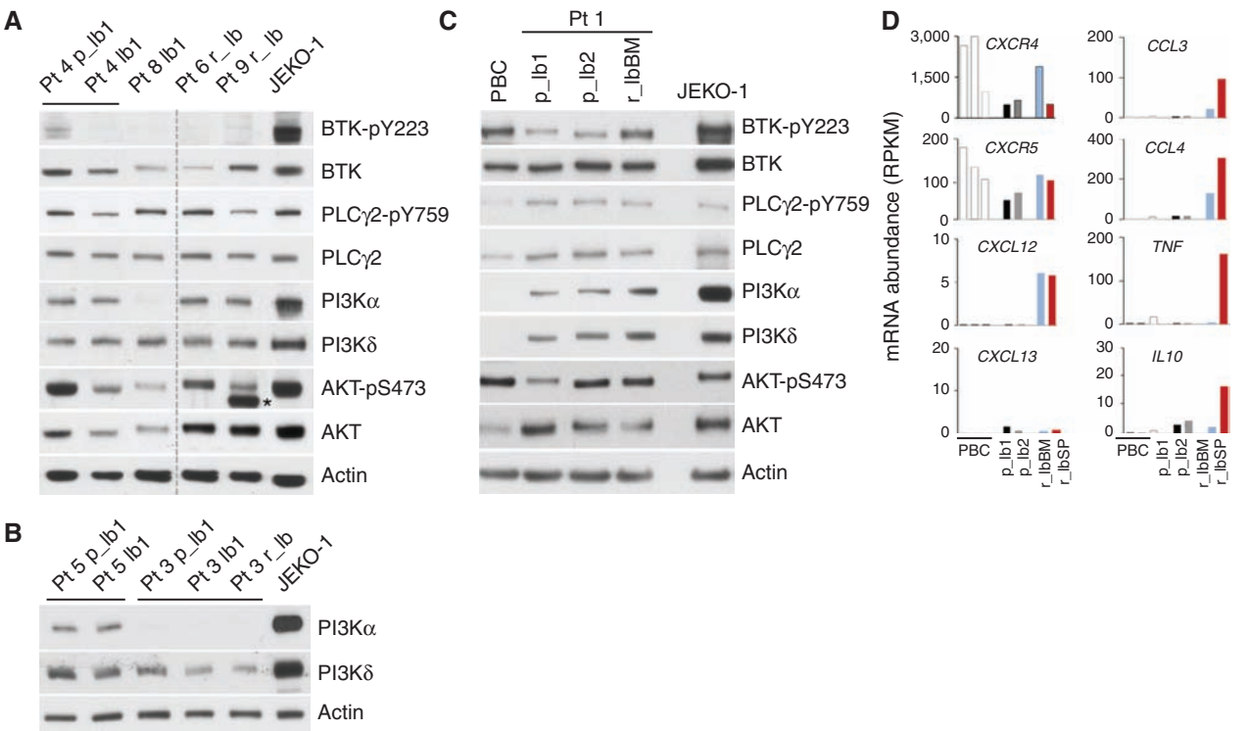

Figure 3. Concurrent inactivation of *BTK*^{WT} and AKT by ibrutinib in responding patients and AKT activation independent of *BTK*^{WT} inactivation in ibrutinib-resistant patients. **A** and **B,** immunoblotting of indicated proteins in MCL cells isolated from responding Patient (Pt) 4 before (Pt 4 p_Ib1) and on day 21 of ibrutinib treatment (Pt 4_Ib1); Pt 8 on day 21 of ibrutinib treatment (Pt 8 Ib_1); primary resistant Pt 6 and Pt 9 on day 21 of ibrutinib treatment; Pt 5 and Pt 3 before ibrutinib treatment (Pt 5 p_Ib1, Pt 3 p_Ib1), on day 21 (Pt 5 Ib1, Pt 3 Ib1) of ibrutinib treatment, and at relapse (Pt 3 r_Ib) after 3 months of ibrutinib response (See Supplementary Table S5 for details). *denotes a nonspecific signal in **A**. **C,** immunoblotting of MCL cells from serial lymph node biopsies of Pt 1 before ibrutinib treatment (p_Ib1, p_Ib2) and from the bone marrow at relapse from ibrutinib (r_IbBM). CD19$^+$ B cells isolated from peripheral blood of healthy donors (PBCs) and JEKO-1 cells were used as controls. **D,** WTS analysis of mRNA abundance (RPKM) of indicated genes expressed in serial biopsies of Pt 1 and PBCs, as shown in Fig. 1.

The increase in PI3Kα and PI3Kδ proteins mirrored the selective increases in the abundance of *PIK3CD* and *PIK3CA* mRNA in MCL cells in the bone marrow and the spleen, suggesting that it stems, in part, from transcriptional activation of PI3Kα and PI3Kδ (data not shown). Collectively, these data suggest that the C481S mutation relieves BTK from ibrutinib inhibition, leading to heightened activation of BTK and AKT-pS473 in resistant bone marrow MCL cells *in vivo*.

Relapse from ibrutinib was also associated with a preferential increase in *CXCR4*, but not *CXCR5*, mRNA in bone marrow MCL cells; and induction of *CXCL12*, but not *CXCL13*, mRNA in MCL cells in both the bone marrow and the spleen and *CCL3*, *CCL4*, *TNF*, and *IL10* in the spleen (Fig. 3D). Because the expression of these chemokines and cytokines has been shown to promote proliferation and survival of MCL cells and to be inhibited by ibrutinib *ex vivo* (25), the tissue-specific upregulation at relapse provides additional functional evidence for ibrutinib resistance *in vivo*.

Tissue-Specific Cell-Cycle Control of Proliferation of *BTK*^{C481S} MCL Cells at Relapse

Unrestrained tumor cell proliferation is characteristic of ibrutinib relapse in MCL. Progression of Patient 1 was associated with massive splenomegaly and mild lymphadenopathy, suggesting a tissue-specific response. Longitudinal WTS analysis of cell-cycle genes showed that, as expected, most cell-cycle genes were expressed at a higher level in MCL cells than in resting PBCs from normal donors (Fig. 4A). However, *MKI67* (Ki67) mRNA was markedly repressed in the bone marrow at relapse, concurrent with selective elevation of *CDK4* mRNA among genes scheduled for early G_1 in both bone marrow and splenic MCL cells, and *CCNA2*, *CCNB1*, and *CDK1* mRNAs (S and G_2–M) in splenic MCL cells (Fig. 4A). These genes were expressed correspondingly at the protein level in bone marrow and splenic MCL cells, along with a reduction of p27 protein and increases in cyclin A and cyclin B in the splenic MCL cells (pretherapy MCL cells were no longer available for protein analysis; Fig. 4B). Surprisingly, the *MYC* mRNA level was lower in the MCL cells of Patient 1 than in the PBCs, and the c-MYC protein was undetectable despite a striking (>200-fold) increase in *MYC* mRNA in splenic MCL cells (Fig. 4B). Collectively, these data indicate that preferential proliferation of MCL cells in the spleen at relapse in this patient is independent of c-MYC, and partly driven by selective upregulation of CDK4, which cooperates with cyclin A, cyclin B, and CDK1 to accelerate the cell cycle in MCL cells.

Published OnlineFirst July 31, 2014; DOI: 10.1158/2159-8290.CD-14-0098

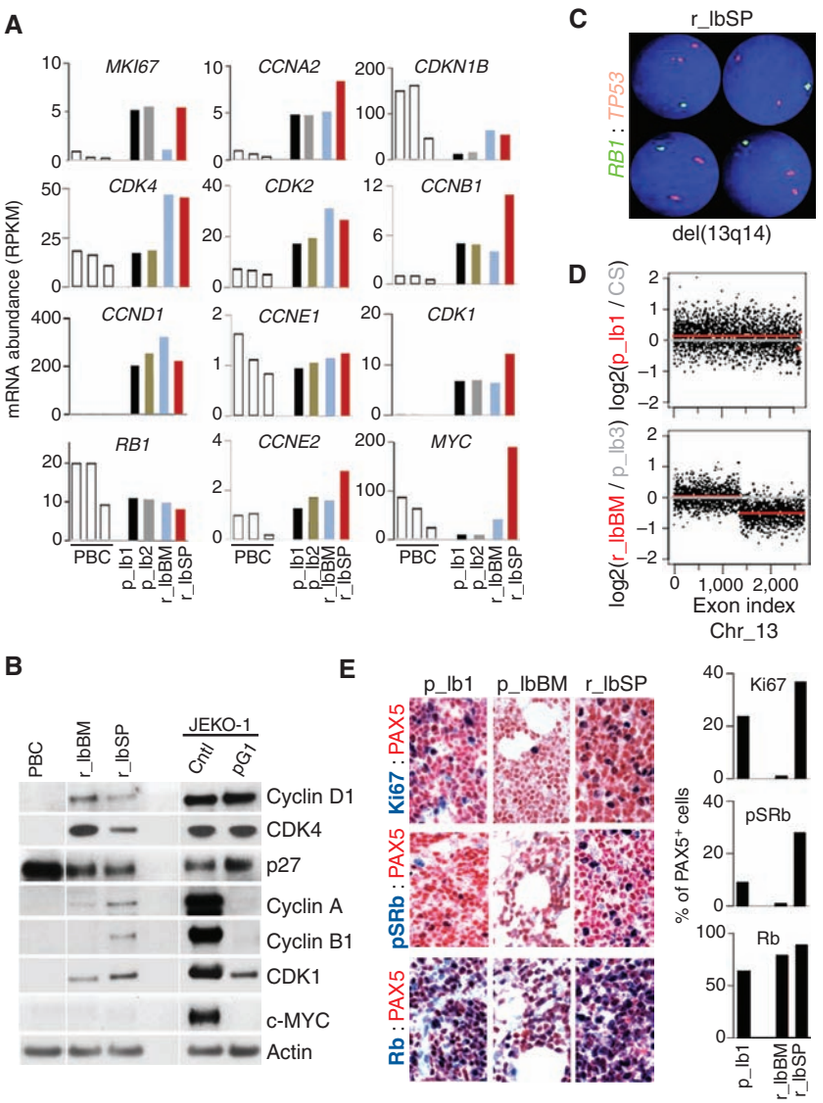

Figure 4. Tissue-specific cell-cycle control of proliferation of *BTK*^{C481S} MCL cells at relapse. **A,** WTS analysis of mRNA abundance (RPKM) of indicated genes in serial biopsies of Patient (Pt) 1 before ibrutinib treatment (p_Ib1, p_Ib2) and at relapse (r_IbBM, r_IbSP) and PBCs. **B,** immunoblotting of indicated proteins in serial biopsies of Pt 1 at relapse from ibrutinib (r_IbBM, r_IbSP) and PBCs. JEKO-1 cells treated with PD 0332991 (PD, 0.3 μmol/L) for 72 hours or left untreated were used as a control. **C,** FISH was performed on a spleen section at relapse using a green-labeled LSI 13 (13q14) probe spanning the *RB1* region, and an orange-labeled LSI TP53 probe as a control. **D,** CNV analysis of chromosome 13 (Chr_13) of the WES data before ibrutinib treatment (p_Ib1; top) and at ibrutinib relapse (r_IbBM) samples (bottom) of Pt 1. CS, cheek swab. **E,** representative images of IHC analysis of Ki67, pSRb, and Rb in MCL cells (PAX5$^+$) cells in the lymph node before ibrutinib treatment (p-Ib1) and at relapse in the bone marrow (r_IbBM) and spleen (r_ibSP; left), and quantification (right).

Cytogenetic and FISH analyses further revealed a complex karyotype in proliferating splenic MCL cells at relapse. Multiple numerical and structural abnormalities were observed, most notably the hemizygous deletion of chromosome 13q that encompasses the *RB1* gene (Fig. 4C). Copy-number variation (CNV) analysis of serial WES of purified MCL cells independently identified the hemizygous 13q deletion at relapse in bone marrow MCL cells (Fig. 4D), and discovered two additional relapse-specific hemizygous deletions in 21q that included the *TRAPPC10* gene (data not shown). However, *RB1* expression was unabated at the mRNA level in MCL cells at relapse (Fig. 4A), presumably through a dosage compensation mechanism to ameliorate the haploinsufficiency. Relapse from ibrutinib in Patient 1 is, thus, associated with exacerbated genomic instability of MCL cells in the presence of sustained *RB1* expression.

Further evaluation of proliferation of MCL cells *in situ* in serial biopsies by IHC demonstrated that more MCL cells (PAX5$^+$) were cycling (Ki67$^+$) in the spleen at relapse (r_IbSP) than in the lymph nodes before ibrutinib therapy (p_Ib1; Fig. 4E). This was apparently driven by accelerated progression through early G_1, given the >3-fold increase in CDK4/CDK6–specific phosphorylation of Rb (pSRb; Fig. 4E). In contrast, few bone marrow MCL cells cycled or expressed pSRb at relapse despite the common *BTK*^{C481S} mutation (Fig. 4E). These results confirm that in Patient 1, MCL cells harboring the C481S mutation preferentially proliferate in the spleen due to CDK4 activation but rarely in the bone marrow at relapse.

pG1 Sensitizes Resistant *BTK*^{WT} MCL Cells to Ibrutinib via Synergic Induction of *PIK3IP1*

Previously, we have shown that induction of pG1 by sustained inhibition of CDK4 with the selective inhibitor PD 0332991 reprograms cancer cells for killing by diverse cytotoxic partners (14, 16). Given that *BTK*^{WT} was inhibited by ibrutinib in highly proliferative primary resistant MCL cells *in vivo* (Fig. 3A), induction of pG1 may lower the threshold

Published OnlineFirst July 31, 2014; DOI: 10.1158/2159-8290.CD-14-0098

of ibrutinib killing in addition to inhibiting the cell cycle (Fig. 5A).

We tested this hypothesis in four RB1-positive MCL cell lines harboring no mutations in *BTK* or *PLCG2* (WES data not shown) by first confirming that PD 0332991 induced pG1, which maintained cyclin D1 and CDK4 expression, elevated p27 protein levels, and prevented the expression of cyclin A, cyclin B, CDK1, and c-MYC protein as expected for pG1 (Fig. 4B). Ibrutinib (0.01–1 μmol/L) was not toxic to JEKO-1, MAVER-1, or Mino MCL cells, although it moderately inhibited S phase entry in Mino cells and potently induced apoptosis in SP53 cells during G_1–S transition by 48 hours, as shown by BrdUrd/PI analysis (Supplementary Fig. S1). pG1 did not augment ibrutinib killing of SP53 cells, but profoundly inhibited the expansion of live cells through cell-cycle control (Fig. 5B). Importantly, induction of pG1 both prevented the ibrutinib-resistant JEKO-1, MAVER-1, and MINO cells from replicating and sensitized them to ibrutinib-induced apoptosis (AnnexinV$^+$/PI$^+$), resulting in a 50- to 100-fold reduction of live cells by 96 hours of ibrutinib treatment (Fig. 5B).

We have recently uncovered that synergistic induction of *PIK3IP1*, a negative regulator of PI3K (26), mediates pG1 reprogramming of MCL cells for durable and enhanced killing by selective PI3K inhibition (16). *PIK3IP1* mRNA expression in MCL cells from all serial biopsies of Patient 1 was 10- to 30-fold lower than in PBCs (Fig. 5C), consistent with previous observations in primary MCL cells (16). It was induced by pG1 and by ibrutinib modestly, but by ibrutinib and pG1 synergistically (~50 fold) in JEKO-1 and MAVER-1 cells (Fig. 5D). Knocking down *PIK3IP1* by two independent shRNA–lentivirus constructs blunted the enhancement of ibrutinib killing in pG1, but not the death induced by pG1 alone in JEKO-1 or MAVER-1 cells (Fig. 5E). Thus, induction of pG1 by selective CDK4 inhibition not only prevents refractory MCL cells that are expressing the wild-type BTK from proliferating, but also reprograms them for ibrutinib killing through synergistic induction of *PIK3IP1*.

pG1 and Ibrutinib Cooperatively Inactivate BTK, AKT, and NF-κB in BCR Signaling

BTK and AKT were coordinately inactivated on ibrutinib treatment in MCL cells of a responding patient (Patient 4). However, AKT activation (pS473) was maintained despite inactivation of *BTK*^{WT} in MCL cells of primary resistant patients (Patient 6 and Patient 9; Fig. 3A). Because pG1 inactivates AKT in primary MCL cells *ex vivo* (16), it may sensitize *BTK*^{WT}-resistant MCL cells to ibrutinib through inactivation of AKT. Indeed, activation of BTK (pY223) and AKT (pS473) in BCR signaling stimulated by anti-IgM was partially neutralized by ibrutinib and in pG1, but completely abolished by ibrutinib in pG1-reprogrammed JEKO-1 cells (Fig. 6A). This finding was reminiscent of synergistic and durable inhibition of AKT activation by a PI3K inhibitor in pG1, which led to enhanced killing of primary MCL cells and MCL cell lines by PI3K inhibitors (16), suggesting that inactivation of PI3K–AKT mediates pG1 reprogramming of MCL cells for killing by both ibrutinib and PI3K inhibitors.

Primary resistance to ibrutinib despite inactivation of *BTK*^{WT} suggests that activation of distal BCR signaling may contribute to ibrutinib resistance. The classic (p50/RELA)

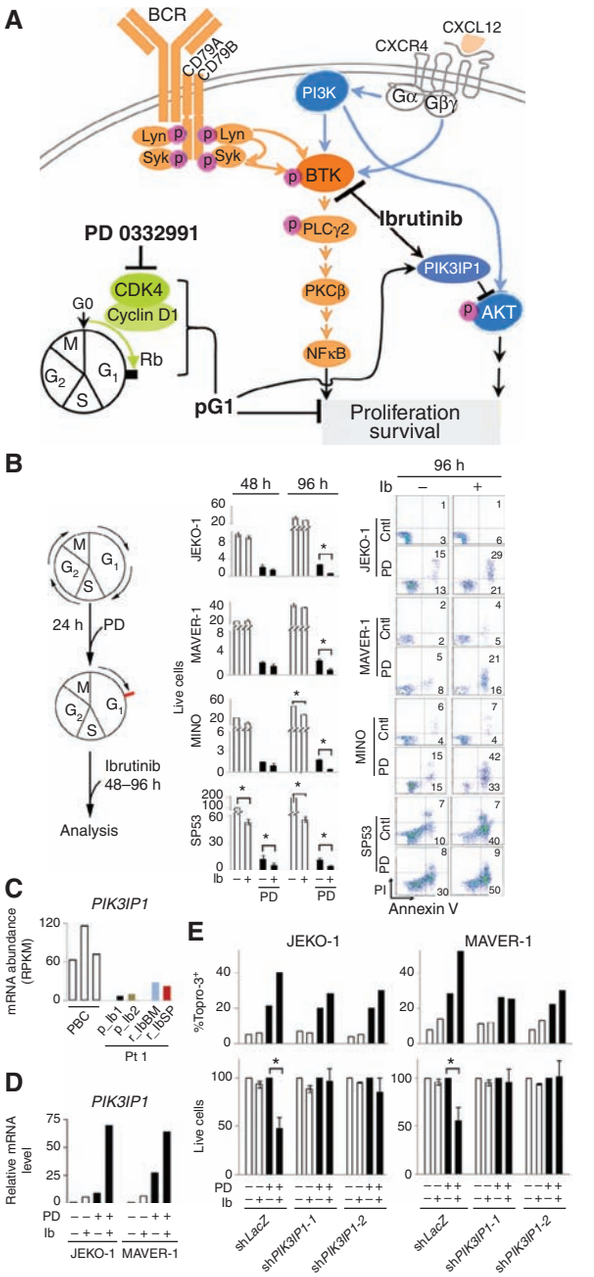

Figure 5. pG1 sensitizes resistant *BTK*^{WT} MCL cells to ibrutinib via synergic induction of *PIK3IP1*. **A,** schema for dual targeting of BTK with ibrutinib and CDK4 with PD 0332991 in MCL cells expressing *BTK*^{WT}. *pG1*, prolonged early G_1 arrest that exceeds the schedule early G_1 transit time (16–20 hours in MCL cells) by selective and sustained inhibition of CDK4. **B,** schema for sequential incubation with PD 0332991 (0.3 μmol/L) and ibrutinib (left), total viable cells (×20,000 cells/mL) at 48 and 96 hours of ibrutinib treatment (1 μmol/L for JEKO-1, MAVER-1, and MINO and 0.1 μmol/L for SP53; middle), FACS analysis of apoptotic (Annexin V$^+$/PI$^+$) MCL cells at 96 hours of ibrutinib treatment (right). **C,** WTS analysis of *PIK3IP1* mRNA abundance in serial biopsies of Patient (Pt) 1 and PBCs. **D,** qRT-PCR analysis of relative *PIK3IP1* mRNA levels in MCL cells cultured with PD for 72 hours and ibrutinib for 48 hours as indicated. **E,** live cells (percentage of untreated cells) and cell death (Topro-3$^+$ cells) in MCL cell lines infected with *PIK3IP1* shRNA or *LacZ* shRNA lentivirus and treated with PD and ibrutinib as in D. Error bars, SD. *, $P < 0.05$, calculated using the Student *t* test. Data are representative of four independent experiments.

Published OnlineFirst July 31, 2014; DOI: 10.1158/2159-8290.CD-14-0098

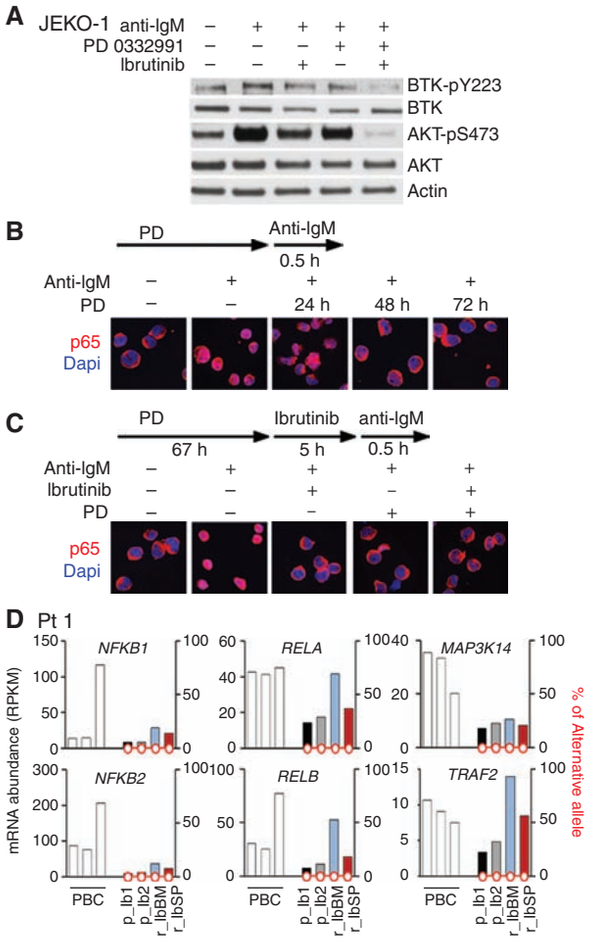

Figure 6. pG1 and ibrutinib cooperatively inhibit BTK, AKT, and NF-κB activation in BCR signaling. **A,** immunoblotting of activated BTK (pY223) and total BTK, and activated AKT (pS473) and total AKT proteins in JEKO-1 cells cultured in the presence or absence of PD 0332991 (0.3 μmol/L) for 24 hours before addition of ibrutinib (1 μmol/L) and goat anti-human IgM (α-IgM; 5 μg/mL) for 24 hours. **B** and **C,** immunofluorescence staining of p65 subcellular localization (red). The nucleus was counterstained with DAPI (blue) in JEKO-1 cells cultured with PD 0332991 for time indicated and α-IgM (5 μg/mL) for 0.5 hours in **B** or cultured with PD 0332991 for 67 hours before addition of Ibrutinib for 5 hours and anti-IgM for 0.5 hours in **C**. Data are representative of three independent experiments. **D,** WTS analysis of mRNA abundance and nonsynonymous SNVs in the CDS of genes indicated in serial biopsies of Patient (Pt) 1 before ibrutinib treatment (p_Ib1, p_Ib2) and at relapse from ibrutinib (r_IbBM, r_IbSP).

NF-κB pathway mediates BCR signaling for B-cell proliferation and survival (4), further indicating that pG1 may reprogram MCL cells by attenuating NF-κB activation. To address this possibility, we showed by immunofluorescence staining (IMF) that nuclear localization of RELA (p65) indicative of NF-κB activation in response to anti-IgM was undetectable in some JEKO-1 cells by 24 hours of PD 0332991 treatment and completely absent by 48 hours (Fig. 6B). Thus, in a time-dependent manner, pG1 reconstitutes the rapid (within 5 hours) inactivation of the classic NF-κB pathway by ibrutinib in BCR signaling (Fig. 6B and C). The alternative (p52/RELB) NF-κB pathway has been shown recently to contribute to ibrutinib resistance in MCL cell lines (20). p52 was expressed in the ibrutinib-resistant JEKO-1 cells used in this study but not appreciably inhibited by ibrutinib in pG1, along with invariable expression of NIK (*MAP3K14*) required for the processing of p100 to p52 (Supplementary Fig. S2).

Longitudinal WES/WTS analysis of serial biopsies of Patient 1 further revealed an association of ibrutinib relapse with upregulation of selective genes of the classic NF-κB pathway such as *NFKB1* and *RELA* as well as *NFKB2* and *RELB* of the alternative NF-κB pathway in bone marrow MCL cells, although *MAP3K14* expression did not vary (Fig. 6D). Taken together, these data suggest tissue-specific upregulation of genes in the NF-κB pathways at relapse in a patient with BTK^{C481S} mutation, and that pG1 reprograms MCL cells for cytotoxic killing, in part by selective inactivation of the classic, but not the alternative, NF-κB pathway.

pG1 Sensitizes Resistant Lymphoma Cells Independent of BTK^{C481S} Mutation to PI3K Inhibitors

PI3K is required for B-cell development and proliferation (27), and acts upstream of BTK for BCR-dependent survival in mature B cells (28). Expression of PI3K and AKT was sustained in all patients with MCL, whereas activation of ATK (pS473) was reduced in an ibrutinib-responding patient, sustained in BTK^{WT} MCL cells of primary resistant patients, and enhanced in BTK^{C481S} MCL cells in a patient at relapse from a durable ibrutinib response (Fig. 3). Because pG1 reprograms primary MCL cells for PI3K inhibitor killing *ex vivo* through durable inhibition of AKT activation (16), it may sensitize ibrutinib-resistant lymphoma cells to PI3K inhibitors independent of the BTK^{C481S} mutation (Fig. 7A).

To test this hypothesis, we reconstituted the expression of V5-tagged BTK^{WT} and BTK^{C481S} in equal molar in the DT40 $BTK^{-/-}$ chicken lymphoma cell line, in which the BTK^{C481S} has been shown to attenuate ibrutinib-mediated inhibition of BTK (ref. 23; Fig. 7B and C). The expression of p110δ, p110α and AKT and AKT activation in DT40 $BTK^{-/-}$ cells were not altered by stable expression of BTK^{WT}, BTK^{C481S}, or the GFP-V5 vector (Fig. 7C). Sustained inhibition of CDK4 by PD 0332991 led to pG1 in DT40 cells expressing either BTK^{WT} or BTK^{C481S} (Fig. 7D), which were then reprogrammed for killing by three clinically relevant selective PI3K inhibitors independent of the BTK^{C481S} mutation. pG1 conferred sensitivity to the PI3Kδ-specific inhibitor GS-1101 (idelalisib; refs. 29–31), which alone did not kill DT40 cells expressing BTK^{WT} or BTK^{C481S}, presumably due to functional compensation by the PI3Kα expressed in these cells. Thus, it seems that when combined with inhibition of PI3Kδ and ATK activation, pG1 bypasses PI3Kα. pG1 also profoundly enhanced killing by the dual PI3Kα/δ inhibitors BAY 80-6946 (copanlisib; ref. 32) and GDC-0941 (pictilisib; ref. 33; Fig. 7E; Supplementary Fig. S3). Sensitization by pG1 led to virtual eradication of live cells by all PI3K inhibitors characterized, even when BTK^{C481S} was expressed at a 5-fold excess of BTK^{WT} (Fig. 7E and Supplementary Fig. S3). Induction of pG1 by sustained CDK4 inhibition thus profoundly reprograms ibrutinib-resistant lymphoma cells for PI3K inhibitor killing independent of the BTK^{C481S} mutation.

Published OnlineFirst July 31, 2014; DOI: 10.1158/2159-8290.CD-14-0098

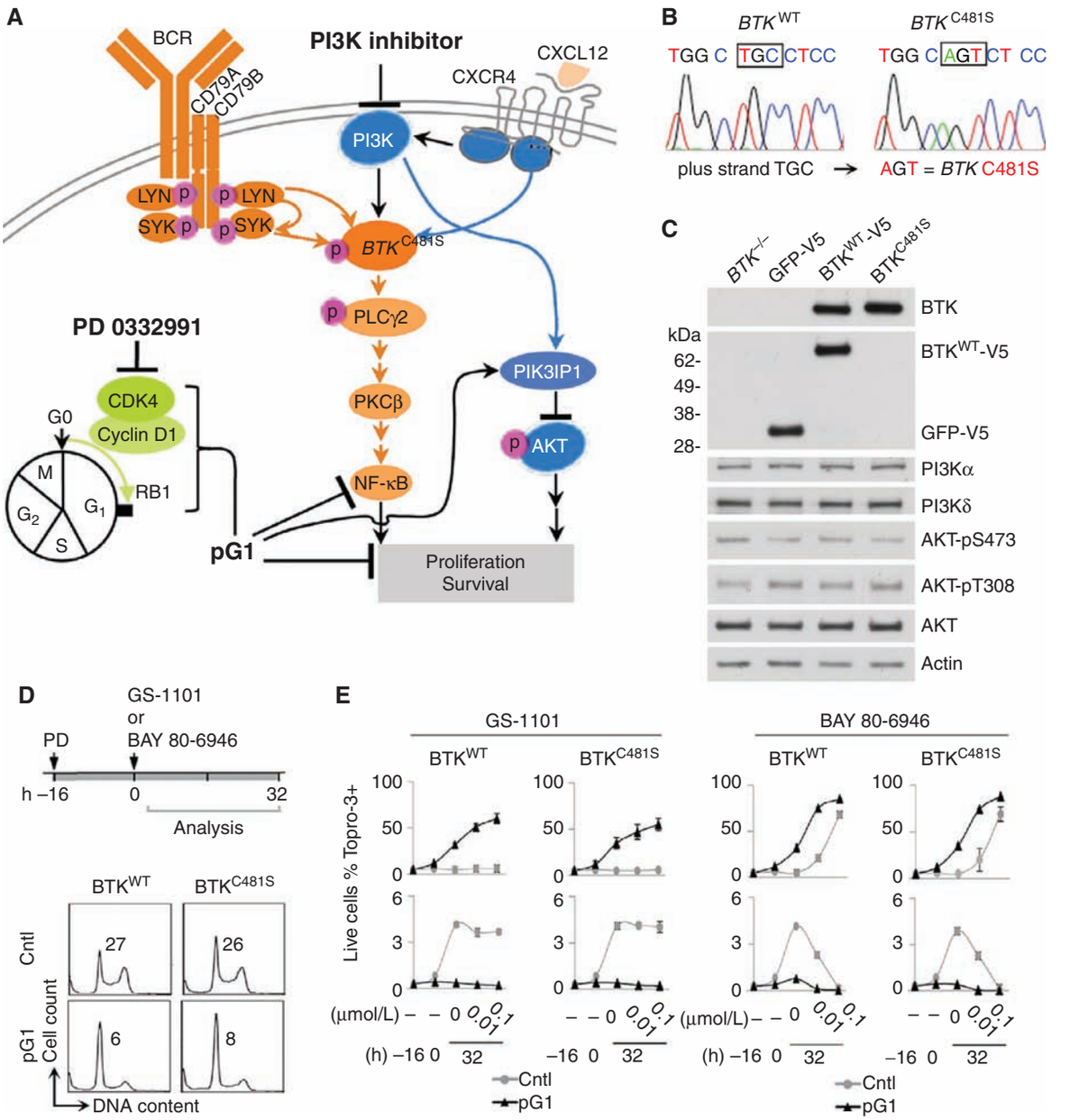

Figure 7. pG1 sensitizes resistant lymphoma cells to inhibition of PI3K independent of *BTK*^{C481S} mutation. **A,** schema for overriding the *BTK*^{C481S} mutation by dual inhibition of CDK4 and PI3K. **B,** confirmation of the *BTK* sequence (WT or C481S) reconstituted in DT40 *BTK*$^{-/-}$ cells by Sanger sequencing. **C,** immunoblotting of the indicated proteins in DT40 *BTK*$^{-/-}$ cells stably infected with a lentivirus expressing human BTK^{WT}-V5, BTK^{C481S}-6xHis, or the GFP-V5 control vector as described in the Supplementary Methods. **D,** cell-cycle analysis by propidium iodide staining of DT40_BTK^{WT} and DT40_BTK^{C481S} cells cultured with PD 0332991 (PD; 0.3 μmol/L) for 16 hours. Number in the FACS profile indicates the percentage of cells in S phase as analyzed by FlowJo. **E,** DT40_BTK^{WT} and DT40_BTK^{C481S} cells were cultured in the absence (Cntl) or presence of PD 0332991 (pG1) as in **D** before addition of GS-1101 or BAY 80-6946 for 32 hours at concentrations indicated in the continuous presence of PD 0332991. Cell death was determined by ToPro-3 staining and FACS analysis. The total number of live cells was determined by Trypan Blue staining (×10^6 cells/mL). Error bars, SD. Data are representative of three independent experiments.

DISCUSSION

Acquired resistance to therapy remains a formidable challenge in human cancer. It is particularly urgent in MCL, which remains incurable due to the development of drug resistance even to the novel BTK inhibitor ibrutinib, despite its exceptional single-agent activity. By longitudinal integrative WES and WTS analysis of MCL cells from serial biopsies of a patient with MCL who progressed following a durable PR, we have now identified the first relapse-specific C481S missense mutation at the ibrutinib-binding site of BTK in MCL. The heightened activation of BTK and AKT,

Published OnlineFirst July 31, 2014; DOI: 10.1158/2159-8290.CD-14-0098

induction of the CXCR4–CXCL12 autocrine loop, and derepression of growth-promoting CCL3 and CCL4, TNFα and IL10, in *BTK*^{C481S} MCL cells at relapse (Figs. 1 and 3) provided the first functional evidence *in vivo* for impaired BTK inhibition caused by a BTK mutation in acquired ibrutinib resistance.

The acquired resistance to ibrutinib could be treatment-related or due to clonal evolution, which are not mutually exclusive. Although no mutations in BTK have been identified by WES or WTS in ibrutinib-naïve MCL patients so far, the existence of a *BTK*^{C481S}-mutant clone at a very low frequency before treatment cannot be excluded, as demonstrated by <0.01% of cells becoming the predominant clone in relapsed leukemia (34). In addition, the *BTK*^{C481S} is likely to confer a selective advantage over MCL cells expressing *BTK*^{WT} and responding to ibrutinib-mediated killing. Consistent with a clonal origin, ibrutinib-resistant MCL cells at relapse in bone marrow and spleen of Patient 1 have in common: (i) identical dinucleotide substitution in *BTK*; (ii) unique concurrent high-frequency *TRAPPC10*^{V600F} mutation; (iii) exacerbated genomic instability in the absence of mutations in *ATM*, the most frequently mutated gene in MCL (35), and hemizygous 13q deletion (Fig. 4).

This raises the question of whether other nonsynonymous potentially damaging mutations, identified by WES and WTS analysis, contribute to the development of acquired ibrutinib resistance in MCL. Of particular interest is the increasing frequency of the N80Y mutation in *BRAP,* a BRCA2–binding protein; the constitutive R273C mutation in *TP53* and S295N mutation in *GTSE1,* a p53-binding protein and G_2–M checkpoint regulator and the K23R mutation in *MEF2B*, a transcriptional activator frequently mutated in MCL (19) and in diffuse large B-cell lymphoma, which led to deregulation of the target oncogene *BCL6* (Fig. 2; ref. 36).

Detection of *BTK*^{C481S} in a second patient with MCL who progressed following an even more durable PR (30 months), but not in any of the 6 patients with MCL who progressed on ibrutinib within 5 months or failed to respond, suggests that the C481S mutation in MCL is specific to acquired ibrutinib resistance after a durable response. Although this possibility is being addressed in a larger MCL patient population, alternative mechanisms must have contributed to primary or rapid resistance to ibrutinib.

The *BTK*^{C481S} mutation has been identified by WES in 5 of 13 CLL patients who relapsed while on ibrutinib (23). Apart from this common genomic aberration, ibrutinib resistance in MCL is distinguishable from that in CLL in other aspects. First, disease progression on ibrutinib is much more frequent in MCL (50 of 115 with a median follow-up of 15.3 months; ref. 6) than in the more indolent CLL (11 of 85 with a median follow-up of 20.9 months; ref. 7), suggesting that more proliferative lymphomas may be less well controlled by ibrutinib. Second, the gain-of-function R665W mutation in PLCγ2 identified in CLL (23) has not been detected in MCL (Supplementary Table S5). Third, BTK was inactivated by ibrutinib in *BTK*^{WT} MCL cells of patients with primary resistance (Fig. 3), suggesting that dysregulation of distal BCR signaling other than through an activating PLCγ2 mutation contributes to rapid ibrutinib resistance. Fourth, the enhanced BTK and PI3K–AKT activation at relapse in *BTK*^{C481S} MCL cells provided the first evidence for divergent functional consequences caused by *BTK*^{C481S} mutation *in vivo* and reinforces the critical importance of developing genome-based combination therapy in MCL.

Relapse from ibrutinib is often characterized by aggressive proliferation of resistant MCL cells and poor clinical outcomes. Here, we show that it was also associated with sustained AKT activation (pS473) in *BTK*^{WT} MCL cells with primary resistance and enhanced AKT activation (pS473) in *BTK*^{C481S} MCL cells at relapse (Fig. 3). These findings demonstrate a pivotal role of PI3K–AKT activation in ibrutinib resistance and provide a strong rationale to override ibrutinib resistance by targeting the cell cycle in combination with inhibition of BTK or PI3K. Indeed, induction of pG1 by PD 0332991 inhibition of CDK4 reprograms MCL cells expressing *BTK*^{WT} for killing by ibrutinib, which, together with inhibition of cell proliferation, resulted in a dramatic reduction of live cells (Fig. 5). Furthermore, pG1 sensitizes ibrutinib-resistant MCL cell lines (16) and DT40 lymphoma cells independent of *BTK*^{C481S} mutation to killing by clinically relevant PI3K inhibitors (Fig. 7), which has important mechanistic and clinical implications.

Previously, we have shown that induction of pG1 by selective CDK4/CDK6 inhibition leads to restricted expression of genes scheduled for early G_1 only, thereby forcing an imbalance in gene expression that reprograms cancer cells for killing by diverse cytotoxic partners (14). *PIK3IP1* was synergistically induced by a PI3K inhibitor (GS-1101 or GDC-0941) and pG1 in MCL cells for enhanced killing through sustained inhibition of pAKT (16). Here, we demonstrated that PIK3IP1 was also synergistically induced by ibrutinib and pG1 in MCL cells to mediate pG1 enhancement of ibrutinib killing, most likely by abrogating the activation of BTK and AKT in BCR signaling (Figs. 5 and 6). PIK3IP1 thus plays a pivotal role in pG1 sensitization of MCL cells to killing by either PI3K or BTK inhibitor. As such, it represents a novel molecular therapeutic biomarker for pG1 combination therapy.

In addition, we have now discovered that pG1 selectively antagonizes the activation of the classic NF-κB pathway in BCR signaling, but not the alternative NF-κB pathway (Fig. 6). Inactivation of NF-κB in pG1 is redundant with inhibition of BTK by ibrutinib, but it may cooperate with inactivation of PI3K–AKT in pG1-reprogrammed MCL cells to enhance PI3K inhibitor killing independent of the *BTK*^{C481S} mutation. By inactivating NF-κB, pG1 antagonizes BCR signaling downstream of PKCβ, and could also bypass various gain-of-function upstream mutations in the BCR signaling pathway (Fig. 5A). Given the importance of NF-κB in transcriptional regulation, inactivation of NF-κB may, in fact, mediate the imbalance in gene expression in pG1, thereby playing a broader role in pG1 reprogramming.

Targeting CDK4 with PD 0332991 in combination with PI3K or BTK inhibition is poised for clinical validation in MCL as well. PD 0332991 had already achieved a durable clinical response with a favorable toxicity profile in the first single-agent clinical trial in patients with recurrent MCL (11). It is now a breakthrough therapy for metastatic breast cancer owing to its exceptional clinical activity when combined with letrozole. Although pG1 reprogramming by PD 0332991

Published OnlineFirst July 31, 2014; DOI: 10.1158/2159-8290.CD-14-0098

requires Rb, the substrate of CDK4 and CDK6 (14, 16), it is independent of *ATM* and *TP53*, the most frequently mutated genes in MCL (17).

As for targeting PI3K, the novel PI3Kδ-specific inhibitor GS-1101 is a breakthrough therapy for CLL that exhibits transient clinical activity in MCL. We showed that pG1 reprogrammed primary MCL cells for sustained and enhanced growth inhibition by GS-1101 via inhibition of AKT activation, and by the dual PI3Kα/δ inhibitor GDC-0941 (16) and BAY 80-6946 (Fig. 7). CDK4 and PI3K are dysregulated at a high frequency in human cancers that develop resistance to therapy (37). To overcome drug resistance by targeting the cell cycle, one of the critical next steps is to define the mechanism by which pG1 inactivates PI3K–AKT. Given that the carboxyl-terminus of AKT is directly phosphorylated by CDK2/cyclin A (38) and that induction of pG1 suppresses cyclin A synthesis (14), it seems likely that pG1 may inactivate AKT via cyclin A suppression (Fig. 4). This exciting possibility is amenable to investigation in targeting CDK4 in clinical studies by longitudinal integrative WTS.

Our unbiased, longitudinal integrative WES and WTS analysis of individual patients represents the first such undertaking in targeted lymphoma therapy. It has provided new insight into the genomic basis and mechanism for acquired resistance in MCL. In conjunction with functional genomics, the availability of exciting new targeting agents offers a unique opportunity to overcome acquired resistance by selective targeting of CDK4 in genome-based combination therapy in lymphoma, which has implications for other human cancers as well.

METHODS

Additional methods are detailed in the Supplementary Data.

Patients and Isolation of Primary MCL Cells

Tissue biopsies from lymph node, bone marrow, and spleen, and peripheral blood samples (Supplementary Table S5) were obtained from 9 patients with MCL at the New York-Presbyterian Hospital (New York, NY). Patient 2 samples were obtained at the Willamette Valley Cancer Institute and Research Center (Springfield, OR). All samples were collected after informed consent as part of a study approved by the local Institutional Review Boards. All patients were treated with ibrutinib after prior therapies. Patient 1 had received four therapies before starting single-agent ibrutinib and achieved a PR that lasted 14 months before disease progression marked by a rapidly enlarging spleen and spontaneous splenic hematoma requiring urgent surgery. Patient 2 achieved a PR lasting 30 months before progression marked by progressive adenopathy and a pleural effusion. Time-to-progression and best response of other patients are indicated in Supplementary Table S5. Primary MCL cells were purified using MACS CD19 MicroBeads (Miltenyi Biotec) at 4°C, and the percentage of MCL tumor cells ($CD19^+/CD5^+$) was determined to be >90% by flow cytometry. PBCs were isolated from healthy volunteers using the same protocol.

MCL Cell Lines

JEKO-1 cells were obtained from DSMZ, and MAVER-1 and MINO from ATCC. SP53 cells were kindly provided by Dr. Jiangao Tao (Moffit Cancer Center, Tampa, FL) and the chicken DT40 lymphoid cells deficient in BTK were described previously (39). No authentication of these cell lines was done by the authors. Cell lines were cultured in the presence of PD 0332991, GS-1101, GDC-0941, and BAY 80-6946 (all from Selleck Chemicals) or ibrutinib (Pharmacyclics) at concentrations and for times indicated.

WTS

For each experimental condition, 100 ng of high-quality total RNA (RNA integrity number > 8 on the Agilent BioAnalyzer 2100) was isolated using the RNeasy kit according to the manufacturer's instructions (Qiagen). All RNAs were converted to cDNA with the SuperScript III First-Strand Synthesis kit (Life Technologies), isolated with the TruSeq mRNA prep kit (v2; Illumina), and then ligated to Illumina adapters, as per the standard TruSeq Illumina protocol. Using these multiplexed cDNA libraries, we generated clusters on the Illumina cBot station and paired-end sequenced each sample to 50 × 50 bp on the Illumina HiSeq2000 at the Weill Cornell Medical College (WCMC) Genomics Core. Cluster generation, sequencing, and processing of the images were done using the Real-Time Analysis (RTA) software on the HiSeq2000 and after processing with CASAVA (v.1.8.2). To optimize library preparation, we used a TACON high-throughput RNA prep station. Raw data were filtered for high median quality (Q-value > 20) and then sent to Cornell's High Performance Computing (HPC) cluster, to be run through our RNA sequencing (RNA-Seq) analysis pipeline. The RNA-Seq data presented in this study, which include libraries from serial biopsies of MCL tumors before ibrutinib treatment (p_Ib1, p_Ib2, p_Ib3) and after ibrutinib relapse (r_IbBM, r_IbSP), and PBCs from 3 healthy volunteers, have been deposited in the Gene Expression Omnibus (GEO).

WES

DNA were isolated from purified MCL cells of five serial biopsies before ibrutinib treatment (p_Ib1, p_Ib2, p_Ib3) and after ibrutinib relapse (r_IbBM, r_IbSP) and a cheek swab of Patient 1, captured with Nextera Rapid Exome Capture Kit (62 MB), and libraries were created according to the manufacturer's protocol. Briefly, purified DNA was fragmented and a sequencing library was created with the Illumina TruSeq (v3) DNA Preparation Kits (FC-121-1031). Following isothermal cluster generation (PE-401-3001) and 75 × 75 paired-end sequencing on the HiSeq2500 (FC-401-3001), the samples underwent primary analysis with the Illumina base calling and primary analysis software (HCS 1.4, CASAVA 1.8.2, and RTA 1.2).

Cell-cycle analysis and cell viability assays were performed as previously described (16).

Disclosure of Potential Conflicts of Interest

P. Martin has received an honorarium from Janssen. J. Sharman has received a commercial research grant from Pharmacyclics. S. Ali is an employee of Foundation Medicine and has ownership interest in the same. B. Chang is employed by Pharmacyclics. J.P. Leonard is a consultant/advisory board member of Pharmacyclics. No potential conflicts of interest were disclosed by the other authors.

Authors' Contributions

Conception and design: D. Chiron, M. Di Liberto, P. Martin, S. Ely, J.P. Leonard, S. Chen-Kiang

Development of methodology: D. Chiron, M. Di Liberto, P. Blecua, B. Chang, S. Ely, O. Elemento, C.E. Mason, S. Chen-Kiang

Acquisition of data (provided animals, acquired and managed patients, provided facilities, etc.): D. Chiron, M. Di Liberto, P. Martin, J. Sharman, P. Blecua, P. Vijay, S. Ely, O. Elemento, C.E. Mason, J.P. Leonard, S. Chen-Kiang

Published OnlineFirst July 31, 2014; DOI: 10.1158/2159-8290.CD-14-0098

Analysis and interpretation of data (e.g., statistical analysis, biostatistics, computational analysis): D. Chiron, M. Di Liberto, P. Martin, X. Huang, P. Blecua, S. Mathew, P. Vijay, K. Eng, S. Ali, S. Ely, O. Elemento, C.E. Mason, S. Chen-Kiang
Writing, review, and/or revision of the manuscript: D. Chiron, M. Di Liberto, P. Martin, X. Huang, J. Sharman, S. Ali, A. Johnson, S. Ely, O. Elemento, C.E. Mason, J.P. Leonard, S. Chen-Kiang
Administrative, technical, or material support (i.e., reporting or organizing data, constructing databases): D. Chiron, M. Di Liberto, P. Vijay, B. Chang, O. Elemento, J.P. Leonard, S. Chen-Kiang
Study supervision: D. Chiron, M. Di Liberto, S. Chen-Kiang
Other (provided laboratory for cytogenetics and FISH studies): S. Mathew

Acknowledgments

The authors thank Drs. Jihye Paik, John Byrd, and Lewis Cantley for helpful discussions, Tricia Ellis for technical support, Dr. Jenny Zhang and the Weill Cornell Genomics Facility for RNA and DNA sequencing, and Pharmacyclics for providing ibrutinib.

Grant Support

This study was supported in part by a Cancer Research and Treatment Fund postdoctoral fellowship (to D. Chiron), grants from The Lymphoma Research Foundation (to S. Chen-Kiang, P. Martin, and J.P. Leonard), The Lymphoma Foundation (to J.P. Leonard), The Leukemia and Lymphoma Society (to S. Chen-Kiang), and R21 CA176362 from the National Cancer Institute (to S. Chen-Kiang and C.E. Mason).

The costs of publication of this article were defrayed in part by the payment of page charges. This article must therefore be hereby marked *advertisement* in accordance with 18 U.S.C. Section 1734 solely to indicate this fact.

Received January 29, 2014; revised June 4, 2014; accepted June 27, 2014; published OnlineFirst July 31, 2014.

REFERENCES

1. Perez-Galan P, Dreyling M, Wiestner A. Mantle cell lymphoma: biology, pathogenesis, and the molecular basis of treatment in the genomic era. Blood 2011;117:26–38.
2. Mohamed AJ, Yu L, Backesjo CM, Vargas L, Faryal R, Aints A, et al. Bruton's tyrosine kinase (Btk): function, regulation, and transformation with special emphasis on the PH domain. Immunol Rev 2009;228:58–73.
3. Bruton OC. Agammaglobulinemia. Pediatrics 1952;9:722–8.
4. Young RM, Staudt LM. Targeting pathological B cell receptor signalling in lymphoid malignancies. Nat Rev Drug Discov 2013;12:229–43.
5. Honigberg LA, Smith AM, Sirisawad M, Verner E, Loury D, Chang B, et al. The Bruton tyrosine kinase inhibitor PCI-32765 blocks B-cell activation and is efficacious in models of autoimmune disease and B-cell malignancy. Proc Natl Acad Sci U S A 2010;107:13075–80.
6. Wang ML, Rule S, Martin P, Goy A, Auer R, Kahl BS, et al. Targeting BTK with ibrutinib in relapsed or refractory mantle-cell lymphoma. N Engl J Med 2013;369:507–16.
7. Byrd JC, Furman RR, Coutre SE, Flinn IW, Burger JA, Blum KA, et al. Targeting BTK with ibrutinib in relapsed chronic lymphocytic leukemia. N Engl J Med 2013;369:32–42.
8. Ibrutinib approved for mantle cell lymphoma. Cancer Discov 2014;4:OF1.
9. Determann O, Hoster E, Ott G, Wolfram Bernd H, Loddenkemper C, Leo Hansmann M, et al. Ki-67 predicts outcome in advanced-stage mantle cell lymphoma patients treated with anti-CD20 immunochemotherapy: results from randomized trials of the European MCL Network and the German Low Grade Lymphoma Study Group. Blood 2008;111:2385–7.
10. Fry DW, Harvey PJ, Keller PR, Elliott WL, Meade M, Trachet E, et al. Specific inhibition of cyclin-dependent kinase 4/6 by PD 0332991 and associated antitumor activity in human tumor xenografts. Mol Cancer Ther 2004;3:1427–38.
11. Leonard JP, Lacasce AS, Smith MR, Noy A, Chirieac LR, Rodig SJ, et al. Selective CDK4/6 inhibition with tumor responses by PD0332991 in patients with mantle cell lymphoma. Blood 2012;119:4597–607.
12. Palbociclib Ups PFS in HER2−/ER+ breast cancer. Cancer Discov 2014;4:624–5.
13. Baughn LB, Di Liberto M, Wu K, Toogood PL, Louie T, Gottschalk R, et al. A novel orally active small molecule potently induces G_1 arrest in primary myeloma cells and prevents tumor growth by specific inhibition of cyclin-dependent kinase 4/6. Cancer Res 2006;66:7661–7.
14. Huang X, Di Liberto M, Jayabalan D, Liang J, Ely S, Bretz J, et al. Prolonged early G(1) arrest by selective CDK4/CDK6 inhibition sensitizes myeloma cells to cytotoxic killing through cell cycle-coupled loss of IRF4. Blood 2012;120:1095–106.
15. Menu E, Garcia J, Huang X, Di Liberto M, Toogood PL, Chen I, et al. A novel therapeutic combination using PD 0332991 and bortezomib: study in the 5T33MM myeloma model. Cancer Res 2008;68:5519–23.
16. Chiron D, Martin P, Di Liberto M, Huang X, Ely S, Lannutti BJ, et al. Induction of prolonged early G_1 arrest by CDK4/CDK6 inhibition reprograms lymphoma cells for durable PI3Kdelta inhibition through PIK3IP1. Cell Cycle 2013;12:1892–900.
17. Greiner TC, Dasgupta C, Ho VV, Weisenburger DD, Smith LM, Lynch JC, et al. Mutation and genomic deletion status of ataxia telangiectasia mutated (ATM) and p53 confer specific gene expression profiles in mantle cell lymphoma. Proc Natl Acad Sci U S A 2006;103:2352–7.
18. Meissner B, Kridel R, Lim RS, Rogic S, Tse K, Scott DW, et al. The E3 ubiquitin ligase UBR5 is recurrently mutated in mantle cell lymphoma. Blood 2013;121:3161–4.
19. Bea S, Valdes-Mas R, Navarro A, Salaverria I, Martin-Garcia D, Jares P, et al. Landscape of somatic mutations and clonal evolution in mantle cell lymphoma. Proc Natl Acad Sci U S A 2013;110:18250–5.
20. Rahal R, Frick M, Romero R, Korn JM, Kridel R, Chun Chan F, et al. Pharmacological and genomic profiling identifies NF-kappaB-targeted treatment strategies for mantle cell lymphoma. Nat Med 2014;20:87–92.
21. Zhang J, Jima D, Moffitt AB, Liu Q, Czader M, Hsi ED, et al. The genomic landscape of mantle cell lymphoma is related to the epigenetically determined chromatin state of normal B cells. Blood 2014;123:2988–96.
22. Yamasaki A, Menon S, Yu S, Barrowman J, Meerloo T, Oorschot V, et al. mTrs130 is a component of a mammalian TRAPPII complex, a Rab1 GEF that binds to COPI-coated vesicles. Mol Biol Cell 2009;20:4205–15.
23. Woyach JA, Furman RR, Liu TM, Ozer HG, Zapatka M, Ruppert AS, et al. Resistance mechanisms for the Bruton's tyrosine kinase inhibitor ibrutinib. N Engl J Med 2014;370:2286–94.
24. Vanhaesebroeck B, Welham MJ, Kotani K, Stein R, Warne PH, Zvelebil MJ, et al. P110delta, a novel phosphoinositide 3-kinase in leukocytes. Proc Natl Acad Sci U S A 1997;94:4330–5.
25. Chang BY, Francesco M, De Rooij MF, Magadala P, Steggerda SM, Huang MM, et al. Egress of CD19+CD5+ cells into peripheral blood following treatment with the BTK inhibitor ibrutinib in mantle cell lymphoma patients. Blood 2013;122:2412–24.
26. Zhu Z, He X, Johnson C, Stoops J, Eaker AE, Stoffer DS, et al. PI3K is negatively regulated by PIK3IP1, a novel p110 interacting protein. Biochem Biophys Res Commun 2007;358:66–72.
27. Fruman DA, Snapper SB, Yballe CM, Davidson L, Yu JY, Alt FW, et al. Impaired B cell development and proliferation in absence of phosphoinositide 3-kinase p85alpha. Science 1999;283:393–7.
28. Srinivasan L, Sasaki Y, Calado DP, Zhang B, Paik JH, DePinho RA, et al. PI3 kinase signals BCR-dependent mature B cell survival. Cell 2009;139:573–86.
29. Herman SE, Gordon AL, Wagner AJ, Heerema NA, Zhao W, Flynn JM, et al. Phosphatidylinositol 3-kinase-delta inhibitor CAL-101 shows promising preclinical activity in chronic lymphocytic leukemia by

Published OnlineFirst July 31, 2014; DOI: 10.1158/2159-8290.CD-14-0098

antagonizing intrinsic and extrinsic cellular survival signals. Blood 2010;116:2078–88.
30. Hoellenriegel J, Meadows SA, Sivina M, Wierda WG, Kantarjian H, Keating MJ, et al. The phosphoinositide 3′-kinase delta inhibitor, CAL-101, inhibits B-cell receptor signaling and chemokine networks in chronic lymphocytic leukemia. Blood 2011;118:3603–12.
31. Lannutti BJ, Meadows SA, Herman SE, Kashishian A, Steiner B, Johnson AJ, et al. CAL-101, a p110delta selective phosphatidylinositol-3-kinase inhibitor for the treatment of B-cell malignancies, inhibits PI3K signaling and cellular viability. Blood 2011;117:591–4.
32. Liu N, Rowley BR, Bull CO, Schneider C, Haegebarth A, Schatz CA, et al. BAY 80-6946 is a highly selective intravenous PI3K inhibitor with potent p110alpha and p110delta activities in tumor cell lines and xenograft models. Mol Cancer Ther 2013;12:2319–30.
33. Folkes AJ, Ahmadi K, Alderton WK, Alix S, Baker SJ, Box G, et al. The identification of 2-(1H-indazol-4-yl)-6-(4-methanesulfonyl-piperazin-1-ylmethyl)-4-morpholin-4-yl-thieno[3,2-d]pyrimidine (GDC-0941) as a potent, selective, orally bioavailable inhibitor of class I PI3 kinase for the treatment of cancer. J Med Chem 2008;51:5522–32.
34. Meyer JA, Wang J, Hogan LE, Yang JJ, Dandekar S, Patel JP, et al. Relapse-specific mutations in NT5C2 in childhood acute lymphoblastic leukemia. Nat Genet 2013;45:290–4.
35. Bea S, Salaverria I, Armengol L, Pinyol M, Fernandez V, Hartmann EM, et al. Uniparental disomies, homozygous deletions, amplifications, and target genes in mantle cell lymphoma revealed by integrative high-resolution whole-genome profiling. Blood 2009;113:3059–69.
36. Ying CY, Dominguez-Sola D, Fabi M, Lorenz IC, Hussein S, Bansal M, et al. MEF2B mutations lead to deregulated expression of the oncogene BCL6 in diffuse large B cell lymphoma. Nat Immunol 2013;14:1084–92.
37. Klempner SJ, Myers AP, Cantley LC. What a tangled web we weave: emerging resistance mechanisms to inhibition of the phosphoinositide 3-kinase pathway. Cancer Discov 2013;3:1345–54.
38. Liu P, Begley M, Michowski W, Inuzuka H, Ginzberg M, Gao D, et al. Cell-cycle-regulated activation of Akt kinase by phosphorylation at its carboxyl terminus. Nature 2014;508:541–5.
39. Takata M, Kurosaki T. A role for Bruton's tyrosine kinase in B cell antigen receptor-mediated activation of phospholipase C-gamma 2. J Exp Med 1996;184:31–40.

Biological rational for sequential targeting of Bruton tyrosine kinase and Bcl-2 to overcome CD40-induced ABT-199 resistance in mantle cell lymphoma

David Chiron[1], Christelle Dousset[1,2,3,*], Carole Brosseau[1,*], Cyrille Touzeau[1,2], Sophie Maïga[1,2], Philippe Moreau[1,2], Catherine Pellat-Deceunynck[1,2], Steven Le Gouill[1,2,3], Martine Amiot[1,2]

[1]INSERM, UMR892 - CNRS, UMR 6299, Université de Nantes, France

[2]Service d'Hématologie Clinique, Unité d'Investigation Clinique, Centre Hospitalier Universitaire de Nantes, France

[3]CIC, INSERM, Nantes, France

[*]These authors have contributed equally to this work

Correspondence to:
Martine Amiot, **e-mail:** martine.amiot@inserm.fr

Keywords: ABT-199, mantle cell lymphoma, apoptosis, Bcl-2 family members, ibrutinib

Received: February 04, 2015 ***Accepted:*** February 08, 2015 ***Published:*** March 05, 2015

ABSTRACT

The aggressive biological behavior of mantle cell lymphoma (MCL) and its short response to current treatment highlight a great need for better rational therapy. Herein, we investigate the ability of ABT-199, the Bcl-2-selective BH3 mimetic, to kill MCL cells. Among MCL cell lines tested (*n* = 8), only three were sensitive (LD_{50} < 200 nM). In contrast, all primary MCL samples tested (*n* = 11) were highly sensitive to ABT-199 (LD_{50} < 10 nM). Mcl-1 and Bcl-x_L both confer resistance to ABT-199-specific killing and *BCL2/(BCLXL+MCL1)* mRNA ratio is a strong predictor of sensitivity. By mimicking the microenvironment through CD40 stimulation, we show that ABT-199 sensitivity is impaired through activation of NF-kB pathway and Bcl-x_L up-regulation. We further demonstrate that resistance is rapidly lost when MCL cells detach from CD40L-expressing fibroblasts. It has been reported that ibrutinib induces lymphocytosis *in vivo* holding off malignant cells from their protective microenvironment. We show here for two patients undergoing ibrutinib therapy that mobilized MCL cells are highly sensitive to ABT-199. These results provide evidence that *in situ* ABT-199 resistance can be overcome when MCL cells escape from the lymph nodes. Altogether, our data support the clinical application of ABT-199 therapy both as a single agent and in sequential combination with BTK inhibitors.

INTRODUCTION

Mantle cell lymphoma (MCL) is a mature B-cell neoplasm characterized by an aggressive clinical course. Although recent progress in the treatment of MCL patients has yielded high complete response rates, relapse invariably occurs and MCL remains incurable [1, 2]. This highlights the necessity to uncover the mechanisms involved in tumor cell survival and drug resistance. The primary oncogenic event in MCL is the t(11;14) translocation resulting in cyclin D1 overexpression and consequent cell cycle dysregulation [3]. However, additional mechanisms are required for MCL progression, including alteration of the mitochondrial apoptotic pathway, which mainly determines cell fate [4–6]. Among the critical components of the apoptotic machinery, the anti-apoptotic protein Bcl-2 is overexpressed in MCL cells and may then represent an attractive target for innovative therapy. BH3 mimetics, such as ABT-737 and ABT-263 (navitoclax), which bind with high affinity Bcl-2 and Bcl-x_L have been developed. They displace pro-apoptotic proteins from Bcl-2 and Bcl-x_L and induce apoptosis through a Bax or Bak dependent manner [7, 8]. Recently, navitoclax has demonstrated antitumor activity

in B-cell malignancies but its clinical development was limited by the significant thrombocytopenia caused by Bcl-x_L inhibition [9]. To overcome this toxicity, the first-in-class orally bioavailable Bcl-2-selective BH3 mimetic ABT-199 was developed and thus far has shown very promising antitumor activity while sparing platelets in chronic lymphoid leukemia (CLL) and B-cell lymphomas, including MCL [10, 11].

Recently it has been demonstrated that tumor microenvironment strongly influence proliferation, survival and drug resistance in MCL cells [12, 13]. Moreover, microenvironment has been implicated in BH3 mimetic resistance via the modulation of Bcl-2 family proteins expression in CLL cells [14–16]. In the present study, we investigated the apoptotic efficiency of ABT-199 in both MCL cell lines and primary cells by integrating the key role of the microenvironment. This led us to propose a rational combination strategy to overcome microenvironment-dependent ABT-199 resistance through prior induction of cellular egress in peripheral blood using the selective BTK inhibitor ibrutinib [17].

RESULTS

Mantle cell lymphoma sensitivity to ABT-199 correlates with *BCL2/(MCL1+BCLXL)* gene expression ratio

To determine sensitivity of MCL cells to ABT-199, cell lines ($n = 8$) were treated with increasing doses of ABT-199 for 48 hours. As shown in Table IA, the efficacy of ABT-199 was heterogeneous among MCL cell lines. Indeed, MAVER-1, MINO and GRANTA-519 cells were found to be highly sensitive to ABT-199 (LD_{50} from 15 to 200 nM) while Z138, JeKo-1, REC-1, JVM2 and UPN-1 were found to be resistant (LD_{50} from 1000 to 10000 nM) (Table IA). We next addressed ABT-199 sensitivity in primary MCL cells obtained from peripheral blood of 11 patients at diagnosis or relapse. In contrast to MCL cell lines, low doses of ABT-199 (10 nM) induced cell death in all samples, ranging from 53% to 98% indicating that primary cells presented a $LD_{50} < 10$ nM (Table IB).

We next analyzed the sensitivity to ABT-199 in regards to the expression of anti-apoptotic Bcl-2 family members determined by RT-qPCR in both cell lines and primary samples (Table I). Whereas *BCL2* and *MCL1* levels were similar in both cell lines and primary cells, *BCLXL* mRNA expression was significantly lower in primary MCL cells ($p = 0.002$) (Fig. 1A). We previously reported that the *BCL2/MCL1* ratio was a powerful biomarker for predicting ABT-737 sensitivity in MCL [18]. Using both MCL cell lines and primary cells we found here a direct correlation between ABT-199 sensitivity threshold and *MCL1* and *BCLXL* anti-apoptotic gene expression. Indeed, whereas neither *BCL2/MCL1 nor BCL2/BCL2XL* mRNA ratios were sufficient (Supplementary Fig. S1A), *BCL2/(MCL1+BCLXL)* mRNA ratio discriminated sensitive from resistant MCL cells with a cut-off value of 0.67 ($p < 0.001$; Fig. 1B). Of note, the Bcl-2/(Mcl-1+Bcl-x_L) protein ratio strongly correlated with the mRNA ratio in MCL cells ($p < 0.001$; Supplementary Fig. S1B–S1C). Taken together, these data suggest that both Bcl-x_L and Mcl-1 expression play a role in ABT-199 resistance in MCL through increase of the apoptotic threshold.

To investigate the role of Bcl-x_L and Mcl-1 in ABT-199 response, these anti-apoptotic proteins were knocked down using siRNA in both Z138 and JeKo-1 resistant cells. Mcl-1 silencing sensitized both cell lines to lower doses of ABT-199 confirming the critical role of Mcl-1 in BH3-mimetics resistance as previously shown (Fig. 1C) [18]. Bcl-x_L silencing also sensitized Z138 and JeKo-1 cells to ABT-199, to a lesser extent than Mcl-1 silencing which may be explained by a lower silencing efficacy (Fig. 1C–1D). These results confirm that both Bcl-x_L and Mcl-1 determine ABT-199-specific response in MCL cells.

CD40 stimulation reduces ABT-199 efficacy in MCL cells

Because MCL cells mainly reside in lymph nodes we next asked whether microenvironment interactions could impact their sensitivity to ABT-199. In order to mimic the lymph node microenvironment where CD40-CD40L interaction takes place, ABT-199 sensitive MCL cell lines (MINO and MAVER-1) were cultured on CD40L-expressing fibroblast L cells (L-40L). Co-culture with L-40L dramatically reduces their sensitivity to ABT-199 while co-culture with parental fibroblast L cells failed to induce significant resistance (Fig. 2A). Of note, primary MCL cells from patients were also significantly more resistant to ABT-199 when cultured on L-40L with 25 nM of ABT-199 ($n = 6$; $p < 0.001$) (Fig. 2B). By contrast, culture of MINO cells with conditioned medium from L-40L culture or with bone marrow stromal cells (HS5) failed to reduce ABT-199 sensitivity (data not shown). These results indicate that the CD40 pathway is directly involved in the resistance to ABT-199 in both MCL cell lines and primary cells.

Bcl-x_L up-regulation by CD40 stimulation confers resistance to ABT-199

To assess the involvement of Bcl-2 family proteins in ABT-199 resistance under CD40 stimulation, we examined their expression following co-culture with either L or L-40L fibroblasts. CD40 stimulation of ABT-199 sensitive MCL cell lines resulted in a strong up-regulation of Bcl-x_L proteins within 6 to 24 hours of co-culture while

A

Cell lines	LD_{50} ABT-199	*BCL2*	*MCL1*	*BCLXL*	*(BCL2)/ (MCL1+BCLXL)*
MAVER-1	15	6.55	0.92	2.01	**2.24**
MINO	100	1.38	0.60	1.25	**0.75**
GRANTA-519	200	3.90	0.89	2.16	**1.28**
Z138	1000	0.98	0.67	1.95	0.37
REC-1	5000	0.68	1.79	3.77	0.12
JVM2	5000	1.48	1.44	2.83	0.35
JeKo-1	7000	1.00	1.00	1.00	0.50
UPN-1	10000	0.01	0.45	1.10	0.00

B

Patient	Status	ABT-199 (10 nM)% of cytotoxicity	*BCL2*	*MCL1*	*BCLXL*	*(BCL2)/ (MCL1+BCLXL)*
#1	Diag	53	2.76	0.82	0.27	**2.53**
#2	Diag	56	2.10	0.78	1.07	**1.14**
#3	Rel	56	3.77	0.9	1.1	**1.96**
#4	Rel	58	ND	ND	ND	ND
#5	Diag	62	3.57	1.59	0.95	**1.41**
#6	Diag	62	1.69	1.08	0.32	**1.22**
#7	Rel	66	1.78	0.8	0.5	**1.43**
#8	Diag	69	1.20	0.90	0.30	**1.00**
#9	Diag	69	2.05	1.03	1.11	**0.96**
#10	Diag	77	1.51	0.40	0.30	**2.16**
#11	Rel	98	ND	ND	ND	ND

Table I: MCL cell sensitivity to ABT-199 correlates with the *BCL2/(MCL1+BCLXL)* ratio. (A) Cell lines were cultured with increasing doses of ABT-199 for 48 hours to determine the median lethal dose (LD_{50}: 15-10000 nM). **(B)** MCL cells from peripheral blood were obtained after gradient density centrifugation on Ficoll Hypaque. MCL cells were cultured with 10 nM of ABT-199 for 24 hours. Diag: diagnosis, Rel: relapse, ND: data not determined. The relative expression of *BCL2*, *MCL1 and BCLXL* mRNA was defined on purified $CD19^+$ cells as described in the Methods section and *BCL2/(MCL1+BCLXL)* mRNA ratio is indicated. Analysis of *BCLXL*, *MCL1 and BCL2* relative expression in primary MCL cells and cell lines are shown in Figure 1A. Correlation between *BCL2/(MCL1+BCLXL)* ratio and ABT-199 sensitivity is shown in Figure 1B.

no modification of Mcl-1 or Bcl-2 levels was observed (Fig. 3A). The CD40-induced Bcl-x_L expression was then confirmed at the mRNA level in MINO and MAVER-1 cell lines (Fig. 3C).

CD40 activation is known to potently activate both classical and alternative NF-kB pathway [19], which mediate Bcl-x_L upregulation [20]. Thus, we investigated NF-kB activation through the phosphorylation of IκBα and accumulation of p52 in MCL cell lines under CD40 stimulation. As shown in Fig. 3A both classical (p-IkB) and alternative (p52) NF-kB pathways were activated under CD40 stimulation in both MINO and MAVER-1

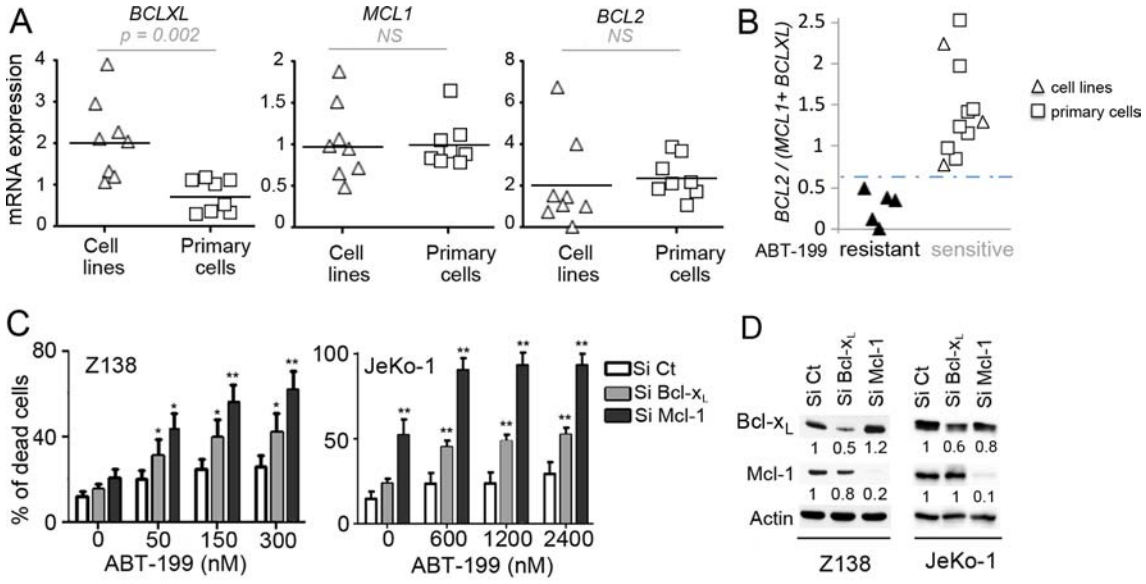

Figure 1: Influence of Bcl-2 family anti-apoptotic proteins on ABT-199 sensitivity in MCL cells. (A) Analysis of the relative expression of *BCLXL, MCL1 and BCL2* mRNA by RT-qPCR in MCL cell lines (n = 8) and primary MCL cells (n = 8). The relative expression was normalized to JeKo-1 cell line. **(B)** The *BCL2/(MCL1+BCLXL)* mRNA ratio correlates with ABT-199 sensitivity in MCL cells. Cells with a LD_{50} < 200 nM were defined as sensitive whereas cells with a LD_{50} > 1000 nM were defined as resistant. The cut-off value (0.67) was determined as the mean of *BCL2/(MCL1+BCLXL)* ratio of resistant cells + (standard deviation) x 2 (True positive rate: 100%) **(C)** Both Mcl-1 and Bcl-x_L confer primary resistance to ABT-199. Z138 and JeKo-1 cell lines were transfected with Si Control (Ct), Mcl-1 or Bcl-x_L. Following transfection, cells were treated with ABT-199 for 24 hours and cell death was quantified by Apo2.7 staining. p-value was determined using the paired Student's t test: *p < .05; **p < .01. **(D)** The protein levels of Mcl-1 and Bcl-x_L were determined by immunoblotting.

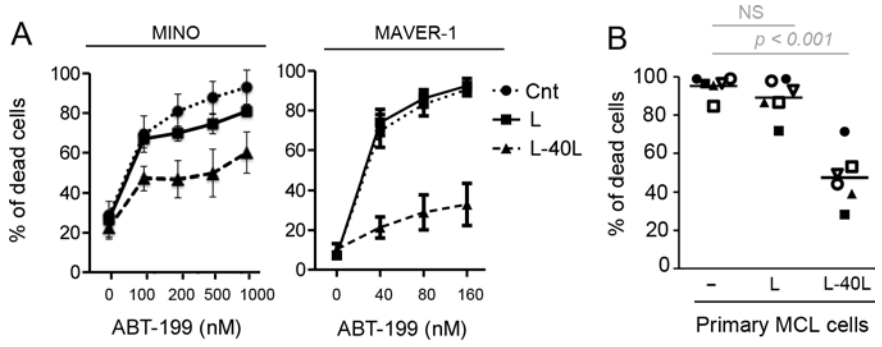

Figure 2: CD40 stimulation resulted in strong resistance to ABT-199. (A) MCL cell lines were cultured alone or on either parental fibroblast L or CD40L-expressing fibroblasts L (L-40L) for 24 hours before being exposed to ABT-199. Cell death was assessed in triplicate by using Apo-2.7 staining. **(B)** Primary MCL cells were cultured alone or on either L or L-40L cells for 24 hours then exposed to 25 nM ABT-199 for 48 hours. Apoptosis was determined by Apo2.7 and CD19 staining.

cells (Fig. 3A). Of interest, CD40 stimulation (24 hours) of primary MCL cells (n = 3) also demonstrated a strong Bcl-x_L upregulation associated to the activation of both classical and alternative NF-kB pathways (Fig. 3B).

To further confirm the critical role of Bcl-x_L in the resistance to ABT-199 induced by CD40 stimulation, we transiently silenced its expression by RNAi. siRNAs against *BCLXL* in MINO cells impaired protein up-regulation upon CD40 stimulation and significantly prevented the resistance to ABT-199 confirming a critical role for Bcl-x_L in cell protection (Fig. 3D).

Because MCL cells frequently disseminate from lymph nodes into circulation, we mimicked this process by removing MINO or primary MCL cells from L40-L before assessing Bcl-x_L levels in order to determine whether resistance to ABT-199 would persist after

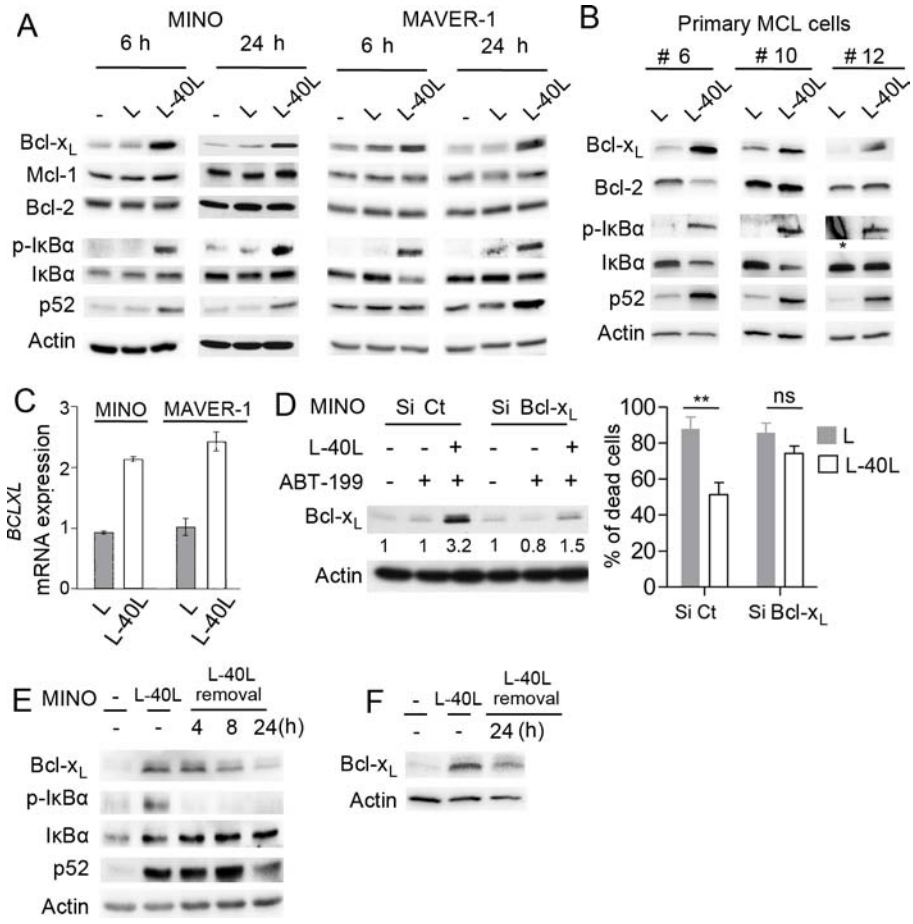

Figure 3: Up-regulation of Bcl-xL by CD40 stimulation confers ABT-199 resistance to MINO cells. (A) Immunoblot analysis of Bcl-2 family (Bcl-x_L, Mcl-1, Bcl-2) and NF-kB (pIkB, IkB, p52) proteins expression in MINO and MAVER-1 cells cultured on either parental L or L-40L for 6 and 24 hours. **(B)** Immunoblot analysis of indicated proteins in primary MCL samples cultured on either L or L-40L cells for 24 hours. * indicates non-specific staining **(C)** *BCLXL* mRNA was measured by RT-qPCR in MINO and MAVER-1 cells treated as indicated in A. **(D)** Left panel: MINO cells were transfected with Si Control (Ct) or Bcl-x_L and silencing at the protein level was confirmed by immunoblotting. Right panel: following 24 hours of transfection, cells were cultured on either L or L-40L cells before being treated with ABT-199 for additional 48 hours. **(E-F)** MINO cells (E) and primary MCL cells (F) cultured on L-40L for 24 hours were removed from coculture support and cultured alone for indicated time and analyzed by immunoblotting.

detachment from L40-L. We observed a rapid decrease of IkBα phosphorylation as well as a progressive reduction of p52 and Bcl-x_L protein level to baseline levels within 24 hours after detachment from L40-L (Fig. 3E–3F). Taken together, these results suggest that ABT-199 resistance due to CD40/CD40L interaction is linked to Bcl-x_L upregulation and that sensitivity could be rapidly restored after egress of MCL cells from their protective microenvironment.

Ex-vivo analysis of the acquired peripheral $CD19^+CD5^+$ population following ibrutinib treatment of MCL patients demonstrates high sensitivity to ABT-199

Ibrutinib is an irreversible BTK inhibitor that displays significant antitumor activity in MCL [21]. By inhibiting BCR and chemokine-mediated stromal adhesion of MCL, ibrutinib has been shown to induce a redistribution of lymph node-resident MCL [22]. Thus, we investigated the lymphocyte population in the peripheral blood of a patient that received ibrutinib (560 mg/d) every day for days 1–7 while treated in the French compassionate use program. Blood was collected and analyzed for the presence of $CD19^+$ $CD5^+$ MCL cells before treatment and at days 2 and 7 following ibrutinib treatment. As shown in Fig. 4, the peripheral $CD19^+$ $CD5^+$ lymphocyte population increased from 16% to 21% after 2 days and to 61% after 7 days of ibrutinib treatment, indicating a cellular mobilization (lymphocytosis) from tissues as previously described (Fig. 4A) [22]. Annexin-V staining demonstrated that only 9% or 25% of the tumor cell population undergoes spontaneous apoptosis at days 2 and 7 following ibrutinib treatment respectively

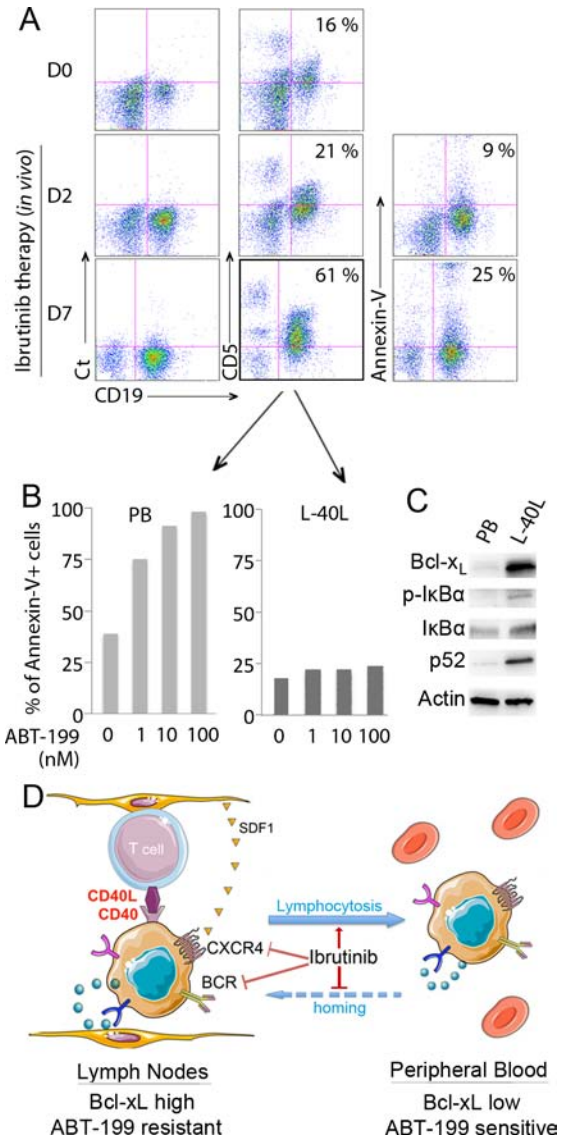

Figure 4: Sensitivity of mobilized primary MCL cells to ABT-199 in a patient treated with ibrutinib. (A) Peripheral blood (PB) cells from a MCL patient were collected before (D0) and after ibrutinib treatment (D2 and D7) and labeled with CD19-APC and CD5-FITC. The percentage of $CD19^+$ $CD5^+$ population is indicated in each dot plot. In addition, apoptosis of $CD19^+$ MCL cells at D2 and D7 was assessed by Annexin V-FITC staining with the percentage of apoptotic cells indicated in each dot plot. **(B)** After 7 days of *in vivo* ibrutinib single-agent treatment, freshly isolated *de novo* $CD19^+CD5^+$ PB cells were cultured with increasing doses of ABT-199 for 24 hours directly or after coculture with L-40L cells. Cell death was assessed by Annexin V-FITC and CD19 staining. **(C)** Expression of Bcl-x_L and activation of the classical (p-IkBα, IkBα) or alternative (p52) NF-kB pathway was analyzed in *de novo* $CD19^+$ MCL peripheral blood cells with or without L-40L coculture. **(D)** Schematic representation of ibrutinib mechanism of action in MCL cells. By inhibiting BTK, ibrutinib neutralize both BCR and CXCR4 axis, resulting in egress of MCL cells from the protective microenvironment into peripheral blood.

(Fig. 4A). In order to analyze the cytotoxic efficiency of ABT-199 on tumor cells mobilized from lymph nodes, peripheral blood population obtained on day 7 was treated with increasing doses of ABT-199 for 24 hours. We found that the $CD19^+$ population was highly sensitive to ABT-199, with a LD50 < 1 nM, confirming that tumor cells mobilized from tissues following ibrutinib treatment could be efficiently targeted by ABT-199 (Fig. 4B). The ABT-199 sensitivity of ibrutinib-mobilized cells was further confirmed in a second patient who displayed an increase absolute lymphocyte count (1.9 fold) 10 days after ibrutinib (Supplementary Figure S2A–S2C). *Ex-vivo* co-culture of the peripheral blood population obtained on day 7 on L-40L confirmed ABT-199-resistance (Fig. 4B, Supplementary Fig. S2C) as well as NFkB activation and Bcl-x_L up-regulation (Fig. 4C). Thus, we hypothesize that without ibrutinib-specific inhibition of homing into the lymph nodes, circulating cells would become resistant to ABT-199. According to our hypothesize, we demonstrated that while ibrutinib increased the sensitivity of MINO cells

to ABT-199, the activity of ibrutinib was not sufficient to significantly reverse the protection observed on L-40L co-culture (Supplementary Fig. S3).

DISCUSSION

The opportunity to induce apoptosis by selectively targeting Bcl-2 with ABT-199 is a potentially promising therapeutic approach in hematological malignancies [10, 23, 24]. MCL cell lines showed a similar sensitivity to ABT-199 than the one previously described for ABT-737 [18], despite the selective affinity of ABT-199 for Bcl-2 but not Bcl-x_L. However, ABT-199 efficiency may be increased thanks to a higher affinity to its selective target Bcl-2 (x100 fold) [10]. Indeed, we observed that ABT-199 kills 3 out of 8 MCL cell lines while it is broadly active against all primary MCL cells tested (n = 11) at low doses (LD_{50} < 10 nM) (Table I). We next demonstrated that ABT-199 sensitivity is significantly correlated to *BCL2/(MCL1+BCLXL)* ratio indicating that both Mcl-1 and Bcl-x_L play a key role in intrinsic ABT-199 resistance (Fig. 1). Of note, until now we didn't observe intrinsic resistance to ABT-199 in the primary MCL cells tested. However, analysis of a larger number of primary cells could potentially reveal ABT-199 resistance due to specific mutation in the Bcl-2 target or in Bax effector protein as recently reported [25].

Accumulating data indicate that the microenvironment is a critical factor for cancer cell survival and thus has to be considered for the development of successful new treatment strategies. In this respect, special attention has been paid to modifications occurring in CLL cells stimulated by fibroblasts expressing CD40L, resulting in ABT-737 resistance [14, 15, 26]. Using this coculture system to mimic the microenvironment within lymph nodes, we have shown here that CD40 stimulation of MCL cell lines and patient samples significantly reduce ABT-199 sensitivity (Fig. 2). We demonstrated that (i) peripheral blood MCL cells express low level of Bcl-x_L and are highly sensitive to ABT-199, (ii) upon CD40 stimulation there is an increase in Bcl-x_L protein level but not Mcl-1 or Bcl-2, and (iii) that silencing of BCL-x_L overcomes ABT-199 resistance induced by CD40 stimulation. Taken together our study highlight a critical role for Bcl-x_L in microenvironment-dependent protection of MCL cells to ABT-199.

As previously reported [20], we confirmed that NF-κB-signaling pathway is involved in CD40-dependent Bcl-x_L up-regulation (Fig. 3). Mechanistically, our results imply that over-expression of Bcl-x_L alters the balance between pro-and anti-apoptotic Bcl-2 family proteins and it is the tempting to hypothesize that Bcl-x_L is able to capture the pro-apoptotic proteins endogenously bound to Bcl-2 and released under ABT-199 treatment. Of note, among the three MCL cell lines highly sensitive to ABT-199, MINO cells lacks Bim expression in contrast to MAVER-1 and GRANTA-519 cells, indicating that the efficacy of ABT-199 is not affected by the absence of Bim (data not shown).

It was shown recently that ibrutinib, a highly potent oral Bruton's tyrosine kinase (BTK) inhibitor, interferes with the homing of MCL cells into secondary lymphoid organs and/or bone marrow through the inhibition of chemokine and BCR signaling [22]. In agreement with this mechanism of action, ibrutinib induces a concomitant increase of circulating MCL cells [22]. Since circulating primary MCL cells are highly sensitive to ABT-199, it would suggest that combining ABT-199 with ibrutinib could be a very effective therapy for MCL patients. Indeed, we have demonstrated that ABT-199 resistance is rapidly lost when MCL cells detach from CD40L expressing fibroblast cells and that peripheral MCL cells isolated from a patient undergoing ibrutinib treatment were sensitized to ABT-199-mediated killing. Taken together, these results indicate that ABT-199 resistance can be overcome when MCL cells escape from the microenvironments (Fig. 4D).

Based on high response rates in a phase 2 clinical data, ibrutinib was recently approved by the FDA for the treatment of MCL [21]. However, approximately one third of patients did not respond and some became resistant to ibrutinib during treatment [21, 27, 28]. Because ABT-199 kills MCL cells through a distinct mechanism of action and is particularly potent against peripheral MCL cells mobilized by ibrutinib, these agents could be highly complementary and beneficial to patients with significant unmet medical need. Their favorable toxicity profiles may also facilitate their combination in future clinical trials. Furthermore, a recent study demonstrated synergistic effect of the ibrutinib and ABT-199 combination on apoptosis induction in several MCL cell lines [29]. However, while ibrutinib increased the sensitivity of MINO cells to ABT-199, this drug combination was not sufficient to reverse the protection induced by the CD40/CD40L interaction. These last results reinforce the interest of sequential strategy taking advantage of ibrutinib-induced lymphocytosis.

In conclusion, the Bcl-2-selective BH3 mimetic ABT-199 is a promising agent for the treatment of B-cell malignancies including MCL and may be especially attractive in combination with BCR signaling inhibitory drugs such as ibrutinib, which can drive malignant cells out of the protective microenvironment of lymph nodes and bone marrow.

MATERIALS AND METHODS

MCL cells and cell lines

MCL cell lines JeKo-1, MINO, REC-1, MAVER-1 were purchased from DSMZ (Braunschweig, Germany), Z138 was purchased from ATCC (Manassas, USA),

GRANTA-519 and UPN-1 were kindly provided by Dr. V. Ribrag (Institut Gustave Roussy, Villejuif, France) and Dr B. Sola (IFR 146, University of Caen, France), respectively. Cell lines were maintained in RPMI-1640 medium supplemented with 10% FCS and 2 mM glutamine. Primary cells were obtained after informed consent from MCL patients treated at the department of clinical hematology from the University hospital of Nantes, France. The patient described in Fig. 4 received ibrutinib single agent therapy (560 mg/d) and achieved a partial response lasting 4 months before progression. The patient described in Supplementary Fig. S2 was still under ibrutinib single agent therapy (560 mg/d) at the time of publication. Peripheral MCL cells from blood were purified after Ficoll-Hypaque separation with immuno-magnetic anti-CD19 beads when MCL infiltration was less than 90% (Miltenyi, Paris, France). Primary MCL cells were cultured in RPMI-1640 supplemented with 10% FCS and 2 mM glutamine.

Parental or CD40L-expressing mouse fibroblast L cells were kindly provided by Dr T. Defrance (Lyon, France). L cells were cultured in RPMI-1640 supplemented with 10% FCS and 2 mM glutamine. For the co-culture experiments, L cell were irradiated with 35 Gray or treated with mitomycin and seeded (2.5×10^4 cells/mL) 6 to 24 hours before MCL cell lines (2.5×10^5 cells/mL) or primary cells (5×10^5 cells/mL). ABT-199 was then added for 48 hours.

Antibodies and reagents

The following antibodies were used for flow cytometry analysis: anti-Apo2.7-PE, anti-CD5-FITC, anti-CD19-APC and control IgG1-FITC mAbs were purchased from BD Biosciences (Le Pont de Claix, France). Analysis of protein expression was conducted by immunoblotting using the following primary antibodies: anti-Bcl-2, anti-IκBα and anti-phosho-IκBα (Cell Signaling, Saint Quentin en Yvelines, France), Anti-Mcl-1 (S19) (Santa Cruz Biotechnology, Santa Cruz, CA), anti-Bcl-x_L (BD Biosciences, Le Pont de Claix, France), Anti-NF-κB p52 Antibody and anti-actin (Merck Millipore, Lyon, France). ABT-199 was kindly provided by Abbvie Laboratories (North Chicago, IL, USA) and the selective BTK inhibitor ibrutinib (PCI-32765) was obtained from Selleck Chemicals (Souffelweyersheim, France).

Viability assays

Cell death in MCL cell lines was assessed by using Apo-2.7 staining (BD Biosciences Le Pont de Claix, France). Cell death in $CD19^+$ primary MCL cells was assessed by Apo-2.7 staining combined with an analysis of altered cellular morphology (lower FSC). Alternatively, apoptosis of primary cells was assessed by Annexin V-FITC staining (Beckman coulter). Fluorescence was analyzed on FACSCalibur (Cytocell, SFR Bonamy).

siRNA transient transfections

Control non-targeted small interfering siRNA (si Ct) and siRNA against *BCLXL* and *MCL1* were purchased from Thermo Scientific (Courtaboeuf, France). Z138 and MINO cell lines were electroporated using a Nucleofector system (Amaxa, Lonza, Basel, Switzerland) according to the manufacturer's instructions. Cells (5×10^5/ml) were suspended in Nucleofector solution T or SF and electroporated in the presence of 10 µmol/L siRNA (T01 for MINO, CM150 for Z138 and DN100 for JeKo-1). The gene-silencing effect was evaluated by immunoblot analysis.

Quantitative real-time PCR

Quantitative PCR was performed as previously described [30]. TaqMan gene expression assays for *BCL2* (Hs00608023_m1), *MCL1* (Hs00172036_m1), *BCLXL* (*BCL2L1*; Hs00236329_m1) and RPL37a (Hs01102345_m1) were purchased from Applied Biosystems. The following thermal cycling parameters were used: 50°C for 2 min for optimal AmpErase UNG activity and then 40 cycles at 95°C for 30 s and 60°C for 1 min. Amplification of the housekeeping gene *RPL37a* was conducted for each sample as an endogenous control.

Immunoblot analysis

Cells were collected and lysed in lysis buffer containing 10 mM Tris, pH 7.6, 150 mM NaCl, 5 mM EDTA and 1% TritonX100, 2 mM PMSF and 2 mg/ml aprotinin. Immunoblot analysis was performed according to published protocols [18].

ACKNOWLEDGEMENTS

We thank AbbVie for supporting in part this study. This study was supported by Ligue Contre le Cancer Grand-Ouest and by Actions Cancer 44. DC was supported by the Ligue Nationale Contre le Cancer and CHU de Nantes (AO jeunes chercheurs). We thank Dr Joel Leverson for helpful discussions and for critical review of the manuscript and Dr Benoit Tessoulin for helpful information on MCL patients.

REFERENCES

1. Dreyling M, Kluin-Nelemans HC, Beà S, Klapper W, Vogt N, Delfau-Larue M-H, Hutter G, Cheah C, Chiappella A, Cortelazzo S, Pott C, Hess G, Visco C, et al. Update on the molecular pathogenesis and clinical

treatment of mantle cell lymphoma: report of the 11th annual conference of the European Mantle Cell Lymphoma Network. Leuk Lymphoma. 2013; 54:699–707.

2. Kluin-Nelemans HC, Hoster E, Hermine O, Walewski J, Trneny M, Geisler CH, Stilgenbauer S, Thieblemont C, Vehling-Kaiser U, Doorduijn JK, Coiffier B, Forstpointner R, Tilly H, et al. Treatment of older patients with mantle-cell lymphoma. N Engl J Med. 2012; 367:520–31.
3. Jares P, Colomer D, Campo E. Molecular pathogenesis of mantle cell lymphoma. J Clin Invest. 2012; 122:3416–3423.
4. Bàe S, Salaverria I, Armengol L, Pinyol M, Fernández V, Hartmann EM, Jares P, Amador V, Hernández L, Navarro A, Ott G, Rosenwald A, Estivill X, Campo E. Uniparental disomies, homozygous deletions, amplifications, and target genes in mantle cell lymphoma revealed by integrative high-resolution whole-genome profiling. Blood. 2009; 113:3059–69.
5. Ek S, Högerkorp C-M, Dictor M, Ehinger M, Borrebaeck CAK. Mantle Cell Lymphomas Express a Distinct Genetic Signature Affecting Lymphocyte Trafficking and Growth Regulation as Compared with Subpopulations of Normal Human B Cells. Cancer Res. 2002; 62:4398–405.
6. Hofmann W-K, Vos de S, Tsukasaki K, Wachsman W, Pinkus GS, Said JW, Koeffler HP. Altered apoptosis pathways in mantle cell lymphoma detected by oligonucleotide microarray. Blood. 2001; 98:787–794.
7. Deng J, Carlson N, Takeyama K, Dal Cin P, Shipp M, Letai A. BH3 profiling identifies three distinct classes of apoptotic blocks to predict response to ABT-737 and conventional chemotherapeutic agents. Cancer Cell. 2007; 12:171–185.
8. Tse C, Shoemaker AR, Adickes J, Anderson MG, Chen J, Jin S, Johnson EF, Marsh KC, Mitten MJ, Nimmer P, Roberts L, Tahir SK, Xiao Y, Yang X, Zhang H, Fesik S, Rosenberg SH, Elmore SW. ABT-263: a potent and orally bioavailable Bcl-2 family inhibitor. Cancer Res. 2008; 68:3421–3428.
9. Roberts AW, Seymour JF, Brown JR, Wierda WG, Kipps TJ, Khaw SL, Carney DA, He SZ, Huang DC, Xiong H, Cui Y, Busman TA, McKeegan EM, et al. Substantial susceptibility of chronic lymphocytic leukemia to BCL2 inhibition: results of a phase I study of navitoclax in patients with relapsed or refractory disease. J Clin Oncol. 2012; 30:488–496.
10. Souers AJ, Leverson JD, Boghaert ER, Ackler SL, Catron ND, Chen J, Dayton BD, Ding H, Enschede SH, Fairbrother WJ, Huang DC, Hymowitz SG, et al. ABT-199, a potent and selective BCL-2 inhibitor, achieves antitumor activity while sparing platelets. Nat Med. 2013; 19:202–8.
11. Davids MS, Letai A. ABT-199: Taking Dead Aim at BCL-2. Cancer Cell. 2013; 23:139–141.
12. Burger JA, Ford RJ. The microenvironment in mantle cell lymphoma: cellular and molecular pathways and emerging targeted therapies. Semin Cancer Biol. 2011; 21:308–312.
13. Kurtova AV, Tamayo AT, Ford RJ, Burger JA. Mantle cell lymphoma cells express high levels of CXCR4, CXCR5, and VLA-4 (CD49d): importance for interactions with the stromal microenvironment and specific targeting. Blood. 2009; 113:4604–4613.
14. Tromp JM, Geest CR, Breij ECW, Elias JA, van Laar J, Luijks DM, Kater AP, Beaumont T, van Oers MH, Eldering E. Tipping the Noxa/Mcl-1 balance overcomes ABT-737 resistance in chronic lymphocytic leukemia. Clin Cancer Res. 2012; 18:487–498.
15. Vogler M, Butterworth M, Majid A, Walewska RJ, Sun X-M, Dyer MJS, Cohen GM. Concurrent up-regulation of BCL-XL and BCL2A1 induces approximately 1000-fold resistance to ABT-737 in chronic lymphocytic leukemia. Blood. 2009; 113:4403–4413.
16. Davids MS, Deng J, Wiestner A, Lannutti BJ, Wang L, Wu CJ, Wilson WH, Brown JR, Letai A. Decreased mitochondrial apoptotic priming underlies stroma-mediated treatment resistance in chronic lymphocytic leukemia. Blood. 2012; 120:3501–3509.
17. Honigberg LA, Smith AM, Sirisawad M, Verner E, Loury D, Chang B, Li S, Pan Z, Thamm DH, Miller RA, Buggy JJ. The Bruton tyrosine kinase inhibitor PCI-32765 blocks B-cell activation and is efficacious in models of autoimmune disease and B-cell malignancy. Proc Natl Acad Sci U S A. 2010; 107:13075–13080.
18. Touzeau C, Dousset C, Bodet L, Gomez-Bougie P, Bonnaud S, Moreau A, Moreau P, Pellat-Deceunynk C, Amiot M, Le Gouill S. ABT-737 Induces Apoptosis in Mantle Cell Lymphoma Cells with a Bcl-2 high/Mcl-1low Profile and Synergizes with Other Antineoplastic Agents. Clin Cancer Res. 2011; 17:5973–5981.
19. Coope HJ, Atkinson PG, Huhse B, Belich M, Janzen J, Holman MJ, Klaus GG, Johnston LH, Ley SC. CD40 regulates the processing of NF-kappaB2 p100 to p52. EMBO J. 2002; 21:5375–5385.
20. Lee HH, Dadgostar H, Cheng Q, Shu J, Cheng G. NF-kappaB-mediated up-regulation of Bcl-x and Bfl-1/A1 is required for CD40 survival signaling in B lymphocytes. Proc Natl Acad Sci U S A. 1999; 96:9136–9141.
21. Wang ML, Rule S, Martin P, Goy A, Auer R, Kahl BS, Jurczak W, Advani RH, Romaguera JE, Williams ME, Barrientos JC, Chmielowska E, Radford J, et al. Targeting BTK with ibrutinib in relapsed or refractory mantle-cell lymphoma. N Engl J Med. 2013; 369:507–516.
22. Chang BY, Francesco M, De Rooij MFM, Magadala P, Steggerda SM, Huang MM, Kuil A, Herman SE, Chang S, Pals ST, Wilson W, Wiestner A, Spaargaren M, et al. Egress of CD19(+)CD5(+) cells into peripheral blood following treatment with the Bruton tyrosine kinase inhibitor ibrutinib in mantle cell lymphoma patients. Blood. 2013; 122:2412–2424.
23. Ko TK, Chuah CT, Huang JW, Ng KP, Ong ST. The BCL2 inhibitor ABT-199 significantly enhances imatinib-induced

cell death in chronic myeloid leukemia progenitors. Oncotarget. 2014; 5:9033–9038.

24. Peirs S, Matthijssens F, Goossens S, Van de Walle I, Ruggero K, de Bock CE, Degryse S, Canté-Barrett K, Briot D, Clappier E, Lammens T, De Moerloose B, Benoit Y, et al. ABT-199 mediated inhibition of BCL-2 as a novel therapeutic strategy in T-cell acute lymphoblastic leukemia. Blood. 2014. pii: blood-2014-05–574566.

25. Fresquet V, Rieger M, Carolis C, García-Barchino MJ, Martinez-Climent JA. Acquired mutations in BCL2 family proteins conferring resistance to the BH3 mimetic ABT-199 in lymphoma. Blood. 2014 Jun 26; 123:4111–9.

26. Hallaert DYH, Jaspers A, van Noesel CJ, van Oers MHJ, Kater AP, Eldering E. c-Abl kinase inhibitors overcome CD40-mediated drug resistance in CLL: implications for therapeutic targeting of chemoresistant niches. Blood. 2008; 112:5141–5149.

27. Saba N, Wiestner A. Do mantle cell lymphomas have an "Achilles heel"? Curr Opin Hematol. 2014; 21:350–357.

28. Chiron D, Di Liberto M, Martin P, Huang X, Sharman J, Blecua P, Mathew S, Vijay P, Eng K, Ali S, Johnson A, Chang B, Ely S, et al. Cell-cycle reprogramming for PI3K inhibition overrides a relapse-specific C81S BTK mutation revealed by longitudinal functional genomics in mantle cell lymphoma. Cancer Discov. 2014; 4:1022–1035.

29. Zhao X, Bodo J, Sun D, Durkin L, Lin J, Smith MR, Hsi ED. Combination of ibrutinib with ABT-199: synergistic effects on proliferation inhibition and apoptosis in mantle cell lymphoma cells through perturbation of BTK, AKT, and BCL2 pathways. Br J Haematol. 2014 doi: 10.1111/bjh.13149.

30. Maïga S, Gomez-Bougie P, Bonnaud S, Gratas C, Moreau P, Le Gouill S, Pellat-Deceunynck C, Amiot M. Paradoxical effect of lenalidomide on cytokine/growth factor profiles in multiple myeloma. Br J Cancer. 2013; 108:1801–1806.

Regular Article

blood

LYMPHOID NEOPLASIA

Rational targeted therapies to overcome microenvironment-dependent expansion of mantle cell lymphoma

David Chiron,[1,2] Céline Bellanger,[1,2,*] Antonin Papin,[1,2,*] Benoit Tessoulin,[1-3] Christelle Dousset,[1,2,4] Sophie Maiga,[1,2] Anne Moreau,[5] Julie Esbelin,[6] Valérie Trichet,[2,7] Selina Chen-Kiang,[8] Philippe Moreau,[1,3] Cyrille Touzeau,[1,3] Steven Le Gouill,[1-3] Martine Amiot,[1,2] and Catherine Pellat-Deceunynck[1,2]

[1]Centre de Recherche en Cancérologie Nantes-Angers, INSERM, Centre National de la Recherche Scientifique (CNRS), Université de Nantes, Nantes, France; [2]Groupement De Recherche 3697 Micronit, CNRS, Tours, France; [3]Service d'Hématologie Clinique, Unité d'Investigation Clinique, [4]Centre d'Investigation Clinique, INSERM, [5]Service d'Anatomie Pathologique, and [6]Service de Gynécologie et Obstétrique, Centre Hospitalier Universitaire, Nantes, France; [7]Laboratoire de Physiopathologie de la Résorption Osseuse, INSERM, Université de Nantes, Nantes, France; and [8]Department of Pathology and Laboratory Medicine, Weill Cornell Medical College, Cornell University, NY

Key Points

- CD40L plus cytokines induces cell-cycle progression and loss of mitochondrial priming, leading to drug resistance in MCL.
- CD40L plus cytokines mimics in situ molecular profiles and allows the development of new approaches by integrating the role of the microenvironment.

Mantle cell lymphoma (MCL) accumulates in lymphoid organs, but disseminates early on in extranodal tissues. Although proliferation remains located in lymphoid organs only, suggesting a major role of the tumor ecosystem, few studies have assessed MCL microenvironment. We therefore cocultured primary circulating MCL cells from 21 patients several weeks ex vivo with stromal or lymphoid-like (CD40L) cells to determine which interactions could support their proliferation. We showed that coculture with lymphoid-like cells, but not stromal cells, induced cell-cycle progression, which was amplified by MCL-specific cytokines (insulin-like growth factor-1, B-cell activating factor, interleukin-6, interleukin-10). Of interest, we showed that our model recapitulated the MCL in situ molecular signatures (ie, proliferation, NF-κB, and survival signatures). We further demonstrated that proliferating MCL harbored an imbalance in Bcl-2 family expression, leading to a consequent loss of mitochondrial priming. Of interest, this loss of priming was overcome by the type II anti-CD20 antibody obinutuzumab, which counteracted Bcl-x_L induction through NF-κB inhibition. Finally, we showed that the mitochondrial priming directly correlated with the sensitivity toward venetoclax and alkylating drugs. By identifying the microenvironment as the major support for proliferation and drug resistance in MCL, our results highlight a selective approach to target the lymphoma niche. (*Blood*. 2016;128(24):2808-2818)

Introduction

Mantle cell lymphoma (MCL) is a rare but incurable subtype of non-Hodgkin lymphoma (NHL) deriving from immunoglobulin M+ (IgM^+) $CD5^+$ B cells, which initially accumulate in secondary lymphoid organs (LO) such as the lymph nodes or spleen. Hallmarks of MCL include aberrant activation of the cyclin D1/CDK4 complex, which supports unrestrained cell-cycle progression, and deregulation of the apoptotic machinery that leads to drug resistance.[1,2] Recently, progress in high-throughput technology provided considerable advancement in our understanding of secondary intrinsic alterations in MCL, such as SOX11 aberrant expression or frequent mutations of *ATM/TP53,* NF-κB regulatory genes, and Notch receptors.[3-5]

As described in other B-cell malignancies,[6,7] extrinsic signaling is believed to favor MCL growth, survival, and migration.[8] Interactions come from multiple microenvironments and support both nodal and extranodal manifestations (bone marrow, gastrointestinal), as highlighted by the early dissemination observed in most MCL patients at presentation. However, there is relatively little information regarding the nature of surrounding cells and soluble factors and the resulting molecular regulations induced in MCL. Further investigations that integrate the key role of the microenvironment are now needed to overcome tumor drug resistance in protective niches. The benefits of such an approach have been recently reinforced by studies reporting that selective inhibition of BTK or phosphatidylinositol 3-kinaseδ, critical kinases of the B-cell receptor (BCR) and CXCR4 pathways, prevents the homing of MCL, leading to peripheral lymphocytosis.[9-12] However, the consequences of cell egress in the peripheral blood (PB) on proliferation and survival are still unclear and need further investigations.

In situ, lymphoma B cells are in close contact with cells of immune origin, including CD40L-expressing T cells or macrophages, and mesenchymal cells such as specialized stromal or follicular dendritic cells.[8,13] Few studies have shown that coculture with stromal cells promoted MCL cell survival through several mechanisms, such as a decrease in Bim expression[14] or cell adhesion-mediated drug resistance.[15] However, regulations induced by coculture are still

Submitted 3 June 2016; accepted 22 September 2016. Prepublished online as *Blood* First Edition paper, 3 October 2016; DOI 10.1182/blood-2016-06-720490.

*C.B. and A.P. contributed equally to this manuscript.

The online version of this article contains a data supplement.

There is an Inside *Blood* Commentary on this article in this issue.

The publication costs of this article were defrayed in part by page charge payment. Therefore, and solely to indicate this fact, this article is hereby marked "advertisement" in accordance with 18 USC section 1734.

unclear, because both cell-cycle arrest[16,17] and cell expansion[18,19] have been described. Difficulties in culturing circulating primary MCL cells (observed in around 20% of patients) greatly impeded their long-term use ex vivo, and in contrast to normal B-cell or chronic lymphocytic leukemia (CLL), CD40 stimulation generally failed to induce absolute long-term expansion.[20,21] These limitations restrained most functional studies to a restricted number of well-described MCL cell lines.

In the present work, we further characterized microenvironment-dependent proliferation, survival, and drug resistance of primary MCL cells (n = 21) and developed a unique ex vivo model for long-term primary MCL cell culture. This model efficiently mimicked molecular signatures observed in lymphoid tissues and allowed us to develop novel mechanism-based strategies that effectively target cancer cells and counteract in situ drug resistance.

Methods

Culture and coculture of primary MCL cells and cell lines

Primary cells were obtained after informed consent from MCL patients treated at the Department of Clinical Hematology from the University Hospital of Nantes, France (ethical approval DC-2011-1399). After Ficoll-Hypaque separation, the percentage of $CD19^+/CD5^+$ cells was assessed by flow cytometry, either directly or after storage in liquid nitrogen (fetal calf serum 10% dimethyl sulfoxide). When $CD19^+/CD5^+$ cells infiltration was <90%, MCL cells were purified with anti-human CD19-conjugated magnetic beads (Miltenyi, Paris, France). Primary cells were plated over preestablished layers of adherent stromal cells (primary human mesenchymal stem cells [hMSC]), mitomycin-C–treated parental [L], or CD40L-expressing fibroblast L cells [L-40L]), as described previously,[22] with or without cytokines (50 ng/mL interleukin-10 [IL-10], 50 ng/mL B-cell activating factor [BAFF], 10 ng/mL insulin-like growth factor-1 [IGF-1], 1 ng/mL IL-6). The ratio of adherent cells and primary MCL cells was 1/10. L-40L cells were kindly provided by Dr. T. Defrance (Lyon, France), and hMSC cells were isolated as described previously.[23,24] Once a week, primary cells were gently unhooked and counted. Cells were then diluted in fresh medium containing cytokines and plated over fresh layer of adherent cells. For comparison with normal naïve $CD5^+$ B cells, cord blood B cells (CBBC) from healthy volunteers were isolated and cultured using the same protocol. MCL cell lines, commercial (JeKo-1, Maver-1, Z138) or generated in our laboratory (NTS1-3, characterized by GEP, GSE86322), were identified using a flow cytometry–based barcode as previously described.[25] They were maintained in RPMI-1640 medium supplemented with 10% fetal calf serum and 2 mM glutamine. JeKo-1 and Maver-1 were purchased from DSMZ (Braunschweig, Germany); Z138 was purchased from ATCC (Manassas, VA).

Cell cycle. Primary cells were incubated overnight with 5-bromo-2′-deoxyuridine (BrdU) on a preestablished layer of mitomycin-C–treated L-40L or hMSC cells and then fixed and permeabilized in 70% ethanol for at least 24 hours at 4°C before staining. Ki67 and pS10H3 staining was performed according to the protocol described by Vignon et al.[26]

BH3 profiling. BH3 profiling was performed using the BH3-mimetic Venetoclax (VNT, 2-20 μM), the BIM BH3 peptide (0.05 μM), and engineered HRK* BH3 (5 μM) and Noxa* BH3 (5 μM) peptides. The peptide sequence for Noxa* (MS1) has been previously described.[27] We used a new sequence peptide for HRK* (Y4eK_21) recently described,[28] which showed significant improved efficacy for identifying cells dependence on Bcl-x_L vs Bcl-2. Permeabilized cells were exposed to peptides for 45 minutes at 27°C before fixation with 2% formaldehyde at room temperature for 15 minutes. After addition of neutralizing buffer (Tris 0.41 mol/L glycine pH 9.1) for 5 minutes, cells were stained with anti-cytochrome c–Alexa647 (BLE612310, Ozyme) 1:40 in 0.1% Saponin/1% bovine serum albumin/phosphate-buffered saline overnight at 4°C. Loss of cytochrome c was quantified by gating the cytochrome c negative population measured by flow cytometry.

RNA extraction from formalin-fixed, paraffin-embedded samples. Purification of total RNA from formalin-fixed, paraffin-embedded lymphoid tissues (patients 5 and 22: lymph nodes; patient 16: spleen) was done on freshly cut 10-μM sections according to manufacturer's protocol (cat. no. 73504; Qiagen).

Cell viability, short interfering RNA (siRNA) transient transfections, real-time quantitative reverse transcription polymerase chain reaction (qRT-PCR) and Immunoblot assays have been previously described.[11] Antibodies and reagents are detailed in supplemental Table 1 (available on the *Blood* Web site) and statistical analyses were performed using Student *t* test, paired Student *t* test, or Wilcoxon test.

Results

$CD40L^+$ cells, but not mesenchymal cells, induce primary MCL proliferation in the presence of specific growth factors

In spite of the significant level of the proliferation index Ki67 (gene *MKI67*) in secondary LOs and the elevated percentage of circulating malignant cells (Figure 1A; Table 1), we did not detect any proliferating ($BrdU^+$) PB MCL cells, which were in the G1-phase of the cell cycle (Figures 1B; supplemental Figure 1A). In contrast to MCL, normal IgM^+ $CD5^+$ B cells, purified from cord blood (CBBC), were quiescent (G0-phase) (Figure 1B; supplemental Figure 1B). Direct comparison of *MKI67* expression in paired samples from MCL LO and PB showed that the proliferation index dramatically dropped in PB (Figure 1C), confirming that in vivo proliferation was related to the LO microenvironment. Thus, we used primary hMSC and CD40L-expressing L-40Ls to mimic stromal and lymphoidlike interactions. L-40L cells, but not hMSCs, were able to induce cell-cycle progression (median $BrdU^+$ cells hMSC, 3%; range, 0-11; L-40L, 29%; range, 10-42; n = 5) (Figure 1D). The progression into the cell cycle observed on the L-40L layer was dependent on CD40 stimulation, with parental L cells being unable to induce proliferation and sCD40L successfully triggered the cell cycle, albeit less potently (supplemental Figure 2A-B). Biopsies from LO revealed a significant RNA level (*CD40LG*) in the tumor niche, confirming that CD40 stimulation can occur in situ (supplemental Figure 2C).

Because cytokines are required for B-cell proliferation, we assessed the expression of cytokine receptors in vivo in MCL cells from LO (RNA-seq) and PB (flow cytometry) (supplemental Figure 3A-B). Given that the receptors for IL-6, IL-10, IGF-1, and BAFF cytokines, which were previously identified to significantly promote MCL survival,[18,29-31] were expressed in LO MCL, we used a cocktail composed of these MCL specific growth factors. Even though IL-4 has been used in most MCL models,[19,32,33] it was excluded from our study because of a low IL-4R level and to a dramatic IL-4–induced expression of CD23, which is typically unexpressed in MCL in vivo (supplemental Figure 3C).[34] Cytokines were critical for enhancing the magnitude of proliferation because they considerably increased $BrdU^+$ cells (S-phase) when cocultured on L-40L cells (3-fold induction, n = 9) (Figure 1E). The cytokine cocktail (Ck) was more efficient than each cytokine alone (supplemental Figure 3D).

Coculture on the L-40L layer in the presence of the Ck (L-40L+Ck) also reproduced the in vivo aggressive behavior of blastoid MCL variants. Indeed, the proportion of cells in S-phase was significantly higher for MCL cells with blastoid morphology (median D7, 50%; n = 3) than cells of the common type (median D7, 15%; n = 4) (Student *t* test, $P = .01$) (Table 1; supplemental Figure 4A). Prolonged stimulation on L-40L+Ck allowed for long-term expansion of primary cells (Figure 1F) and expression of cyclin-D1 and monoclonality confirmed that expanded cells were MCL cells (supplemental Figure 4B-C). Using this system, we were able to maintain proliferation of primary MCL cells for several weeks, and most MCL samples remained dependent on the extrinsic signal over time. After several months of culture, t(11;14) Epstein-Barr

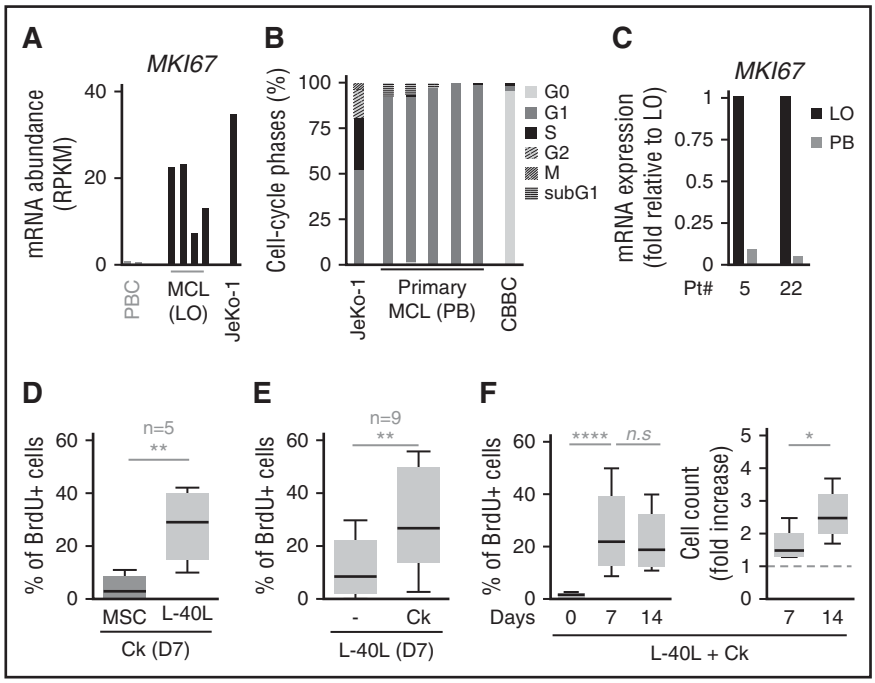

Figure 1. CD40L$^+$ but not mesenchymal cells support primary MCL cell proliferation ex vivo. (A) Whole transcriptome sequencing analysis of mRNA abundance (RPKM) of *MKI67* (Ki67 gene) in cyclinD1$^+$ primary MCL cells from LO, CD19$^+$ PB B cells (PBC)s from 2 healthy volunteers, and JEKO-1, as previously described.[54] (B) Cell distribution in the different cell-cycle phases (%) for 1 proliferating cell line (JeKo-1), 5 primary PB MCL samples, and CD5$^+$ CBBCs (healthy donor). The results are detailed in supplemental Figure 1B. (C) qRT-PCR analysis of the *MKI67* gene in primary cells concomitantly isolated from LO and PB for 2 MCL patients. Pt, patient. (D) BrdU/propidium iodide staining of primary MCL cells (n = 5) in the presence of hMSC or L-40L coculture layer and cytokines for 7 days as indicated; paired Student *t* test. (E) BrdU/propidium iodide staining of primary MCL cells (n = 9) in the presence of L-40L coculture layer with or without cytokines for 7 days as indicated; paired Student *t* test. (F) Left (n = 9): cell-cycle analysis (% of BrdU$^+$ cells) of primary MCL cells for the time and condition indicated; Student *t* test. Right (n = 5): total number of live cells is represented as fold increase from input on day 0; Student *t* test. n.s., not significant. $^*P < .05$, $^{**}P < .01$, $^{****}P < .0001$.

virus$^+$ subclones gave rise to 2 microenvironment independent cell lines (NTS-1 from patient 10; NTS-2 from patient 15), whereas the t(11;14) Epstein-Barr virus$^-$ MCL cell line NTS-3 (from patient 16) remained dependent on CD40L and displayed a molecular profile close to widely used commercial MCL cell lines (supplemental Figure 4D-E).

Ex vivo L-40L+Ck coculture model induces a lymphoid organ-like molecular profile in peripheral MCL cells

To assess whether our ex vivo model did recapitulate an LO-like MCL profile, we compared L-40L+Ck cocultured primary MCL cells with LO/PB paired MCL samples. We first showed that, compared with PB, *MKI67* increased in situ in LO and ex vivo in coculture. The cell-cycle activation was also confirmed at the protein level by the increase in phosphorylation of Rb (pRb) or in proliferating cell nuclear antigen (PCNA) expression in the Rb-negative sample (patient 11) (Figure 2A-B).

In addition, the analysis of NF-κB target genes (*IL2RG*, *PLEK*, and *CD74*)[35] in paired LO/PB MCL samples revealed an induction in LO, suggesting that NF-κB activation by the microenvironment occurred in vivo (Figure 2C). This induction was recapitulated in L-40L+Ck coculture and, accordingly, was associated with a potent and lasting NF-κB activation through the

Table 1. Characteristics of patients with MCL

Patient	Status	Age	Sex	sIg	Blastoid variant	Ki67$^+$ (%)	CD19$^+$CD5$^+$ (% in PB)	CD5 (ratio MFI)
1	D	67	M	κ	No	ND	60	21.0
2	R	86	M	κ	ND	ND	50	7.1
3	D	73	M	ND	ND	ND	80	16.8
4	R	80	F	κ	No	ND	80	7.9
5	D	74	F	κ	No	10	85	17.6
6	R	62	M	λ	Yes	90	80	18.3
7	D	61	F	λ	ND	ND	28	25.6
8	R	67	M	λ	ND	ND	33	8.8
10	D	69	F	κ	No	ND	60	4.0
11	R	73	F	κ	No	ND	60	5.2
12a	D	69	F	κ	No	30	22	7.5
12b	D	69	F	κ	No	ND	68	30.2
13	D	73	M	κ	No	30	55	3.5
14	R	73	M	λ	ND	ND	70	16.0
15	R	79	F	κ	Yes	40	85	84.3
16	R	73	F	κ	Yes	40	90	22.0
17	D	82	F	κ	ND	ND	33	1.7
18	D	76	M	κ	No	30	25	18.4
19	R	81	M	κ	ND	ND	22	5.0
20	R	72	M	κ	Yes	65	67	16.7
21	D	70	F	λ	ND	ND	75	1.3
22	D	75	M	ND	Yes	70	84	60.0

Ki67 expression was determined in CCND1$^+$ cells by immunohistochemistry. All but 1 (12b, pleural effusion) sample was obtained from PB.
D, diagnosis; F, female; M: male; MFI, mean fluorescence intensity; ND, not determined; R, relapse.

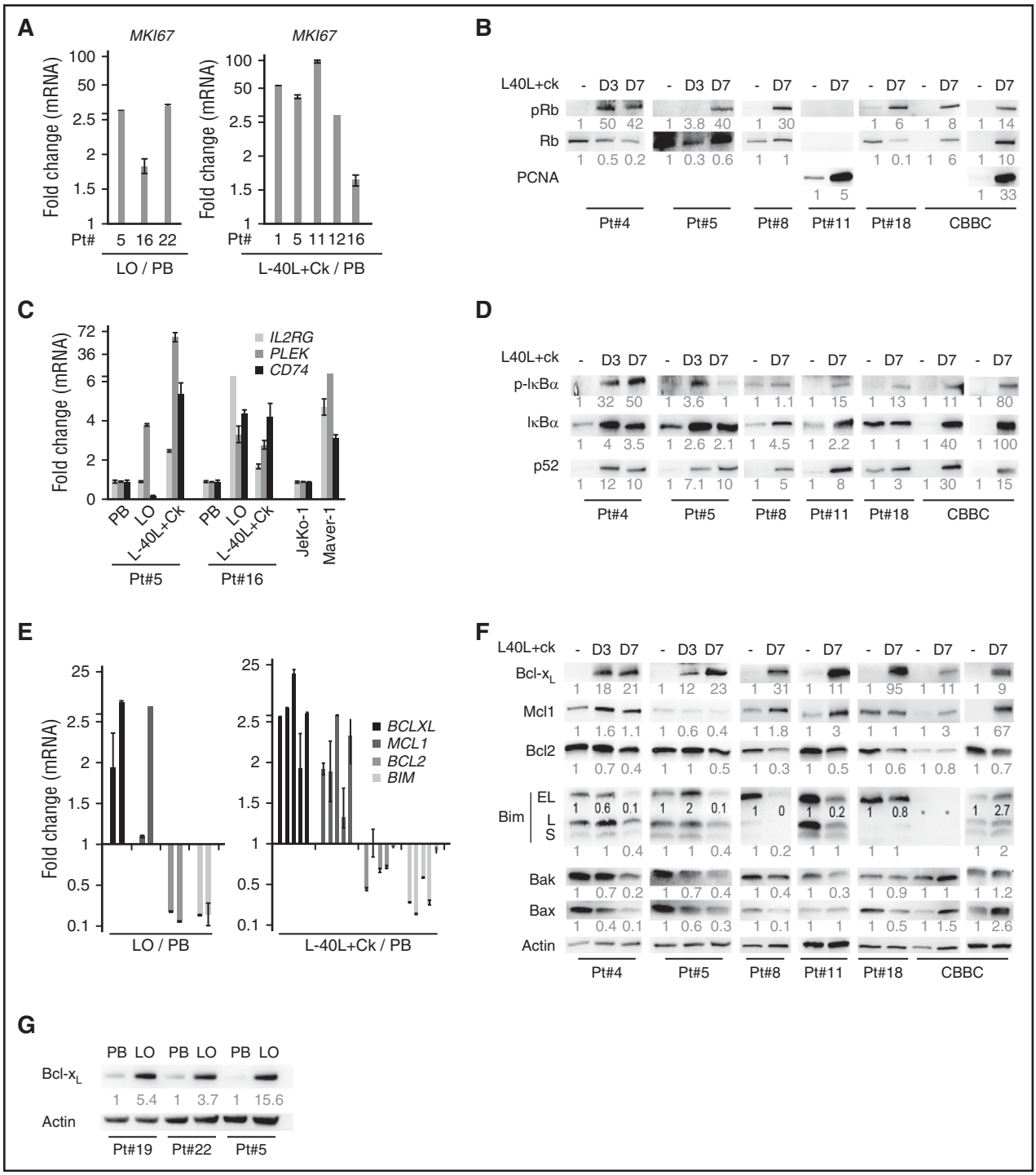

Figure 2. Extrinsic stimulations result in proliferation, NF-κB activation and in an unbalanced modulation of the Bcl-2 family in primary MCL cells. (A) qRT-PCR analysis of MKI67 from: left, primary MCL cells concomitantly isolated from LO (Pts 5 and 22: lymph node, Pt16: spleen) and PB; right, PB primary MCL cells cocultured on an L-40L layer in the presence of cytokines (D7) and relative to PB. (B) Immunoblotting of cell-cycle related proteins (pRb, Rb, PCNA) in primary $CD5^+$ cells isolated from healthy donor (CBBC) or MCL patients (PB) at D0 and after coculture on L-40L+Ck at the time indicated (D3, D7). (C) qRT-PCR analysis of NF-κB target genes (*IL2RG*, *PLEK*, and *CD74*)[35] in primary MCL cells cultured as in panel A. Maver-1 and JeKo-1 were used as NF-κB signaling positive and negative controls, respectively.[4] (D) Immunoblotting of classical (*p*-IκBα) and alternative (p52) NF-κB pathway proteins in primary MCL cells as in panel B. (E) qRT-PCR analysis of indicated genes in primary MCL cells cultured as in panel A. (F) Immunoblotting of Bcl-2 family proteins in primary MCL cells as in panel B. *Highlights Bim underexposure resulting from high expression in sample 18. (G) Immunoblotting analysis of indicated proteins in primary MCL cells concomitantly isolated from LO and PB. Quantification of protein level was normalized to actin and indicated below each protein.

phosphorylation of NF-κB inhibitor alpha (*p*-IκBα) and accumulation of p52. Of note, Maver-1 (known as constitutive NF-κB activated cells)[4] but not JeKo-1 cells displayed similar expression of NF-κB target genes (Figure 2C-D). Moreover, primary MCL cells isolated from LO displayed elevated level of NF-κB target genes as well as other NF-κB signature genes (*NFKBIA*, *NFKBIE*,

RELB, *BIRC3*, *TNFAIP3*, *MALT1*)[35] compared with JeKo-1 cells (supplemental Figure 5).

Finally, in good agreement with gene and protein expression in situ, we observed an increase in Bcl-x_L and Mcl-1 and a decrease in Bcl-2 and Bim expression ex vivo (Figure 2E-G). In addition, expression of both effector proteins Bak and Bax was decreased (Figure 2F). These microenvironment regulations were in favor of survival and appeared to be restricted to tumor cells. Indeed, although coculture induced proliferation (pRb^+PCNA^+) of CBBC and increased expression of Bcl-xL and Mcl-1, it did not decrease the expression of Bim, Bak, or Bax (Figure 2F).

Taken together, these results showed that PB MCL cultured with L-40L+Ck displayed a molecular signature of proliferation, NF-κB pathway, and survival, which was similar to MCL in LO. In contrast, we did not observe similar NF-κB activation or modulation of Bcl-x_L, Bcl-2, and Mcl-1 in primary MCL cells cocultured on hMSC. Nevertheless, expression of Bim (EL) was decreased as previously reported (supplemental Figure 6A).[14]

Microenvironment-dependent upregulation of Bcl-x_L mediates loss of priming

To determine the functional involvement of microenvironment-induced modulation in expression of Bcl-2 family proteins at the mitochondrial level, we performed flow cytometry BH3 profiling. Using this functional assay, we determined the global priming of the cells using a BIM peptide, which targets all antiapoptotic proteins, and MCL cells dependency on individual antiapoptotic proteins through the use of selective peptides (HRK*, NOXA*) or the BH3 mimetics (VNT) highly specific for Bcl-x_L, Mcl-1, or Bcl-2.[36] Resting cells from PB were highly primed for death because BIM peptide induced dramatic cytochrome c release in 77 ± 7% of cells. They were mostly primed on Bcl-2 (strong VNT response, 54 ± 28%) and moderately on Bcl-x_L (weak HRK* response, 19 ± 16%) but not at all on Mcl-1 (no NOXA* response, 2 ± 5%). By contrast, MCL cultured on L-40L+Ck were far less primed (decrease in BIM response, 34 ± 20%) and unprimed to Bcl-2 and Bcl-x_L (2 ± 2% and 6 ± 8%, respectively) (Figure 3A). The loss of priming was specific to MCL cells cultured on L-40L+Ck and was not observed when primary cells were cultured on hMSC (supplemental Figure 6B).

To assess the functional consequences of this priming loss at the cellular level, we compared the drug sensitivity of primary MCL cells freshly isolated from PB and after 7 days on L-40L+Ck coculture. As expected, and in accordance with the priming assays, prolonged coculture resulted in full resistance to 25 nM VNT (Figure 3B). L-40L+Ck cocultured MCL cells also became more resistant to the alkylating drug bendamustine but remained sensitive to the proteasome inhibitor bortezomib (BTZ; Figure 3C). siRNA against Bcl-x_L similarly impaired CD40L-dependent resistance to both bendamustine and VNT, highlighting the central role of Bcl-x_L in CD40L-dependent MCL resistance (Figure 3D).

In accordance with the lack of Bcl-x_L induction, the loss of priming, the resistance to VNT and bendamustine were not observed in MCL cells cocultured with hMSC (supplemental Figure 6C-D).

Given the high expression of Bcl-x_L in MCL cell cocultured on L-40L+Ck, lack of priming on Bcl-x_L was unexpected and suggested that Bcl-x_L could be "empty" of proapoptotic proteins at mitochondria. Indeed, no association with Puma and Bid BH3-only activators or the proapoptotic multidomain Bax was detected and only weak Bcl-x_L/Bim and Bcl-x_L/Bak complexes were observed (Figure 4A and data not shown). We then hypothesized that Bcl-x_L could bind Bcl-2–released BH3 only, leading to loss of priming and consequent drug resistance. Indeed, in L-40L+Ck cultured cells pretreated with VNT, which selectively disrupted Bcl-2-BH3–only complexes, we demonstrated that Bim released from Bcl-2 was associated with Bcl-x_L after VNT exposure (Figure 4B). This was confirmed by BH3-profiling, VNT pretreatment making the cells now selectively primed on Bcl-x_L as shown by cytochrome c release induced by HRK* peptide (Figure 4C). Taken together, our results demonstrated that CD40L-dependent Bcl-x_L induction triggered loss of mitochondrial priming through its ability to capture back BH3-only released from its complex with Bcl-2 (Figure 4D). Dual inhibition of Bcl-2 and Bcl-x_L are thus needed to target MCL cells located in both peripheral blood and protective niches. This was confirmed by the high efficiency of Bcl-2 (VNT) and BclxL (A131852) BH3 mimetics sequential combination, which overrode microenvironment drug resistance (Figure 4E).

Microenvironment/NF-κB–dependent Bcl-x_L upregulation is counteracted by the type II anti-CD20 monoclonal antibody obinutuzumab

BH3-mimetic targeting both Bcl-2 and Bcl-x_L (Navitoclax) could counteract the loss of priming observed, but its clinical use has been limited by induction of toxicity such as thrombocytopenia.[37] Novel approaches to impair microenvironment-dependent induction of Bcl-x_L selectively in tumor cells are thus needed. Previous studies have demonstrated that even if Bcl-x_L is regulated by multiple transcription factors, NF-κB preferentially controlled CD40L-dependent Bcl-x_L induction.[38] The NF-κB inhibitor Bay-11-7082, which inhibits both classical (*p*-IκBα) and alternative (p52) CD40L-dependent activation, also totally impaired Bcl-x_L induction in primary MCL cells (Figure 5A). BTZ has also been shown to rapidly impair NF-κB activity through proteasome inhibition and accumulation of *p*-IκBα in MCL cell lines.[39] As observed in Figure 5A, in addition to blocking *p*-IκBα degradation, BTZ counteracted the CD40L-dependent p52 increase, leading to a substantial decrease in Bcl-x_L protein level.

Previous studies have shown that anti-CD20 monoclonal antibody (mAb, rituximab [RTX]) was able to downregulate Bcl-x_L through NF-κB inhibition in a model of B-cell NHL cell lines.[40] We then further investigated whether of anti-CD20 RTX (type I mAb) or obinutuzumab (type II mAb, OBN) could overcome microenvironment dependent Bcl-x_L upregulation. We demonstrated that OBN directly impaired IκBα and p52 expression (Figure 5B) and inhibited expression of NF-κB target genes (Figure 5C) in $CD20^{High}$ but not in $CD20^{Low}$ primary samples (ratio MFI <3; Figure 5D). Accordingly, *BCLXL* expression decrease (both at the messenger RNA [mRNA] and protein level) was deeper in $CD20^{High}$ primary MCL cells than $CD20^{Low}$ samples (Figure 5E). As observed in primary MCL cells, pretreatment of Maver-1 and Z138 cells with OBN induced the downregulation of *BCLXL*, whereas it did not significantly modulate expression of *BCL-2* and *MCL-1*. OBN induced the downregulation of both constitutive and CD40L-induced *BCLXL* expression (Figure 5F-G), and we wondered whether it could prevent loss of priming. Indeed, OBN counteracted loss of priming as highlighted by the increased cytochrome c release using Bim peptide or different concentration of VNT (Figure 5H). Taken together, our results demonstrate that OBN overcome microenvironment-dependent Bcl-x_L upregulation and consequent loss of mitochondrial priming through inhibition of the NF-κB axis.

In good agreement with BH3 profiling, OBN sensitized MCL cells to VNT cytotoxicity (Figure 6A). In Maver-1 cells, pretreatment with OBN counteracted CD40L-dependent resistance to VNT. Similarly a

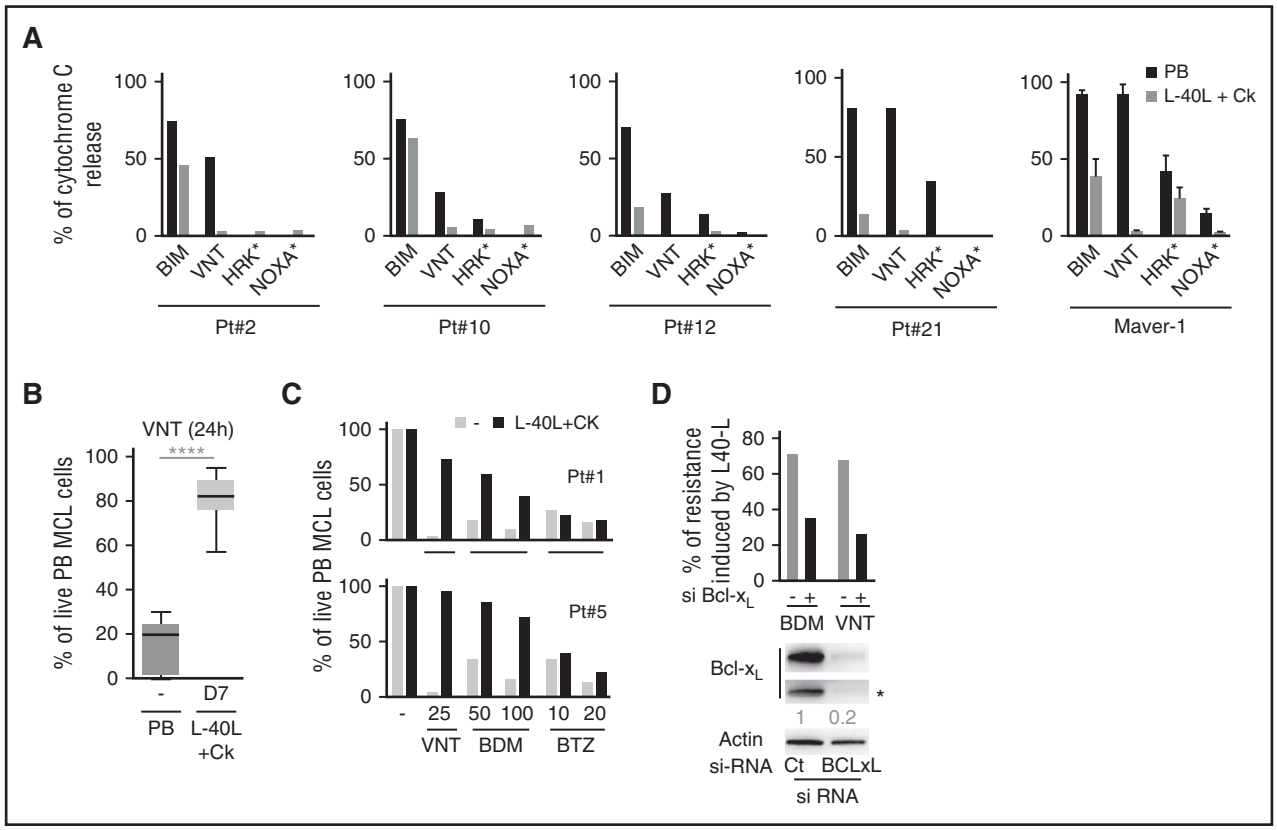

Figure 3. Microenvironment-dependent loss of mitochondrial priming and acquired drug resistance in primary MCL cells. (A) BH3 profiling of primary MCL from 4 patients and Maver-1 cells performed as described in "Methods." Values for Maver-1 cells are the mean of 3 independent experiments. (B-C) Primary MCL cells freshly isolated from PB (−) or after 7 days on an L-40L or hMSC layer in the presence of cytokines were cultured with VNT (25 nM), bendamustine (BDM; 50-100 μM), or BTZ (10-20 nM) for 24 hours. Viability was then addressed by annexin-V staining, the % of live cells is represented as the % of control (without treatment). ****$P < .0001$; paired Student *t* test. (D) siRNA against *BCLXL* reduced Bcl-x_L protein expression and impaired L-40L–induced protection against BDM (24 hours, 100 μM) or VNT (24 hours, 50 nM) cytotoxicity in Maver-1 cells. *Lower exposure. Representative western blot of 3 experiments.

supraadditive effect of the combination was also observed for intrinsically VNT-resistant JeKo-1 and Z138 cells (observed value > expected value, Figure 6A). OBN pretreatment also counteracted CD40L-dependent resistance to bendamustine and to AraC to a lesser extent (Figure 6B).

Although both RTX and OBN bind to CD20, OBN is a type II antibody described as displaying stronger direct cell death activity.[41] In contrast, RTX (0.5-5 μg/mL) neither induced direct cytotoxicity nor sensitized MCL cell lines to VNT (data not shown). Similarly, primary MCL cells were more sensitive to direct OBN than to RTX cytotoxicity (median cell death: OBN, 40%; RTX, 16%; Figure 6C).

Of interest, whereas low doses of single agent OBN (0.5 μg/mL) did not induce cell death in cell lines, cocultured primary cells were sensitive (Figure 6D). Finally, VNT and OBN alone triggered 15% (range, 2-28) and 30% (9-54) cell death, respectively, and in combination induced 54% (18-71) (Figure 6E), $CD20^{High}$ samples being more sensitive to the combination than $CD20^{Low}$ samples (supplemental Table 2).

Discussion

Recently, considerable effort has been invested on the identification of intrinsic MCL abnormalities,[3-5] but little attention has been paid to the importance of the microenvironment in this pathology. Herein, our observations confirmed that well-known intrinsic abnormalities such as overexpression of cyclin-D1 and Bcl-2 are not sufficient to recapitulate the proliferation observed in situ or to protect malignant cells against spontaneous apoptosis ex vivo. To further understand the central role of extrinsic signaling in MCL cells, we established ex vivo models using stromal (hMSC) or lymphoid-like (L-40L) coculture and demonstrated that L-40L, associated with specific growth factors, not only promoted extended survival but also the progression into the cell cycle in primary MCL cells.

Cytokines play a critical role in hematological malignancies and receptors for IL-6, BAFF, IL-10, and IGF-1 have been previously identified as important survival factors in MCL.[18,29-31] Because all MCL cells did not homogeneously express the 4 growth factor receptors, we did not investigate the individual role of each cytokine and decided to keep the same cocktail for all samples. Even though CD40L allows cells to go through G1 into S phase, we demonstrated that these specific cytokines potentiated cell-cycle progression and allow long-term expansion in all samples tested. In contrast, although hMSC similarly protected MCL cells against spontaneous apoptosis, they were unable to promote proliferation (Figure 1), which was consistent with the previously described cell-cycle arrest upon stromal interaction[16] and the tissue-specific cell-cycle control observed in vivo.[42]

A study recently highlighted activation of BCR/NF-κB signaling as well as tumor proliferation in LO resident cells in situ.[43] Of interest, we demonstrated that modulations observed after L40L+Ck coculture

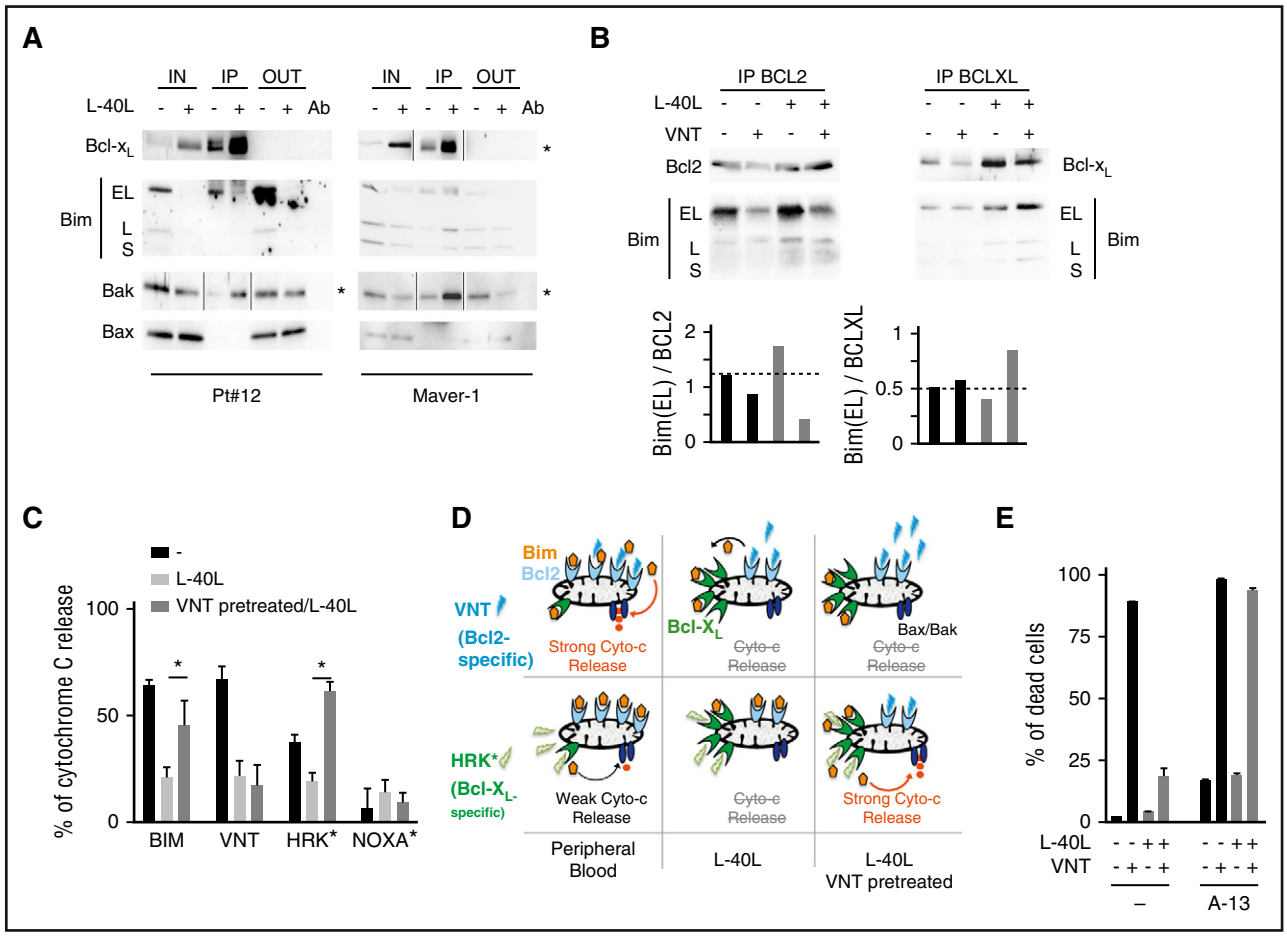

Figure 4. Microenvironment-dependent upregulation of Bcl-x_L mediates loss of priming. (A) Bcl-x_L immunoprecipitation in primary MCL cells (Pt 12) and Maver-1 cells cocultured or not on L-40L+Ck. The lysate (IN), immunoprecipitates (IP), and IP supernatants (OUT) were analyzed by immunoblotting for the indicated proteins. *Highlights different exposure for IP and IN/OUT. (B) Bcl-2 and Bcl-x_L immunoprecipitation in Maver-1 cells cocultured or not on L-40L with or without VNT (3 hours, 50 nM) pretreatment. Lower, Quantification of protein level. (C) BH3-profiling of Maver-1 cells cultured as in panel B and performed as described in "Methods." Values are the mean of 3 independent experiments. (D) Schematic representation of how microenvironment-dependent upregulation of Bcl-x_L mediates loss of priming. (E) Maver-1 cells cultured or not on L-40L with or without VNT (50 nM) and Bcl-xL mimetic A1331852 (0.5 μM). Cell death was assessed using annexin-V staining. Values are the mean of 3 independent experiments.

mimicked the differential proliferation, NF-κB, and BCR signature observed in malignant cells from LO vs PB (Figure 2 and data not shown). This observation highly suggests that our ex vivo model is relevant and that CD40L-expressing T cells in situ might play a role in tumor maintenance. T cells are present in MCL LO,[44] and we showed the CD40L mRNA expression in tissue biopsies. In addition, colocalization of primary MCL cells with T cells were recently evidenced in a xenograft model of NSG mice.[45] By using peripheral circulating MCL cells, our model also offers a process not only for expanding primary MCL cells to perform genomic/cellular analyses, but also for establishing MCL cell lines.

In addition to inducing progression into the S-phase of the cell cycle, L-40L+Ck coculture also resulted in anti- and proapoptotic Bcl-2 family member modulation, leading to a decrease in mitochondrial priming and a consequent drug resistance. We observed that increase in the expression of the antiapoptotic Bcl-x_L protein was associated with a striking downregulation in the expression of the proapoptotic Bim, Bax, and Bak proteins in primary MCL cells. Of note, this unbalanced regulation seemed to be restricted to MCL cells because it did not occur in naïve CBBC (Figure 2) or normal memory B cells, as previously described.[22] We demonstrated that CD40L-NF-κB–mediated Bcl-x_L upregulation was responsible for loss of mitochondrial priming and drug resistance. Using BH3 profiling, we showed a dynamic sequestration of the BH3-only activator Bim by Bcl-x_L proteins at the mitochondrial level. Our results are consistent with previous studies showing microenvironment-dependent unpriming[46] and Bcl-x_L induction[47] in CLL primary cells, reinforcing the central role of microenvironment-dependent signaling in lymphoid malignancies drug resistance.

Although the dramatic Bcl-x_L increase was the direct consequence of CD40L-dependent NF-κB induction, mechanisms of the differential regulation of other BCL-2 family members are still unclear. Further investigation is now needed to decipher specific cytokine effects as well as potential indirect regulation resulting from cell-cycle progression or epigenetic regulations.

Given the central role of CD40-NF-κB-Bcl-x_L signaling in mitochondrial regulation, we investigated how to overcome this extrinsically induced drug resistance. As expected, CD40L-cocultured MCL cells remained sensitive to BTZ because it rapidly neutralizes NF-κB activity[39] and consequently impairs Bcl-x_L upregulation. Although BTZ recently received US Food and Drug Administration approval for first-line use in patients with MCL, its efficacy is limited by major side effects.[48] We further assessed the ability of anti-CD20 mAbs to inhibit the CD40-NF-κB-Bcl-x_L pathway because they were

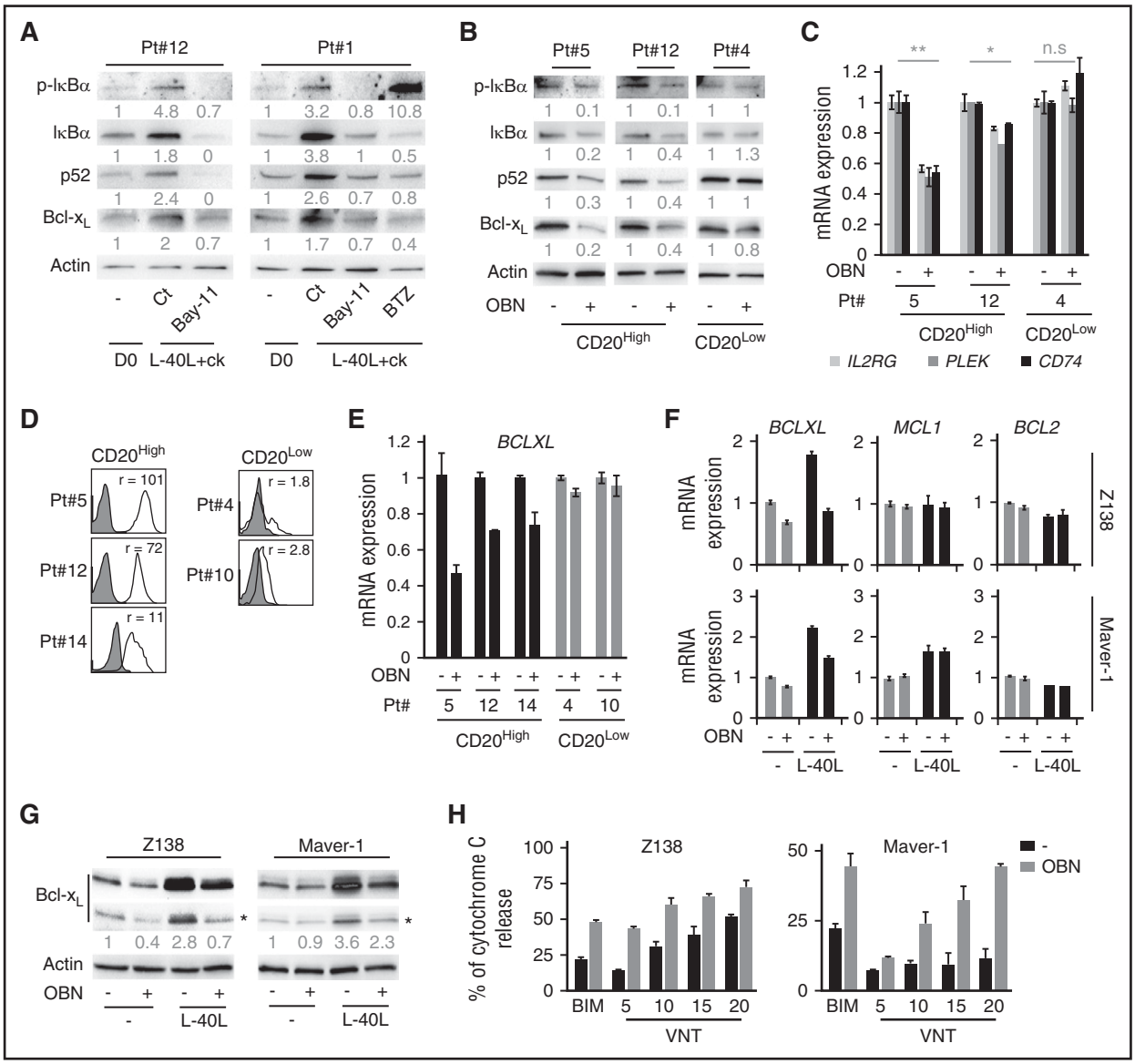

Figure 5. Obinutuzumab counteracts microenvironment-dependent loss of priming through NF-κB inhibition and Bcl-x_L downregulation in primary MCL cells. (A) Immunoblotting of indicated proteins in primary MCL cells cocultured on L-40L for 6 hours in the presence or absence of the NF-κB inhibitor Bay11-7082 (Bay11: 5 μM) or proteasome inhibitor BTZ (50 nM). (B) Immunoblotting analysis of the indicated proteins in $CD20^{High}$ or $CD20^{Low}$ primary MCL cells in the presence or absence of OBN (48 hours; 5 μg/mL). (C) qRT-PCR analysis of NF-κB targets (*IL2RG*, *PLEK*, and *CD74*)[35] in $CD20^{High}$ or $CD20^{Low}$ primary cells. (D) CD20 expression levels measured by fluorescence-activated cell sorting analysis on $CD19^{+}CD5^{+}$ primary MCL cells. (E) qRT-PCR analysis of *BCLXL* gene in $CD20^{High}$ (black bars) or $CD20^{Low}$ (gray bars). L-40L+Ck cocultured primary MCL cells in the presence or absence of OBN (24 hours; 5 μg/mL). (F-G) qRT-PCR analysis of *BCLXL*, *BCL-2*, and *MCL-1* (F) and immunoblotting of Bcl-x_L (G) in Z138 and Maver-1 cells cocultured or not on L-40L cells in the presence or absence of OBN (24 hours; 5 μg/mL). (H) BH3-profiling of Z138 and Maver-1 cells cocultured on L-40L+Ck in the presence or absence of OBN (24 hours; 0.5 μg/mL), was performed as described in "Methods."

reported to counteract microenvironment protection in CLL.[49] We demonstrated that the type II anti-CD20 antibody OBN, but not the type I RTX, was able to counteract NF-κB–induced overexpression of Bcl-x_L and the consequent loss of mitochondrial priming and drug sensitivity. This is consistent with previous works showing an increased direct cell death induction and superior B cell–depleting activity in lymph nodes and spleen treated with OBN in comparison with RTX.[50,51] In contrast to BTZ, anti-CD20 mAb specifically targets B cells and thus induces limited in vivo adverse events.[52] OBN has already demonstrated promising clinical activity as a single agent in MCL,[52] and recent results from a phase 3 study in indolent NHL suggested an increased progression-free survival in combination with bendamustine.[53] In accordance, our preclinical data highlighted that OBN significantly increased bendamustine cytotoxicity in CD40L-stimulated MCL cells. Our results also showed that OBN could be particularly efficient in combination with VNT. This Bcl-2–selective BH3 mimetic was highly cytotoxic for Bcl-2–dependent peripheral MCL cells, but became less efficient in CD40L-induced Bcl-x_L cells that displayed a similar profile to LO MCL cells. Although VNT shows encouraging results as a single agent, our results highly suggest that combinatorial therapy with OBN would improve patient response. Moreover, ibrutinib, which mediates indirect Bcl-x_L down-modulation upon BTK-dependent egress in the PB, could also increase in vivo VNT efficacy.[11] Our results predict that the combined use of these complementary and highly selective inhibitors may improve clinical responses with more

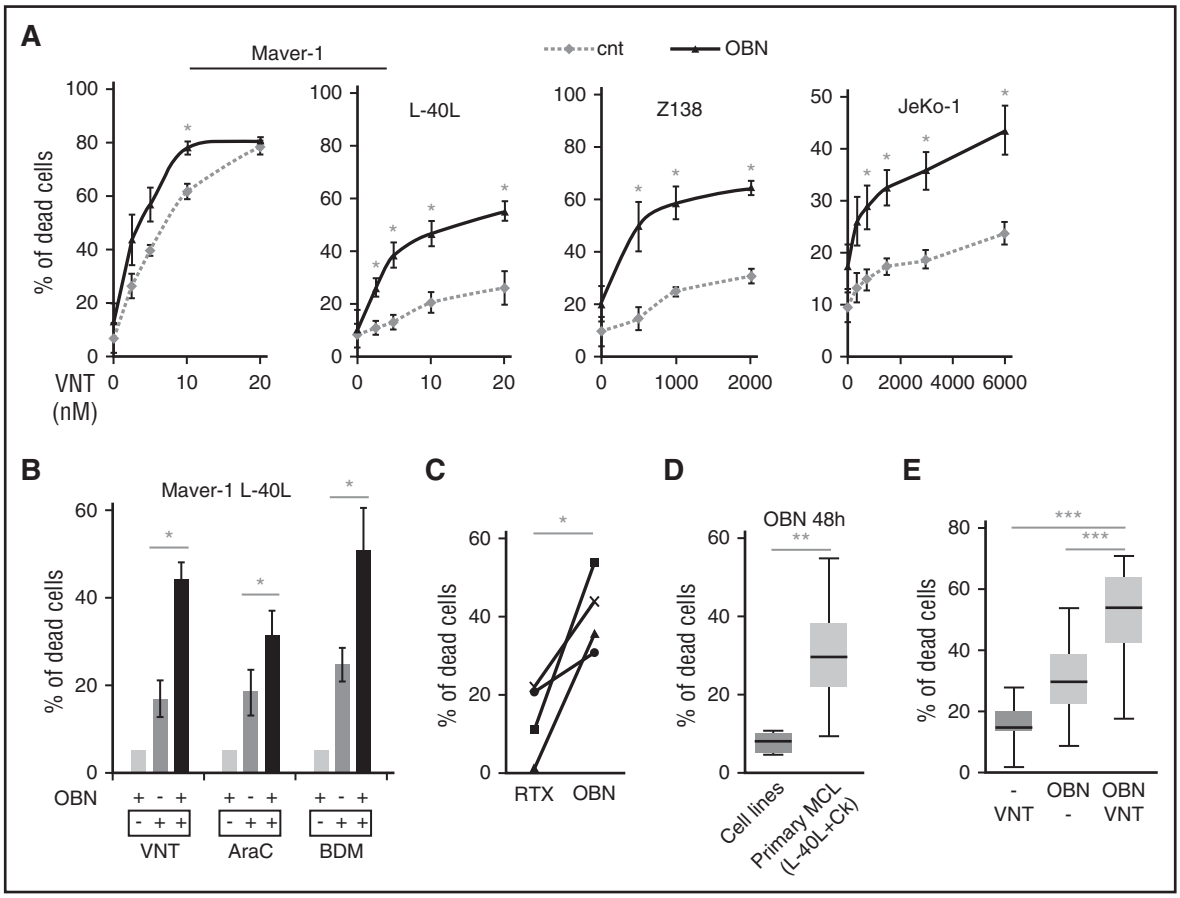

Figure 6. OBN counteracts microenvironment-dependent drug resistance in MCL cells. (A) Maver-1 cocultured or not on L-40L cells, and Z138 and JeKo-1 cell lines were treated with VNT for 48 hours at the indicated doses with or without OBN pretreatment (0.5 μg/mL). *Observed value > expected value. (B) Maver-1 cells, in the presence of an L-40L coculture layer, were cultured with OBN (24 hours, 5 μg/mL) alone or in sequential combination with OBN (24 hours, 5 μg/mL) and then VNT (48 hours, 50 nM), cytarabine (AraC; 48 hours, 80 ng/mL) or BDM (48 hours, 100 μM). (C) OBN (48 hours; 0.5 μg/mL) but not RTX (48 hours; 0.5 μg/mL) induced direct cell death in reactivated primary MCL cells (7 days on L-40L+Ck; n = 4); paired Student *t* test. (D) OBN (48 hours; 0.5 μg/mL) induced direct cell death in L-40L+Ck cocultured primary MCL cells (7 days on L-40L+Ck; n = 12) but not in MCL cell lines (n = 4); Student *t* test. (E) L-40L+Ck cocultured primary MCL cells (n = 11) were cultured with VNT (24 hours; 25 nM), OBN (48 hours; 0.5 μg/mL), or the sequential combination of OBN and then VNT, paired Wilcoxon test. Cell death was assessed using annexin-V staining. *$P < .05$, **$P < .01$, paired Student *t* test.

efficiency and less toxicity than the current standard of care. Our ongoing Obinutuzumab, GDC-0199 Plus Ibrutinib in Relapsed/Refractory Mantle Cell Lymphoma Patients (OAsIs) Trial for MCL patients (OBN, ibrutinib, and venetoclax, www.nationalclinicaltrials.gov, #NCT02558816) will rapidly determine in vivo efficacy.

In summary, we reported here the development of a reproducible ex vivo coculture model for primary MCL cells. This model has provided new insights into microenvironment-dependent proliferation and Bcl-2 family regulation, which are central components of survival and drug resistance. Our increased understanding of intrinsic abnormalities, the development of highly selective inhibitors and integration of the microenvironment offer new opportunities to design mechanism-based strategies that should overcome drug resistance in MCL and potentially other B-cell malignancies.

Acknowledgments

The authors thank the institut Régional du Cancer Nantes Atlantique tissue bank for providing samples and Roche for supporting in part this study.

This study was supported by Ligue Contre le Cancer Grand-Ouest and the Ligue Nationale Contre le Cancer and CHU de Nantes (D.C.).

Authorship

Contribution: D.C. designed and performed experiments, analyzed data, and wrote the article. C.B. and A.P. performed experiments. B.T. participated in bioinformatics analysis. C.D. and S.M. performed experiments. A.M. provided biopsy samples. J.E. provided cord blood samples. V.T. provided human mesenchymal stem cells. S.C.-K. provided data and reviewed the article. P.M. participated in the design of the study and reviewed the article. C.T. participated in BH3 profiling assays. S.L.G. participated in the design of the study and data analysis and reviewed the article. M.A. and C.P.-D. participated in the design of the study and data analysis and in the writing of the article.

Conflict-of-interest disclosure: S.L.G. is a consultant/advisory board member and has received an honorarium from Roche. The remaining authors declare no competing financial interests.

Correspondence: David Chiron, Centre de Recherche en Cancérologie Nantes-Angers, INSERM, CNRS, Université de Nantes, 8 quai Moncousu, 44007 Nantes, France; e-mail: david.chiron@univ-nantes.fr.

References

1. Campo E, Rule S. Mantle cell lymphoma: evolving management strategies. *Blood.* 2015;125(1): 48-55.
2. Jares P, Colomer D, Campo E. Molecular pathogenesis of mantle cell lymphoma. *J Clin Invest.* 2012;122(10):3416-3423.
3. Meissner B, Kridel R, Lim RS, et al. The E3 ubiquitin ligase UBR5 is recurrently mutated in mantle cell lymphoma. *Blood.* 2013;121(16): 3161-3164.
4. Rahal R, Frick M, Romero R, et al. Pharmacological and genomic profiling identifies NF-κB-targeted treatment strategies for mantle cell lymphoma. *Nat Med.* 2014;20(1):87-92.
5. Beà S, Valdés-Mas R, Navarro A, et al. Landscape of somatic mutations and clonal evolution in mantle cell lymphoma. *Proc Natl Acad Sci USA.* 2013;110(45):18250-18255.
6. Burger JA, Gribben JG. The microenvironment in chronic lymphocytic leukemia (CLL) and other B cell malignancies: insight into disease biology and new targeted therapies. *Semin Cancer Biol.* 2014;24:71-81.
7. Amé-Thomas P, Tarte K. The yin and the yang of follicular lymphoma cell niches: role of microenvironment heterogeneity and plasticity. *Semin Cancer Biol.* 2014;24:23-32.
8. Burger JA, Ford RJ. The microenvironment in mantle cell lymphoma: cellular and molecular pathways and emerging targeted therapies. *Semin Cancer Biol.* 2011;21(5):308-312.
9. Chang BY, Francesco M, De Rooij MF, et al. Egress of CD19(+)CD5(+) cells into peripheral blood following treatment with the Bruton tyrosine kinase inhibitor ibrutinib in mantle cell lymphoma patients. *Blood.* 2013;122(14):2412-2424.
10. Wang ML, Rule S, Martin P, et al. Targeting BTK with ibrutinib in relapsed or refractory mantle-cell lymphoma. *N Engl J Med.* 2013;369(6):507-516.
11. Chiron D, Dousset C, Brosseau C, et al. Biological rational for sequential targeting of Bruton tyrosine kinase and Bcl-2 to overcome CD40-induced ABT-199 resistance in mantle cell lymphoma. *Oncotarget.* 2015;6(11):8750-8759.
12. Furtado M, Wang ML, Munneke B, McGreivy J, Beaupre DM, Rule S. Ibrutinib-associated lymphocytosis corresponds to bone marrow involvement in mantle cell lymphoma. *Br J Haematol.* 2015;170(1):131-134.
13. Pham LV, Vang MT, Tamayo AT, et al. Involvement of tumor-associated macrophage activation in vitro during development of a novel mantle cell lymphoma cell line, PF-1, derived from a typical patient with relapsed disease. *Leuk Lymphoma.* 2015;56(1):186-193.
14. Lwin T, Lin J, Choi YS, et al. Follicular dendritic cell-dependent drug resistance of non-Hodgkin lymphoma involves cell adhesion-mediated Bim down-regulation through induction of microRNA-181a. *Blood.* 2010;116(24):5228-5236.
15. Kurtova AV, Tamayo AT, Ford RJ, Burger JA. Mantle cell lymphoma cells express high levels of CXCR4, CXCR5, and VLA-4 (CD49d): importance for interactions with the stromal microenvironment and specific targeting. *Blood.* 2009;113(19): 4604-4613.
16. Lwin T, Hazlehurst LA, Dessureault S, et al. Cell adhesion induces p27Kip1-associated cell-cycle arrest through down-regulation of the SCFSkp2 ubiquitin ligase pathway in mantle-cell and other non-Hodgkin B-cell lymphomas. *Blood.* 2007; 110(5):1631-1638.
17. Jin Z, Teramoto N, Hayashi K, et al. CD40 ligand stimulation inhibits the proliferation of mantle cell lymphoma lines. *Anticancer Res.* 2004;24(2B): 691-697.
18. Medina DJ, Goodell L, Glod J, Gélinas C, Rabson AB, Strair RK. Mesenchymal stromal cells protect mantle cell lymphoma cells from spontaneous and drug-induced apoptosis through secretion of B-cell activating factor and activation of the canonical and non-canonical nuclear factor κB pathways. *Haematologica.* 2012;97(8): 1255-1263.
19. Castillo R, Mascarenhas J, Telford W, Chadburn A, Friedman SM, Schattner EJ. Proliferative response of mantle cell lymphoma cells stimulated by CD40 ligation and IL-4. *Leukemia.* 2000;14(2):292-298.
20. Andersen NS, Larsen JK, Christiansen J, et al. Soluble CD40 ligand induces selective proliferation of lymphoma cells in primary mantle cell lymphoma cell cultures. *Blood.* 2000;96(6): 2219-2225.
21. Planken EV, Dijkstra NH, Willemze R, Kluin-Nelemans JC. Proliferation of B cell malignancies in all stages of differentiation upon stimulation in the 'CD40 system'. *Leukemia.* 1996;10(3): 488-493.
22. Geffroy-Luseau A, Chiron D, Descamps G, Jégo G, Amiot M, Pellat-Deceunynck C. TLR9 ligand induces the generation of CD20+ plasmablasts and plasma cells from CD27+ memory B-cells. *Front Immunol.* 2011;2:83.
23. Arpin C, Déchanet J, Van Kooten C, et al. Generation of memory B cells and plasma cells in vitro. *Science.* 1995;268(5211):720-722.
24. Brennan MA, Renaud A, Gamblin AL, et al. 3D cell culture and osteogenic differentiation of human bone marrow stromal cells plated onto jet-sprayed or electrospun micro-fiber scaffolds. *Biomed Mater.* 2015;10(4):045019.
25. Maïga S, Brosseau C, Descamps G, et al. A simple flow cytometry-based barcode for routine authentication of multiple myeloma and mantle cell lymphoma cell lines. *Cytometry A.* 2015;87(4): 285-288.
26. Vignon C, Debeissat C, Georget MT, et al. Flow cytometric quantification of all phases of the cell cycle and apoptosis in a two-color fluorescence plot. *PLoS One.* 2013;8(7):e68425.
27. Foight GW, Ryan JA, Gullá SV, Letai A, Keating AE. Designed BH3 peptides with high affinity and specificity for targeting Mcl-1 in cells. *ACS Chem Biol.* 2014;9(9):1962-1968.
28. Dutta S, Ryan J, Chen TS, Kougentakis C, Letai A, Keating AE. Potent and specific peptide inhibitors of human pro-survival protein Bcl-xL. *J Mol Biol.* 2015;427(6 Pt B):1241-1253.
29. Baran-Marszak F, Boukhiar M, Harel S, et al. Constitutive and B-cell receptor-induced activation of STAT3 are important signaling pathways targeted by bortezomib in leukemic mantle cell lymphoma. *Haematologica.* 2010; 95(11):1865-1872.
30. Zhang L, Yang J, Qian J, et al. Role of the microenvironment in mantle cell lymphoma: IL-6 is an important survival factor for the tumor cells. *Blood.* 2012;120(18):3783-3792.
31. Vishwamitra D, Shi P, Wilson D, et al. Expression and effects of inhibition of type I insulin-like growth factor receptor tyrosine kinase in mantle cell lymphoma. *Haematologica.* 2011;96(6):871-880.
32. Guidoboni M, Zancai P, Cariati R, et al. Retinoic acid inhibits the proliferative response induced by CD40 activation and interleukin-4 in mantle cell lymphoma. *Cancer Res.* 2005;65(2):587-595.
33. Dal Col J, Zancai P, Terrin L, et al. Distinct functional significance of Akt and mTOR constitutive activation in mantle cell lymphoma. *Blood.* 2008;111(10):5142-5151.
34. Dorfman DM, Pinkus GS. Distinction between small lymphocytic and mantle cell lymphoma by immunoreactivity for CD23. *Mod Pathol.* 1994; 7(3):326-331.
35. Annunziata CM, Davis RE, Demchenko Y, et al. Frequent engagement of the classical and alternative NF-kappaB pathways by diverse genetic abnormalities in multiple myeloma. *Cancer Cell.* 2007;12(2):115-130.
36. Dousset C, Maïga S, Gomez-Bougie P, et al. BH3 profiling as a tool to identify acquired resistance to venetoclax in multiple myeloma [published online ahead of print 29 July 2016]. *Br J Haematol.* doi: 10.1111/bjh.14251.
37. Vogler M, Hamali HA, Sun XM, et al. BCL2/BCL-X (L) inhibition induces apoptosis, disrupts cellular calcium homeostasis, and prevents platelet activation. *Blood.* 2011;117(26):7145-7154.
38. Habens F, Lapham AS, Dallman CL, et al. Distinct promoters mediate constitutive and inducible Bcl-XL expression in malignant lymphocytes. *Oncogene.* 2007;26(13):1910-1919.
39. Pham LV, Tamayo AT, Yoshimura LC, Lo P, Ford RJ. Inhibition of constitutive NF-kappa B activation in mantle cell lymphoma B cells leads to induction of cell cycle arrest and apoptosis. *J Immunol.* 2003;171(1):88-95.
40. Jazirehi AR, Huerta-Yepez S, Cheng G, Bonavida B. Rituximab (chimeric anti-CD20 monoclonal antibody) inhibits the constitutive nuclear factor-kappaB signaling pathway in non-Hodgkin's lymphoma B-cell lines: role in sensitization to chemotherapeutic drug-induced apoptosis. *Cancer Res.* 2005;65(1):264-276.
41. Illidge T, Klein C, Sehn LH, Davies A, Salles G, Cartron G. Obinutuzumab in hematologic malignancies: lessons learned to date. *Cancer Treat Rev.* 2015;41(9):784-792.
42. Chiron D, Di Liberto M, Martin P, et al. Cell-cycle reprogramming for PI3K inhibition overrides a relapse-specific C481S BTK mutation revealed by longitudinal functional genomics in mantle cell lymphoma. *Cancer Discov.* 2014;4(9):1022-1035.
43. Saba NS, Liu D, Herman SE, et al. Pathogenic role of B-cell receptor signaling and canonical NF-κB activation in mantle cell lymphoma. *Blood.* 2016;128(1):82-92.
44. Nygren L, Wasik AM, Baumgartner-Wennerholm S, et al. T-cell levels are prognostic in mantle cell lymphoma. *Clin Cancer Res.* 2014;20(23):6096-6104.
45. Iyengar S, Ariza-McNaughton L, Clear A, et al. Characteristics of human primary mantle cell lymphoma engraftment in NSG mice. *Br J Haematol.* 2016;173(1):165-169.
46. Davids MS, Deng J, Wiestner A, et al. Decreased mitochondrial apoptotic priming underlies stroma-mediated treatment resistance in chronic lymphocytic leukemia. *Blood.* 2012;120(17): 3501-3509.
47. Vogler M, Butterworth M, Majid A, et al. Concurrent up-regulation of BCL-XL and BCL2A1 induces approximately 1000-fold resistance to ABT-737 in chronic lymphocytic leukemia. *Blood.* 2009;113(18):4403-4413.
48. Robak T, Huang H, Jin J, et al; LYM-3002 Investigators. Bortezomib-based therapy for newly diagnosed mantle-cell lymphoma. *N Engl J Med.* 2015;372(10):944-953.
49. Thijssen R, Slinger E, Weller K, et al. Resistance to ABT-199 induced by microenvironmental signals in chronic lymphocytic leukemia can be counteracted by CD20 antibodies or kinase inhibitors. *Haematologica.* 2015;100(8): e302-e306.
50. Heinrich DA, Weinkauf M, Hutter G, et al. Differential regulation patterns of the anti-CD20

antibodies obinutuzumab and rituximab in mantle cell lymphoma. *Br J Haematol.* 2015;168(4): 606-610.

51. Mössner E, Brünker P, Moser S, et al. Increasing the efficacy of CD20 antibody therapy through the engineering of a new type II anti-CD20 antibody with enhanced direct and immune effector cell-mediated B-cell cytotoxicity. *Blood.* 2010;115(22): 4393-4402.

52. Morschhauser FA, Cartron G, Thieblemont C, et al. Obinutuzumab (GA101) monotherapy in relapsed/refractory diffuse large b-cell lymphoma or mantle-cell lymphoma: results from the phase II GAUGUIN study. *J Clin Oncol.* 2013;31(23): 2912-2919.

53. Sehn LH, Chua N, Mayer J, et al. Obinutuzumab plus bendamustine versus bendamustine monotherapy in patients with rituximab-refractory indolent non-Hodgkin lymphoma (GADOLIN): a randomised, controlled, open-label, multicentre, phase 3 trial. *Lancet Oncol.* 2016;17(8): 1081-1093.

54. Chiron D, Martin P, Di Liberto M, et al. Induction of prolonged early G1 arrest by CDK4/CDK6 inhibition reprograms lymphoma cells for durable PI3Kδ inhibition through PIK3IP1. *Cell Cycle.* 2013;12(12):1892-1900.

frontiers in Oncology

ORIGINAL RESEARCH
published: 07 January 2019
doi: 10.3389/fonc.2018.00645

BCL2-Family Dysregulation in B-Cell Malignancies: From Gene Expression Regulation to a Targeted Therapy Biomarker

Benoît Tessoulin[1,2,3*†], *Antonin Papin*[1,2,4†], *Patricia Gomez-Bougie*[1,2,4], *Celine Bellanger*[1,2,4], *Martine Amiot*[1,2,4], *Catherine Pellat-Deceunynck*[1,2,4] *and David Chiron*[1,2,4*]

[1] CRCINA, INSERM, CNRS, Université d'Angers, Université de Nantes, Nantes, France, [2] L'Héma-NexT, i-Site NexT, Nantes, France, [3] Department of Hematology, Centre Hospitalier Universitaire, Nantes, France, [4] CNRS GDR3697 Micronit, Tours, France

OPEN ACCESS

Edited by:
Massimo Libra,
Università degli Studi di Catania, Italy

Reviewed by:
Apostolos Zaravinos,
European University Cyprus, Cyprus
Rehan Khan,
Mayo Clinic, United States

***Correspondence:**
Benoît Tessoulin
benoit.tessoulin@chu-nantes.fr
David Chiron
david.chiron@univ-nantes.fr

[†]These authors have contributed equally to this work

Specialty section:
This article was submitted to Hematologic Malignancies, a section of the journal Frontiers in Oncology

Received: *09 October 2018*
Accepted: *10 December 2018*
Published: *07 January 2019*

Citation:
Tessoulin B, Papin A, Gomez-Bougie P, Bellanger C, Amiot M, Pellat-Deceunynck C and Chiron D (2019) BCL2-Family Dysregulation in B-Cell Malignancies: From Gene Expression Regulation to a Targeted Therapy Biomarker. Front. Oncol. 8:645. doi: 10.3389/fonc.2018.00645

BCL2-family proteins have a central role in the mitochondrial apoptosis machinery and their expression is known to be deregulated in many cancer types. Effort in the development of small molecules that selectively target anti-apoptotic members of this family i.e., Bcl-2, Bcl-xL, Mcl-1 recently opened novel therapeutic opportunities. Among these apoptosis-inducing agents, BH3-mimetics (i.e., venetoclax) led to promising preclinical and clinical activity in B cell malignancies. However, several mechanisms of intrinsic or acquired resistance have been described *ex vivo* therefore predictive markers of response as well as mechanism-based combinations have to be designed. In the present study, we analyzed the expression of the BCL2-family genes across 10 mature B cell malignancies through computational normalization of 21 publicly available Affimetrix datasets gathering 1,219 patient samples. To better understand the deregulation of anti- and pro-apoptotic members of the BCL2-family in hematological disorders, we first compared gene expression profiles of malignant B cells to their relative normal control (naïve B cell to plasma cells, $n = 37$). We further assessed BCL2-family expression according to tissue localization i.e., peripheral blood, bone marrow, and lymph node, molecular subgroups or disease status i.e., indolent to aggressive. Across all cancer types, we showed that anti-apoptotic genes are upregulated while pro-apoptotic genes are downregulated when compared to normal counterpart cells. Of interest, our analysis highlighted that, independently of the nature of malignant B cells, the pro-apoptotic BH3-only *BCL2L11* and *PMAIP1* are deeply repressed in tumor niches, suggesting a central role of the microenvironment in their regulation. In addition, we showed selective modulations across molecular subgroups and showed that the BCL2-family expression profile was related to tumor aggressiveness. Finally, by integrating recent data on venetoclax-monotherapy clinical activity with the expression of BCL2-family members involved in the venetoclax response, we determined that the ratio *(BCL2+BCL2L11+BAX)/BCL2L1* was the strongest predictor of venetoclax response for mature B cell malignancies *in vivo*.

Keywords: BCL2, B-cell malignancy, lymphoma, cell death, microenvironment, data mining, predictive markers

INTRODUCTION

B cell differentiation is a tightly controlled process that leads to the generation and selection of memory B cells and antibody-secreting plasma cells (1, 2). B cells constitute an essential part of our adaptive immune system but the genomic instabilities necessary for the development of high affinity antibodies are also involved in the initiation of malignant B-cell neoplasms (3, 4). Thereby, hematological malignancies can arise from most steps of B cell differentiation and more than 40 types of mature B cell lymphomas are referenced in the latest World Health Organization classification. The most frequent types include diffuse large B cells lymphoma, DLBCL (25%), plasma cell neoplasms [including multiple myeloma, MM (23%)], chronic lymphocytic leukemia, CLL (19%), follicular lymphoma, FL (12%), splenic marginal zone lymphoma, SMZL (7%), mantle cell lymphoma, MCL (3%), hairy cell leukemia, HCL (2%), and Burkitt lymphoma, BL (1%) (5). All of these hematological malignancies are characterized by their own genetic hallmarks, even though most of them display deregulation of the B-cell receptors (BCR), NFkB, Notch (*see articles associated to this Frontiers topic*) or BCL2-family networks, leading to increased survival and enhanced chemoresistance.

BCL2-family proteins, which play a central role in the control of apoptosis, include multidomain anti-apoptotic members (Bcl-2, Bcl-xL, Mcl-1, Bcl-w, Bfl-1), BH3-only sensitizers (Bad, Bik, Noxa, Hrk, Bmf), BH3-only activators (Bid, Puma, Bim), and pro-apoptotic effectors (Bax, Bak) (6). The deregulation of the "B-cell lymphoma-2" (BCL2) family in mature B cell malignancies has been first highlighted through a translocation between the chromosomes 14 and 18 that led to the overexpression of the Bcl-2 oncogene in follicular lymphoma (7). Additional deregulations were then described such as 1q amplification leading to Mcl-1 overexpression in MM (8), Bim deletion in lymphoma cell lines (9) or miRNA deregulation leading to Bcl-2 overexpression in CLL (10, 11).

Given the central role of the BCL2-family in the apoptosis machinery, several strategies have been developed to target this network in hematological malignancies, such as synthetic antisense, specific peptides or BH3-mimetics (12, 13). Up to day, BH3-mimetics displayed the best efficacy both *in vitro* and *in vivo* (14, 15). Indeed, BH3-mimetics selectively bind anti-apoptotic members of the BCL2-family with high affinity, leading to the release of pro-apoptotic members that consequently induce cell death (16). Several clinical trials are currently ongoing using the first in class orally bioavailable BCL2-selective BH3-mimetic venetoclax, demonstrating clinical efficacy as a single agent in several B cell malignancies such as CLL, MCL, and MM (17–21).

Nevertheless, mature B cell neoplasms do not harbor similar dependence to anti-apoptotic members of the BCL2-family. For example, whereas both CLL and DLBCL overexpress Bcl-2 protein (10, 22), the overall response rate (ORR) of patients to venetoclax-monotherapy strongly diverged with 79 and 18%, respectively. In addition to intrinsic resistance, acquired resistance to BH3-mimetics has also been recently described (23–25). The challenge is now to set up markers and functional assays that predict responses to BCL2-family targeted strategies and to design mechanism-based combinations to overcome resistance.

To gain insight into BCL2-family expression and regulation across most frequent mature B cell malignancies, we analyzed the BCL2-family expression in ten different hematological disorders i.e., MCL, BL, DLBCL, FL, B-cell prolymphocytic leukemia (BPLL), CLL, HCL, mucosa-associated lymphoid tissue (MALT), SMZL, MM, through normalization of Affymetrix Human Genome U133 Plus 2.0 public datasets. We analyzed: (1) the common modulations across all B-cell neoplasms in comparison with their respective normal counterpart, (2) the modulations associated to the microenvironment and molecular subtypes, and (3) established a ratio of expression involving Bcl-2, Bcl-xL, Bax, and Bim that is associated with the response rate to venetoclax.

MATERIALS AND METHODS

Gene expression profiling datasets were selected on Gene Expression Omnibus (https://www-ncbi-nlm-nih-gov.gate2.inist.fr/geo/) and ArrayExpress (https://www.ebi.ac.uk/arrayexpress/), for all mature B-cell malignancies series and normal B-cell series (**Table S1**). In order to overcome data normalization biases, only Affymetrix Human Genome U133 Plus 2.0 series with raw data were retained. Raw data (cel files) were acquired as a whole and normalized using Affy and gcrma packages and outlier samples were removed and data were further quantile normalized (**Figure S1A**). Normalization quality and the absence of a remnant batch-effect were further assessed by the analysis of "anchoring genes" expression (*CD27*, *CCND1*, *SOX11*, *MKI67*, *BCL6*, *MME*, *CD200*, *ITGAE*, *CD38*, and *SDC1*), highlighting histological and/or B-cell differentiation specificities, independent of source series (**Figure S1**). Normal counterpart B-cell were associated to B cell malignancies according to cell-of-origin classification (26). For genes with multiple Affymetrix probes, probes were selected according to correlations between GEP and RNA-seq data for MM and MCL cell lines when available (https://www.keatslab.org/data-repository) ($n = 19$) (**Table S2**). Given that none of the *BAD* and *HRK* probes available gave a correlation with RNA-seq, these genes were excluded from our study. In addition, expression of *BBC3* (coding for Puma protein) has not been evaluated because of putative *MIR3191/MIR3190* cross-hybridization (Affymetrix HGU133plus2.0 Annotation, Revision 35).

Factor maps were constructed by FactoMiner and further represented by factoextra package. Data used in the Principal Component for each graph were a subset of the Bcl2-family dataset we firstly constructed.

For quantitative variables, statistical testing was performed using Wilcoxon-Mann-Whitney tests for two groups and Kruskal-Wallis for more than two groups. For qualitative variables, Fisher-test was performed. Statistical significance was retained under α-risk of 0.05. Random forest analysis was carried-out with 1,000 trees, using randomForest R-package.

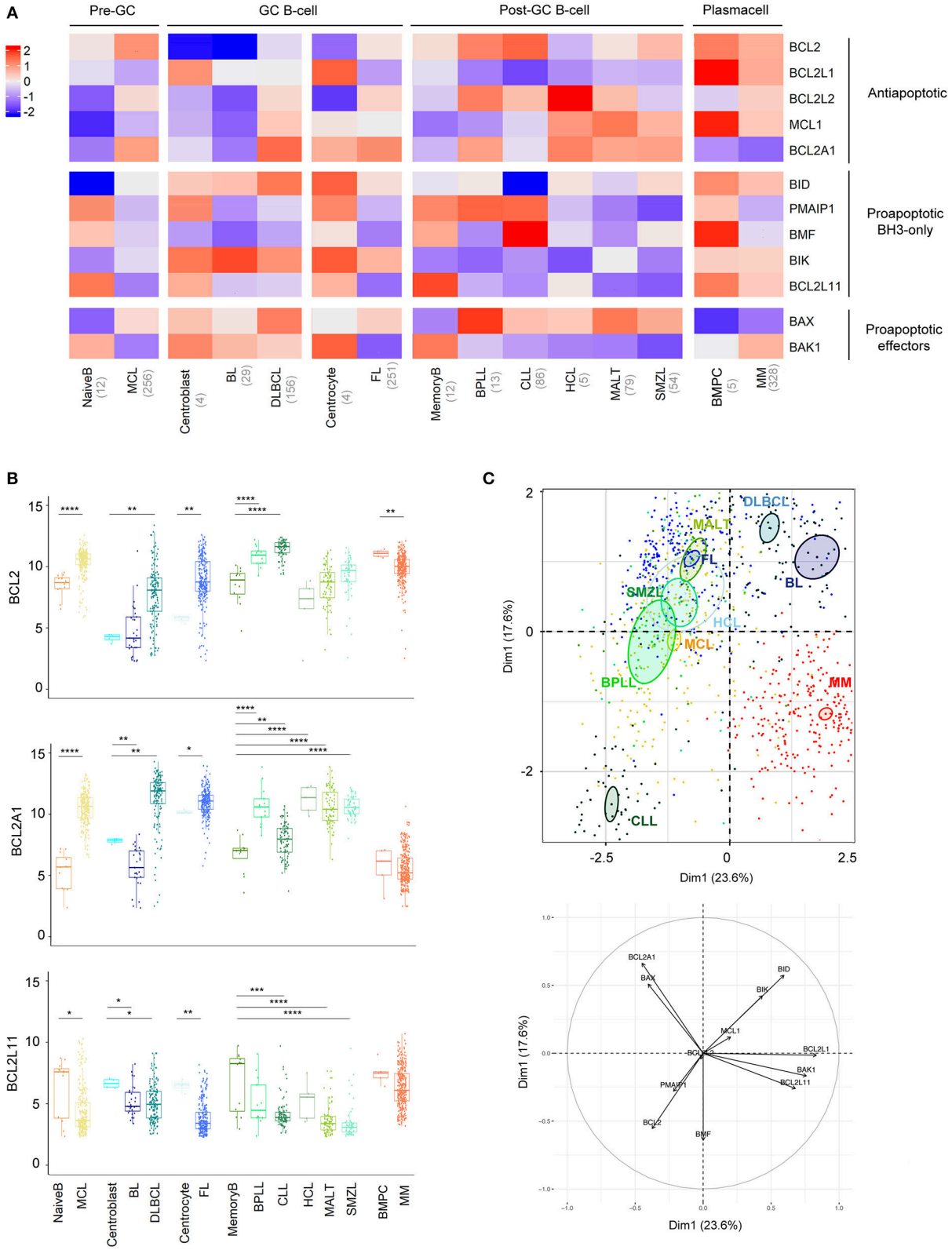

FIGURE 1 | BCL2-family is strongly deregulated in the landscape of B-cell malignancies. **(A)** Heat-map of Bcl-2 gene expression profiles among B-cell malignancies. The color corresponds to the intensity of the median gene expression. Blue indicates lower and red higher transcript abundance. MCL, Mantle Cell Lymphoma; BL,

(Continued)

FIGURE 1 | Burkitt lymphoma; DLBCL, Diffuse Large B-cell Lymphoma; FL, Follicular Lymphoma; BPLL, B-cell Prolymphocytic Leukemia; CLL, Chronic lymphocytic leukemia; HCL, Hairy Cell Lymphoma; MALT, mucosa-associated lymphoid tissue lymphoma; SMZL, Splenic Marginal Zone Lymphoma; BMPC, Bone Marrow Plasma Cell, MM: multiple Myeloma. **(B)** Expression of *BCL2*, *BCL2A1,* and *BCL2L11* in the different B-cell malignancies compared to their respective control. Wilcoxon-Mann-Whitney tests. $^{*}p < 0.05$, $^{**}p < 0.01$, $^{***}p < 0.001$, $^{****}p < 0.0001$. **(C)** Representation of the individual factor map of each sample for the PCA and according to the two first dimensions. Colored ellipses are drawn around the mean of the group (=barycenter), with the 95% confidence interval of the mean in the corresponding plan. *BCL2* is coding for Bcl-2 protein, *BCL2L1* for Bcl-xL, *MCL1* for Mcl-1, *BCL2L2* for Bcl-w, *BCL2A1* for Bfl1, *BIK* for Bik, *PMAIP1* for Noxa, *BMF* for Bmf, *BID* for Bid, *BCL2L11* for Bim, *BAX* for Bax, and *BAK1* for Bak.

RESULTS

B-cell Malignancies Display Unbalanced Regulations of their Anti- and Pro-apoptotic Genes

B cell malignancies were classified and compared to their normal B cell counterparts according to the latest WHO classification (26). Whereas, MCL was defined as a pre-GC (germinal-center) neoplasm, FL, BL, and DLBCL were defined as GC neoplasms and SMZL, MALT, BPLL, CLL, HCL, and MM as post-GC neoplasms (**Figure 1A**). Within GC neoplasms, we further compared highly proliferative BL and DLBCL to centroblasts and the mostly indolent FL to centrocytes.

Anti-apoptotic members of the BCL2-family have a tendency to be overexpressed in most malignancies compared to their relative normal control, with the striking exception of *BCL2L1*, coding for BCLxL protein (**Figure 1A**, **Figure S2**). *BCL2* was overexpressed in MCL, DLBCL, FL, BPLL, and CLL. Of note, *BCL2A1*, coding for Bfl1 protein, appeared to be the most frequently elevated genes (8 out 10 malignancies, **Figure 1B**). As previously described, overexpression of *BCL2A1* was not observed in MM (27). Furthermore, in contrast to most mature B cell malignancies, MM and BL did not show major modulations of anti-apoptotic genes when compared to their normal counterparts (**Figure 1A**, **Figure S2**).

Pro-apoptotic BH3-only have a tendency to be downregulated in all mature B cell malignancies compared to their relative normal control, *BCL2L11*, coding for Bim protein, being the most frequently significantly deregulated gene (7 out of 10 malignancies, **Figure 1B**, **Figure S2**). Regarding pro-apoptotic effectors we observed a *BAX*/*BAK1* switch of expression in malignant B cells compared to their normal counterparts. Indeed, whereas *BAX* was elevated, *BAK1* appeared downregulated in all malignancies, excepted in MM and BL (**Figure 1A**, **Figure S2**).

To compare the 10 entities studied in regard to their BCL2-family profile, we performed a Principal Component Analysis (PCA, **Figure 1C**). We observed that CLL and MM displayed unique profiles. The variable plot highlighted that CLL profile was mostly carried by the expression of *BCL2*, *BMF*, *PMAIP1*, coding for Noxa protein, and the absence of *BID* whereas MM cells were characterized by the projection of *BCL2L1*, *BAK1,* and *BCL2L11* and the absence of *BCL2A1* (**Figure 1C**, lower panel).

BCL2-family Genes Display Differential Expression According to the Microenvironment

We, and others, previously demonstrated that microenvironment-dependent modulations of BCL2-family members were involved in the survival and chemoresistance of B cell malignancies (23, 28, 29). To get insight into the role of the microenvironment in the BCL2-family regulation, we compared the expression profile of lymphoma cells from peripheral blood (PB) and tumoral niches i.e., lymph nodes (LN), bone marrow (BM) or spleen (SPL) for MCL, FL, CLL, and SMZL. MCL displayed the most frequent modulations with 11 out of 12 genes being significantly differently expressed between LN and PB with a general increase of all anti-apoptotic members within LN (**Figure 2A**, **Figure S3**). Although PB and LN samples were not paired, these data suggest that MCL cells have divergent BCL2 profiles depending on their microenvironment.

Of interest, our analysis highlighted that, independently of the nature of malignant B cells, the pro-apoptotic BH3-only *BCL2L11* and *PMAIP1* genes were deeply repressed in tumor niches (**Figure 2B**). In contrast, anti-apoptotic regulation seemed to be cell-type specific and only *BCL2L1* was commonly upregulated in the LN of both MCL and FL (**Figures 2A,B**).

PCA of these entities showed that tumor localization prevailed over entity intrinsic hallmarks (**Figure 2C**). Indeed, PB lymphoma cells from FL, MCL, and SMZL segregated together and apart from their relative LN cells. In contrast, CLL samples form a separated group independent of their tumor localization (PB, LN, and BM), confirming the specific profile of this malignancy as mentioned before (**Figures 1C**, **2C**).

Intra-entities BCL2-family Heterogeneity Is Related to Molecular Subtypes and Aggressiveness

Molecular subgroups have been previously described in several B cell disorders (26). We thus compared the BCL2 profile according to molecular subtypes in DLBCL, MCL, and MM (**Figure 3**, **Figures S4, S5**).

Conventional MCL cells are characterized by a strong expression of the oncogene *SOX11*. A *SOX11*-negative (*SOX11*-) leukemic non-nodal minor MCL subtype is now well-characterized and displays a limited number of genomic alterations and a more indolent clinical course (30). The BCL2-family profile of conventional PB *SOX11*+ MCL was mostly similar to the one of leukemic non-nodal *SOX11*- MCL (**Figure 3A**). Nevertheless, *SOX11*- MCL cells displayed a moderate increase in MCL1 expression and a dramatic decrease in BIK expression when compared to *SOX11*+.

We next compared the profile of 3 subtypes of DLBCL, GC-type (GCB), ABC-type (ABC), and primary mediastinal (PMBL, **Figure 3B**). Our analysis showed that ABC cells were characterized by a high level of *BCL2*, *BID,* and *BMF*, which is consistent with previous reports (31). In contrast, PMBL cells displayed a high expression of *BCL2L1* (**Figure 3B**).

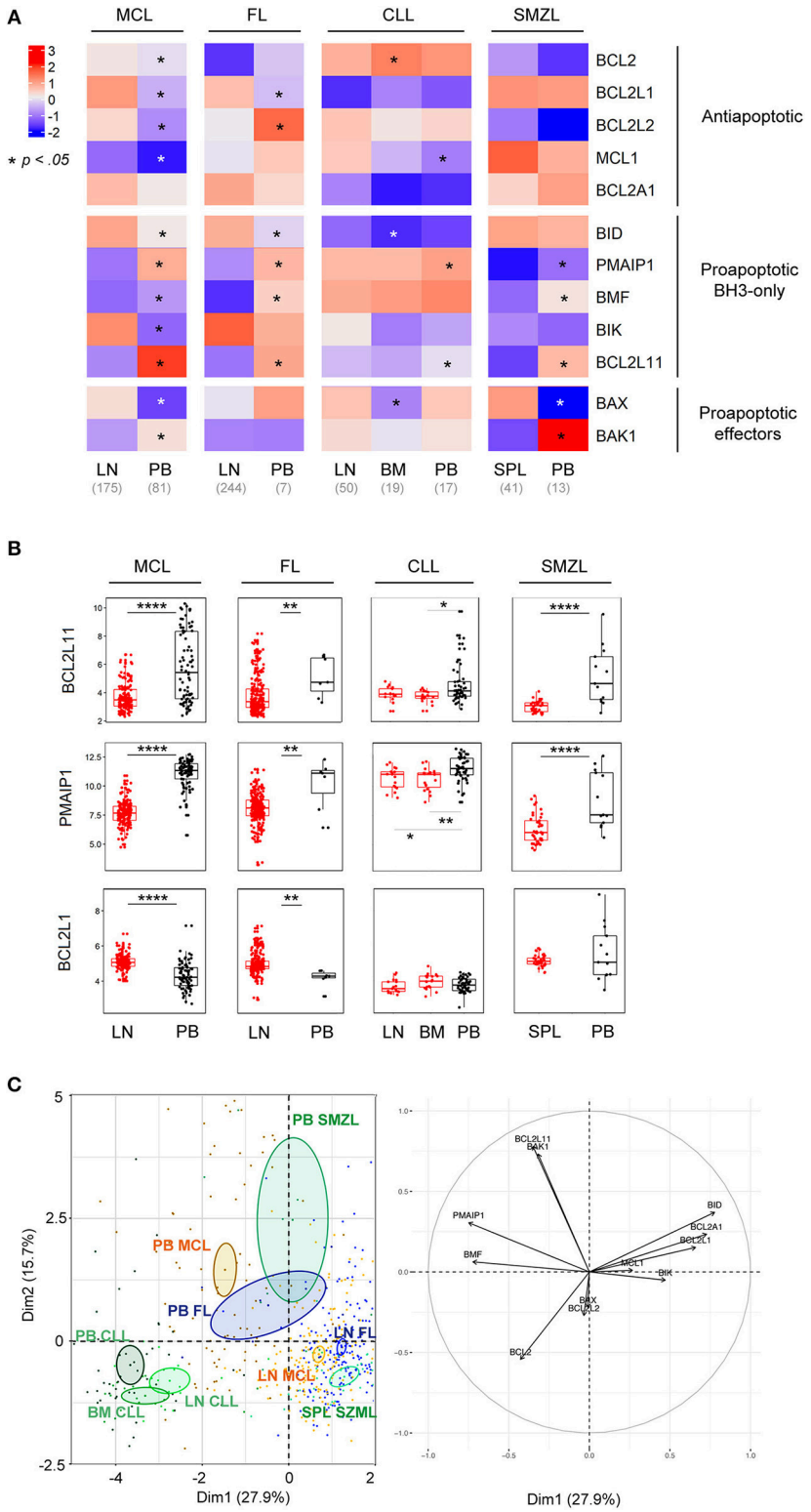

FIGURE 2 | BCL2-family is regulated by the tumor microenvironment. **(A)** Heat-map of Bcl-2 gene expression profiles for MCL, FL, CLL, and SMZL in function of their tissue localization. Wilcoxon-Mann-Whitney tests. *$p < 0.05$. **(B)** Comparison of *BCL2L11*, *PMAIP1,* and *BCL2L1* gene expression according to their localization. LN, lymph nodes; PB, peripheral blood; BM, bone marrow. Wilcoxon-Mann-Whitney tests. **$p < 0.01$, ****$p < 0.0001$. **(C)** Representation of the individual factor map for the PCA according to the two first dimensions and their respective correlation circle. Colored ellipses are drawn around the mean of the group (=barycenter), with the 95% confidence interval of the mean in the corresponding plan.

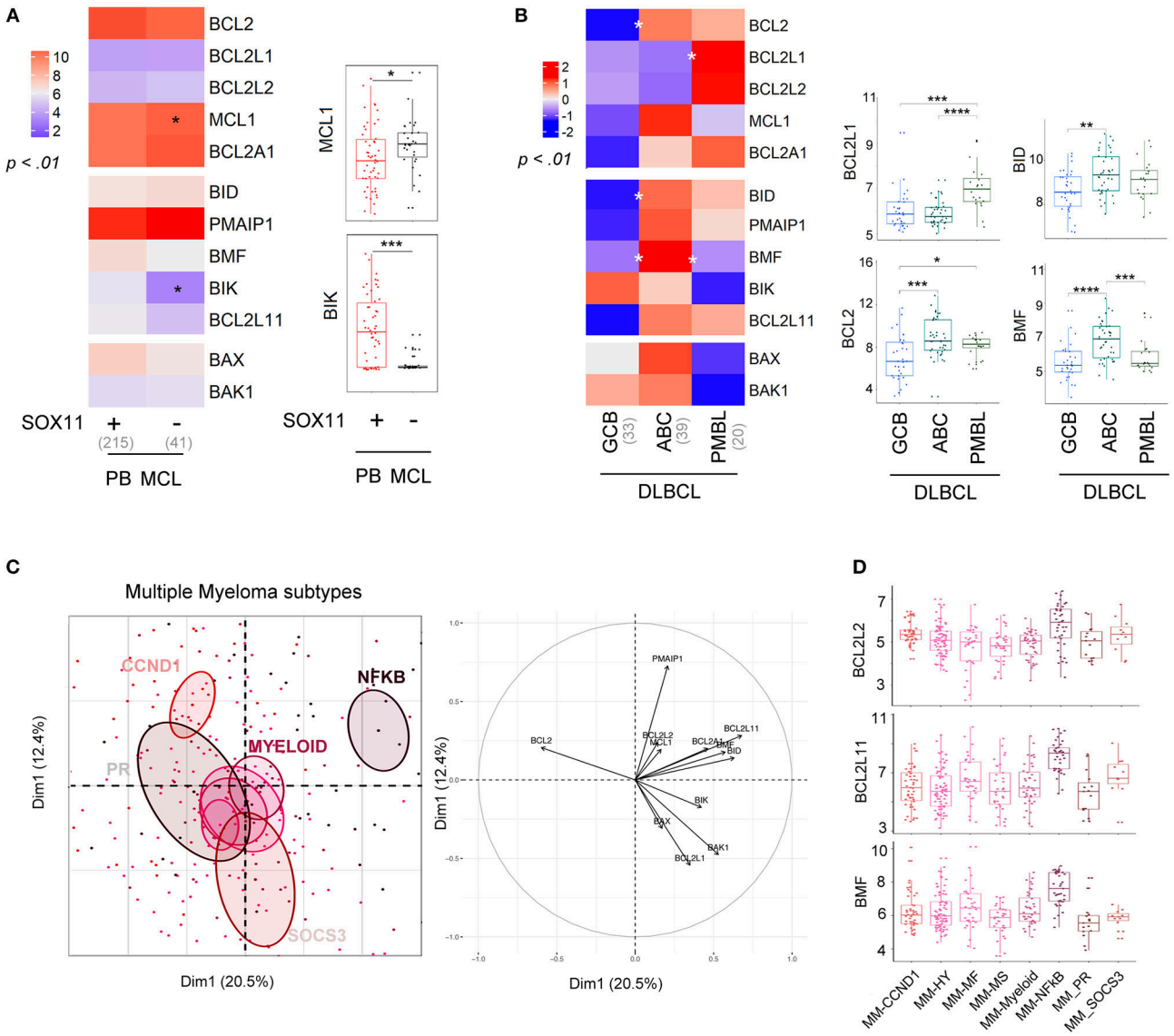

FIGURE 3 | Molecular subtypes display differential expression of the BCL2-family. **(A)** left; Heat-map of BCL2-family expression profile comparing PB MCL according to *SOX11* gene expression (right). *MCL1* and *BIK* expression in the two molecular subgroups. **(B)** left; Heat-map of BCL2-family expression profile comparing the different subtypes of DLBCL: GCB (germinal center B cell, ABC (activated B-cell) and PMBL (Primary mediastinal B-cell lymphoma). right; Gene expression of *BCL2L1*, *BCL2*, *BID,* and *BMF* for the three subtypes of DLBCL. **(C)** Representation of the individual factor map for the PCA and according to the two first dimensions of multiple myeloma samples and their respective correlation circle. Colored ellipses are drawn around the mean of the group (=barycenter), with the 95% confidence interval of the mean in the corresponding plan. **(D)** *BCL2L2*, *BCL2L11,* and *BMF* expression in the different multiple myeloma subtypes. $*p < 0.05$, $**p < 0.01$, $***p < 0.001$, $****p < 0.0001$.

Several gene-expression profiling analyses of primary MM cells have led to a molecular classification of MM subtypes (32–34). This classification now includes 8 subgroups characterized either by an IgH translocation with the CyclinD1 [$t_{(11;14)}$; CCND1 group], the MMSET oncogene [$t_{(4;14)}$; MS group], MAF oncogenes [$t_{(14;16)}$ and $t_{(14;20)}$], or by specific gene signatures (PR, HY, Myeloid, SOCS3, and NFKB) (35, 36). We previously reported the apoptotic machinery diversity in MM major subgroups (HY, CCND1, MF, and MS) (37). Here, we enlarged the analysis by taking into account the 8 molecular subgroups (33). As represented by PCA, the NFKB subgroup displayed a specific BCL2-family profile and was characterized by an overexpression of *BCL2L2*, *BCL2L11,* and *BMF*, while the other groups overlapped without any exclusive signatures (**Figures 3C,D**).

Histologic transformation of indolent B cell lymphomas such as FL or MALT into an aggressive lymphoma (mostly DLBCL) is a well-described phenomenon (38). Our analysis highlighted that histologic transformation was associated with common deregulations of the BCL2-family in both FL and MALT

(**Figure 4A**, **Figure S6**). Indeed, we observed a downregulation of BCL2 as well as an increase of the pro-apoptotic *BCL2L11*, *BID,* and *BAX* and *BAK1* in both entities after transformation (**Figure 4B**). As observed in the PCA, the BCL2-family profile of the aggressive forms of both FL and MALT segregated apart from their respective indolent forms toward a profile close to the one of DLBCL (**Figure 4C**). Of note, we investigated whether BCL2-family expression patterns would differentiate the non-transformed FL/MALT from the transformed one. To do so, an ensemble machine-learning algorithm (random forest) was trained on BCL2-family expression dataset to predict the different B-cell malignancies. Using this trained algorithm on FL and MALT, it classified the transformed forms of the latters as DLBCL, thus efficiently predicting the aggressive transformation in both FL [Odds Ratio [OR] for transformation = 31, $p = 2x10^{-14}$] and MALT (OR = 30, $p = 9 \times 10^{-5}$).

BCL2-family Expression Profile Predicts the Sensitivity to BCL2 Specific BH3-mimetics in Mature B Cell Malignancies

We previously demonstrated that a ratio of *BCL2* expression with the resistance factors *MCL1* and *BCL2L1* could predict sensibility to venetoclax in MCL and MM *ex vivo* and *in vivo* (20, 39, 40). Here, to determine the best predictive ratio across mature B cell malignancies, we analyzed the correlations between expression of previously described factors involved in venetoclax resistance (*MCL1*, *BCL2L1*, *BCL2A1*) (14, 23, 25, 39–41) as well as factors involved in venetoclax efficacy (*BCL2*, *BCL2L11*, *BAX*) (24, 25, 42) with overall response rate (ORR) in patients treated with venetoclax. Recent publications have shown an elevated ORR of venetoclax monotherapy in CLL and MCL (79 and 75%, respectively) (18, 20), intermediate for FL (38%) (17) and low for DLBCL and MM (18 and 21%, respectively) (17, 20). We showed that the ratio *(BCL2+BCL2L11+BAX)/(BCL2L1)* was the best predictor of venetoclax response across all mature B cell malignancies ($r = 0.81$, $p = 7e\text{-}4$, **Figure S7**). Of note, BPLL and HCL, entities for which venetoclax efficacy is unknown, were characterized by a high ratio whereas BL was characterized by a low ratio (**Figure 5A**).

We next analyzed whether subgroups of patients (genomic heterogeneity or transformation) displayed different ratios. In good agreement with the *in vivo* and *in vitro* sensitivity to venetoclax, we showed that the CCND1 MM subgroup displayed the highest *(BCL2+BCL2L11+BAX)/(BCL2L1)* ratio among MM subtypes (**Figure 5B**) (14, 20). Interestingly, subgroups of patients with MCL (*SOX11*+/–) harbored similar ratio, while ABC DLBCL cells were characterized by a higher ratio compared to GCB and PMBL. Histologic transformation only slightly influenced the ratio in FL but not in MALT lymphoma (**Figures 5C,D**).

Lastly, we compared the *(BCL2+BCL2L11+BAX)/(BCL2L1)* ratio according to the microenvironment and showed that MCL within the LN are predicted to be more resistant to venetoclax that MCL cells in the PB, confirming our previous functional *in vitro* observations (23, 39). Similarly, our analysis predicted that CLL cells should be less sensitive to venetoclax in BM as compared to PB (**Figure 5E**).

DISCUSSION

The BCL2-family is known to be deregulated in cancer, including hematological malignancies (43). Whereas, most studies focused on the regulation of selective BCL2-family members within a specific pathology, here we provided a global RNA expression analysis of 12 members of the BCL2-family across 10 mature B-cell malignancies and their relative normal counterparts. To do so, we took advantage of the numerous Affymetrix HGU133Plus2.0 series datasets previously published for mature B cell malignancies and gathered in the GEO database. We controlled the normalization quality by addressing hallmarks expression such as *CCND1*, *SOX11*, *MKI67*, *MME*, *CD200*, CD38, or *SDC1*, confirming malignancies specificities, independently of source series (**Figure S1**). Using similar data mining strategy, Adams et al. recently highlighted an overexpression of *BCL2* and *BCL2L2* in Hodgkin Lymphomas and several NHL (BL, DLBCL, FL, MZL, and MCL) (44). This overexpression was confirmed in our study with the exception of BL, a discrepancy that might be due to the use of different normal counterparts. Nevertheless, this technology has limitations such as probes aspecificity (*HRK*, *BAD*) or cross-hybridization within some probes such as *BBC3* (45), impeding the integration of these critical member of the BCL2 network in the present study (see Material and Methods section). Although this drawback could be resolved using RNA-sequencing technologies, datasets availability was too limited for most of the cellular entities analyzed in the present work.

Having these limitations in mind, our analysis provided a global picture of the BCL2-family dysregulation in mature B-cell malignancies, from their transcriptional regulation to their potential use as targeted therapy biomarker. We first highlighted a global upregulation of anti-apoptotic genes as well as a global downregulation of pro-apoptotic genes in most B cell lymphomas compared to their normal control, confirming that the BCL2-family deregulation is a hallmark of most B cell malignancies. We did not observe upregulation of the anti-apoptotic genes in MM compared to BMPC. On the one hand, this might be due to the elevated level of anti-apoptotic genes in BMPC, which are necessary for the survival of these long-lived cells (46). On the other hand, we cannot exclude that posttranscriptional modifications could directly influence protein levels, particularly for Mcl-1 (47–49).

We also showed specific modulations in BCL2-family expression associated to molecular subgroups in MCL, DLBCL and MM. In the *SOX11*- MCL subtype, we highlighted a selective dramatic downregulation of *BIK*. Given that this BH3-only is tightly regulated by DNA methylation (50), its silencing might be the direct consequence of the specific epigenetic profile recently described in this MCL subtype (51). Further investigations are now needed to document the consequences of these modulations in the survival and chemoresistance of *SOX11*- MCL cells.

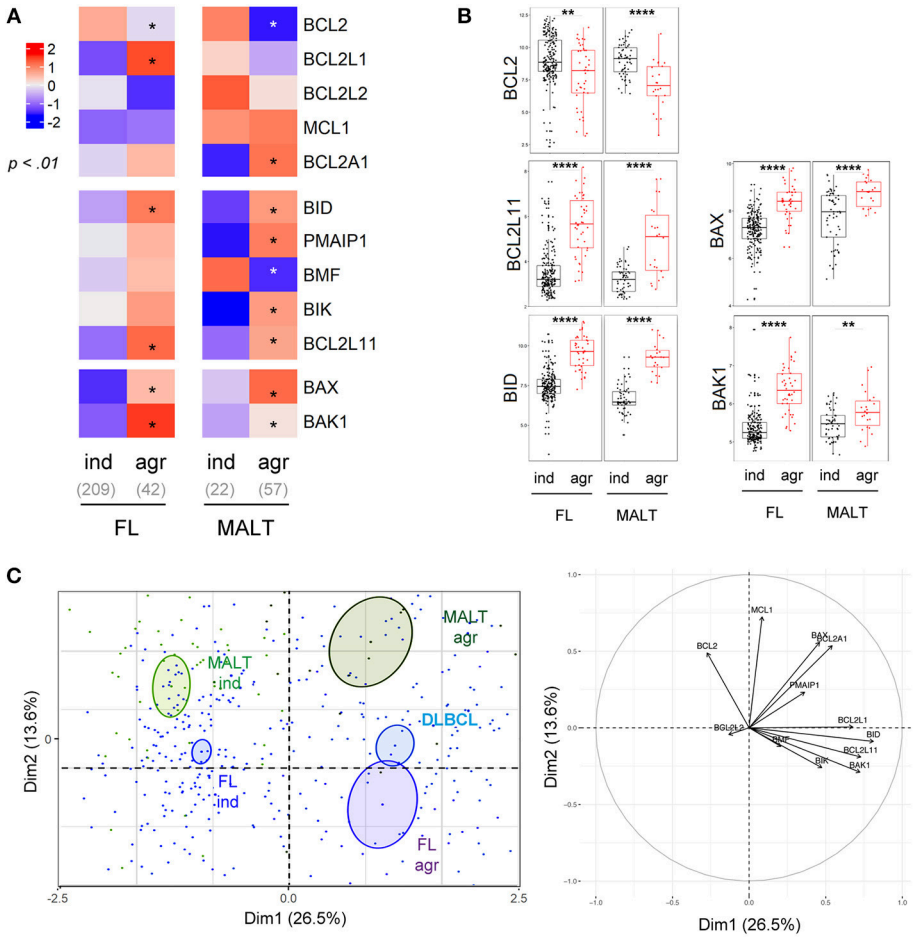

FIGURE 4 | Intra-entities BCL2-family heterogeneity is related to aggressiveness. **(A)** Heat-map of BCL2-family expression profile comparing FL and MALT samples according to their indolent (ind) or aggressive (agr) status. **(B)** *BCL2*, *BCL2L11*, *BID*, *BAX,* and *BAK1* expression in FL and MALT sample according to their aggressiveness. **(C)** Representation of the individual factor map for the PCA and according to the two first dimensions of lymphoma samples and their respective correlation circle. Colored ellipses are drawn around the mean of the group (=barycenter), with the 95% confidence interval of the mean in the corresponding plan. $^{*}p < 0.05$, $^{**}p < 0.01$, $^{****}p < 0.0001$.

Similarly, the "NFkB" molecular subgroup displayed a unique BCL2-family profile within MM samples, highlighted by the overexpression of *BCL2L2, BMF,* and *BCL2L11*. Given that this subgroup is characterized by an elevated expression of NFkB targets, it is tempting to speculate that the NFkB pathway regulates these genes in MM, as it has been previously described for *BCL2L2* in B cell lymphoma (52). Nevertheless, the "NFkB" entity represents <10% of the disease and the lack of relevant *in vitro* models for this molecular subgroup makes its study challenging (53).

By evaluating BCL2-family expression according to tissue localization, we observed a strong microenvironment-dependent regulation, especially in MCL and FL. Several studies have demonstrated the critical role of the microenvironment in the expansion and the chemoresistance of these hematological malignancies (54–56). Furthermore, we recently showed that a microenvironment-dependent upregulation of *BCL2L1* and downregulation of *BCL2L11* was involved in MCL chemoresistance (23). Of interest, a global pro- and anti-apoptotic imbalance was confirmed here in MCL. In addition, we showed that both *BCL2L11* and *PMAIP1* were downregulated by the tumor microenvironment in all the B-cell malignancies studied (MCL, FL, CLL, and SMZL), suggesting a fundamental role of these 2 specific BH3-only proteins in the microenvironment-dependent survival of lymphoma cells. Rational strategies to counteract their downregulation could then be critical to target lymphoma cells within the protective niches.

This global tissue-specific modulation in the BCL2 profile also directly impacted the predictive ratio to venetoclax sensitivity in MCL. Indeed, the *(BCL2+BCL2L11+BAX)/BCL2L1* ratio was much lower in LN-MCL samples compared to PB-MCL. Even though clinical studies highlighted an encouraging

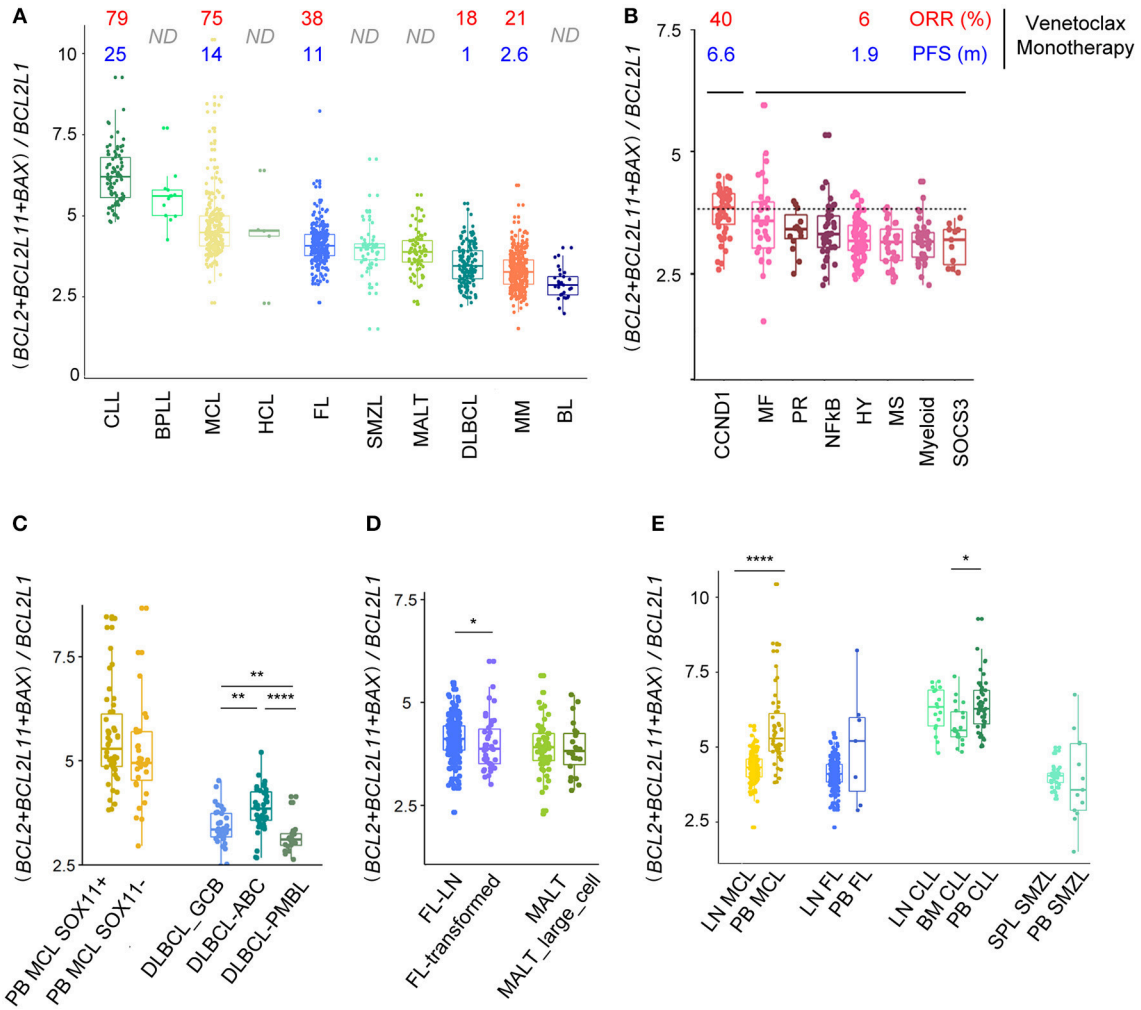

FIGURE 5 | (*BCL2+BCL2L11+BAX*)/*BCL2L1* ratio predicts response to Bcl2 specific BH3 mimetic. **(A)** Evaluation of the (*BCL2+BCL2L11+BAX*)/*BCL2L1* ratio for the different B-cell malignancies associated to ORR and PFS of patients treated with venetoclax-monotherapy when available. **(B,C)** Evaluation of the (*BCL2 + BCL2L11 + BAX*)/*BCL2L1* ratio for the different subtypes of **(B)** MM and **(C)** MCL and DLBCL. **(D)** Evaluation of the (*BCL2 + BCL2L11 + BAX*)/*BCL2L1* ratio for the different subtypes of FL and MALT. **(E)** Evaluation of the (*BCL2 + BCL2L11 + BAX*)/*BCL2L1* ratio for MCL, FL, CLL, SMZL according to their tissue localization (peripheral blood, PB, lymph nodes, LN, spleen, SPL). $^{*}p < 0.05$, $^{**}p < 0.01$, $^{****}p < 0.0001$.

ORR in MCL patients treated by venetoclax monotherapy, the PFS observed appeared much lower than in CLL. Our study suggested that MCL cells in the LN could be more resistant to venetoclax than PB-MCL and consequently could be involved in the rapid relapse observed in this pathology. Strategies targeting the microenvironment in association with venetoclax could then increase treatment efficacy and delay relapse. We recently show that MCL primary cells egressing in the PB through BTK inhibition have a *BCL2* high/*BCL2L1* low profile and were highly sensitive to venetoclax (39). Similarly, we showed that microenvironment-dependent *BCL2L1* induction was counteracted with the anti-CD20 antibody obinutuzumab, leading to an increased venetoclax efficacy *ex vivo* (23). Similar results showing the benefit of targeting microenvironmental interactions to potentiate BH3-mimetics efficacy have been published in other B cell malignancies such as CLL and MM (28, 29).

Of note, the above-mentioned predictive ratio highlighted that previously untested entities in venetoclax clinical trials, especially B-PLL and HCL, have sensitive-like BCL2-family profile, suggesting that they should be included in future clinical trials. Lastly, given the heterogeneity among entities (molecular subgroups, aggressiveness, tissue), this ratio could help predicting the B cell lymphoma patients who would benefit to BCL2 specific BH3-mimetic based therapy.

AUTHOR CONTRIBUTIONS

BT and AP designed the project, performed bioinformatics analyses, and wrote the paper. CB participated in the

bioinformatics analyses. PG-B, MA, and CP-D participated in the design of the study and in the writing of the article. DC designed the project and wrote the paper.

ACKNOWLEDGMENTS

This work was supported by grants from FFRMG, AF3M, Action Cancer 44, i-Site NexT (ANR-16-IDEX-0007) and the SIRIC ILIAD (INCa-DGOS-Inserm_12558). BT was supported by INSERM (poste d'accueil) and Foundation ARC.

SUPPLEMENTARY MATERIAL

The Supplementary Material for this article can be found online at: https://www.frontiersin.org/articles/10.3389/fonc.2018.00645/full#supplementary-material

REFERENCES

1. Kurosaki T, Kometani K, Ise W. Memory B cells. *Nat Rev Immunol*. (2015) 15:149–59. doi: 10.1038/nri3802
2. Nutt SL, Hodgkin PD, Tarlinton DM, Corcoran LM. The generation of antibody-secreting plasma cells. *Nat Rev Immunol*. (2015) 15:160–71. doi: 10.1038/nri3795
3. Basso K, Dalla-Favera R. Germinal centres and B cell lymphomagenesis. *Nat Rev Immunol*. (2015) 15:172–84. doi: 10.1038/nri3814
4. Kuppers R. Mechanisms of B-cell lymphoma pathogenesis. *Nat RevCancer* (2005) 5:251–62. doi: 10.1038/nrc1589
5. Teras LR, DeSantis CE, Cerhan JR, Morton LM, Jemal A, Flowers CR. 2016 US lymphoid malignancy statistics by World Health Organization subtypes. *CA Cancer J Clin*. (2016) 66:443-59. doi: 10.3322/caac.21357
6. Kuwana T, Bouchier-Hayes L, Chipuk JE, Bonzon C, Sullivan BA, Green DR, et al. BH3 domains of BH3-only proteins differentially regulate Bax-mediated mitochondrial membrane permeabilization both directly and indirectly. *Mol Cell* (2005) 17:525–35. doi: 10.1016/j.molcel.2005.02.003
7. McDonnell TJ, Deane N, Platt FM, Nunez G, Jaeger U, McKearn JP, et al. bcl-2-immunoglobulin transgenic mice demonstrate extended B cell survival and follicular lymphoproliferation. *Cell* (1989) 57:79–88. doi: 10.1016/0092-8674(89)90174-8
8. Beroukhim R, Mermel CH, Porter D, Wei G, Raychaudhuri S, Donovan J, et al. The landscape of somatic copy-number alteration across human cancers. *Nature* (2010) 463:899–905. doi: 10.1038/nature08822
9. Tagawa H, Karnan S, Suzuki R, Matsuo K, Zhang X, Ota A, et al. Genome-wide array-based CGH for mantle cell lymphoma: identification of homozygous deletions of the proapoptotic gene BIM. *Oncogene* (2005) 24:1348–58. doi: 10.1038/sj.onc.1208300
10. Cimmino A, Calin GA, Fabbri M, Iorio MV, Ferracin M, Shimizu M, et al. miR-15 and miR-16 induce apoptosis by targeting BCL2. *Proc Natl Acad Sci USA*. (2005) 102:13944–9. doi: 10.1073/pnas.0506654102
11. Raveche ES, Salerno E, Scaglione BJ, Manohar V, Abbasi F, Lin YC, et al. Abnormal microRNA-16 locus with synteny to human 13q14 linked to CLL in NZB mice. *Blood* (2007) 109:5079–86. doi: 10.1182/blood-2007-02-071225
12. Huang J, Fairbrother W, Reed JC. Therapeutic targeting of Bcl-2 family for treatment of B-cell malignancies. *Exp Rev Hematol*. (2015) 8:283–97. doi: 10.1586/17474086.2015.1026321
13. Lessene G, Czabotar PE, Colman PM. BCL-2 family antagonists for cancer therapy. *Nat Rev Drug Discov*. (2008) 7:989–1000. doi: 10.1038/nrd2658
14. Touzeau C, Dousset C, Le Gouill S, Sampath D, Leverson JD, Souers AJ, et al. The Bcl-2 specific BH3 mimetic ABT-199: a promising targeted therapy for t(11;14) multiple myeloma. *Leukemia* (2014) 28:210–2. doi: 10.1038/leu.2013.216
15. Touzeau C, Le Gouill S, Mahe B, Boudreault JS, Gastinne T, Blin N, et al. Deep and sustained response after venetoclax therapy in a patient with very advanced refractory myeloma with translocation t(11;14). *Haematologica* (2017) 102:e112–14. doi: 10.3324/haematol.2016.160408
16. Dai H, Meng XW, Kaufmann SH. Mitochondrial apoptosis and BH3 mimetics. *F1000Research* (2016) 5:2804. doi: 10.12688/f1000research.9629.1
17. Davids MS, Roberts AW, Seymour JF, Pagel JM, Kahl BS, Wierda WG, et al. Phase I first-in-human study of venetoclax in patients with relapsed or refractory non-hodgkin lymphoma. *J Clin Oncol*. (2017) 35:826–33. doi: 10.1200/JCO.2016.70.4320
18. Roberts AW, Davids MS, Pagel JM, Kahl BS, Puvvada SD, Gerecitano JF, et al. Targeting BCL2 with venetoclax in relapsed chronic lymphocytic leukemia. *N Eng J Med*. (2016) 374:311–22. doi: 10.1056/NEJMoa1513257
19. Leverson JD, Sampath D, Souers AJ, Rosenberg SH, Fairbrother WJ, Amiot M, et al. Found in translation: how preclinical research is guiding the clinical development of the BCL2-selective inhibitor venetoclax. *Cancer Discov*. (2017) 7:1376–93. doi: 10.1158/2159-8290.CD-17-0797
20. Kumar S, Kaufman JL, Gasparetto C, Mikhael J, Vij R, Pegourie B, et al. Efficacy of venetoclax as targeted therapy for relapsed/refractory t(11;14) multiple myeloma. *Blood* (2017) 130:2401–9. doi: 10.1182/blood-2017-06-788786
21. Davids MS. Targeting BCL-2 in B-cell lymphomas. *Blood* (2017) 130:1081–8. doi: 10.1182/blood-2017-04-737338
22. Tsuyama N, Sakata S, Baba S, Mishima Y, Nishimura N, Ueda K, et al. BCL2 expression in DLBCL: reappraisal of immunohistochemistry with new criteria for therapeutic biomarker evaluation. *Blood* (2017) 130:489–500. doi: 10.1182/blood-2016-12-759621
23. Chiron D, Bellanger C, Papin A, Tessoulin B, Dousset C, Maiga S, et al. Rational targeted therapies to overcome microenvironment-dependent expansion of mantle cell lymphoma. *Blood* (2016) 128:2808–18. doi: 10.1182/blood-2016-06-720490
24. Dousset C, Maiga S, Gomez-Bougie P, Le Coq J, Touzeau C, Moreau P, et al. BH3 profiling as a tool to identify acquired resistance to venetoclax in multiple myeloma. *Br J Haematol*. (2017) 179:684–8. doi: 10.1111/bjh.14251
25. Tahir SK, Smith ML, Hessler P, Rapp LR, Idler KB, Park CH, et al. Potential mechanisms of resistance to venetoclax and strategies to circumvent it. *BMC Cancer* (2017) 17:399. doi: 10.1186/s12885-017-3383-5
26. Swerdlow SH, Campo E, Pileri SA, Harris NL, Stein H, Siebert R, et al. The 2016 revision of the World Health Organization classification of lymphoid neoplasms. *Blood* (2016) 127:2375–90. doi: 10.1182/blood-2016-01-643569
27. Tarte K, Jourdan M, Veyrune JL, Berberich I, Fiol G, Redal N, et al. The Bcl-2 family member Bfl-1/A1 is strongly repressed in normal and malignant plasma cells but is a potent anti-apoptotic factor for myeloma cells. *Br J Haematol*. (2004) 125:373–82. doi: 10.1111/j.1365-2141.2004.04908.x
28. Gupta VA, Matulis SM, Conage-Pough JE, Nooka AK, Kaufman JL, Lonial S, et al. Bone marrow microenvironment-derived signals induce Mcl-1 dependence in multiple myeloma. *Blood* (2017) 129:1969–79. doi: 10.1182/blood-2016-10-745059
29. Thijssen R, Slinger E, Weller K, Geest CR, Beaumont T, van Oers MH, et al. Resistance to ABT-199 induced by microenvironmental signals in chronic lymphocytic leukemia can be counteracted by CD20 antibodies or kinase inhibitors. *Haematologica* (2015) 100:e302–6. doi: 10.3324/haematol.2015.124560
30. Puente XS, Jares P, Campo E. Chronic lymphocytic leukemia and mantle cell lymphoma: crossroads of genetic and microenvironment interactions. *Blood* (2018) 131:2283–96. doi: 10.1182/blood-2017-10-764373
31. Iqbal J, Neppalli VT, Wright G, Dave BJ, Horsman DE, Rosenwald A, et al. BCL2 expression is a prognostic marker for the activated B-cell-like type of diffuse large B-cell lymphoma. *J Clin Oncol*. (2006) 24:961–8. doi: 10.1200/JCO.2005.03.4264
32. Bergsagel PL, Kuehl WM, Zhan F, Sawyer J, Barlogie B, Shaughnessy J Jr. Cyclin D dysregulation: an early and unifying pathogenic event in multiple myeloma. *Blood* (2005) 106:296–303. doi: 10.1182/blood-2005-01-0034

33. Broyl A, Hose D, Lokhorst H, de Knegt Y, Peeters J, Jauch A, et al. Gene expression profiling for molecular classification of multiple myeloma in newly diagnosed patients. *Blood* (2010) 116:2543–53. doi: 10.1182/blood-2009-12-261032
34. Zhan F, Huang Y, Colla S, Stewart JP, Hanamura I, Gupta S, et al. The molecular classification of multiple myeloma. *Blood* (2006) 108:2020–8. doi: 10.1182/blood-2005-11-013458
35. Bergsagel PL, Kuehl WM. Molecular pathogenesis and a consequent classification of multiple myeloma. *J Clin Oncol*. (2005) 23:6333–8. doi: 10.1200/JCO.2005.05.021
36. Szalat R, Avet-Loiseau H, Munshi NC. Gene expression profiles in myeloma: ready for the real world? *Clin Cancer Res*. (2016) 22:5434–42. doi: 10.1158/1078-0432.CCR-16-0867
37. Gomez-Bougie P, Amiot M. Apoptotic machinery diversity in multiple myeloma molecular subtypes. *Front Immunol*. (2013) 4:467. doi: 10.3389/fimmu.2013.00467
38. Montoto S, Fitzgibbon J. Transformation of indolent B-cell lymphomas. *J Clin Oncol*. (2011) 29:1827–34. doi: 10.1200/JCO.2010.32.7577
39. Chiron D, Dousset C, Brosseau C, Touzeau C, Maiga S, Moreau P, et al. Biological rational for sequential targeting of Bruton tyrosine kinase and Bcl-2 to overcome CD40-induced ABT-199 resistance in mantle cell lymphoma. *Oncotarget* (2015) 6:8750–9. doi: 10.18632/oncotarget.3275
40. Gomez-Bougie P, Maiga S, Tessoulin B, Bourcier J, Bonnet A, Rodriguez MS, et al. BH3-mimetic toolkit guides the respective use of BCL2 and MCL1 BH3-mimetics in myeloma treatment. *Blood* (2018). doi: 10.1182/blood-2018-03-836718. [Epub ahead of print].
41. Vogler M, Butterworth M, Majid A, Walewska RJ, Sun XM, Dyer MJ, et al. Concurrent up-regulation of BCL-XL and BCL2A1 induces approximately 1000-fold resistance to ABT-737 in chronic lymphocytic leukemia. *Blood* (2009) 113:4403–13. doi: 10.1182/blood-2008-08-173310
42. Bodo J, Zhao X, Durkin L, Souers AJ, Phillips DC, Smith MR, et al. Acquired resistance to venetoclax (ABT-199) in t(14;18) positive lymphoma cells. *Oncotarget* (2016) 7:70000–10. doi: 10.18632/oncotarget.12132
43. Vogler M, Walter HS, Dyer MJS. Targeting anti-apoptotic BCL2 family proteins in haematological malignancies - from pathogenesis to treatment. *Br J Haematol*. (2017) 178:364–79. doi: 10.1111/bjh.14684
44. Adams CM, Mitra R, Gong JZ, Eischen CM. Non-hodgkin and hodgkin lymphomas select for overexpression of BCLW. *Clin Cancer Res*. (2017) 23:7119–29. doi: 10.1158/1078-0432.CCR-17-1144
45. Chipuk JE, Green DR. PUMA cooperates with direct activator proteins to promote mitochondrial outer membrane permeabilization and apoptosis. *Cell Cycle* (2009) 8:2692–6. doi: 10.4161/cc.8.17.9412
46. Papatriantafyllou M. B cells: secrets to plasma cell longevity. *Nat Rev Immunol*. (2013) 13:156–7. doi: 10.1038/nri3410
47. Wuilleme-Toumi S, Robillard N, Gomez P, Moreau P, Le Gouill S, Avet-Loiseau H, et al. Mcl-1 is overexpressed in multiple myeloma and associated with relapse and shorter survival. *Leukemia* (2005) 19:1248–52. doi: 10.1038/sj.leu.2403784
48. Wertz IE, Kusam S, Lam C, Okamoto T, Sandoval W, Anderson DJ, et al. Sensitivity to antitubulin chemotherapeutics is regulated by MCL1 and FBW7. *Nature* (2011) 471:110–4. doi: 10.1038/nature09779
49. Zhong Q, Gao W, Du F, Wang X. Mule/ARF-BP1, a BH3-only E3 ubiquitin ligase, catalyzes the polyubiquitination of Mcl-1 and regulates apoptosis. *Cell* (2005) 121:1085–95. doi: 10.1016/j.cell.2005.06.009
50. Brosseau C, Dousset C, Touzeau C, Maiga S, Moreau P, Amiot M, et al. Combination of lenalidomide with vitamin D3 induces apoptosis in mantle cell lymphoma via demethylation of BIK. *Cell Death Dis*. (2014) 5:e1389. doi: 10.1038/cddis.2014.346
51. Queiros AC, Beekman R, Vilarrasa-Blasi R, Duran-Ferrer M, Clot G, Merkel A, et al. Decoding the DNA methylome of mantle cell lymphoma in the light of the entire B cell lineage. *Cancer Cell* (2016) 30:806–21. doi: 10.1016/j.ccell.2016.09.014
52. Zhang M, Xu-Monette ZY, Li L, Manyam GC, Visco C, Tzankov A, et al. RelA NF-kappaB subunit activation as a therapeutic target in diffuse large B-cell lymphoma. *Aging* (2016) 8:3321–40. doi: 10.18632/aging.101121
53. Moreaux J, Klein B, Bataille R, Descamps G, Maiga S, Hose D, et al. A high-risk signature for patients with multiple myeloma established from the molecular classification of human myeloma cell lines. *Haematologica* (2011) 96:574–82. doi: 10.3324/haematol.2010.033456
54. Ame-Thomas P, Tarte K. The yin and the yang of follicular lymphoma cell niches: role of microenvironment heterogeneity and plasticity. *Semin Cancer Biol*. (2014) 24:23–32. doi: 10.1016/j.semcancer.2013.08.001
55. Balakrishnan K, Burger JA, Fu M, Doifode T, Wierda WG, Gandhi V. Regulation of Mcl-1 expression in context to bone marrow stromal microenvironment in chronic lymphocytic leukemia. *Neoplasia* (2014) 16:1036–46. doi: 10.1016/j.neo.2014.10.002
56. Papin A, Le Gouill S, Chiron D. Rationale for targeting tumor cells in their microenvironment for mantle cell lymphoma treatment. *Leuk Lymph*. (2018) 59:1064–72. doi: 10.1080/10428194.2017.1357177

Conflict of Interest Statement: The authors declare that the research was conducted in the absence of any commercial or financial relationships that could be construed as a potential conflict of interest.

Leukemia
https://doi.org/10.1038/s41375-019-0463-3

ARTICLE

Lymphoma

CSF1R and BTK inhibitions as novel strategies to disrupt the dialog between mantle cell lymphoma and macrophages

Antonin Papin[1,2,3] · Benoit Tessoulin[1,3,4] · Céline Bellanger[1,2,3] · Anne Moreau[3,5] · Yannick Le Bris[1,3,6] · Hervé Maisonneuve[3,7] · Philippe Moreau[1,3,4] · Cyrille Touzeau[1,3,4] · Martine Amiot[1,2,3] · Catherine Pellat-Deceunynck[1,2,3] · Steven Le Gouill[1,3,4] · David Chiron[1,2,3]

Received: 26 October 2018 / Revised: 18 March 2019 / Accepted: 19 March 2019

Abstract

The microenvironment strongly influences mantle cell lymphoma (MCL) survival, proliferation, and chemoresistance. However, little is known regarding the molecular characterization of lymphoma niches. Here, we focused on the interplay between MCL cells and the associated monocytes/macrophages. Using circulating MCL cells ($n = 58$), we showed that, through the secretion of CSF1 and, to a lesser extent, IL-10, MCL polarized monocytes into specific CD163$^+$ M2-like macrophages (MϕMCL). In turn, MϕMCL favored lymphoma survival and proliferation ex vivo. We next demonstrated that BTK inhibition abrogated CSF1 and IL-10 production in MCL cells, leading to the inhibition of macrophage polarization and consequently resulting in the suppression of microenvironment-dependent MCL expansion. In vivo, we showed that CSF1 and IL-10 plasma concentrations were higher in MCL patients than in healthy donors, and that monocytes from MCL patients overexpressed CD163. Further analyses of serial samples from ibrutinib-treated patients ($n = 8$) highlighted a rapid decrease of CSF1, IL-10, and CD163 in responsive patients. Finally, we showed that targeting the CSF1R abrogated MϕMCL-dependent MCL survival, irrespective of their sensitivity to ibrutinib. These data reinforced the role of the microenvironment in lymphoma and suggested that macrophages are a potential target for developing novel therapeutic strategies in MCL.

Introduction

Mantle cell lymphoma (MCL) is a rare and incurable B-cell malignancy, representing 3–10% of non-Hodgkin lymphomas (NHLs) [1, 2]. MCL cells are naive CD19$^+$ IgM$^+$ B cells characterized by the expression of the B1-cell marker CD5 and the absence of CD23 [3]. Conventional MCL cells initially accumulate in the lymph nodes (LN) and disseminate early on into the peripheral blood (PB) or the bone marrow [4]. In addition to the translocation t(11;14)(q13;q32), leading to the overexpression of cyclin D1, conventional MCL cells are characterized by the overexpression of the oncogene SOX11. A SOX11-negative leukemic non-nodal MCL subtype is now well characterized and displays a limited number of genomic alterations, indolent clinical course, spleen involvement, and a high percentage of circulating tumoral cells [5]. Both subtypes can evolve into more aggressive forms (blastoid/pleomorphic) characterized by increased genomic instability and a high proliferation index [5]. Several studies have described the nature of MCL genomic secondary alterations, such as frequent *ATM* or

These authors contributed equally: Benoit Tessoulin, Céline Bellanger, Steven Le Gouill, David Chiron

Supplementary information The online version of this article (https://doi.org/10.1038/s41375-019-0463-3) contains supplementary material, which is available to authorized users.

✉ David Chiron
david.chiron@univ-nantes.fr

1 CRCINA, INSERM, CNRS, Université d'Angers, Université de Nantes, Nantes, France

2 GDR3697 Micronit, CNRS, Nantes, France

3 L'Héma-NexT, i-Site NexT, Nantes, France

4 Service d'Hématologie Clinique, Unité d'Investigation Clinique, CHU, Nantes, France

5 Service d'Anatomie Pathologique, CHU, Nantes, France

6 Service d'Hématologie Biologique, CHU, Nantes, France

7 Centre Hospitalier de la Roche sur Yon, La Roche sur Yon, France

Published online: 02 April 2019

TP53 mutations, as well as recurrent copy-number abnormalities and the deletion of *CDKN2A* or *TP53*, those being associated with a bad prognosis [6–8].

In addition to intrinsic tumoral abnormalities, the major role of the immune and stromal microenvironments in the expansion and chemoresistance of B-cell lymphomas is now widely accepted [9, 10]. MCL, one of the most aggressive B-cell lymphomas, does not escape this logic, and several studies have recently confirmed the role of the microenvironment in the survival, proliferation, and chemoresistance of this NHL [11–16]. Nevertheless, the composition of the MCL microenvironment and the resulting interactions that occur in the tumor niches remain largely unknown.

Among accessory cells, tumor-associated macrophages (TAM) are known to play a critical role in solid tumor progression [17, 18] and have also been described in several B-cell malignancies [19–22]. Previous studies suggested the presence of macrophages in MCL LN [23, 24], but their phenotype and the molecular dialog that occurs between MCL cells and the associated macrophages remain unknown.

In this work, we have studied the dynamic interactions between MCL and its myeloid microenvironment. Using primary coculture models ex vivo, we have demonstrated that primary MCL cells polarize monocytes into specific associated macrophages (MϕMCL), which support MCL growth and survival. Furthermore, we identified mechanism-based targeted strategies that disrupt the dialog between MCL and MϕMCL ex vivo and in vivo.

Methods

Culture and coculture of primary cells

Primary MCL cells were obtained after informed consent from patients according to protocols approved by local institutional review boards (REFRACT-LYMA cohort; ethical approval GNEGS-2015-09-13 [25]) and in accordance with the Declaration of Helsinki. Patients' characteristics are summarized in supplemental Table S1. Briefly, samples from 58 patients (69% male; median age, 70 years) were used in this study, 61% at diagnosis and representing the different subtypes of the disease (37 conventional, 10 blastoid/pleomorphic, and 9 leukemic nonnodal). PB MCL cells were isolated after Ficoll–Hypaque separation and stored in liquid nitrogen. PB MCL cells (median of circulating cells, 50%) were separated from other mononuclear cells using antihuman CD19-conjugated magnetic beads (Miltenyi, Paris, France) with purity >90%. For autologous cocultures, monocytes from patients were isolated using anti-CD14-conjugated magnetic beads (Miltenyi, Paris, France). For allogeneic coculture experiments, PB primary monocytes from healthy donors (HD) were obtained by elutriation (CIC Biotherapy 0503, Nantes, France). For IL-10, CSF1 plasma concentrations, and CD163 expression on monocytes, PB was obtained from age-matched (>60 years) HD. Samples used for in vitro cocultures or molecular characterizations were listed in Table S1.

For in vitro generation of classically activated M1 and alternatively activated M2 macrophages, monocytes were differentiated with CSF2 (GM-CSF, 20 ng/mL, 5 days) or CSF1 (M-CSF, 50 ng/mL, 5 days) before activation with IFNγ (10 ng/mL, 2 days) or IL-10 (25 ng/mL, 2 days), respectively [26, 27].

$CD19^+$ primary MCL cells were cultured at 10^6 cells/mL alone or with monocytes or in vitro pre-differentiated macrophages at 2×10^5 cells/mL (5:1 ratio). Transwell assays were realized with a 0.4-µm pore polycarbonate membrane and 6.5 mm inserts (Corning, NY, USA). After cocultures, MCL cells were separated from macrophages by removal of non-adherent cells and identified using B-cell markers by flow cytometry (CD19, CD20). Adherent macrophages were detached using PBS–EDTA 0.02% (15 min at 4 °C). All cells were maintained in RPMI-1640 medium (Gibco) supplemented with 10% fetal calf serum and 2 mM glutamine.

MCL cell lines

JeKo-1, MINO, REC-1, MAVER-1, and GRANTA-519 were purchased from DSMZ (Braunschweig, Germany) and Z138 from ATCC (Manassas, USA). UPN1 and SP53 were kindly provided by Dr. V. Ribrag (Institut Gustave Roussy Villejuif, France) and Pr. S. Chen-Kiang (Cornell University, NY), respectively. NTS-3 and NTS-4 have been generated in our laboratory (CRCINA) [12]. Cell lines are routinely identified using a flow cytometry-based barcode as previously described [28], as well as MHC class I sequencing and are tested for mycoplasma contamination. Values for MCL cell lines are the mean of at least three independent experiments.

Bioinformatics analysis

For mRNA relative expression level, $CD19^+$ PB B cells from HD (normal B cell, NBC, $n = 15$), MCL cells ($n = 183$), and myeloid cells (monocytes, $n = 6$; MϕMCL, $n = 4$; M1, $n = 3$; M2, $n = 5$) datasets were collected from the GEO database (GSE50006, GSE19243, GSE35426, GSE16455, GSE36000, GSE21452, GSE70910, GSE76803, GSE28490, GSE124931, GSE95405, and GSE20484). In order to overcome data normalization biases, only Affimetrix Human Genome U133 Plus 2.0 series

with raw data were retained. Briefly, raw .CEL files were downloaded and processed in R-3.5.1 using the affy package, optical noise/background correction was performed by MAS5.0 or gcrma with standard options, and expression batches were finally normalized by quantiles using the limma package [29, 30]. Principal component analysis (PCA) was performed by FactoMineR and factoextra packages. A hierarchical ascendant clustering was performed using Euclidean distances and Ward.D2 method. Heatmap and radarchart were carried out with the ComplexHeatmap and fmsb package, respectively.

For deconvolution analysis of tumor bulk gene expression data (LN MCL, $n = 161$, GSE16455, GSE93291, GSE16024, GSE36000, and GSE70910) we used the Cibersort program [31]. $CD19^+$ sorted MCL cells from four LN (GSE70910) were used as an internal control for the deconvolution analysis.

Other methods

Cell cycle and viability assays as well as real-time quantitative reverse transcription polymerase chain reaction (qRT-PCR, control gene *RPL37A*) and Immunoblot protocols have been previously described [15]. Antibodies and reagents are detailed in supplemental Table S2. Statistical analyses were performed using two-sided Mann–Whitney, Wilcoxon-matched pairs signed-rank, or *t*-tests as stated in the figure legends. Analyses were performed using GraphPad Prism and R statistical software and all tests were considered statistically significant at $p < 0.05$.

Results

Monocyte-derived macrophages support primary MCL cell survival and proliferation

Using a deconvolution algorithm for tumor bulk gene expression data [31], we first observed that MCL LN were characterized by macrophage infiltration (median, 12%, $n = 161$, Fig. S1A). $CD68^+$ macrophages were also highlighted in MCL LN by IHC ($n = 10$), arguing for a potential dialog between MCL and its myeloid microenvironment in vivo (Fig. S1B).

To understand the potential role of this interplay, we first set up an ex vivo coculture of PB primary MCL cells (PB MCL cells) and monocytes isolated from HD. After 7 days of coculture, we observed that monocytes differentiated into adherent macrophages (Fig. S1C), which we called MCL-associated macrophages (MϕMCL) throughout this study. PB MCL cells poorly survived when cultured alone. In contrast, the presence of monocytes greatly improved their survival after 7 days ex vivo (median Annexin-V^{neg}, alone, 6.5%; coculture, 85.9%; $n = 17$; $p < 0.001$; Fig. 1a). The pro-survival advantage of the coculture, observed as early as 48 h, was maintained for several weeks and after several months of culture, the t(11;14) EBV^{neg} MCL cell line NTS-4 (from sample 2b) remained dependent on MϕMCL for survival (data not shown). Using culture inserts to avoid contact between the two cell types, we determined that the pro-survival impact of monocytes was partly dependent on soluble factors (median survival alone, 5%; coculture, 32.9%; $p < 0.001$; Fig. 1a). Indeed, whereas direct contact with monocytes induced a 13-fold increase of PB MCL cell survival, soluble factors supported a 6.5-fold survival increase (Fig. 1a).

We have previously shown that in contrast to lymph node MCL cells, circulating MCL cells rarely proliferate (Fig. S2A) [12]. Here, we have demonstrated that monocyte coculture supported the proliferation of primary MCL cells in 8/16 samples tested (median $BrdU^+$ cells in coculture, 14.75%; Fig. 1b, S2B), confirming the microenvironment-dependent expansion of MCL cells. Of note, monocyte-dependent proliferation was significantly lower in leukemic non-nodal (light gray bars, $n = 5$) compared with conventional (dark gray bars, $n = 7$) or aggressive (black bars; $n = 4$) MCL subtypes ($p < 0.05$, Fig. 1b). This monocyte-dependent increase in proliferation was confirmed at the molecular level by the induction of *MKI67* expression and the inhibition of the tumor suppressor Rb (ratio phospho (p) Rb/Rb) (Fig. S2C, D). As observed for survival, cell cycle induction was, at least, partly dependent on soluble factors (Fig. S2E). Of note, autologous monocytes/MCL cocultures displayed similar results ($n = 4$, autologous vs. allogeneic coculture, $p > 0.35$, Fig. 1c).

MϕMCL are M2-like macrophages

In order to better characterize the interplay between MCL and its myeloid microenvironment, cocultures of PB MCL cells in contact with in vitro pre-differentiated, classically activated (M1), or alternatively activated (M2) macrophages were set up. Even though M1 macrophages display anti-tumoral activities in several models, both M1 and M2 macrophages provided a similar pro-survival benefit to PB MCL cells (Fig. S3A). As observed for monocytes, this pro-tumoral effect was, at least, partly due to soluble factors (Fig. S3B), suggesting that both M1 and M2 macrophages secrete MCL pro-survival factors. Of note, M2 macrophages induced significantly more proliferation in PB MCL cells compared with M1 macrophages (median with M1 = 3%, with M2 = 9%, $p < 0.01$; Fig. S3C).

To define the precise nature of MCL-associated macrophages (MϕMCL), we analyzed their transcriptome along with the one of undifferentiated monocytes, M1 and M2 macrophages. To compare the different groups, we

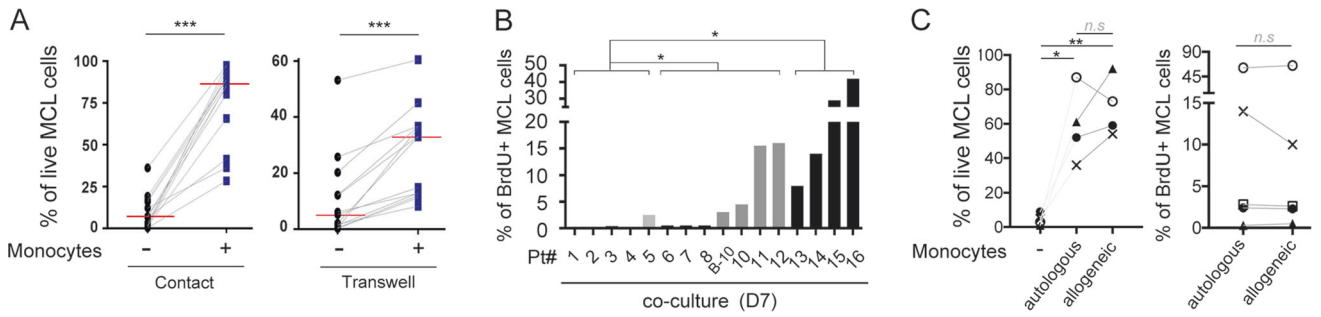

Fig. 1 Allogeneic and autologous monocytes support MCL cell survival and promote cell proliferation. **a** The percentage of PB MCL live cells was assessed by Annexin-V staining after 7 days of culture alone (–) or with allogeneic monocytes, either in contact ($n = 17$, left panel) or separated by transwell inserts ($n = 13$, right panel). Wilcoxon-matched pairs sign-rank test. ***$p < .001$. Red lines represent medians. **b** Cell cycle analysis (BrdU/PI) of PB MCL cells ($n = 16$) after 7 days of cocultures with monocytes according to their molecular subtypes (light gray: leukemic non-nodal ($n = 5$), dark gray: conventional ($n = 7$), and black: aggressive ($n = 4$)). Mann–Whitney test. *$p < 0.05$. **c** Percentage of live cells (Annexin-V staining, $n = 4$, left panel) and cell cycle analysis (BrdU/PI, $n = 5$, right panel) of PB MCL cells cultured alone or in contact with autologous or allogeneic monocytes for 7 days. Paired *t*-test. *$p < 0.05$; **$p < 0.01$

performed a PCA and observed that MϕMCL segregated with M2 macrophages (Fig. S4A). Accordingly, hierarchical clustering based on 17,256 genes highlighted greater similarities of MϕMCL with alternatively activated M2 macrophages (Fig. 2a).

Previously defined gene signatures allowed the robust prediction of monocytes, M1-like or M2-like phenotypes (Fig. S4B) [31]. It is noteworthy that ex vivo-generated MϕMCL and macrophages infiltrated in MCL LN in vivo displayed a similar CSF1-differentiated M2-like macrophage signature (Fig. 2b). In line with an M2-like profile, MϕMCL were characterized by the expression of the M2-like marker CD163, even though at a lower level than in vitro pre-differentiated M2 macrophages (Fig. 2c, S4C). MϕMCL arising from allogeneic or autologous $CD14^+$ monocytes displayed a similar phenotype (Fig. S4C) and the presence of $CD163^+$ cells was confirmed in MCL LN by IHC or cytometry (Fig. S4D-E).

Given the key role of soluble factors in MϕMCL/MCL interplay (Fig. 1), we analyzed the expression profile of genes coding for cytokines ($n = 24$) and chemokines ($n = 28$) in MϕMCL (Fig. S4F). Even though hierarchical clustering based on these 52 genes highlighted greater similarities with M2 macrophages (Fig. S4G), PCA demonstrated that MϕMCL formed a specific subtype of macrophages, producing both M2 and M1-associated factors (Fig. S4H). Among them, the expression of known protumoral cytokines in MCL, such as IGF1, IL-10, and IL6 [32–34], were confirmed in additional MϕMCL samples ($n = 5$, Fig. 2c).

MCL cells secrete the M2-polarizing factors IL-10 and CSF1

To determine how primary MCL cells polarized monocytes into specific $CD163^+$ M2-like MϕMCL, the expression of known macrophage-polarizing factors [35] was analyzed. We first interrogated publicly available gene expression datasets and observed that *CSF1* and *IL-10* transcripts, in contrast to *CSF2*, *IL4*, *IL34*, or *IL13 (data not shown)*, were significantly overexpressed in MCL samples in vivo, when compared with normal B cells (NBC) (Fig. 3a). Of note, *CSF1* but not *IL-10* expression was significantly higher in MCL LN compared with MCL PB (Fig. S5A). To confirm that these soluble factors were indeed produced by MCL cells, we assessed their expression in MCL cell lines ($n = 9$) and purified PB MCL cells ($n = 20$) by RT-qPCR (Fig. 3b, c). Whereas only 3/9 cell lines (JeKo, Mino, Granta) co-expressed *CSF1* and *IL-10*, transcripts for both factors were detected in 19 out of 20 primary MCL samples. *CSF1*, but not *IL-10* mRNA, was significantly overexpressed in aggressive (blastoid/pleomorphic) MCL subtypes and correlated with proliferation in coculture ex vivo ($BrdU^+$ cells in coculture) and in tissues in vivo (*MKI67*) (Fig. S5B–D). IL-10 (7/10) and CSF1 (7/10) expressions were then confirmed at the protein level in the MCL/MϕMCL coculture supernatant (D7), with all samples tested, secreting detectable amounts of at least one of both the factors (median CSF1, 4.35 pg/mL; median IL-10, 5.67 pg/mL) (Fig. 3d).

To understand the role of the CSF1 and IL-10 in the initiation of MCL/monocyte interplay, we cultured monocytes with previously generated MCL/monocyte coculture supernatants (7 days) in the presence of inhibitors of the CSF1R (GW2580 [36–38], blocking antibodies) or IL-10R (blocking antibodies). We demonstrated that inhibition of the CSF1R significantly reduced monocyte survival (median viability reduction of 80% with GW2580, of 44% with anti-CSF1R, $n = 6$, Fig. 3e). Inhibition of CSF1R with GW2580 significantly reduced the M2-like marker CD163 on the remaining viable monocytes (median CD163 reduction of 45%, $n = 5$) (Fig. 3e). Significant inhibition was also observed with anti-CSF1R monoclonal antibodies

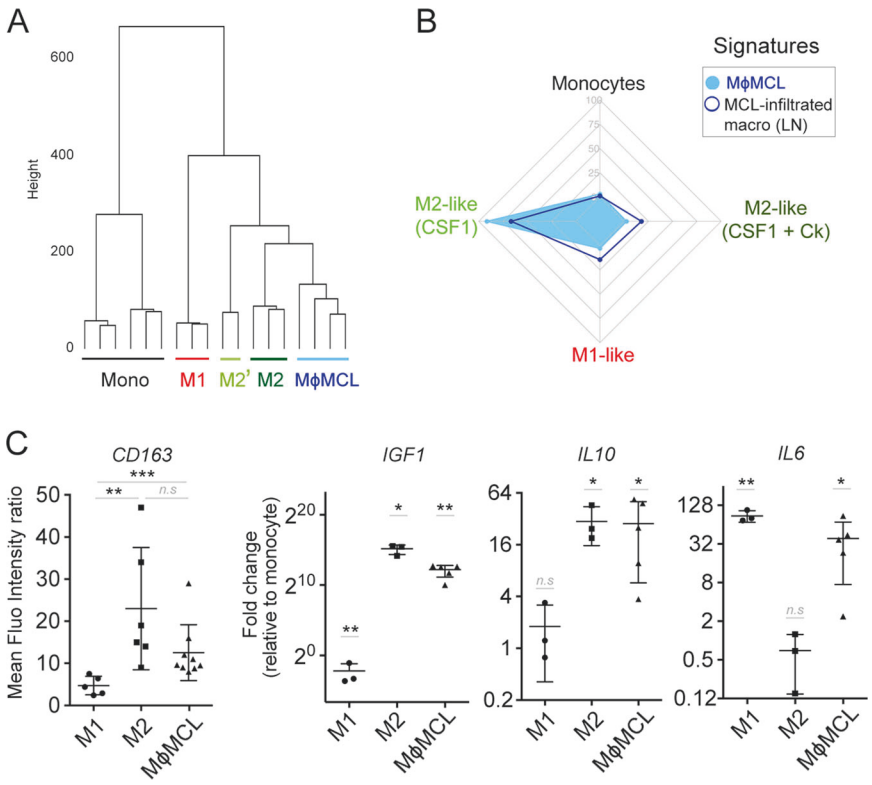

Fig. 2 MCL cells polarize monocytes into specific MϕMCL with M2-like features. **a** An ascendant hierarchical clustering was constructed with ward.D2 method of Euclidian distance. M2 macrophages were generated from human monocytes cultured with CSF1/IL-10 (see the section Methods), M2' with CSF1 alone (GSE20484), and M1 with LPS/IFNg (GSE95405). **b** Radarchart representation of the cibersort signature for MϕMCL and MCL-infiltrated macrophages in lymph nodes. **c** (left panel) CD163 mean fluorescence intensity ratio assessed by flow cytometry for M1 ($n = 6$), M2 ($n = 6$), and MϕMCL ($n = 9$) macrophages. Mann–Whitney test. $^{**}p < 0.01$, $^{***}p < 0.001$. (right panel) *IGF1*, *IL-10,* and *IL6* induction measured by qRT-PCR (relative to undifferentiated human monocytes) for M1 ($n = 3$), M2 ($n = 3$), and MϕMCL ($n = 5$) macrophages. *t*-test. $^{*}p < 0.05$; $^{**}p < 0.01$

(median reduction of 28%, $n = 5$). Inhibition of IL-10R resulted in a slight, but not significant, reduction of the CD163 level on MϕMCL (median reduction of 16%, $n = 5$, Fig. 3e). These data showed that MCL-secreted CSF1, but not IL-10, was essential for initiating the dialog between MCL and monocytes.

In addition to inhibiting monocyte survival and polarization, CSF1R neutralization resulted in the inhibition of monocyte-dependent survival in all primary MCL samples tested (Fig. 3f) (median monocyte-dependent survival reduction by GW2580 of 91%). Besides, we observed that CSF1R inhibition also resulted in an inhibition of primary MCL cells viability, as well as a downregulation of macrophage CD163 expression in coculture experiments with pre-differentiated MϕMCL and M2, but not M1, macrophages (Fig. S6A).

In accordance with the absence of CSF1R expression on MCL cells (data not shown), GW2580 did not display any direct cytotoxicity on primary MCL cells (Fig. S6B), confirming that the loss of viability was the consequence of the inhibition of MCL/MϕMCL interplay. In addition, CSF1R inhibition with other inhibitors such as BLZ945 [37], the clinically available PLX3397 or anti-CSF1R mAb confirmed the results obtained with GW2580 (Fig. S6C).

Taken together, the results showed that MCL cells secrete the M2-polarizing factors IL-10 and CSF1, the latter being essential for the initiation of the pro-tumoral dialog between malignant B cells and the associated macrophages.

Ibrutinib disrupts the dialog with MϕMCL by inhibiting MCL-specific CSF1 and IL-10 secretion

Previous studies reported modulations of the MCL secretome, including IL-10, upon BTK inhibition with ibrutinib, both in vitro [39] and in vivo [40]. To study the modulation of IL-10 and CSF1 upon ibrutinib treatment, Mino and Granta cell lines, which produce both factors, were first used (Fig. 3b). As previously reported [41], it was confirmed that, in contrast to Mino cells, Granta was resistant to both cytotoxic and cytostatic ibrutinib effects in vitro (0.5 µM; data not shown). Both *CSF1* and *IL-10* mRNA were dramatically reduced after 72 h of ibrutinib treatment (0.5 µM) in the ibrutinib-sensitive Mino cells, whereas no modulation was observed in the ibrutinib-resistant Granta

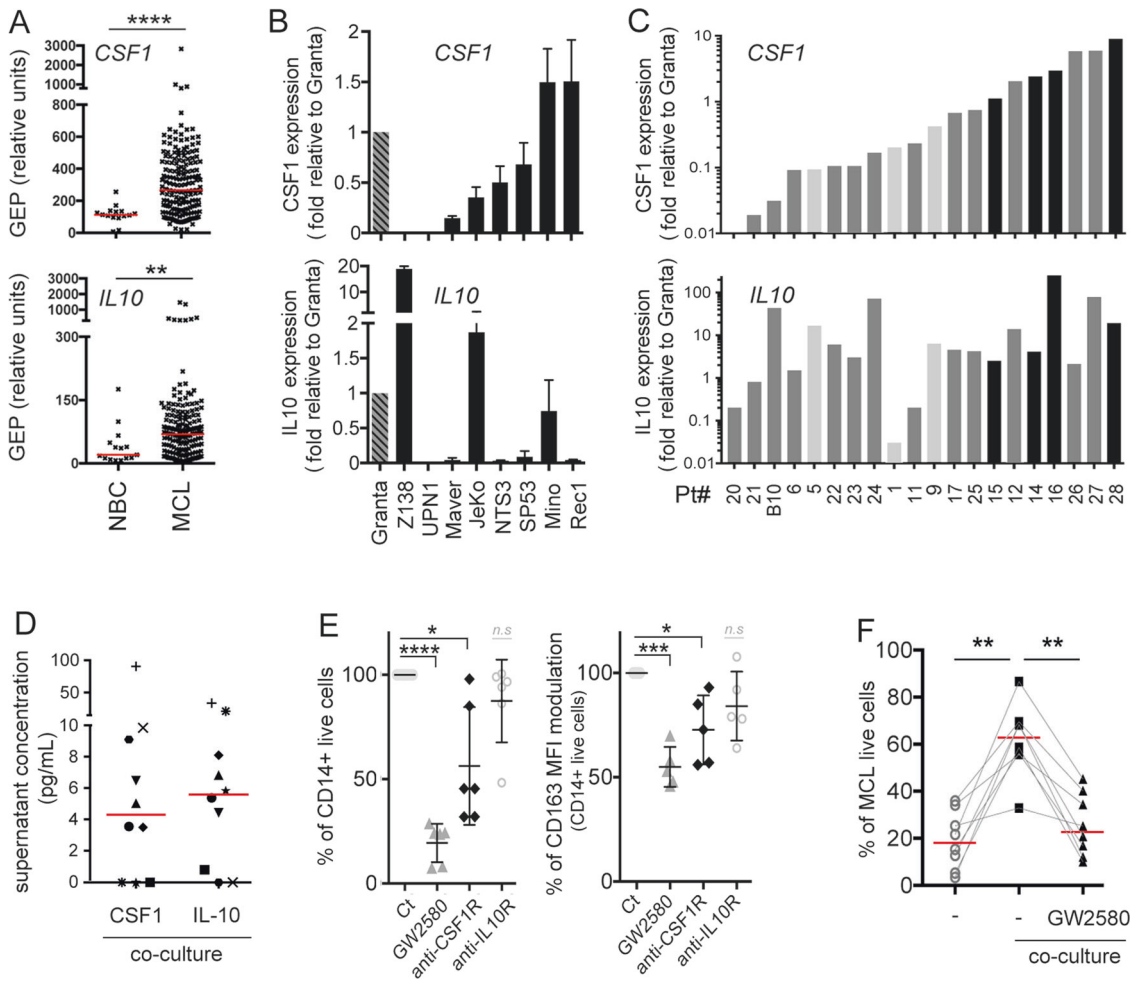

Fig. 3 MCL cells express the M2-polarizing factors CSF1 and IL-10. **a** Expression of *CSF1* and *IL-10* in MCL cells ($n = 183$) compared with normal B cells (NBC, $n = 15$) according to GEP public databases (see Methods). Mann–Whitney test. $^{****}p < 0.0001$; $^{**}p < 0.01$. **b** qRT-PCR analysis of *CSF1* and *IL-10* gene expression in nine MCL cell lines (realized in triplicate) and **c** 20 $CD19^+$ MCL samples purified from PB. Expression was normalized to Granta cell line. **d** Concentration of CSF1 and IL-10 proteins evaluated by ELISA in the supernatant of MϕMCL/MCL coculture (7 days, $n = 10$). **e** Percentage of live CD14 cells (left panel) and CD163 MFI modulation (on CD14 live cells) (right panel) after 3 days of culture with previously generated MCL/MϕMCL coculture supernatants ($n = 5$) in the presence of CSF1R inhibitors (GW2580 1 µM, anti-CSF1R antibodies 5 µg/mL), or of anti-IL-10R antibodies (5 µg/mL). Paired *t*-test. $^{*}p < 0.05$; $^{***}p < 0.001$; $^{****}p < 0.0001$. **f** Percentage of primary MCL live cells in coculture with monocytes with or without GW2580 treatment (1 µM) ($n = 8$). Cell death was assessed by Annexin-V staining. Wilcoxon-matched pairs sign-rank test. $^{**}p < .01$. Red lines represent medians

cells (Fig. 4a). These modulations were confirmed at the protein level using ELISA (Fig. 4b). Of note, we observed an induction of the CSF1 expression in cell lines with a low baseline level (UPN1, JeKo) after BCR activation upon anti-IgM stimulation, confirming that CSF1 is a direct target of the BCR signaling network (Fig. S7A).

In accordance with production of M2-polarizing factors, the coculture of both cell lines induced CD163 expression on PB primary monocytes from HD (Fig. 4c). As expected, ibrutinib inhibited the M2-like polarization exclusively with the ibrutinib-sensitive Mino cells (mean reduction of 43%, $n = 3$, Fig. 4c). Taken together, the results suggested that ibrutinib treatment counteracted $CD163^+$ MϕMCL polarization through inhibition of MCL-specific IL-10 and CSF1 secretion.

In addition to impairing MϕMCL polarization, ibrutinib treatment resulted in the inhibition of MϕMCL-dependent pro-survival and proliferative effects in 8 out of 14 and 4 out of 4 samples, respectively ($p < 0.01$) (Fig. 4d, e). Even though BCR signaling was constitutively activated, independently of monocyte coculture (Fig. S7B), ibrutinib did not induce any cytotoxicity in primary MCL cells cultured alone ex vivo (Fig. S7C). Besides, ibrutinib did not induce any cytotoxicity in monocytes/macrophages alone (data not shown). Thus, given that BCR inhibition abrogated MCL survival in coculture, it appears that ibrutinib acted mainly

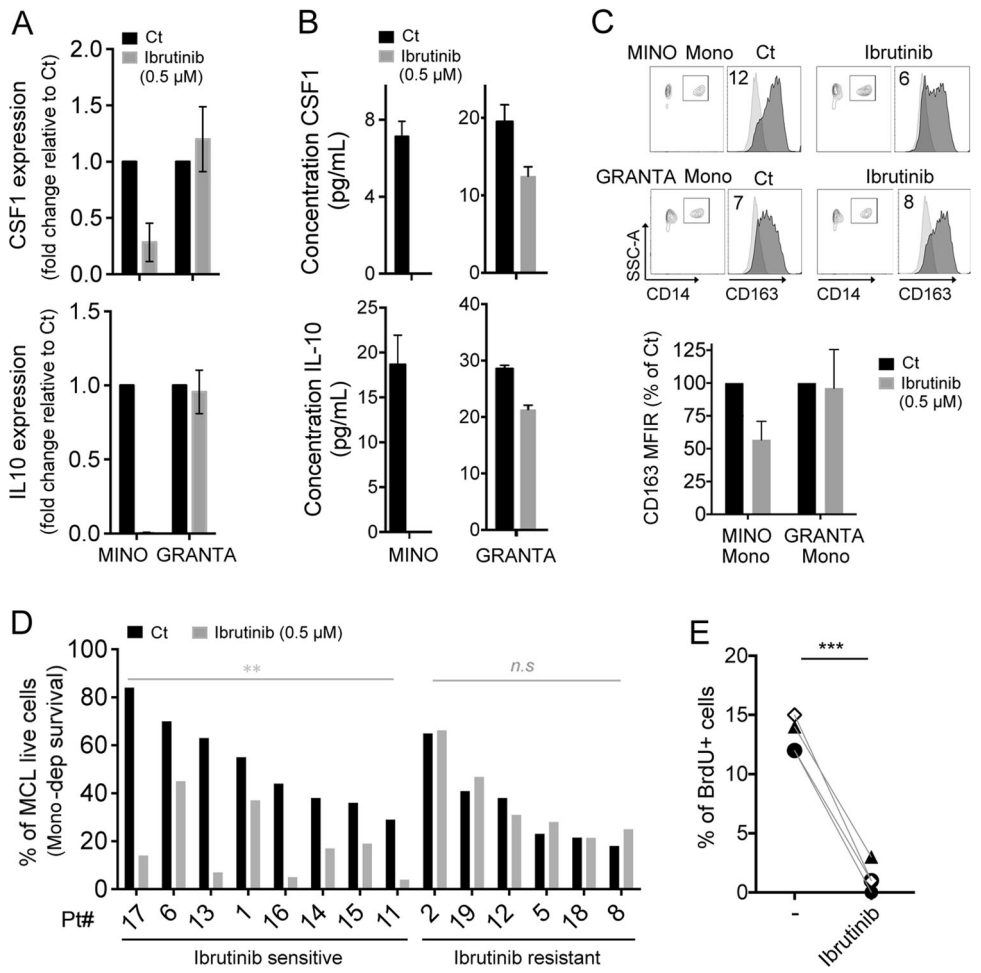

Fig. 4 Ibrutinib counteracts MCL/MϕMCL dialog through inhibition of CSF1. **a** qRT-PCR analysis of *CSF1* and *IL-10* expression in ibrutinib-sensitive Mino cells and ibrutinib-resistant Granta cells with or without ibrutinib treatment (72 h; 0.5 µM). Gene expression has been normalized to the non-treated control condition of each cell line (realized in triplicate). **b** Concentration of CSF1 and IL-10 proteins evaluated by ELISA in the supernatant of Mino and Granta cells with or without ibrutinib treatment (72 h; 0.5 µM; triplicate). **c** (upper panel) Gating strategy to evaluate the CD163 expression on $CD14^+$ after 3 days of coculture between monocytes and Mino or Granta cells with or without ibrutinib treatment (72 h; 0.5 µM). (lower panel) CD163 MFI modulation on $CD14^+$ cells representing three independent experiments. **d** Percentage of primary MCL live cells in coculture with monocytes (Annexin-V staining) with or without ibrutinib treatment (72 h; 0.5 µM; $n = 14$). Wilcoxon-matched pairs sign-rank test. $^{**}p < 0.01$, n.s. not significant. **e** Cell cycle analysis (BrdU/PI) of primary MCL cells after 5 days of cocultures with monocytes with or without ibrutinib treatment (72 h; 0.5 µM; $n = 4$). Paired *t*-test. $^{***}p < 0.001$

through the disruption of the interplay between tumoral cells and MϕMCL.

Early in vivo CD163 modulation on PB monocytes is observed upon ibrutinib treatment of MCL patients

In accordance with the ability of primary MCL cells to produce CSF1 and IL-10, a significantly higher level of these M2-polarizing factors was detected in the plasma of MCL patients compared with age-matched HD (median HD IL-10, 0 pg/mL; CSF1, 0 pg/mL; $n = 9$; median MCL IL-10, 1.2 pg/mL; CSF1, 5.6 pg/mL; $n = 28$, Fig. 5a). Likewise, CD163 was overexpressed at the surface of $CD14^+$ PB monocytes in several MCL samples compared with HD (median CD163 MFIr HD = 4.3, $n = 8$; MCL = 7.5, $n = 32$, Fig. 5a), which was consistent with the CD163-inducing properties of CSF1 and IL-10. There was no significant correlation between the level of IL-10, CSF1 nor CD163 and the status of the disease (Diagnosis/Relapse).

We next evaluated IL-10 and CSF1 plasma concentrations, as well as CD163 expression on $CD14^+$ PB monocytes in eight patients treated with anti-CD20 monoclonal antibody (Obinutuzumab) in combination with ibrutinib (protocol detailed in Fig. S8A). PB samples were collected before (D0) and after 8 days of treatment (D8). IL-10 or CSF1 concentration was decreased at D8 in 8/8 and 2/3 evaluable plasma samples, respectively (IL-10, $n = 8$, $p < 0.01$) (Fig. 5b). In addition, CD163 expression on

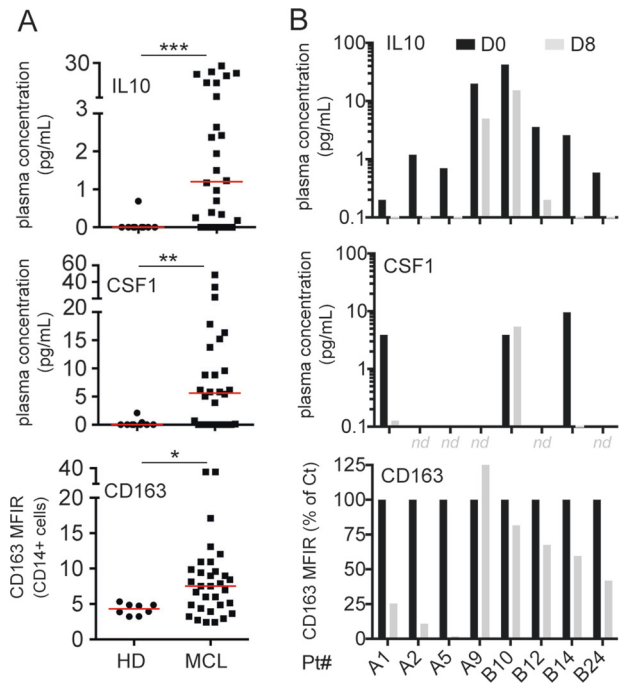

Fig. 5 CD163 modulation on circulating monocytes in vivo might be an early marker of ibrutinib response. **a** Plasma concentration of CSF1 and IL-10 proteins in MCL patients ($n = 28$) and age-matched healthy donors (HD, $n = 9$) by ELISA. (lower panel) Mean fluorescence intensity ratio (MFIr) of CD163 on circulating monocytes ($CD14^+$ cells) in MCL patients ($n = 32$) compared with age-matched HD ($n = 8$). Mann–Whitney test. $*p < 0.05$; $**p < 0.01$; $***p < 0.001$. **b** Plasma concentration of CSF1 and IL-10 and CD163 MFIr modulation on monocytes ($CD14^+$) of patients treated with anti-CD20 and ibrutinib (Clinical trial: NTC02558816). Biological parameters have been evaluated before treatment with ibrutinib and obinutuzumab (D0, black bars) and after 8 days of treatment (D8, gray bars). Variation of CD163 expression is normalized to D0 (% of D0)

$CD14^+$ PB monocytes was decreased in seven out of eight patients at D8 (median $CD163^+$ reduction of 58%, $n = 7$, $p < 0.05$, Fig. 5b). In contrast to ibrutinib (Fig. 4a), the anti-CD20 mAb Obinutuzumab did not directly modulate *IL-10* or *CSF1* in vitro (Fig. S8B).

The follow-up of patients treated with anti-CD20 mAb and ibrutinib for several cycles (Pt# A1, A2, A5, and A9) revealed that CD163 inhibition was durable and associated with a clinical response (>2 years) (Fig. S8C). In fact, whereas the three patients characterized by a dramatic reduction in CD163 at D8 (Pt# A1, A2, and A5) achieved a durable complete response, Pt# A9, who displayed an increase in CD163 expression and a limited decrease of IL-10 plasma concentration, progressed under treatment. Taken together, our retrospective analysis suggested that CD163 modulation upon ibrutinib treatment is associated with a clinical response. These results warrant further investigation with a larger cohort of ibrutinib-treated patients.

CSF1R inhibition as an alternative for disrupting MCL/MϕMCL dialog in ibrutinib-resistant patients

Ibrutinib did not efficiently counteract MϕMCL-dependent MCL survival in 6 out of 14 samples (Fig. 4d), including two patients who previously demonstrated ibrutinib resistance in vivo (Pt#2 and #12). To assess whether alternative strategies targeting the MCL/MϕMCL dialog could bypass ibrutinib resistance, the CSF1R inhibitor GW2580 was tested in both ibrutinib-sensitive (Pt#7, 11, 15, and 16) and resistant (Pt#2, 5, 18, and 19) primary cells. We showed that GW2580 reduced MCL cell viability in all samples tested, irrespective of their sensitivity to ibrutinib (Fig. 6a), suggesting that targeting the CSF1/CSF1R axis could be of major interest in ibrutinib-resistant patients. To assess whether the association of BTK and CSF1R inhibitors could also be beneficial for ibrutinib-sensitive patients, the efficacy of ibrutinib/GW2580 combination was tested at lower concentrations (125 nM). We showed additive (Pt#11 and #47) or supra-additive (Pt#7 and #15) effects of the combination in ibrutinib-sensitive samples ($n = 4$, $p < 0.05$, Fig. 6b, left) but not in ibrutinib-resistant samples ($n = 4$, Fig. 6b, right).

Discussion

Several studies have highlighted the central role of the microenvironment in the expansion and chemoresistance of B-cell lymphomas, including MCL [11–16, 42]. The few works that have examined the role of macrophages in MCL suggested a pro-tumoral function [23, 24], especially through the induction of a VEGF-dependent lymphangiogenesis [24]. However, little was known about the molecular interplay between MCL cells and the associated monocytes/macrophages. Here we showed that, through secretion of IL-10 and CSF1, MCL polarizes monocytes into M2-like macrophages, which in turn favor tumor survival and proliferation.

IL-10 production by MCL cells has been previously reported in vitro and in vivo [39, 40]. In contrast, this is, to our knowledge, the first study reporting a CSF1 paracrine loop in MCL. CSF1 and IL-10 are involved in monocyte polarization into alternatively activated M2-like TAM [43]. In addition, CSF1 and its receptor CSF1R are central to myeloid cell biology and promote migration, survival, and proliferation of monocytes [44]. It is noteworthy that both ex vivo-generated MϕMCL and in vivo MCL-infiltrated macrophages displayed a M2-like signature close to macrophages differentiated by the CSF1 (Fig. 2b, S4B), highlighting the relevance of our ex vivo coculture model and reinforcing the key role of the CSF1 in MCL/monocyte interplay.

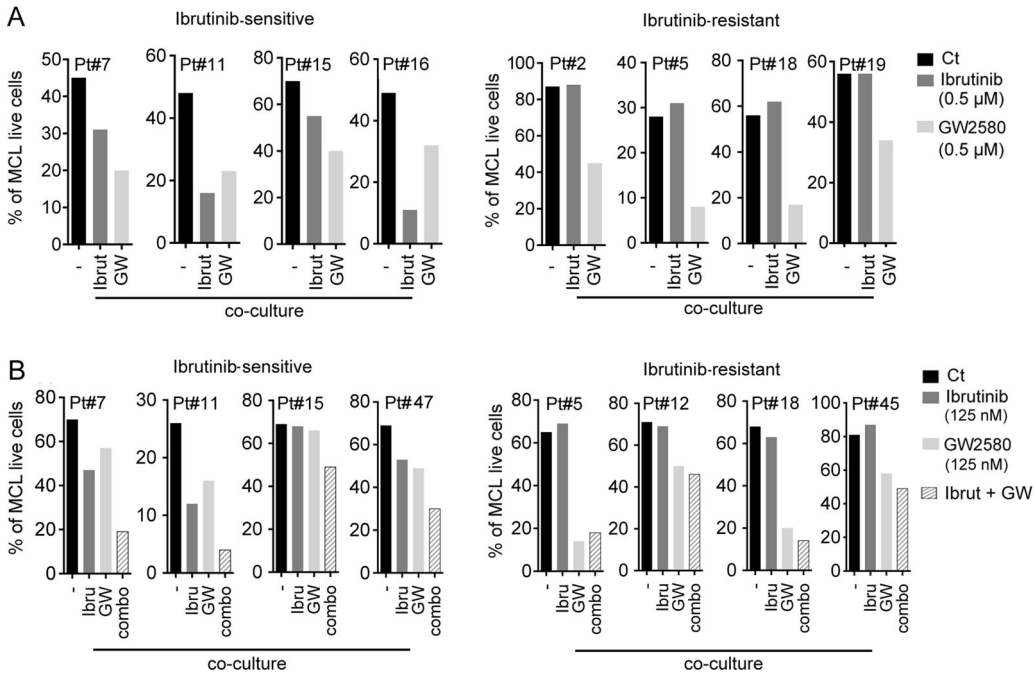

Fig. 6 CSF1R as a potential therapeutic target for ibrutinib-resistant patients. **a** Ibrutinib-sensitive (Pt#7, 11, 15, and 16) and ibrutinib-resistant (Pt#2, 5, 18, and 19) primary MCL cells were cocultured with monocytes and treated with ibrutinib (0.5 µM) or GW2580 (0.5 µM) for 72 h. **b** Ibrutinib-sensitive (Pt#7, 11, 15 and 47) and ibrutinib-resistant (Pt#5, 12, 18 and 45) primary MCL cells were cocultured with monocytes and treated with low doses of ibrutinib (125 nM) or GW2580 (125 nM) or both for 72 h. Cell death was assessed by Annexin-V staining

CSF1 production has been reported in several solid tumor models and has been associated with a poor prognosis [45, 46]. Regarding B-cell malignancies, *CSF1* transcript overexpression correlated with chronic lymphocytic leukemia (CLL) progression; however, CSF1 protein was not detected in the plasma of CLL patients [47]. In our study, and using the same technology (ELISA), we detected a significant amount of CSF1 protein in 17 out of 28 MCL plasmas studied, highlighting a high production in MCL (Fig. 5). In addition, we showed that *CSF1* was more expressed in the most aggressive forms of MCL and was associated with primary MCL cells proliferation ($BrdU^+$) ex vivo. This was reinforced by a positive correlation between *CSF1* and *MKI67* (proliferation index) expression in vivo (GEP analysis, $n = 183$) and suggested an association between MCL/MϕMCL interplay and tumor aggressiveness (Fig. S5).

Even though transcriptome analysis showed that MCL-associated macrophages (MϕMCL) shared more similarities with M2 macrophages (Fig. 2), M**ϕ**MCL expressed both M1 and M2-associated soluble factors (Fig. S4F–H). This reflected the phenotypic and functional plasticity of macrophage polarization and suggested that additional factors to IL-10 and CSF-1 might be involved in MϕMCL polarization. Besides soluble factors, cellular contacts might also play a role in MCL/MϕMCL interplay. We observed that MϕMCL displayed a specific immune checkpoint profile and expressed both PD1 and PDL1 (Fig. S4F), suggesting that immune checkpoint inhibitors could be of interest as another therapeutic avenue in MCL.

Given the central role of the myeloid microenvironment in numerous solid and hematological malignancies, several targeted strategies are under investigation. Among them, the CSF2-dependent re-education of M2-like TAM into classically activated antitumoral M1 macrophages has been proposed in several models such as glioblastoma or multiple myeloma [48, 49]. However, based on our ex vivo data, M1 macrophages could also provide a pro-survival signal in MCL. The depletion of TAM using targeted therapies has therefore appeared to be more attractive in MCL. Accordingly, we demonstrated that targeting the CSF1R using the small molecule GW2580 efficiently counteracted MϕMCL pro-tumoral effects ex vivo (Figs. 3 and 6). GW2580 is an orally bioavailable and selective CSF1R kinase inhibitor whose efficacy and selectivity have been previously demonstrated in different models [36–38, 50, 51]. In addition, potential off-target effects have been ruled out using other well-described selective small molecules, such as PLX3397 or BLZ945 as well as anti-CSF1R mAb. Success of such a strategy has been recently confirmed in vivo using clodrolip or anti-CSF1R mAb in a CLL mouse model [22]. In humans, several anti-CSF1R mAb

(LY3022855, Emactuzumab, AMG820) and CSF1R inhibitors (PLX3397, Pexidartinib) are currently being evaluated in phase I/II clinical studies that will soon document the efficacy of these targeted therapies [36].

In this study, we demonstrated that ibrutinib also directly counteracted the MCL/MϕMCL dialog through the modulation of the malignant B-cell secretome. We showed that BTK inhibition resulted in a dramatic decrease of CSF1 and IL-10 ex vivo and in vivo. Indeed, whereas higher levels of CSF1 and IL-10 were detected in the plasma of MCL compared with HD, ibrutinib treatment rapidly decreased the concentrations of both cytokines. Furthermore, CD163 was overexpressed at the surface of circulating monocytes in MCL compared with HD, which was consistent with the CD163-inducing properties of CSF1 and IL-10. Of interest, the longitudinal follow-up of four patients treated with ibrutinib highlighted a downregulation of CD163 on PB monocytes in three responsive patients in vivo. In contrast, only a limited modulation was observed in the resistant patient (Pt #A9). Taken together, our results are in favor of monitoring of CSF1, IL-10, and CD163 for the follow-up of patients' response to ibrutinib-based treatment. Even though a larger cohort of MCL patients treated with ibrutinib is now necessary to confirm the strength of this soluble and cellular signature, it is noteworthy that modulation of PB cytokines has also been associated with in vivo ibrutinib response in other B-cell malignancies [52].

Single-agent ibrutinib displayed an unprecedented clinical efficacy in MCL and is now approved for use in several B-cell malignancies. Nevertheless, several mechanisms of resistance such as mutation acquisition [53], compensatory pathway activation, i.e., NFκB [41], or kinome-adaptive reprogramming [42] have been described and retrospective studies revealed poor outcomes for ibrutinib relapsed/refractory MCL patients [54]. Here we showed that targeting the CSF1R could be an alternative for disrupting the MCL/MϕMCL pro-tumoral dialog, especially for ibrutinib-refractory patients for whom poor therapeutic alternatives are available. In addition, we observed (supra)additive cytotoxicity when BTK and CSF1R inhibitors were combined at low doses ex vivo, suggesting that this strategy could also be beneficial for ibrutinib-sensitive patients.

In conclusion, by modeling the dialog between MCL cells and their protective immune niches, we uncovered a novel rational combination that could overcome drug resistance. Our data reinforce the central role of the microenvironment in MCL and show that monocytes/macrophages are a potential target for developing novel therapeutic strategies in MCL.

Acknowledgements This study was supported by la Ligue Contre le Cancer Grand-Ouest, i-Site NexT (ANR-16-IDEX-0007), and the SIRIC ILIAD (INCa-DGOS-Inserm_12558). We thank Janssen-Cilag and Roche for supporting in part this study. The authors thank Elise Douillard (CRCINA) for excellent technical expertise. BT is the recipient for a fellowship from Fondation ARC.

Author contributions AP designed and performed experiments, analyzed data, and wrote the article. BT participated in bioinformatics analysis. CB performed experiments and participated in bioinformatics analysis. AM provided biopsy samples and analyzed data. YLB provided samples. HM provided samples. PM participated in the design of the study. CT provided samples. MA participated in the design of the study and reviewed the article. CPD participated in the design of the study, in the data analysis, and in the writing of the article. SLG participated in the design of the study, in the data analysis, and in the writing of the article. DC designed and performed experiments, analyzed data, and wrote the article.

Compliance with ethical standards

Conflict of interest SLG is a consultant/advisory board member and has received an honorarium from Roche and Janssen-Cilag. The remaining authors declare that they have no conflict of interest.

Publisher's note: Springer Nature remains neutral with regard to jurisdictional claims in published maps and institutional affiliations.

References

1. Campo E, Rule S. Mantle cell lymphoma: evolving management strategies. Blood. 2015;125:48–55.
2. Jares P, Colomer D, Campo E. Molecular pathogenesis of mantle cell lymphoma. J Clin Invest. 2012;122:3416–23.
3. Weisenburger DD, Armitage JO. Mantle cell lymphoma—an entity comes of age. Blood. 1996;87:4483–94.
4. Swerdlow SH, Campo E, Pileri SA, Harris NL, Stein H, Siebert R, et al. The2016 revision of the World Health Organization classification of lymphoid neoplasms. Blood. 2016;127:2375–90.
5. Puente XS, Jares P, Campo E. Chronic lymphocytic leukemia and mantle cell lymphoma: crossroads of genetic and microenvironment interactions. Blood. 2018;131:2283–96.
6. Delfau-Larue M-H, Klapper W, Berger F, Jardin F, Briere J, Salles G, et al. High-dose cytarabine does not overcome the adverse prognostic value of CDKN2A and TP53 deletions in mantle cell lymphoma. Blood. 2015;126:604–11.
7. Beà S, Valdés-Mas R, Navarro A, Salaverria I, Martín-Garcia D, Jares P, et al. Landscape of somatic mutations and clonal evolution in mantle cell lymphoma. Proc Natl Acad Sci USA. 2013;110:18250–5.
8. Queirós AC, Beekman R, Vilarrasa-Blasi R, Duran-Ferrer M, Clot G, Merkel A, et al. Decoding the DNA methylome of mantle cell lymphoma in the light of the entire B cell lineage. Cancer Cell. 2016;30:806–21.
9. Burger JA, Gribben JG. The microenvironment in chronic lymphocytic leukemia (CLL) and other B cell malignancies: insight into disease biology and new targeted therapies. Semin Cancer Biol. 2014;24:71–81.
10. Amé-Thomas P, Tarte K. The yin and the yang of follicular lymphoma cell niches: role of microenvironment heterogeneity and plasticity. Semin Cancer Biol. 2014;24:23–32.
11. Papin A, Le Gouill S, Chiron D. Rationale for targeting tumor cells in their microenvironment for mantle cell lymphoma treatment. Leuk Lymphoma. 2017;59:1064–72.

12. Chiron D, Bellanger C, Papin A, Tessoulin B, Dousset C, Maiga S. Rational targeted therapies to overcome microenvironment-dependent expansion of mantle cell lymphoma. Blood. 2016;128:2808–18.
13. Saba NS, Liu D, Herman SEM, Underbayev C, Tian X, Behrend D, et al. Pathogenic role of B-cell receptor signaling and canonical NF-κB activation in mantle cell lymphoma. Blood. 2016;128:82–92.
14. Chen Z, Teo AE, McCarty N. ROS-induced CXCR4 signaling regulates mantle cell lymphoma (MCL) cell survival and drug resistance in the bone marrow microenvironment via autophagy. Clin Cancer Res. 2016;22:187–99.
15. Chiron D, Dousset C, Brosseau C, Touzeau C, Maïga S, Moreau P, et al. Biological rational for sequential targeting of Bruton tyrosine kinase and Bcl-2 to overcome CD40-induced ABT-199 resistance in mantle cell lymphoma. Oncotarget. 2015;6:8750–9.
16. Kurtova AV, Tamayo AT, Ford RJ, Burger JA. Mantle cell lymphoma cells express high levels of CXCR4, CXCR5, and VLA-4 (CD49d): importance for interactions with the stromal microenvironment and specific targeting. Blood. 2009;113:4604–13.
17. Noy R, Pollard JW. Tumor-associated macrophages: from mechanisms to therapy. Immunity. 2014;41:49–61.
18. Qian B-Z, Pollard JW. Macrophage diversity enhances tumor progression and metastasis. Cell. 2010;141:39–51.
19. Steidl C, Lee T, Shah SP, Farinha P, Han G, Nayar T, et al. Tumor-associated macrophages and survival in classic Hodgkin's lymphoma. N Engl J Med. 2010;362:875–85.
20. Amin R, Mourcin F, Uhel F, Pangault C, Ruminy P, Dupré L, et al. DC-SIGN-expressing macrophages trigger activation of mannosylated IgM B-cell receptor in follicular lymphoma. Blood. 2015;126:1911–20.
21. Nguyen P-H, Fedorchenko O, Rosen N, Koch M, Barthel R, Winarski T, et al. LYN kinase in the tumor microenvironment is essential for the progression of chronic lymphocytic leukemia. Cancer Cell. 2016;30:610–22.
22. Galletti G, Scielzo C, Barbaglio F, Rodriguez TV, Riba M, Lazarevic D, et al. Targeting macrophages sensitizes chronic lymphocytic leukemia to apoptosis and inhibits disease progression. Cell Rep. 2016;14:1748–60.
23. Song K, Herzog BH, Sheng M, Fu J, McDaniel JM, Chen H, et al. Lenalidomide inhibits lymphangiogenesis in preclinical models of mantle cell lymphoma. Cancer Res. 2013;73:7254–64.
24. Pham LV, Vang MT, Tamayo AT, Lu G, Challagundla P, Jorgensen JL, et al. Involvement of tumor-associated macrophage activation in vitro during development of a novel mantle cell lymphoma cell line, PF-1, derived from a typical patient with relapsed disease. Leuk Lymphoma. 2015;56:186–93.
25. Hanf M, Chiron D, de Visme S, Touzeau C, Maisonneuve H, Jardel H, et al. The REFRACT-LYMA cohort study: a French observational prospective cohort study of patients with mantle cell lymphoma. BMC Cancer [Internet]. 2016;16:802. https://www.ncbi.nlm.nih.gov/pmc/articles/PMC5064959/
26. Derlindati E, Dei Cas A, Montanini B, Spigoni V, Curella V, Aldigeri R, et al. Transcriptomic analysis of human polarized macrophages: more than one role of alternative activation? PLoS One. 2015;10:e0119751.
27. Murray PJ, Allen JE, Biswas SK, Fisher EA, Gilroy DW, Goerdt S, et al. Macrophage activation and polarization: nomenclature and experimental guidelines. Immunity. 2014;41:14–20.
28. Maïga S, Brosseau C, Descamps G, Dousset C, Gomez-Bougie P, Chiron D, et al. A simple flow cytometry-based barcode for routine authentication of multiple myeloma and mantle cell lymphoma cell lines. Cytometry A. 2015;87:285–8.
29. Ritchie ME, Phipson B, Wu D, Hu Y, Law CW, Shi W, et al. limma powers differential expression analyses for RNA-sequencing and microarray studies. Nucleic Acids Res. 2015;43:e47.
30. Gautier L, Cope L, Bolstad BM, Irizarry RA. affy—analysis of Affymetrix GeneChip data at the probe level. Bioinformatics. 2004;20:307–15.
31. Newman AM, Liu CL, Green MR, Gentles AJ, Feng W, Xu Y, et al. Robust enumeration of cell subsets from tissue expression profiles. Nat Methods. 2015;12:453–7.
32. Vishwamitra D, Shi P, Wilson D, Manshouri R, Vega F, Schlette EJ, et al. Expression and effects of inhibition of type I insulin-like growth factor receptor tyrosine kinase in mantle cell lymphoma. Haematologica. 2011;96:871–80.
33. Baran-Marszak F, Boukhiar M, Harel S, Laguillier C, Roger C, Gressin R, et al. Constitutive and B-cell receptor-induced activation of STAT3 are important signaling pathways targeted by bortezomib in leukemic mantle cell lymphoma. Haematologica. 2010;95:1865–72.
34. Zhang L, Yang J, Qian J, Li H, Romaguera JE, Kwak LW, et al. Role of the microenvironment in mantle cell lymphoma: IL-6 is an important survival factor for the tumor cells. Blood. 2012;120:3783–92.
35. Shapouri-Moghaddam A, Mohammadian S, Vazini H, Taghadosi M, Esmaeili S-A, Mardani F, et al. Macrophage plasticity, polarization, and function in health and disease. J Cell Physiol. 2018;233:6425–40.
36. Mantovani A, Marchesi F, Malesci A, Laghi L, Allavena P. Tumour-associated macrophages as treatment targets in oncology. Nat Rev Clin Oncol. 2017;14:399–416.
37. Yeh Y-M, Hsu S-J, Lin P-C, Hsu K-F, Wu P-Y, Su W-C, et al. The c.1085A>G genetic variant of CSF1R gene regulates tumor immunity by altering the proliferation, polarization, and function of macrophages. Clin Cancer Res. 2017;23:6021–30.
38. Edwards DK, Watanabe-Smith K, Rofelty A, Damnernsawad A, Laderas T, Lamble A, et al. CSF1R inhibitors exhibit anti-tumor activity in acute myeloid leukemia by blocking paracrine signals from support cells. Blood. 2018;133:588–99
39. Bernard S, Danglade D, Gardano L, Laguillier C, Lazarian G, Roger C, et al. Inhibitors of BCR signalling interrupt the survival signal mediated by the micro-environment in mantle cell lymphoma. Int J Cancer. 2015;136:2761–74.
40. Chang BY, Francesco M, De Rooij MFM, Magadala P, Steggerda SM, Huang MM, et al. Egress of CD19(+)CD5(+) cells into peripheral blood following treatment with the Bruton tyrosine kinase inhibitor ibrutinib in mantle cell lymphoma patients. Blood. 2013;122:2412–24.
41. Rahal R, Frick M, Romero R, Korn JM, Kridel R, Chan FC, et al. Pharmacological and genomic profiling identifies NF-κB-targeted treatment strategies for mantle cell lymphoma. Nat Med. 2014;20:87–92.
42. Zhao X, Lwin T, Silva A, Shah B, Tao J, Fang B, et al. Unification of de novo and acquired ibrutinib resistance in mantle cell lymphoma. Nat Commun. 2017;8:14920.
43. Ruffell B, Affara NI, Coussens LM. Differential macrophage programming in the tumor microenvironment. Trends Immunol. 2012;33:119–26.
44. Hamilton JA, Cook AD, Tak PP. Anti-colony-stimulating factor therapies for inflammatory and autoimmune diseases. Nat Rev Drug Discov. 2016;16:53–70.
45. Ries CH, Cannarile MA, Hoves S, Benz J, Wartha K, Runza V, et al. Targeting tumor-associated macrophages with anti-CSF-1R antibody reveals a strategy for cancer therapy. Cancer Cell. 2014;25:846–59.
46. Zhu X-D, Zhang J-B, Zhuang P-Y, Zhu H-G, Zhang W, Xiong Y-Q, et al. High expression of macrophage colony-stimulating factor in peritumoral liver tissue is associated with poor survival after curative resection of hepatocellular carcinoma. J Clin Oncol. 2008;26:2707–16.

47. Polk A, Lu Y, Wang T, Seymour E, Bailey NG, Singer JW, et al. Colony-stimulating factor-1 receptor is required for nurse-like cell survival in chronic lymphocytic leukemia. Clin Cancer Res. 2016;22:6118–28.
48. Pyonteck SM, Akkari L, Schuhmacher AJ, Bowman RL, Sevenich L, Quail DF, et al. CSF-1R inhibition alters macrophage polarization and blocks glioma progression. Nat Med. 2013; 19:1264–72.
49. Gutiérrez-González A, Martínez-Moreno M, Samaniego R, Arellano-Sánchez N, Salinas-Muñoz L, Relloso M, et al. Evaluation of the potential therapeutic benefits of macrophage reprogramming in multiple myeloma. Blood. 2016;128:2241–52.
50. Moughon DL, He H, Schokrpur S, Jiang ZK, Yaqoob M, David J, et al. Macrophage blockade using CSF1R inhibitors reverses the vascular leakage underlying malignant ascites in late-stage epithelial ovarian cancer. Cancer Res. 2015;75:4742–52.
51. Priceman SJ, Sung JL, Shaposhnik Z, Burton JB, Torres-Collado AX, Moughon DL, et al. Targeting distinct tumor-infiltrating myeloid cells by inhibiting CSF-1 receptor: combating tumor evasion of antiangiogenic therapy. Blood. 2010;115:1461–71.
52. Chen JG, Liu X, Munshi M, Xu L, Tsakmaklis N, Demos MG, et al. BTKCys481Ser drives ibrutinib resistance via ERK1/2 and protects BTKwild-type MYD88-mutated cells by a paracrine mechanism. Blood. 2018;131:2047–59.
53. Chiron D, Di Liberto M, Martin P, Huang X, Sharman J, Blecua P, et al. Cell-cycle reprogramming for PI3K inhibition overrides a relapse-specific C481S BTK mutation revealed by longitudinal functional genomics in mantle cell lymphoma. Cancer Discov. 2014;4:1022–35.
54. Martin P, Maddocks K, Leonard JP, Ruan J, Goy A, Wagner-Johnston N, et al. Postibrutinib outcomes in patients with mantle cell lymphoma. Blood. 2016;127:1559–63.